Glucose Regulated Protein Synthesis in Pancreatic β-cells

Isabel Greenman

Department of Biochemistry
University of Leicester

UMI Number: U487871

UMI U487871

Abstract

The pancreatic β-cell rapidly releases insulin in response to glucose and in order to maintain insulin stores within the β-cell, there is a rapid and specific increase in proinsulin (PI) synthesis (10-20 fold within 60min). This rapid increase in PI synthesis is mediated entirely at the post-transcriptional level, likely through an increase in the rate of protein synthesis. As the regulation of glucose-stimulated proinsulin synthesis is poorly understood, the first objective of this thesis was to investigate the mechanism of glucose-regulated proinsulin synthesis in pancreatic β-cells. This thesis shows that contrary to previous reports, there is no pool of 'free' preproinsulin (PPI) mRNA at low glucose concentrations and that glucose does not stimulate the rate of *de novo* initiation. However, glucose does stimulate the recruitment of ribosomes onto ribosome-associated PPI mRNA, indicative of an increase in the rate of initiation of translation. Additionally, glucose stimulates the recruitment of PPI, PC2 and CPH mRNAs to the ER. Moreover, PPI mRNA is preferentially recruited to the ER over the other secretory protein mRNAs. This preferential recruitment of PPI mRNA may be an important mechanism for the specific up-regulation of PI synthesis at high glucose concentrations. Indeed, data presented here shows that the recruitment of PPI mRNA to the ER plays an important role in glucose stimulated PI synthesis.

In addition to an increase in PI synthesis, glucose stimulates a rapid increase in the synthesis of more than 260 unidentified β-cell proteins. It is likely that this rapid up-regulation of β-cell proteins is important in β-cell function. Therefore, microarray analysis of polysomal mRNAs was used to identify β-cell proteins that were translationally regulated in response to increases in glucose concentration. Interestingly, the majority of polysomal mRNAs whose levels changed between low and high glucose encoded proteins important in transcription and oxidative stress.

Publications

Gomez, E., Powell, M. L., Greenman, I. C. and Herbert, T. P. (2004). Glucose-stimulated protein synthesis in pancreatic beta-cells parallels an increase in the availability of the translational ternary complex (eIF2-GTP.Met-tRNAi) and the dephosphorylation of eIF2 alpha. J Biol Chem **279**, 53937-46

Greenman, I.C., Gomez, E., Moore, C.E.J., and Herbert, T.P. (2005). The selective recruitment of preproinsulin mRNA to the ER and an increase in ribosome recruitment onto ribosome associated preproinsulin mRNA are important mediators of glucose stimulated proinsulin synthesis in pancreatic β-cells. Biochem J. 2005 Jun 23; [Epub ahead of print].

Acknowledgements

Thanks to my supervisor, Terry Herbert for his guidance and supervision.

Special thanks must go to members of the lab, Mike Powell, Edith Gomez, Claire Moore and Kate Evans. I would especially like to thank Mike for taking apart the occasional Northern blot etc etc and for putting up with my singing and lack of musical knowledge for the last 3 and a half years! Thanks to Edith for all of her help and guidance, especially her cloning 'green fingers!'

Thank you must also go to my equally insane Biochemistry housemates, Jo and Kirsty who understood. Extra thanks to Mona, my non-biochemistry housemate – how did you put up with us?!

Thanks to all of my supportive friends in Bookham, especially Allie, Ben, Katie, Hedge and Gibson.

Thanks to Andy Broughton for his support, especially for keeping me happy with noodle bars!

The most thanks have got to go to my family. Simon for not being at all understanding but still making me laugh and Grandad for his very wise words and support, which I shall always treasure. Last but not least enormous thanks to Mum and Dad who have always been on the end of a phone at any time and kept me going through the last 4 years.

I dedicate this thesis to my Grandparents, Eric and Noella Jordan and Edwin and Freda Greenman.

Abbreviations

Abbreviation	Meaning
4E-BP	eIF4E binding protein
Amp	ampicillin
APS	ammonium persulphate
ATF4	activating transcription factor 4
bp	base pair
BiP	Immunoglobulin heavy chain-binding protein
BSA	bovine serum albumin
c-fos	FBJ osetosarcoma oncogene
CIAP	calf intestinal alkaline phosphatase
CPH	carboxypeptidase H
cpm	counts per minute
DMEM	Dulbecco's Modified Eagle's Medium
DMSO	Dimethyl Sulfoxide
DTT	dithiothreitol
ECL	Enhanced chemi-illuminescence
EDTA	Ethylenediaminetetraacetic Acid
eEF	eukaryotic elongation factor
EGTA	[ethylenebis(oxonitrilo)]tetra-acetate
eIF	eukaryotic initiation factor
ER	endoplasmic reticulum
eRF	eukaryotic release factor
EtBr	ethidium bromide
FCS	foetal calf serum
Ffh	Fifty-fourth homologue
Fluc	firefly luciferase
FRET	fluorescence resonance electron transfer
FtsY	signal recognition particle docking protein
GADD34	growth Arrest and DNA Damage inducible protein
GAP	GTPase activating protein
GAPDH	glyceraldehyde 3-phosphate dehydrogenase
GCN4	general control non-derepressible 4
GEF	guanine exchange factor
GFP	green fluorescent protein
GST	glutathione S transferase
HBS	HEPES buffered saline
HEPES	N-2-Hydroxyethylpiperazine-N'-2-ethanesulfonic acid
HRI	Heme-regulated eIF2α kinase
IPTG	Isopropyl thiogalactoside
JNK	c-jun NH$_2$-terminal kinase

Abbreviation	Meaning
Kan	kanamycin
Kb	kilobase
Kda	kilodalton
KHM buffer	potassium/HEPES/magnesium buffer
KRB	Kreb's Ringer Buffer
LB	Luria-Bertani Medium
M	molar
MAS5	MicroArray Suite 5
MCS	multiple cloning site
MIN6	mouse insulinoma 6
mM	millimolar
MM	mismatch
MOPS	3-(N-Morpholino)propanesulfonic acid
mRNP	messenger ribonucleoprotein
MTCH1	mitochondrial carrier homologue 1
NLS	nuclear localisation signal
PABP	poly(A)binding protein
PAGE	polyacrylamide gel electrophoresis
PBS	phosphate buffered saline
PC2	prohormone convertase 2
PC3	prohormone convertase 3
PCR	polymerase chain reaction
PI	proinsulin
PM	perfect match
PMSF	phenylmethylsulfonyl fluoride
PMT	photon multiplier tube
PPI	preproinsulin
PTB	polypyrimidine tract binding protein
RNC	ribosome nascent chain complex
RRL	rabbit reticulocyte lysate
SDS	sodium dodecyl sulphate
SRP	signal recognition particle
SR	SRP receptor
SSC	Saline Sodium Citrate
TAE	Tris-Acetate-EDTA Buffer
TBS	tris buffered saline
TCA	trichloroacetic acid
TE	Tris Ethylenediamine-Tetraacetic Acid
TE	tris EDTA
TEMED	N,N,N',N'-tetramethylethylenediamine
Tm	melting temperature

Abbreviation	Meaning
TOP	track of polypyrimidines
TRICINE	N-tris(hydroxymethyl)methylglycine
Tris	tris(hydroxymethyl)aminomethane
Tris-HCl	Tris Hydrochloride
TXNIP	thioredoxin interacting protein
uORF	upstream open reading frame
UTR	untranslated region
UV	Ultra-violet
v/v	volume/volume
w/v	weight/volume

Contents

<u>Addenda</u>

CD-ROM containing microarray unfiltered data from MAS5 and dChip as Microsoft

Excel files:
MAS5 experiment 1.xls
MAS5 experiment 2.xls
DChip experiment 1.xls
Dchip experiment 2.xls

Chapter 1: Introduction

1.1: Translation

At the end of transcription a 7-methyl guanylate cap is added to the 5' end of all polymerase II transcripts (Banerjee, 1980). Meanwhile, a string of usually 50 to 70 adenine residues is added to the 3' end to form the poly (A) tail, which is bound by poly(A) binding protein (PABP) (Brawerman, 1981). After splicing mRNA is exported from the nucleus and emerges into the cytosol as a messenger ribonucleoprotein (mRNP); an mRNA coated with RNA binding proteins.

The bases of the mRNA are organised into codons, each of which directs translation: the stepwise addition of amino acids to form the polypeptide chain. Translation takes place on the ribosome, which is a ribonucleoprotein (RNP) made up of two subunits, and is conventionally divided into three stages: initiation, elongation and termination (figure 1.1). In addition to the ribosome a large number of factors are required for each process to ensure that translation is a fast but highly regulated and accurate process (reviewed in (Kapp and Lorsch, 2004)).

1.1.1: Initiation of translation

In eukaryotes, initiation of translation (figure 1.2) requires a number of eukaryotic initiation factors (eIFs), GTP, ATP, Met-tRNA, mRNA and the 40S and 60S ribosomal subunits, which form the 80S ribosome. Initiation is completed when the first methionine of the polypeptide chain enters the P site of the ribosome. The first initiation event results in the formation of a monosome, an mRNA with one ribosome; any subsequent initiation events on the same mRNA whilst the first ribosome is attached result in the formation of a polysome.
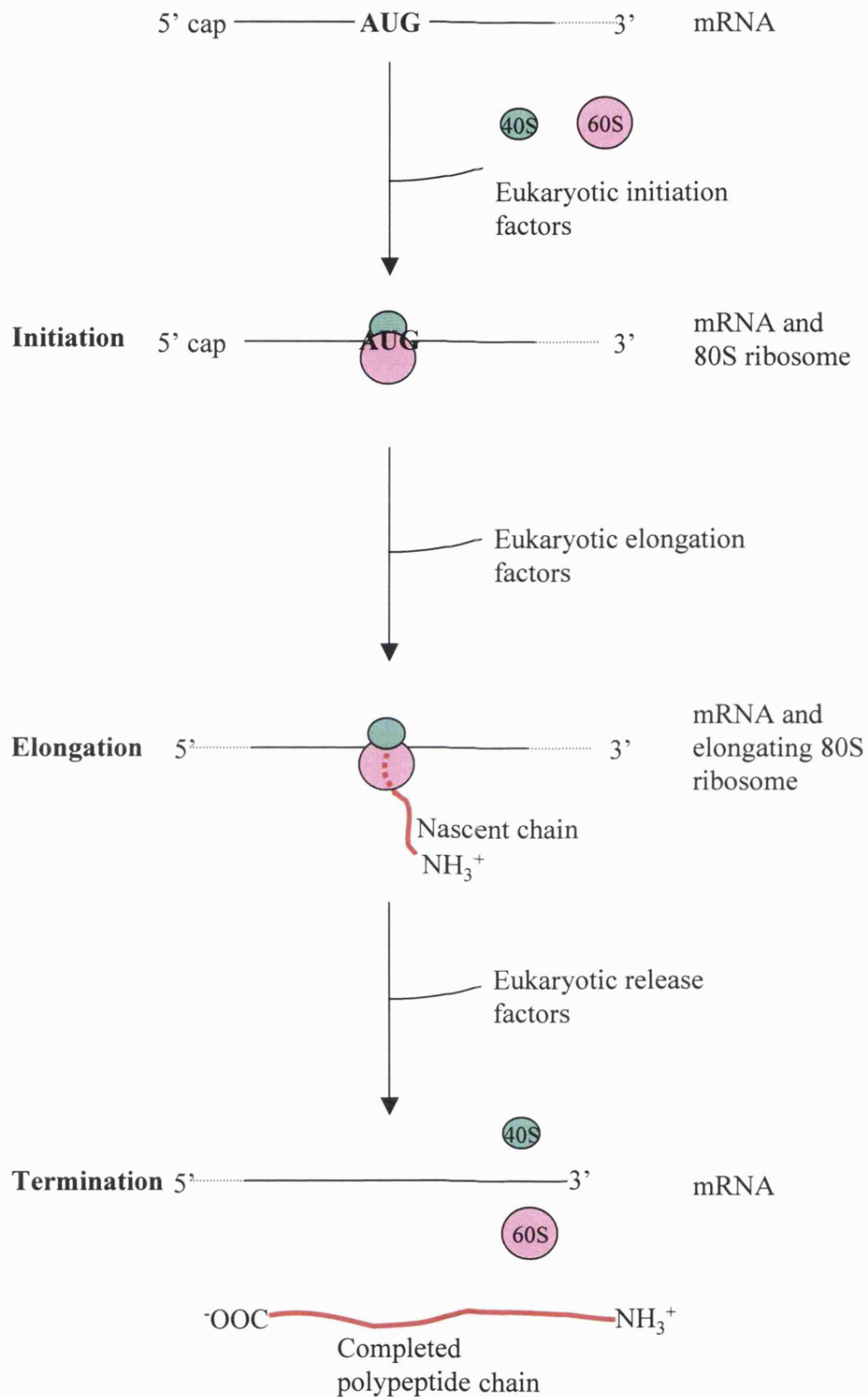
Figure 1.1: Eukaryotic translation

Translation is conventionally divided into three stages: initiation, which requires eukaryotic initiation factors (eIFs); elongation, which requires eukaryotic elongation factors (eEFs) and termination, which requires eukaryotic release factors (eRFs).
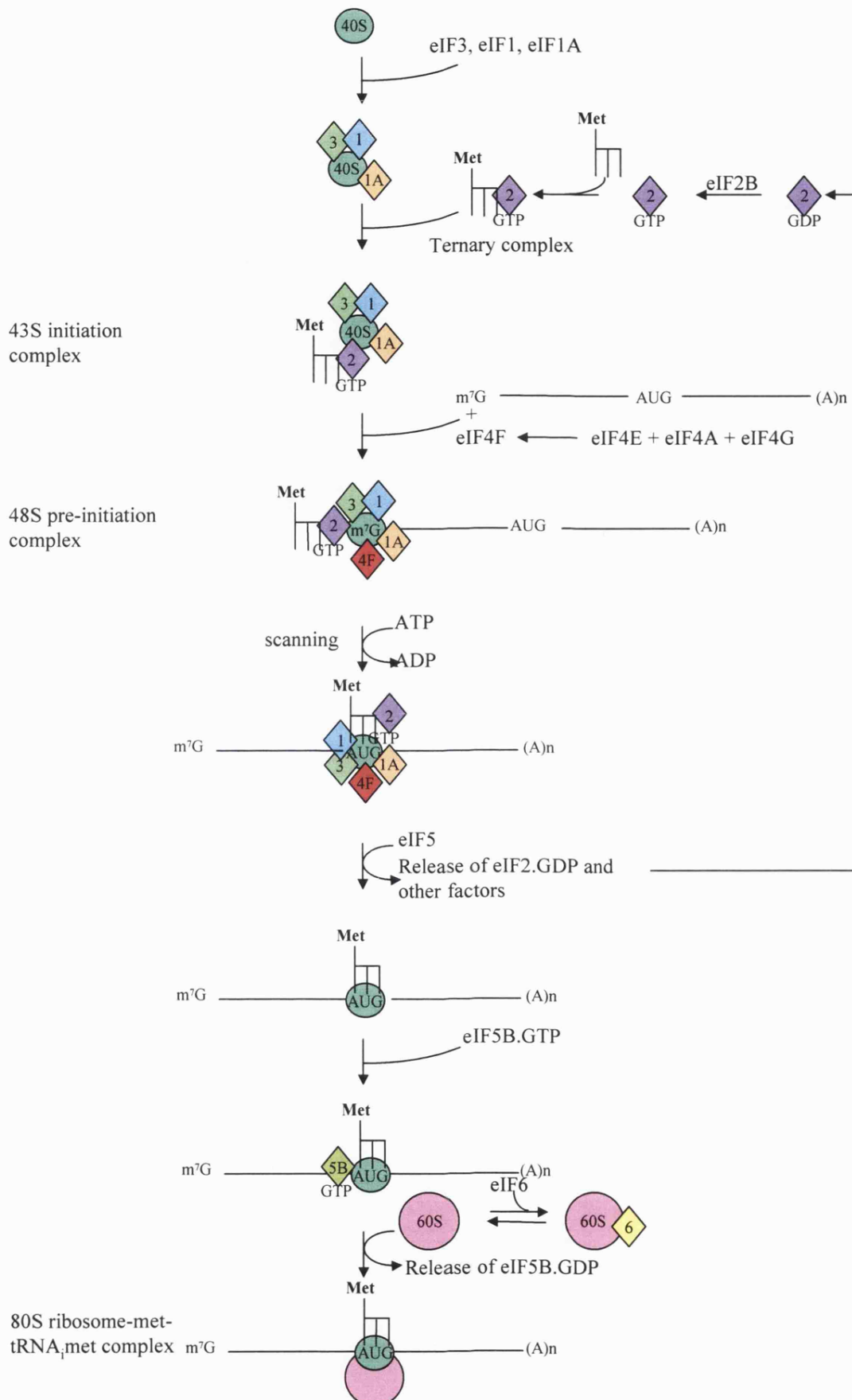
Figure 1.2: Steps involved in eukaryotic initiation of translation

◇ = initiation factors   ● = ribosomal subunits

Adapted from Hershey et al, 2000.

8

Availability of the ribosomal subunits

The binding of the ribosomal subunits by initiation factors keeps them from forming 'empty' 80S ribosomes that is redundant ribosomes without mRNA and initiation complexes. Indeed, prior to initiation, eIF6, which must be released prior to 80S formation binds the 60S ribosomal subunit and eIF1, eIF1A and eIF3 bind the 40S ribosomal subunit (Ceci et al., 2003; Goss et al., 1988; Majumdar et al., 2003; Nakaya et al., 1973).

Formation of the ternary complex

Before mRNA binding, the heterotrimeric eukaryotic initiation factor 2 (eIF2) bound to GTP binds to the Met-tRNA$_i$ to form the translational ternary complex (Smith and Henshaw, 1975). The initiator tRNA-met differs from the elongator tRNA-met in that it binds eIF2 and not eukaryotic elongation factor 1 (eEF-1) (Farruggio et al., 1996). It also binds the P site of the ribosome and not the A site of the ribosome (Farruggio et al., 1996). Unique elements in the initiator tRNA enable eIF2 to recognise the methionylated initiator tRNA over methionylated elongator tRNA (Sprinzl et al., 1987). The most important of these is an A1:U72 base pair at the end of the acceptor stem of the tRNA (Astrom et al., 1993; Farruggio et al., 1996; von Pawel-Rammingen et al., 1992).

Binding of the ternary complex to the 40S ribosomal subunit

Association of the ternary complex with the 40S ribosomal subunit leads to the formation of the 43S preinitiation complex and in mammals requires eIF1, eIF1A and eIF3 (Chaudhuri et al., 1999; Chaudhuri et al., 1997; Choi et al., 1998; Majumdar et al., 2003; Olsen et al., 2003; Shin et al., 2002). It has been proposed that eIF3 binds the 40S ribosomal subunit with eIF1 and eIF1A and the whole complex then binds the ternary complex (Majumdar et al., 2003). Furthermore, it has been suggested that these factors may facilitate easier access of the ternary complex to the ribosome through a change in the ribosome's conformation (Kapp and Lorsch, 2004). Interestingly, it has been shown that eIF1A alone catalyses ternary complex binding to the 40S ribosomal subunit but that this catalysis is inhibited by the presence of 60S ribosomal subunits (Chaudhuri et al., 1997). Indeed, eIF3 is required to relieve this inhibition by the 60S ribosomal subunit and to allow stable binding to occur between the ternary complex and the 40S ribosomal subunit (Chaudhuri et al., 1997).

9

eIF5 has also been shown to promote recruitment of the ternary complex to the ribosome, most likely through directly interacting with the ternary complex and binding the ribosome via eIF1 and eIF3 (Asano et al., 2001; He et al., 2003).

Binding of eIF4F to the mRNA and recruitment of the 43S preinitiation complex

In cap-dependent translation, binding of the 43S preinitiation complex to mRNA requires recognition of the cap by eIF4F. eIF4F assembles from the 5' cap-binding protein, eIF4E, the RNA helicase, eIF4A and the large scaffolding protein, eIF4G. The primary role of eIF4F is the recruitment of other initiation factors, which facilitate and direct binding of the 43S complex to the 5' end of the mRNA (Hentze, 1997, reviewed in Gingras et al., 1999).

eIF4G acts as a scaffold for the components required to direct the ribosome to the 5' end of the mRNA and to unwind RNA secondary structure (figure 1.3). It binds eIF4E, eIF4A, eIF3 and PABP. In addition, an RNA binding motif has been identified in the yeast homologue of eIF4G and binding sites for the eIF4E Mnk kinases have been identified in mammalian eIF4G (Goyer et al., 1993; Pyronnet et al., 1999). eIF4E binds eIF4G via the N-terminal domain (cp_N) of eIF4G (Johannes and Sarnow, 1998; Lamphear et al., 1995; Piron et al., 1998). eIF4A binds eIF4G in two places; one is in the C-terminal domain (cp_{C2}) and one is in the middle of eIF4G (cp_{C3}) (Lamphear et al., 1995; Waskiewicz et al., 1999). eIF4A shares the cp_{C3} binding site on eIF4G with eIF3 (Lamphear et al., 1995). Because eIF3 binds the ribosome and eIF4G it can aid the recruitment of the preinitiation complex to the mRNA (Lamphear et al., 1995; Mader et al., 1995).
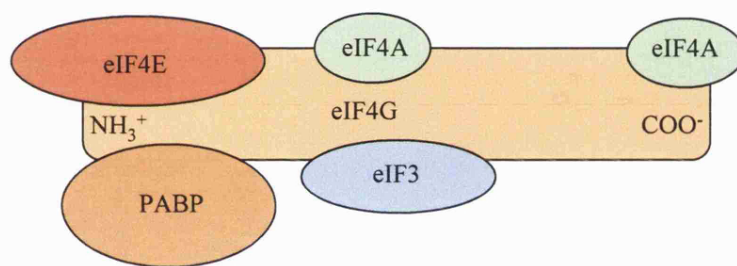
Figure 1.3: eIF4G is a scaffolding protein
eIF4G acts as a scaffolding protein for eIF4E, eIF4A, eIF3 and PABP.

The 5' untranslated region (UTR) of the mRNA must be free of secondary structure for the ternary complex to bind. Therefore, the first role of eIF4E binding to the cap is the recruitment of the ATP-dependent helicase, eIF4A to the 5' end of the RNA so that it can remove secondary structure from the mRNA (Abramson et al., 1987; Grifo et al., 1982). eIF4B and eIF4H stimulate the RNA binding and helicase activity of eIF4A; while eIF4B and eIF4F both act to reduce the K_m for the RNA in the helicase reaction (Abramson et al., 1988; Abramson et al., 1987; Richter et al., 1999; Richter-Cook et al., 1998; Rogers et al., 1999). Recently eIF4G was found to increase the ATP hydrolysis activity of eIF4A and increase its binding to RNA (Korneeva et al., 2004). It has also been suggested that eIF4A may act to remove RNA-binding proteins that would inhibit translation, indeed the addition of eIF4F relieves the inhibition of 48S complex formation by RNA binding protein p50/YB-1 (Pisarev et al., 2002).

In yeast and mammalian *in vitro* and *in vivo* systems capped mRNA and poly-adenylated mRNA translates more efficiently than uncapped or unadenylated mRNA (Iizuka et al., 1994; Michel et al., 2000; Munroe and Jacobson, 1990). Enhancement of initiation by the poly (A) tail is dependent on the cap structure (Gallie, 1991). Furthermore, the cap and poly(A) tail act synergistically to further enhance initiation of translation (Michel et al., 2000). Moreover, it has been shown that eIF4G associates with PABP when PABP is bound to the poly(A) tail, which may result in the circularisation of mRNA, although it should be made clear that evidence for this occurring during translation has not been provided (Imataka et al., 1998; Kozak, 2004; Tarun and Sachs, 1996; Wells et al., 1998).

Cap-poly(A) synergy is dependent on the interaction between eIF4G and PABP (Kahvejian et al., 2005; Michel et al., 2000). It has been proposed that it may stimulate 48S formation (Tarun and Sachs, 1996), 60S subunit joining (Kahvejian et al., 2005; Sachs and Davis, 1989; Searfoss et al., 2001) or ribosome recycling (Hershey and Merrick, 2000).

There is strong evidence that the circularisation of mRNA through eIF4G binding to PABP leads to an increase in initiation factor assembly and 80S formation (Borman et al., 2000; Preiss and Hentze, 1998; Tarun and Sachs, 1996). Interestingly, PABP depletion had a larger effect on 80S formation than 40S recruitment suggesting that

these processes are separately stimulated by PABP. Interaction of PABP with eIF4F increases eIF4E affinity for the cap structure (Borman et al., 2000; Kahvejian et al., 2005; Le et al., 1997) and additionally PABP increases the helicase activity of eIF4F in plants (Bi and Goss, 2000). Furthermore, PABP has been shown to enhance 80S formation (Sachs and Davis, 1989; Searfoss et al., 2001), which supports data that show the poly(A) tail influences 60S joining (Munroe and Jacobson, 1990)

Interestingly, circularisation also ensures that mRNAs which have degraded 3' ends and poly(A) tails are less efficiently translated, therefore reducing the synthesis of potentially toxic truncated proteins.

mRNA scanning and AUG recognition
Once the preinitiation complex has bound the mRNA it begins scanning the 5'-UTR for an AUG codon. For efficient initiation to occur the AUG must be within the consensus sequence: GCC(A/G)CCAUGG. (Kozak, 1986b; Kozak, 1987a; Kozak, 1987b) The initiator AUG is underlined and intiation at this AUG is most sensitive to changes in the bases in bold (Kozak, 1986b; Kozak, 1987a; Kozak, 1987b).

Ribosomal scanning has not been visualised or directly assayed so it is not known if the ribosome scans the 5'UTR by linear diffusion or by discrete association and dissociation. However, the scanning of structured mRNA is dependent on ATP although it is not known whether this dependence on ATP is required for ribosome scanning or just unwinding RNA secondary structure (Kozak, 1980a; Kozak, 1980b; Kozak, 1989b).

The 40S ribosome requires a minimum of eIF1, eIF2-ternary complex and eIF3 for binding to and scanning unstructured RNA although eIF1A, eIF4A, eIF4B and eIF4F do enhance scanning and are essential in scanning mRNA with any secondary structure (Pestova and Kolupaeva, 2002). Interestingly, eIF4A and eIF4B only promote scanning in the presence of eIF4F (Pestova and Kolupaeva, 2002). eIF1 and eIF1A act synergistically to promote scanning (Pestova et al., 1998). In the absence of eIF1 and eIF1A, 43S preinitiation complexes form at the 5' cap but do not start scanning the 5'-UTR (Pestova et al., 2001). In the absence of eIF1 low levels of 48S complexes were formed, which commenced scanning but did not discriminate between cognate and non-

cognate initiation codons (Pestova and Kolupaeva, 2002; Yoon and Donahue, 1992). Furthermore, eIF1 is required for destabilisation of these preinitiation complexes associated with 'incorrect' AUG codons (Pestova and Kolupaeva, 2002). Meanwhile, eIF1A is believed to stabilise 48S complexes, and facilitate eIF1's function of mediating scanning.

In yeast, hydrolysis of GTP associated with eIF2 is thought to be instigated by the base pairing of the initiation codon of the mRNA and the anti codon of the initiator tRNA (Huang et al., 1997). This hydrolysis of GTP is dependent on the GTPase-activating protein (GAP), eIF5 (Chakrabarti and Maitra, 1991; Das et al., 2001; Das and Maitra, 2001). Furthermore, mutations in eIF5 or eIF2 that result in over-stimulation of GTP hydrolysis or early release of eIF2 result in mismatched codon/anticodon pairing of the initiator tRNA (Huang et al., 1997). It was therefore suggested that the hydrolysis of GTP and ensuing release of eIF2 perform a checkpoint for correct AUG recognition. Additionally, met-tRNAi has been shown to interact with eIF2-GTP but not eIF2-GDP, supporting the fact that hydrolysis of GTP does indeed lead to the release of initiator tRNA from eIF2 (Kapp and Lorsch, 2004). Following GTP hydrolysis and release of eIF2-GDP the guanine exchange factor, eIF2B recycles eIF2-GDP to eIF2-GTP. This process is discussed in more detail below.

Mutation analysis has shown that eIF4G and eIF3 may also play roles in AUG recognition (He et al., 2003; Naranda et al., 1996; Phan et al., 1998). Additionally, it has been proposed that general RNA binding proteins encourage cap dependent translation and therefore prevent spurious initiation at 'incorrect' initiation codons (Svitkin et al., 1996).

Joining of 60S ribosomal subunit to the 48S preinitiation complex
Once eIF2-GDP has left the initiation complex, it has been proposed that eIF5B bound to GTP joins the complex at the AUG by interacting with eIF1A, which is in the A site of the ribosome (Lee et al., 2002). It has then been suggested that eIF5B acts as a translocase by occupying the A site of the ribosome, thereby shifting the initiator tRNA into the P site of the ribosome (Schmitt et al., 2002). In support of this, eIF5B has been shown to stabilise Met-tRNA in the P site of the ribosome (Choi et al., 2000).

Once bound to the initiation complex, eIF5B promotes the joining of the 60S ribosomal subunit to form the 80S ribosome (Choi et al., 2000; Lee et al., 2002; Pestova et al., 2000; Shin et al., 2002). Hydrolysis of GTP is not required for subunit joining as a non-hydrolysable analogue of GTP will still form an 80S ribosome, although these 80S ribosomes are not translationally competent (Pestova et al., 2000). Rather, GTP hydrolysis changes the conformation of eIF5B so that it has reduced affinity for the ribosome and therefore promotes release of eIF5B (Shin et al., 2002). Interestingly, the addition of a mutation that reduces ribosome affinity to the GTPase-deficient eIF5B mutants suppresses growth defects of the GTPase-deficient mutant (Shin et al., 2002). It is therefore believed that the GTPase activity is primarily important in release of eIF5B, which allows the 80S ribosome to partake in elongation. Indeed it has been suggested that eIF5B release triggers the release of eIF1A from the A site of the ribosome to allow entry of the second amino acyl tRNA (Choi et al., 2000; Olsen et al., 2003).

Association of the 60S subunit with the 48S complex results in the formation of the 80S ribosome-Met-tRNA$_i$met complex, which is now ready for the stepwise addition of amino acids by the in-frame translation of the mRNA.

1.1.2: Recycling and Re-initiation

Ribosome recycling is defined as the initiation of ribosomes that have already been through a round of translation onto the same or a different mRNA (Hershey and Merrick, 2000). Recent work has shown that progression of ribosomes through the 3'-UTR of the mRNA was not necessary for cap-poly(A) synergy or ribosome recycling, (Michel et al., 2000; Rajkowitsch et al., 2004). Therefore, ribosome recycling most likely occurs directly from the stop codon. Indeed PABP has been shown to interact both *in vitro* and *in vivo* with a member of the termination machinery, eukaryotic release factor 3 (eRF3), which interacts with the terminating ribosome through eRF1 (Cosson et al., 2002; Hoshino et al., 1999; Uchida et al., 2002). Furthermore, inhibition of the PABP-eRF3 interaction does not inhibit de novo 80S formation but does appear to inhibit subsequent rounds of initiation (Uchida et al., 2002). Uchida *et al*, 2002 propose that the interaction between PABP and eRF3 'loops out' the 3'UTR (which can result in a large distance between the stop codon and the poly(A) tail) and connects the

terminating ribosome with the 5'UTR and cap structure (figure 1.4). The distance between the termination site and the initiation site influences the local ribosome concentration around the initiation site and therefore influences the overall translation rate (Chou, 2003).

1.1.3: Regulation of initiation

Initiation of translation is considered the rate-limiting step of translation and is therefore thought to be the most important stage in the regulation of translation. Interaction between eIFs facilitates the speed and accuracy of initiation and provides a means of regulating both global translation and gene-specific translation. The major regulatory step of initiation is the binding of the 43S-initiation complex to the 5' end of the mRNA. This is largely regulated through regulation of ternary complex formation and assembly of the eIF4F complex.

Regulation of eIF4F assembly (figure 1.5)

Assembly of the eIF4F complex is regulated by a variety of stimuli through multiple signal transduction pathways, which in turn regulate initiation of translation (reviewed in Gingras et al., 1999). Initially it was thought that eIF4E is the limiting factor in eIF4F assembly (Duncan et al., 1987; Hiremath et al., 1985) and therefore it was logical that the availability of eIF4E was the primary mechanism for regulating eIF4F assembly. The availability of eIF4E can be regulated by three main mechanisms: gene expression (Rosenwald et al., 1993), eIF4E phosphorylation and inhibition of eIF4E by eIF4E-binding proteins (4E-BPs) (figure 1.5).

Initially, it was believed that eIF4E was phosphorylated on Ser53, therefore the earlier mutagenesis work focused on this residue. However, it was later found that eIF4E is phosphorylated once on Ser209, which resides within a consensus sequence for protein kinase C phosphorylation (Joshi et al., 1995; Whalen et al., 1996). The location of Ser209 by the cap-binding pocket, suggests that its phosphorylation influences cap binding (Marcotrigiano et al., 1997; Matsuo et al., 1997).

initiation

AUG

5'cap

eIF4E

eIF4G

80S ribosome

PABP

elongation

AAAA....AAAA

eRF3

eRF1

TGA

3'UTR

termination
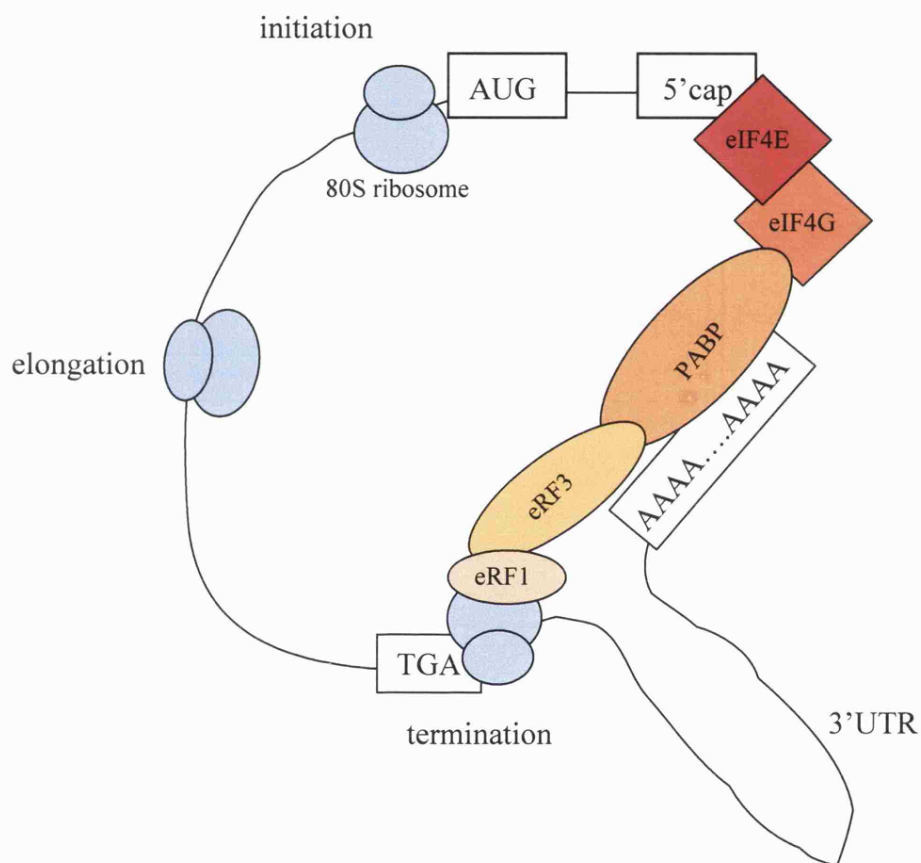
Figure 1.4: Circularisation of mRNA and ribosome recycling
Adapted from Uchida et al, 2002.

17
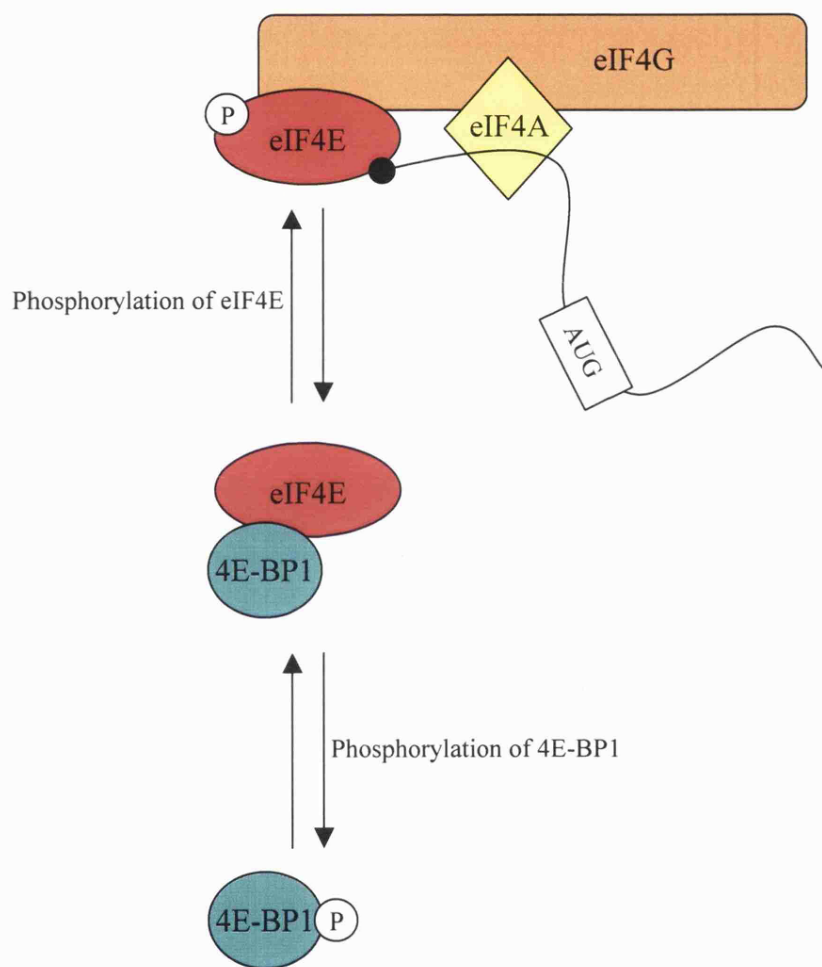
Figure 1.5: Regulation of eIF4F assembly

Early work shows that increases in phosphorylation of eIF4E parallel increases in translation and vice versa (Bonneau and Sonenberg, 1987; Duncan and Hershey, 1989). For example, translation rates are reduced during mitosis and this coincides with a reduction in [^{32}P] labelling of eIF4E (Bonneau and Sonenberg, 1987). Furthermore, in some studies phosphorylated eIF4E has been shown to have higher affinity for eIF4G, cap analogues and capped globin mRNA than non-phosphorylated eIF4E (Bu et al., 1993; Minich et al., 1994). This is supported by structural data, which predicts a salt bridge between phosphorylated Ser209 and Lys159, which would form a clamp around the mRNA 5' cap (Marcotrigiano et al., 1997). However, Duncan *et al*, 1987 commented that phosphorylated eIF4E and non-phosphorylated eIF4E are both active in cap-binding when purified by m7G affinity chromatography. More recently recombinant non-phosphorylated eIF4E and phosphorylated eIF4E have been used to quantify binding of pure eIF4E to the cap structure (Scheper et al., 2002). Scheper *et al*, 2002 showed that phosphorylated eIF4E in fact has lower affinity for the cap than non-phosphorylated eIF4E. In the study it is suggested that the negative charge of the phosphate group creates an electrostatic repulsion from the negative charge of the mRNA (Scheper et al., 2002). In support of this, replacement of Ser209 with acidic residues has the same effect as phosphorylation of Ser209 and reduces the affinity of eIF4E for the cap. Furthermore, they propose that Lys159 is important in binding the cap structure, but most likely through interacting with the phosphate groups of the cap structure and not other eIF4E residues.

In vitro, the mitogen activated protein kinase interacting kinases 1 and 2 (Mnk1 and Mnk2) phosphorylate eIF4E (Fukunaga and Hunter, 1997; Scheper et al., 2001; Waskiewicz et al., 1997). Meanwhile, data has been produced in support of these kinases phosphorylating eIF4E *in vivo*. *In vivo*, constitutively active mutants of Mnk1 and Mnk2 increase eIF4E phosphorylation and expression of kinase-dead forms of Mnk1 decrease eIF4E phosphorylation (Scheper et al., 2001; Waskiewicz et al., 1999). Studies of knockout mice for Mnk1 and Mnk2 suggest that Mnk2 is responsible for maintaining the basal level of eIF4E phosphorylation, while Mnk1 reacts to signals to increase eIF4E phosphorylation (Ueda et al., 2004). This is supported by work that shows Mnk2 has a high level of basal phosphorylation actvity in mammalian cells (Scheper et al., 2001).

Binding sites for Mnk1 and Mnk2 have been identified on the C-terminal region of eIF4G, suggesting that the scaffolding protein congregates eIF4E and its kinases (Pyronnet et al., 1999; Scheper et al., 2001). Interestingly, eIF4E associated with eIF4G is more phosphorylated than free eIF4E (Lamphear and Panniers, 1990; Rau et al., 1996; Tuazon et al., 1990). Furthermore the binding of Mnk1 and Mnk2 to eIF4G is reduced by the stimulation of cells with phorbol ester, which suggests that Mnk interaction with eIF4G can also be regulated (Scheper et al., 2001). Moreover, Mnk1 has been shown to bind p97/DAP5, a protein that shares homology with only the C-terminal region of eIF4G and therefore can potentially act as a translational inhibitor by binding select translation factors such as eIF4A but not eIF4E (Pyronnet et al., 1999). It has been proposed that by binding p97, Mnk1 is sequestered away from eIF4G, thereby decreasing eIF4E phosphorylation.

The function of eIF4E phosphorylation is disputed. Most recently, Mnk1 and Mnk2 knockout mice and double knockout mice have been generated. Although the embryonic fibroblasts and adult tissues from these mice lacked phosphorylated eIF4E, they showed no abnormalities and were fertile (Ueda et al., 2004). Furthermore a S209A mutant of eIF4E can rescue eIF4E-dependent *in vitro* translation systems (McKendrick et al., 2001). This confirms work in 293 cells that showed phosphorylation of eIF4E had no effect on general translation rates or eIF4F assembly (Herbert et al., 2000; Scheper et al., 2001). However, in Drosophila a mutation in the phosphorylatable serine (Ser251) resulted in growth defects (Lachance et al., 2002). Additionally, phosphorylation of Mnk1 and eIF4E is regulated by IL-2 in natural killer cells and expression of a dominant negative form of Mnk1 inhibits Mnk1 phosphorylation and specifically inhibits expression of the transcription factor Ets1 (Grund et al., 2005). Therefore, the precise role of eIF4E phosphorylation is still unknown. It has been suggested that phosphorylation of eIF4E is a requirement for either the fine-tuning of translation or for *de novo* initiation but not for reinitiation (Novoa and Carrasco, 1999). Interestingly, eIF4E has a second function of nucleocytoplasmic transport of growth promoting mRNAs such as cyclin D1 (Cohen et al., 2001; Rousseau et al., 1996; Topisirovic et al., 2003). Decreased eIF4E phosphorylation has been shown to decrease transport of cyclin D1mRNA into the cytoplasm and therefore reduce cyclin D1 protein levels (Topisirovic et al., 2004).

eIF4E-binding proteins (4E-BPs) inhibit formation of eIF4F and therefore inhibit cap-dependent translation (Morley and Pain, 1995; Pause et al., 1994). There are three known 4E-BPs although the majority of work has been carried out on 4E-BP1 also known as PHASI. 4E-BPs share a 49 amino acid binding motif with eIF4G and compete with eIF4G for binding eIF4E (Haghighat et al., 1995; Mader et al., 1995). Consequently, binding of eIF4E by 4E-BP results in the inhibition of eIF4F complex formation. Indeed, removal of this motif from 4E-BP1 abolishes interaction of 4E-BP1 with eIF4E and abolishes translational repression that occurs in *in vitro* translation systems (Haghighat et al., 1995).

The affinity of 4E-BPs for eIF4E is regulated through their phosphorylation (Lin et al., 1994; Pause et al., 1994). Phosphorylation of 4E-BP1 decreases its affinity for eIF4E and leaves eIF4E free to bind eIF4G, potentially leading to an increase in the rate of protein synthesis (Beretta et al., 1996; Brunn et al., 1997; Haghighat et al., 1995; Lin et al., 1994; Pause et al., 1994). However, phosphorylation of 4E-BPs is independent from phosphorylation of eIF4E and is regulated though different signalling pathways (Brunn et al., 1997; Flynn and Proud, 1996; Frederickson et al., 1992; Gingras et al., 1998). 4E-BP1 contains five phosphorylation sites, which differentially regulate 4E-BP1 binding to eIF4E either through influencing phosphorylation of other sites or by directly affecting its binding to eIF4E (Fukunaga and Hunter, 1997; Rau et al., 1996; Waskiewicz et al., 1997).

Interestingly, eIF4E that is bound to 4E-BP1 cannot be phosphorylated by PKC or Mnk1 (Wang et al., 1998b; Whalen et al., 1996). Therefore, it was suggested that eIF4E is activated in two stages. First, 4E-BP1 is phosphorylated to encourage its dissociation from eIF4E, and subsequently, eIF4E is free to be phosphorylated and bind the cap. However, if phosphorylation of eIF4E reduces cap binding, a model has been proposed whereby eIF4E binds to the cap and is then joined by other initiation factors to form eIF4F (Scheper et al., 2001). The formation of eIF4F would bring eIF4G and the associated eIF4E kinases, Mnk1 and Mnk2, therefore allowing eIF4E phosphorylation and dissociation from the cap thus allowing the migration of factors required for mRNA unwinding and scanning.

The phosphorylation of eIF4G may also regulate eIF4F assembly. Phosphorylation of eIF4G has been demonstrated *in vitro* by protein kinase A, protein kinase C and protease-activated kinase II (Tuazon et al., 1989). *In vivo* eIF4G is phosphorylated in response to treatment with EGF or TPA (Donaldson et al., 1991; Morley and Pain, 1995). Three sites have been idenitifed in eIF4GI that are phosphorylated in response to serum (Raught et al., 2000). The role of eIF4G phosphorylation is unknown but increases in eIF4G phosphorylation appear to correlate with increases in eIF4F assembly (Bu et al., 1993). As already mentioned, eIF4G may also regulate translation initiation indirectly through binding PABP and therefore causing circularisation of the mRNA.

Regulation of ternary complex formation (figure 1.6)

The ternary complex consists of eukaryotic initiation factor 2 (eIF2) bound to GTP and Met-tRNAi and its formation relies on the activity of the guanine exchange factor (GEF), eIF2B, which recycles eIF2.GDP to eIF2.GTP. eIF2B activity can be regulated through a number of mechanisms including: allosteric regulation of eIF2B by sugar phosphates, NADH, inositol phosphates and adenine nucleotides (Price and Proud, 1994; Webb and Proud, 1997), inhibition through phosphorylation of eIF2B (Welsh et al., 1998) and competitive inhibition by phosphorylated eIF2 (Clemens et al., 1982; Ramaiah et al., 1994).

eIF2B contains multiple phosphorylation sites, which can regulate its activity (Campbell et al., 1999; Wang et al., 2001). Glycogen synthase kinase 3 (GSK-3) phosphorylates the ε-subunit of eIF2B, which brings about its inactivation (Welsh et al., 1998). Insulin inactivates GSK3, and also results in the dephosphorylation of the ε subunit of eIF2B and activation of eIF2B (Welsh et al., 1998). However, additional mechanisms are required for the activation of eIF2B, as activation does not occur upon the addition of compounds that inhibit GSK-3 and result in the dephosphorylation of eIF2B (Wang et al., 2002).
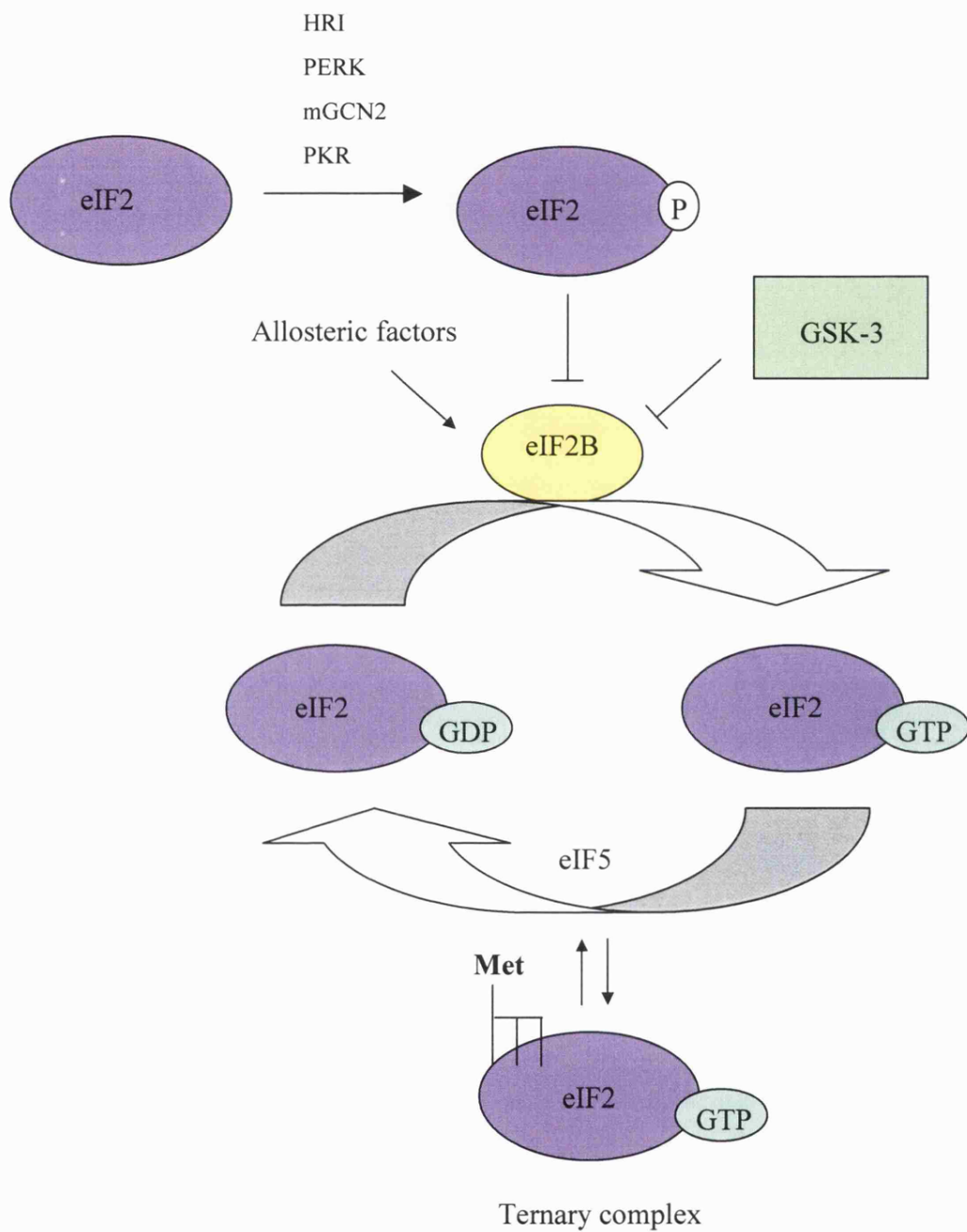
Figure 1.6: Regulation of ternary complex formation

One of the key mechanisms for regulating ternary complex formation and therefore, global translation is through the competitive inhibition of eIF2B by the phosphorylated form of the alpha subunit of eIF2 (eIF2α) (Clemens et al., 1982; Ramaiah et al., 1994). Phosphorylation of serine 51 on the alpha subunit of eIF2 changes it from a substrate to a competitive inhibitor of eIF2B (Colthurst et al., 1987; Dever et al., 1993; Rowlands et al., 1988). Because eIF2 is two to five folds in excess of eIF2B, phosphorylation of only a fraction of eIF2 inhibits eIF2B and can block protein synthesis (Oldfield et al., 1994; Rowlands et al., 1988). Four eIF2α kinases have been identified in mammalian cells: the double stranded RNA-dependent eIF2 kinase (PKR) (Clemens, 1997; Jagus et al., 1999), the mammalian orthologue of yeast GCN2 protein kinase (mGCN2, (Sood et al., 2000; Yang et al., 2000)), the heme-regulated eIF2 kinase (HRI, (Chen et al., 1994)) and the PKR-like endoplasmic reticulum kinase (PERK/PEK, (Harding et al., 2000b; Harding et al., 2000c; Harding et al., 1999)). Each of the eIF2 kinases responds to different physiological stimuli. For example, PERK plays a role in regulating global translation in conditions of ER stress (Harding et al., 2000b; Harding et al., 2000c; Harding et al., 1999).

Two regulatory subunits of protein phosphatase I are known to mediate eIF2α dephosphorylation. These are the constituitively active CreP, which maintains basal phosphorylation of eIF2α and GADD34 (growth Arrest and DNA Damage inducible protein), which is up-regulated in conditions of cell stress (Jousse et al., 2003; Kojima et al., 2003; Lu et al., 2004b). The up-regulation of GADD34 takes a few hours and acts to stimulate the recovery of protein synthesis after high phosphorylation of eIF2α.

1.2: Gene specific regulation of initiation of translation

Sequences within specific mRNAs can affect their translation. In particular, secondary structures such as stem loops or pseudoknots in the 5'-untranslated region of the mRNA act to inhibit translation (Kozak, 1986a; Kozak, 1989a; Vega Laso et al., 1993), possibly by inhibiting eIF4E from interacting with other initiation factors (Lawson et al., 1986; Lee et al., 1983; Muckenthaler et al., 1998).

Alternatively, sequences within the mRNA may serve as sites for attachment of trans-acting factors. For example, binding of pyrimidine-tract binding protein (PTB) and upstream of n-ras (unr) binding protein to specific binding sites within the mRNA have been shown to increase/decrease translation (Hunt et al., 1999; Kaminski and Jackson, 1998). Furthermore, in *C.elegans*, small non-coding RNAs *lin-4* and *let-7* bind complementary sequences in the 3'UTR of the target mRNAs, thereby inhibiting translation (Banerjee and Slack, 2002).

The untranslated regions of mRNA have been shown to be important in the regulation of protein synthesis. Indeed, recombinant techniques in which the 3' and/or 5' UTRs are altered or exchanged or removed and then transfected into cells in culture shows that regulatory elements are present in the untranslated regions of a number of mRNAs (Wicksteed et al., 2001). The 5' UTR is often important in regulating translation, while the 3' UTR can be from 100s to 1000s of bases and has a wide range of functions including the regulation of polyadenylation, translocation and the stability and localisation of mRNA by interaction with trans-acting proteins (Kozak, 1992).

A large number of mRNAs have been shown to contain sequences complementary to both 18S and 28S rRNA (Mauro and Edelman, 1997). It has been proposed that the ribosome may influence translation through binding mRNAs and either enhancing translation due to increased recruitment of ribosome or inhibiting translation by sequestering mRNAs from the required initiation factors (Mauro and Edelman, 1997).

Changes in the general translational machinery can also regulate gene-specific protein synthesis. Regulation of gene-specific protein synthesis was first proposed by Lodish

(Lodish, 1976; Lodish et al., 1976; Lodish and Small, 1976). It was demonstrated that the α and β-globin mRNAs are translated at different rates due to less efficient initiation on the α-globin mRNA. It has been proposed that this is due to increased sensitivity to changes in translation initiation efficiency by the weaker α-globin mRNA. Indeed, recently it has been shown that certain cap analogues with reduced affinities for eIF4E have reduced translation efficiencies *in vitro* (Niedzwiecka et al., 2002), this supports the theory that access to the cap structure may affect the translation efficiencies of different mRNAs.

Although eIF4E phosphorylation does not appear to play an essential role in mammalian cells, it has been speculated that eIF4E phosphorylation may play a role in the fine-tuning of translation and regulate the translation of a specific subset of mRNAs (Ueda et al., 2004). Phosphorylation of eIF4E has been shown to increase translation of mRNAs with a large amount of secondary structure (Koromilas et al., 1992; Manzella et al., 1991). In support of this Tuxworth et al., 2004 show that overexpression of Mnk1 results in increased translation of a reporter mRNA which has a large amount of 5' secondary structure. Furthermore, Mnk1 phosphorylation of eIF4E is essential for viral gene expression and herpes simplex virus replication in quiescent cells (Walsh and Mohr, 2004).

Certain mRNAs are preferentially translated under stress-induced conditions when eIF2 is phosphorylated. The most characterised of these is the mRNA for general control non-derepressible 4 (GCN4) in yeast, which is translated in response to amino acid deprivation resulting in GCN2 phosphorylation of eIF2 (Hinnebusch, 2000). GCN4 mRNA contains four upstream open reading frames (uORFs) in its 5'UTR. Under non-stressed conditions, the ribosome initiates at the 5' proximal uORF and once this peptide is synthesised, the ribosome remains associated with the mRNA and reinitiates at inhibitory ORF 2, 3 or 4 which continue into the coding region of GCN4, therefore inhibiting translation of the coding region. In stressed conditions, when ternary complex availability is low there is a delay in reinitiation that allows the ribosome to by-pass the inhibitory uORFs and initiate at the initiation codon for GCN4.

In mammals it has been demonstrated that translation of transcription factor, ATF4 mRNA is up-regulated in response to a decrease in the formation of the ternary complex (Harding et al., 2000b). Recently, the 5' UTR of ATF4 has been shown to contain two uORFs (Harding et al., 2000b). uORF1 stimulates translation of ATF4 in stressed cells and uORF2 inhibits translation of ATF4 in non-stressed cells in a similar manner to the inhibition of GCN4 translation by uORF 2 to 4 (Vattem and Wek, 2004). When ternary complex availability is low, the delay in reinitiation allows the ribosome to by-pass the initiation codon for uORF2 and translates the coding region for ATF4.

1.3: Protein Targeting and Translocation at the Endoplasmic Reticulum Membrane

1.3.1: Overview of SRP-dependent protein targeting

Secretory pathway mRNAs are recruited from a cytoplasmic pool to the rough endoplasmic reticulum (ER) in order to ensure polypeptide translocation across the ER and entry into the secretory pathway (Palade, 1975). Polypeptides can be targeted to the ER by two distinct pathways, the post-translational pathway or the co-translational pathway. However, the majority of eukaryotic secretory proteins are co-translationally targeted to the ER (reviewed in (Keenan et al., 2001)). Here, protein synthesis is coupled to the targeting and translocation of the nascent polypeptide chain to the ER. This has the advantage of preventing the mis-folding of the nascent chain in the cytosol. Recruitment of secretory proteins to the ER can be separated into two biochemically distinct processes: targeting to the ER and translocation through the membrane (Nicchitta et al., 1991). Secretory proteins are targeted to the ER due to a hydrophobic N-terminal signal sequence. Once the signal sequence has emerged from the ribosome it is recognised and bound by the signal recognition particle (SRP) (figure 1.7), which induces elongation arrest (Walter and Blobel, 1981). SRP then targets the ribosome-nascent chain complex to the ER by binding to the SRP receptor (SR), a heterodimeric integral ER protein. The SR then catalyses the transfer of the ribosome nascent chain complex from SRP to the translocon of the ER. The polypeptide chain is inserted into the translocon and translation resumes with the polypeptide chain being synthesised into the lumen of the ER.

1.3.2: Structure of Signal Recognition Particle (SRP) and the SRP Receptor

SRP is an evolutionarily conserved ribonucleoprotein particle. It is an elongated rod-like structure divided into two domains: the S and Alu domains (Gundelfinger et al., 1983). The S domain binds to the signal sequence of the nascent polypeptide chain (Krieg et al., 1986; Kurzchalia et al., 1986) and interacts with the SRP receptor (Connolly et al., 1991), while the Alu domain mediates elongation arrest (Siegel and Walter, 1988). Mammalian SRP consists of a 300-nucleotide 7S backbone RNA
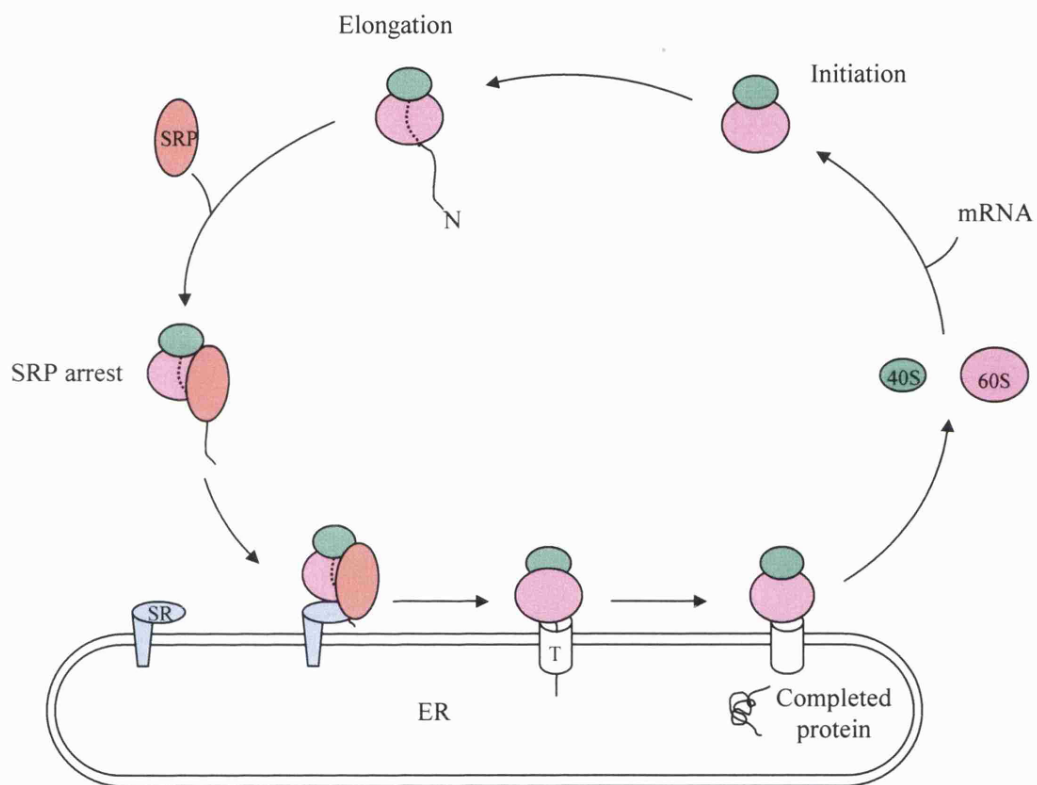
Figure 1.7: SRP-dependent targeting to the ER
Adapted from Keenan et al,. 2001.

molecule onto which the six SRP polypeptides (SRP72, SRP68, SRP54, SRP19, SRP14 and SRP9) assemble (figure 1.8) (Walter and Blobel, 1980; Walter and Blobel, 1982).

The S domain of SRP comprises of helices 6-8 and part of helix 5 of the 7S RNA and SRP19, SRP54, SRP68 and SRP72 (Siegel and Walter, 1988). The SRP68-SRP72 heterodimer binds to the central region of SRP RNA through SRP68 and functions as a brace connecting the Alu and S domains (Halic et al., 2004; Lutcke et al., 1993; Siegel and Walter, 1988). SRP19 holds the S domain together by binding to the apices of helices 6 and 8 of SRP RNA and is required for the binding of SRP54 to 7S RNA (Hainzl et al., 2002; Oubridge et al., 2002; Siegel and Walter, 1988). The SRP core is the only part common to all SRPs and is the most structurally conserved and functionally significant part of SRP. It consists of SRP54 bound to helix 8 of 7S (Bernstein et al., 1989; Poritz et al., 1990; Siegel and Walter, 1988). SRP54 consists of three domains, an N terminal four-helix bundle domain (N), a central GTPase domain (G) and a methionine-rich C terminal domain (M) (Walter and Johnson, 1994). The N domain packs against the G domain to form a connected NG domain (Freymann et al., 1997; Montoya et al., 2000). The NG domain is then connected to the M domain by a protease-sensitive flexible hinge (Lutcke et al., 1992; Zheng and Gierasch, 1997). The M domain anchors SRP54 to 7S RNA and binds to the signal sequence (Batey et al., 2000).

The Alu domain of SRP comprises of an SRP9-SRP14 heterodimer bound to the 5' and 3' ends of 7S RNA with two branched helices 3 and 4 (Poritz et al., 1988; Siegel and Walter, 1988). The 3-dimensional structure of SRP9/14 heterodimer shows a symmetrical complex with the two proteins adopting the same fold despite the large differences in their primary sequences (Birse et al., 1997). Removal of the Alu domain or the protein SRP9/14 heterodimer abrogates the elongation arrest activity of the particle (Siegel and Walter, 1986; Siegel and Walter, 1988).

The SRP receptor is a heterodimeric integral ER membrane protein composed of the alpha and beta subunits (Tajima et al., 1986). The beta subunit contains a single N terminal transmembrane domain and anchors the alpha subunit onto the endoplasmic reticulum by interacting with the amino terminus of SRα (Miller et al., 1995; Young et al., 1995). After the amino terminus of SRα is synthesised, a translational pause site on
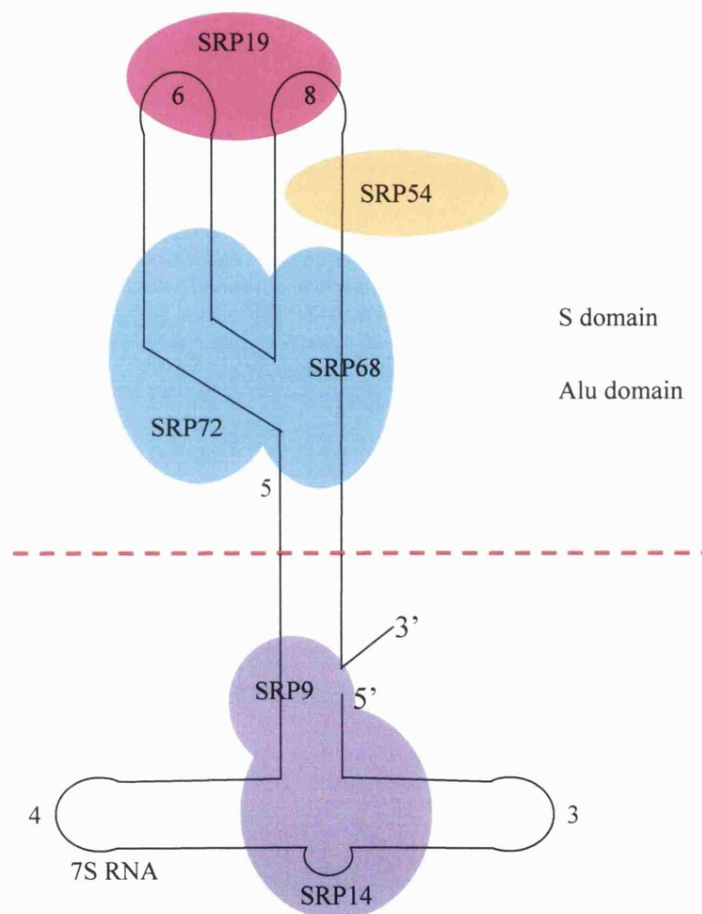
Figure 1.8: Schematic representation of mammalian SRP
SRP is made up of the S domain and the Alu domain. The S domain
contains helices 6-8 and part of helix 5 of the 7S RNA (numbered on
figure) and the protein subunits: SRP19, SRP54, SRP68 and SRP72.
The Alu domain contains helices 3 and 4 with the protein subunits
SRP9 and SRP14 bound to the 5' and 3' ends of the 7S RNA.
Adapted from Nagai et al,. 2003.

SRα mRNA allows the amino terminus to fold and interact with SRβ before translation of SRα is completed, thereby allowing efficient targeting of SRα to the ER (Young and Andrews, 1996). A yeast deletion of SRβ's transmembrane domain dramatically reduces binding of SR to the ER (Ogg et al., 1998). However, this deletion does not affect dimerisation or function of the SRP receptor, suggesting that SRβ interacts with other proteins of the ER (Ogg et al., 1998).

Both the SRα and SRβ domains contain GTP binding domains (Connolly and Gilmore, 1989; Miller et al., 1995). The GTP binding domain of SRα is closely related to that of the GTP binding domain in SRP54 and has a similar low affinity for the nucleotide (Bacher et al., 1999; Rapiejko and Gilmore, 1997). However, the GTP binding domain of SRβ belongs to the Ras superfamily of GTPases and has a much higher affinity for GTP (20nM) than the SRP-type GTPase domains (Bacher et al., 1999; Hattori et al., 1985).

1.3.3: SRP Binding to the Ribosome and Signal Sequence

SRP can associate with the ribosome in the absence or presence of a signal sequence (Ogg and Walter, 1995). Recently cross-linking and structure studies in bacteria have identified that SRP associates with ribosomal proteins L23a and L35 through the N domain of SRP54 in the absence and presence of a signal sequence (Halic et al., 2004; Pool et al., 2002). These proteins are located on the large ribosomal subunit close to the exit site from which the nascent chain emerges, which allows SRP54 to sample the emerging nascent chain for the presence of a signal sequence. In bacteria, further connections between SRP and the ribosome have been shown between the N-terminal and C-terminal regions of SRP54 M domain and 25S rRNA (Halic et al., 2004). An additional connection has been predicted between SRP RNA and 25S RNA and rpL16 (Halic et al., 2004).

Recently Flanagan and colleagues have used competitive binding experiments to show that SRP can distinguish between translating (K_D 8nM) and non-translating ribosomes (K_D=71nM) (Flanagan et al., 2003). This means that SRP will preferentially bind translating ribosomes over non-translating ribosomes (Flanagan et al., 2003). These K_D

values and therefore the preference exist before the nascent chain has emerged from the ribosome. Therefore it is most likely that SRP identifies a translating ribosome through a ribosomal conformational change and not through interaction with the nascent chain.

In eukaryotes the signal sequence is a continuous stretch of 6-20 N-terminal hydrophobic amino acids that form an alpha helical conformation (Valent et al., 1995). One or two basic residues often flank the hydrophobic amino acids (Lee and Bernstein, 2001). Once the signal peptide emerges from the ribosome the affinity of SRP for the ribosome increases to a K_D of 0.05 – 0.38nM (Flanagan et al., 2003). It is likely that the ribosome plays an important role in signal sequence recognition as SRP will not bind signal sequences of nascent chains that have been released from the ribosome (Garcia and Walter, 1988; Wiedmann et al., 1987).

The signal peptide binds into the hydrophobic groove of the M domain of SRP54 (Romisch et al., 1990; Zopf et al., 1990). However, crosslinking studies show that the M domain of SRP54 binds the signal sequence with a lower affinity than whole SRP54 protein, suggesting that the NG domain is also important in signal sequence binding (Zopf et al., 1993). This is supported by results that show alkylation of cysteine residues in the NG domain of SRP54 hinders the binding of the signal sequence (Lutcke et al., 1992; Siegel and Walter, 1988). The N domain of SRP54 may aid binding to the signal sequence through its ALLEADV motif (Newitt and Bernstein, 1997).

1.3.4: Elongation Arrest

Upon binding of SRP to the signal sequence, translation elongation is slowed down (Lipp et al., 1987). However, all elongation arrest studies to date have been carried out *in vitro*. In the wheatgerm system elongation arrest by canine SRP was observed as a complete halt (Walter and Blobel, 1981), but in the rabbit reticulocyte lysate, canine SRP only slows elongation (Wolin and Walter, 1989). In all cases, elongation arrest-deficient systems lacked efficient transfer of ribosome-nascent chain complexes to the ER lumen, suggesting that elongation arrest is important for full SRP function (Hauser et al., 1995; Mason et al., 2000; Siegel and Walter, 1985; Siegel and Walter, 1986; Thomas et al., 1997).

So far the mechanism of elongation arrest remains to be elucidated, although it is known that elongation arrest requires the Alu domain of SRP (Siegel and Walter, 1986). Initially, it was suggested that the Alu domain of SRP may slow elongation through binding the A site of the ribosome and mimicking tRNA (Walter and Johnson, 1994; Zwieb, 1985). However, structural studies later showed that the Alu domain was not significantly similar to tRNA (Weichenrieder et al., 2000). Mutational analysis of SRP14 revealed that the C terminal region of SRP14 is essential for elongation arrest activity but is not required for SRP9/14 binding to the ribosome, therefore, this mutant likely represents an exclusive elongation arrest specific SRP-ribosome interaction (Hauser et al., 1995; Mason et al., 2000; Powers and Walter, 1996; Thomas et al., 1997; Wolin and Walter, 1989).

Recent cross-linking data shows that in the absence of a signal sequence, SRP14 cross-links with a large ribosomal subunit protein (Terzi et al., 2004). Once the signal sequence has emerged, further cross-linking products become detectable suggesting a change in the interface between the Alu domain and the ribosome (Terzi et al., 2004). Since SRP14 can be cross-linked to small and large ribosomal subunit proteins, the Alu domain of SRP is probably located at the ribosomal subunit interface (Terzi et al., 2004). Indeed, structural data shows that the Alu domain fits tightly into the 65Å gap between the large and small ribosomal subunits (Halic et al., 2004). Furthermore, all of the ribosome points contacted by Alu are well conserved in ribosomes across all species and also make up the elongation-factor-binding site. This has led to the suggestion that upon signal sequence emergence, a conformational change in the S domain of SRP results in the Alu domain closing into the elongation factor-binding site of the ribosome thus preventing elongation factors from binding, inhibiting elongation and therefore causing elongation arrest (Halic et al., 2004).

1.3.5: Targeting to the ER

Once SRP has bound to the ribosome nascent chain complex (RNC), the SRP-RNC complex is targeted to the SRP receptor (SR) on the surface of the ER (Meyer et al., 1982; Rapiejko and Gilmore, 1992).

Site-directed mutagenesis studies suggest that signal sequence binding to SRP54 and interaction of SRα with membrane components cause a conformational change across the interface of the N and G domains (NG domain) of SRP54 and SRα respectively (Lu et al., 2001). These interactions most likely occur directly through the N domain and 'prime' SRP54 and SRα for binding each other (Lu et al., 2001). Indeed, interaction of SRP54 and SRα appears to be through their NG domains (Bernstein et al., 1989; Rapiejko and Gilmore, 1992; Zopf et al., 1993). Priming of SRP and SRα would also act as a control mechanism to prevent them associating with each other in the absence of a signal sequence and the necessary membrane components.

SRP, SRα and SRβ are GTP binding proteins and undergo GTP cycles that ensures the targeting of the ribosome nascent chain complex to the ER is a unidirectional process (figure 1.9). However, both the translocon and GTP are dispensable for the initial targeting of the SRP-RNC to the SRP receptor (Rapiejko and Gilmore, 1994; Song et al., 2000) and both free SRP and free SRα have surprisingly low affinities for GTP (Miller et al., 1993; Rapiejko and Gilmore, 1997). Therefore it was proposed that prior to SRP-RNC-SR complex formation both the GTP binding sites in SRP54 and SRα are in their 'empty site' conformation (Rapiejko and Gilmore, 1994; Rapiejko and Gilmore, 1997). The unusual stable empty state of SRP54 is explained by structural data of the prokaryotic homologues of SRP54 and SRα, Ffh (fifty-fourth homologue) and FtsY respectively (Freymann et al., 1997; Freymann et al., 1999; Montoya et al., 1997).

Upon binding of the SRP-RNC complex to SRα, the affinity of both SRP54 and SRα for GTP is increased and they both bind GTP (Rapiejko and Gilmore, 1997). In support of this, upon binding SRP, FtsY increases its specificity for guanine-containing nucleotides and allows GTP to bind tightly (Shan and Walter, 2003). It has been suggested that when SRP interacts with SRα the GTPases undergo a conformational change from an open state, where the affinity and specificity for GTP is low, to a closed state where the affinity and specificity for GTP is high (Rapiejko and Gilmore, 1997). This is supported by biochemical data that shows the active site of FtsY and Ffh only associate with the γ-phosphate of GTP when associated with each other (Peluso et al., 2001). Furthermore, it has been shown that nucleotide binding and SRP binding to FtsY causes a reversible conformational change in FtsY (Jagath et al., 2000).
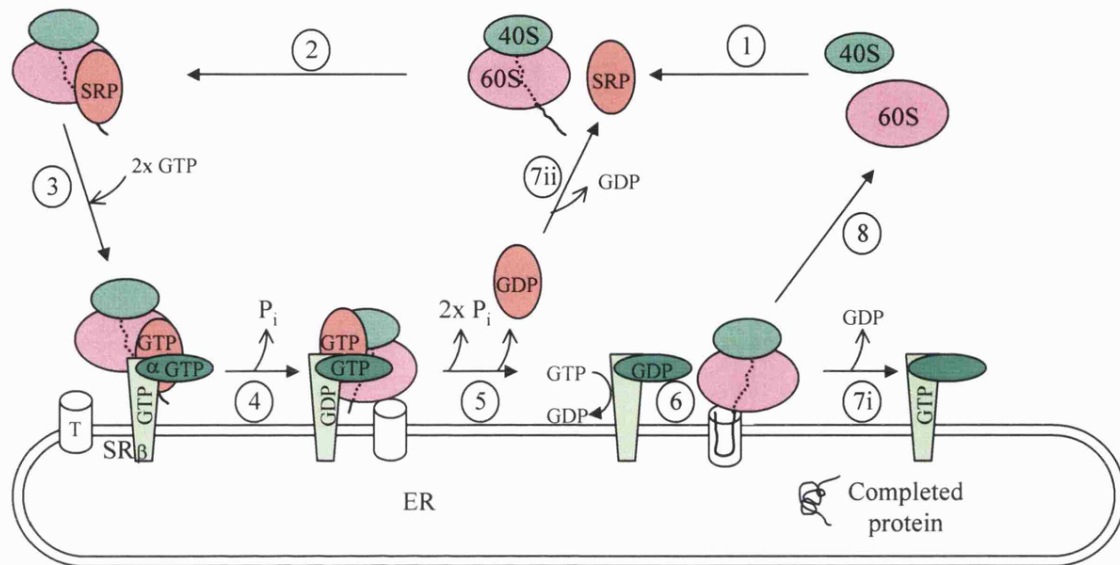
Figure 1.9: GTP cycles at the ER

The 40S and 60S ribosomal subunits initiate and begin protein synthesis on an mRNA encoding a secretory protein (1). The emerging signal sequence is recognised and bound by SRP, which is in its empty state conformation (i.e. not bound to GTP nor GDP) (2). SRP then targets the ribosome nascent chain complex to the SRP receptor (SR) on the ER (3). Before binding the ER both SRα and SRP are in their empty state conformations and SRβ is bound to GTP. Upon binding of SRP-RNC to the SR, both SRP54 and SRα bind GTP. The RNC is transferred to the translocon while SRP54, SRα and SRβ are bound to GTP (4). Upon targeting of the RNC to the translocon (4), GTP bound to SRβ is hydrolysed, possibly by the ribosome acting as a GAP. SRP54 and SRα act as GAPs for each other to hydrolyse GTP (5). Hydrolysis of GTP associated with SRP54 and SRα reduces their affinity for each other and SRP dissociates from the SR. It has then been proposed that the translocon acts as a GEF for SRβ, resulting in full transfer of the RNC to the translocon (6). Once SRα and SRP have dissociated, GDP is released leaving them in their empty state conformation, ready to start a new round of targeting (7i and 7ii). Meanwhile, the completion of protein synthesis results in the availability of the 40S and 60S ribosomal subunits for further rounds of initiation (8). Adapted from Keenan et al,. 2001.

36

It has been suggested that the ribosome makes the first point of contact with SRβ and this allows SRα to scan the RNC for SRP. The dual involvement of SR with the ribosome and with SRP ensures that complexes containing both RNC and SRP are targeted to the ER. In fact, the affinity of SRP for the SRP receptor (SR) is surprisingly low at a Kd of 125nM in physiological ionic strength buffers (Connolly and Gilmore, 1993). The ribosome has a 100 fold higher affinity for the SR than SRP; however, it also has a faster dissociation rate for the SR than SRP (Mandon et al., 2003). It has been proposed that the SR recognise both the ribosome and SRP but maintains its fidelity through rejecting ribosomes that lack bound SRP.

The precise orders of events for transfer of the RNC from the SR to the translocon are unknown. However, it is known that transfer of the RNC to the translocon requires SRP54, SRα and SRβ in GTP-bound states and the presence of an available translocon. (Fulga et al., 2001; Rapiejko and Gilmore, 1997; Song et al., 2000). Furthermore, GTP hydrolysis does not appear to be required for transfer of the nascent chain to the translocon (Song et al., 2000).

In eukaryotes SRα forms a heterodimer with SRβ, which anchors SRα to the ER membrane primarily through its transmembrane domain (Miller et al., 1993; Ogg et al., 1998). Recent work has shown that SRβ and SRα will only stably bind when SRβ is bound to GTP (Legate and Andrews, 2003; Ogg et al., 1998; Schwartz and Blobel, 2003). After targeting of the RNC to the translocon, SRβ is bound to GDP and SRα will only re-associate with SRβ when the GDP of SRβ is exchanged for GTP by a guanidine exchange factor. Recently, it has been shown in yeast that subunits of the translocon act as GEFs for SRβ (Helmers et al., 2003). It has been proposed that when the translocon is occupied by an active translating ribosome these β-subunits are inaccessible to SRβ and therefore targeting of a nascent chain complex to this particular SR and 'busy' translocon is blocked.

The GTP binding site of SRβ but not the transmembrane domain is essential for SR function (Ogg et al., 1998), however, the precise timing of the SRβ GTPase cycle is unknown and many models have been proposed. Purified SRβ has been found to have a

high affinity for GTP, however the effect of the ribosome on the nucleotide binding of SRβ is disputed. Work from the Dobberstein and Pool laboratories suggests that the ribosome bound to SRβ-GTP acts as a GTPase-activating protein (GAP) (Bacher et al., 1999; Fulga et al., 2001). Once GTP is hydrolysed, SRβ's affinity for guanine nucleotide drops and the ribosome stabilises SRβ in the GDP/free state (Bacher et al., 1999; Fulga et al., 2001). They suggest that the subsequent binding of the ribosome to an available translocon would allow GTP to re-bind SRβ, which is consistent with data from Helmer et al, 2003 that suggests the translocon act as a GEF for SRβ. Fulga et al, 2001 then suggest that the re-binding of GTP to SRβ results in the release of the signal peptide from SR-SRP and full transfer of the ribosome nascent chain complex to the translocon. However, as mentioned above the hydrolysis of GTP by the ribosome would result in the dissociation of SRα and SRβ (Schwartz and Blobel, 2003). Furthermore, it has been reported that the ribosome does not stimulate the GTPase activity of SRβ (Helmers et al., 2003; Legate and Andrews, 2003). Therefore the main discrepancy in the data so far is the ribosome's role in the binding and hydrolysis of GTP associated with SRβ. This will need to be elucidated before the precise sequence of events for nascent chain transfer to the translocon can be known.

After the nascent chain is transferred to the translocon, SRP and the SRP receptor act as GTPase activating proteins (GAPs) for each other and reciprocally stimulate each others GTPases to hydrolyse GTP (Powers and Walter, 1995). The hydrolysis of GTP results in the dissociation of SRP from SRα (Connolly et al., 1991). After hydrolysis of GTP, GDP is exchanged for GTP (Connolly et al., 1991). Most other GTPases use a separate nucleotide exchange factor. However, SRP GTPases have a low affinity for GTP *in vitro* and are unusually stable in their empty state (Rapiejko and Gilmore, 1997). Moser *et al*, 1997 suggested that SRP54 and SRα contain their own GTPase exchange factor activity, possible through the insertion box domain (IBD) of the G domain of SRP54 or SRα. More recently it has been shown that Ffh contains other structural features that could allow it to cause nucleotide release in the absence of a nucleotide exchange factor (Freymann et al., 1999).

1.3.6: Structure of the translocon

The translocon is the aqueous pore responsible for the trafficking of nascent chains into the lumen of the ER (Simon and Blobel, 1991). The core components of the eukaryotic ER translocon are the Sec61 complex comprising of the α, β and γ subunits and the translocating-chain-associating membrane (TRAM) protein (Gorlich et al., 1992). The Sec61α subunit is a 40kDa protein with 10 transmembrane domains and is the major component forming the aqueous pore through which the nascent chain is transported into the lumen of the ER (Gorlich et al., 1992; Gorlich and Rapoport, 1993; Mothes et al., 1994; Wilkinson et al., 1996). The 12kDa β-subunit spans the membrane, facilitates co-translational translocation of the nascent chain across the ER and is thought to interact with signal peptidase at the ER translocation site (Kalies et al., 1998). The γ subunit of Sec61 is a 10kDa protein and like the β subunit has one transmembrane domain at its carboxyl terminus (Gorlich et al., 1992; Gorlich and Rapoport, 1993). Although the function of the γ subunit is unknown, the yeast homologue has been shown to be essential for protein translocation *in vivo* (Esnault et al., 1993).

Initial structural data used electron microscopy to show that the ribosome induces 3-4 mammalian and yeast Sec61 complexes to come together to form cylindrical oligomers with a diameter of 85Å and an average central pore size of 20Å (Hanein et al., 1996). Hanein *et al*, 1996 proposed that this central pore provided the hydrophilic environment for the translocation of the nascent chain. The same ring structures have been observed for the bacterial homologue of Sec61, SecY/E (Meyer et al., 1999). Three-dimensional mapping of two-dimensional crystals of the SecY showed the SecY complex existed as a dimer, with the pore at its centre (Breyton et al., 2002). However, biochemical analysis suggested that the SecY complex is fully functional as a monomer (Yahr and Wickner, 2000). Recently Van den Berg *et al*, 2004 showed the X-ray structure of the *Methanococcus* SecY complex. This data supports the theory of a single SecY/Sec61 complex and shows that the pore is formed by 10 transmembrane segments, made up from the α subunit with the β and γ subunits located on the periphery of the α subunit. Van den Berg *et al*, 2004 agreed that the SecY complex may oligomerize but that only one SecY monomer would function in protein translocation. The reason for this oligomerization therefore remains unknown.

The size of the translocon pore was further investigated by Hamman et al., 1997 who incorporated fluorescent probes into a nascent chain and then determined the size of the pore by introducing quenching agents of different sizes. This study suggested that the pore was in fact 40-60Å in diameter, making it the largest pore observed in any impermeable membrane and contradicting Hanein et al., 1996 who suggested that the pore was 20Å in diameter. (Hamman et al., 1997). The differences in pore size between the two experiments could be explained by the difference between closed and open pores as those in the second study were translocating a nascent chain (Hanein et al., 1996).

1.3.7: Binding of the RNC to the translocon

It is still relatively unknown as to which translocon subunits that the ribosome actually binds. Both the α and γ subunits of Sec61 are essential for yeast viability, however a yeast mutant lacking Sec61β is still viable (Deshaies and Schekman, 1987; Esnault et al., 1993; Esnault et al., 1994; Finke et al., 1996). Kalies *et al*, 1994 and 1998 showed that the Sec61α but not β subunits are protected from proteolytic digest by the bound ribosome and that the β subunit is not necessary for ribosome binding to the translocon. Furthermore limited proteolysis of Sec61α has suggested which domains of Sec61α are involved in binding the ribosome (Raden et al., 2000). This all suggests that the α but not the β subunits are bound by the ribosome. Work has also shown that the ribosome will bind the β subunit *in vitro* (Levy et al., 2001) and although the β subunit of the translocon is not necessary for translocation, in the absence of Sec61β, translocation occurs at a much slower rate (Kalies et al., 1998). Therefore, the β subunit of the translocon probably facilitates quick and efficient insertion of the nascent chain into the translocon,

It has been shown that both translating and non-translating ribosomes bind the Sec61 complex (Gorlich et al., 1992; Kalies et al., 1994). However, binding of non-translating ribosomes does not inhibit SRP-targeted RNCs from binding to the translocon (Murphy et al., 1997; Neuhof et al., 1998). Furthermore, non-translating ribosomes can be distinguished from translating ribosomes by removal with high salt concentrations;

whereas, translating ribosomes require the addition of puromycin as well as high salt concentrations to cause premature termination and release of the nascent chain (Adelman et al., 1973; Jungnickel and Rapoport, 1995).

Beckman *et al* showed that the exit tunnel of the ribosome is aligned over the opening of the protein-conducting channel, perhaps to allow direct entry of the nascent chain into the translocon (Beckmann et al., 1997). Indeed, after targeting of the RNC to the ER, the ribosome binds the translocon through four connections. In mammals, these connections are via the large ribosomal subunit 28S rRNA and ribosomal proteins L19, L23 (L25 in yeast), L26 and L35 and similar connections have been observed in yeast (Beckmann et al., 1997; Menetret et al., 2000; Morgan et al., 2002; Prinz et al., 2000). The L23 and L35 proteins also bind SRP54, therefore SRP and Sec61 binding sites may be alike and indeed SRP inhibits RNC binding to the translocon in the absence of an SRP receptor (Hauser et al., 1995; Jungnickel and Rapoport, 1995).

In addition to the ribosome, the signal sequence has been implicated in regulating RNC binding to the ER. The signal sequence most probably acts as the second ligand to bind the Sec61 complex, as secretory protein RNC complexes but not cytoplasmic RNCs will bind partially digested Sec61 complexes that non-translating ribosomes will not bind (Raden et al., 2000). Indeed, in the absence of SRP and SR, RNCs with a wild type but not a mutant signal sequence will bind to Sec61p and efficiently translocate the nascent chain suggesting that a component of the ER does bind and discriminate genuine signal sequences (Jungnickel and Rapoport, 1995). Furthermore, photo-crosslinking analysis in yeast suggests that the signal sequence associates with transmembrane helices two and seven of the Sec61 complex and this is confirmed by X-ray structure analysis of the translocon (Plath et al., 1998; Van den Berg et al., 2004).

1.3.8: Gating of the translocon

Gating of the ER translocation channel is required to maintain the permeability barrier across the ER and preserve gradients established across it, in particular that of Ca^{2+}. It was initially believed that the permeability barrier is maintained through the tight binding of the ribosome on the cytoplasmic side and the binding of BiP on the lumenal side of the ER. Early work showed that prior to the ribosome forming a tight seal with

the translocon, the luminal side is sealed by nucleotide-dependent binding of BiP (also known as immunoglobulin heavy chain-binding protein) (Hamman et al., 1998). Meanwhile, the ribosome nascent chain complex initially forms a weak binding to the translocon until substrate-specific N-terminal signal sequences determine tight binding of the ribosome to the Sec61 complex (Crowley et al., 1994; Crowley et al., 1993; Gorlich et al., 1992; Rutkowski et al., 2001). The tightly bound ribosome maintains the permeability barrier on the cytosolic side of the ER as well as ensuring direct transport of the nascent chain into the membrane channel of the ER (Crowley et al., 1993). After tight binding of the ribosome, insertion of the signal sequence into the aqueous pore causes the pore to undergo a conformational change and increase its diameter (Crowley et al., 1993; Hamman et al., 1998). Once the nascent chain reaches approximately 70 amino acids BiP dissociates from the translocon and the luminal side of the translocon opens (Crowley et al., 1994; Hamman et al., 1998).

Interestingly, structural studies have shown that there is a 10-20Å gap between the ribosome and the translocon, contradicting work suggesting that the ribosome acts as a permeability barrier (Beckmann et al., 1997; Menetret et al., 2000; Morgan et al., 2002; Prinz et al., 2000). They propose that the pore itself narrows and closes in the absence of a nascent chain (Morgan et al., 2002) and indeed recent X-ray crystallography has confirmed this (Van den Berg et al., 2004).

Van den Berg et al., 2004 demonstrated that the translocon pore is funnel shaped with a narrow constriction in the centre of the membrane, widening at the edges. This narrowing was found to consist of six hydrophobic residues, which could form a gasket-like seal around the translocating polypeptide chain. It was suggested that the transmembrane segments of the α subunit could shift and allow the pore to open and allow larger amino acid residues and possibly alpha helices through the translocon. Part of transmembrane segment 2 from the α subunit (TM2a) was found to be a short distorted helix that filled half of the pore on the non-cytoplasmic side of SecY. It was proposed that this helix acts as a plug maintaining the permeability barrier until the bound signal sequence binds TM2 and TM7 of Sec61α, which destabilises the plug, moving it out of the centre of the pore. Once the polypeptide chain is fully translocated into the ER lumen the plug can return to its position in the centre of the pore.

The earlier theories of a tight ribosome-membrane junction are therefore contradicted by the more recent structural data that suggests there is a gap between the ribosome and membrane. However, it should be noted that Van den Berg's X-ray crystal structure was in the absence of a RNC and therefore was most likely in the closed state (Van den Berg et al., 2004). Therefore this issue still remains to be resolved.

1.3.9: Ribosome Detachment from the ER

The logical extension of the SRP hypothesis was that following nascent chain release into the ER lumen, the ribosomal subunits dissociated from the ER so as to be available for the next round of initiation. However, run-off *in situ* translation experiments demonstrated that while the small ribosomal subunit dissociates from the ER, the large ribosomal subunit remains bound to the translocon (Potter and Nicchitta, 2002; Seiser and Nicchitta, 2000). Follow-up work showed that the ER-associated 60S ribosomal subunits were able to participate in *de novo* initiation of both cytosolic and secretory proteins by binding to 48S initiation complexes presumably formed in the cytosol (Potter and Nicchitta, 2002). However, while secretory proteins were targeted to the translocon in an SRP-independent manner, cytosolic RNCs detached from the ER (Potter and Nicchitta, 2002). It was therefore proposed that the 60S ribosomal subunit has a high affinity for the membrane but upon commencement of translation this affinity decreases. The signal sequence is then required for anchorage of the RNC to the ER and in the absence of this, the RNC dissociates (Potter et al., 2001).

1.3.10: Differential regulation of protein targeting and translocation

The emerging nascent chain can differentially regulate protein targeting and translocation and this has been demonstrated through its interactions with SRP, the translocon and translocon associated protein (TRAP). Interestingly the affinity of SRP differs for different signal sequences. For example the signal sequence for BiP has a high affinity (K_D: 0.05nM) for SRP compared to that of PI (K_D: 0.38nM) (Flanagan et al., 2003). This is probably to ensure that under cell stress conditions the efficient translation and translocation of BiP is a priority for the unfolded protein response.

Comparison of the early stages of translocation of different nascent chains suggests that the ribosome-translocon junction is regulated by the nature of the nascent chain (Rutkowski et al., 2001; Wolin and Walter, 1993). Some nascent chains such as the prion protein quickly formed tight ribosome-translocon junctions, while others such as pre β-lactamase remained exposed to the cytosol for longer. Rutkowski *et al*, 2001 propose that TRAM may play a role in specific signal sequence recognition as it has been shown to be involved in signal sequence recognition and regulation of the ribosome-translocon junction (Hegde et al., 1998; Rutkowski et al., 2001; Voigt et al., 1996). Specific signal sequences also determine whether the protein complex TRAP is required for translocation (Fons et al., 2003). Protein signal sequences such as prolactin's signal sequence do not require TRAP for efficient transport across the ER membrane, whereas the prion protein signal sequence relies on TRAP for efficient translocation.

Nascent chains can also influence the ribosome to act as a messenger for targeting and translocation processes. Liao *et al*, 1997 first showed that the ribosome and not the translocon recognises that the polypeptide is destined for the ER membrane and not secretion. Membrane proteins are co-translationally targeted to the ER by the same mechanism as secretory proteins, however, upon translocation through Sec61α the translocon is thought to open laterally and allow release of the transmembrane segment into the ER membrane (Van den Berg et al., 2004). Once the ribosome has identified the membrane protein this is communicated across a distance of 150Å to the translocon (Liao et al., 1997). These results and fluorescence resonance electron transfer (FRET) data show that the ribosome can communicate and influence the behaviour of the translocon depending on the folding of the nascent chain (Woolhead et al., 2004).

1.4: Nutrient regulation of protein synthesis

In order to survive an organism must be able to respond to changes in environmental factors. For example, in order to fulfil nutritional needs, an organism must be able to sense nutrient deficiency and excess. Expression of proteins involved in a variety of different metabolic functions can be governed by nutrient regulation. Indeed, both direct and indirect nutrient regulators of gene and protein expression can control: transcription, mRNA processing, mRNA stability, translation and post-translational modifications.

Nutrients can regulate both global protein synthesis and gene-specific protein synthesis. There is evidence to indicate that amino acids and glucose facilitate an increase in the rate of global translation by eukaryotic initiation translation factors (Gomez et al., 2004; Proud et al., 2001). Indeed, activation of eIF2B by insulin in Chinese hamster ovary (CHO) cells is dependent on the presence of both amino acids and glucose (Campbell et al., 1999). In addition, removal of amino acids from the media results in the dephosphorylation of 4E-BP1, which increases its binding to eIF4E and reduces formation of eIF4F complexes (Wang et al., 1998a). Upon re-introduction of amino acids into the media there is an increase in the phosphorylation of 4E-BP1 leading to its dissociation from eIF4E and an increase in eIF4F complex formation. These changes are often associated with global changes in translation.

There is increasing evidence that translational events play an important role in nutrient regulation of specific mRNA translation as well as global mRNA translation. This can be evident from discrepancies between mRNA abundance and translation rates. An example of nutrient regulation of translation for a specific protein is general control non-derepressible 4 (GCN4) in yeast, which is translated in response to amino acid deprivation resulting in GCN2 phosphorylation of eIF2 (Hinnebusch, 2000).

mRNA binding proteins are often associated with the 5' UTR or 3' UTR of mRNAs. A well-documented example of the role of UTRs as regulatory elements is in the case of the expression of both transferrin receptor and ferritin in the regulation of cellular iron levels (reviewed in Ponka et al., 1998). The transferrin receptor is responsible for

uptake of iron into the cell, while ferritin is responsible for detoxifying and storing cellular iron. Transferrin mRNA has 5 iron regulatory elements (IRE) in the 3' UTR. In the absence of iron, trans-acting factors bind the IRE and prevent transferrin mRNA from degradation by ribonucleases. In the presence of iron these factors dissociate which results in destabilisation of transferrin mRNA. The destabilsation of transferrin mRNA at high levels of cellular iron results in a decrease in transferrin mRNA synthesis and therefore a decrease in iron uptake into the cell. In contrast to the transferrin mRNA, where the IRE regulate mRNA stability via the 3'UTR, ferritin mRNA IRE regulate translation through the 5'UTR. At low iron levels iron regulatory protein binds IRE and represses translation. However, in the presence of iron, iron regulatory protein dissociates and allows translation of ferritin mRNA, which increases synthesis of ferritin and storage of iron. Additionally in the absence of IRP, the 5' UTR IRE of ferritin enhances binding of initiation factors to ferritin mRNA.

1.5: Pancreatic β-cell Protein Synthesis

When isolated rat islets are incubated in 16.7mM glucose they incorporate twice as much [^{3}H]-leucine into protein as those incubated in 2.8mM glucose (Permutt, 1974; Permutt and Kipnis, 1972a). This increase in protein synthesis is over only one hour and is independent of new mRNA synthesis, which suggests that glucose up-regulates pancreatic β-cell protein synthesis at a post-transcriptional level.

The majority of work shows that glucose stimulates total islet protein synthesis through an increase in the rate of initiation of translation. For example, changes in glucose resulted in an increase in [^{3}H]-leucine-containing nascent peptides on larger polysome aggregates at high glucose (Permutt and Kipnis, 1973). Recently, polysome analysis data from our lab has shown that glucose stimulates an increase in the size of polysomes, indicative of an increase in the rate of initiation (Gomez et al., 2004). Additionally, the initiation inhibitor, aurintricarboxylic acid caused a 50% reduction in protein synthesis and a reduction in the size of polysomes in islets incubated in high glucose but not low glucose (Permutt, 1974). Although there is strong evidence that an increase in glucose concentration leads to a two-fold increase in β-cell protein synthesis at the level of initiation, there is limited information as to the mechanism of this increase. Changes in the rate of initiation may be through changes in the activity and availability of translation initiation factors in the β-cell. In particular, studies have focused on the regulation of eIF4F formation and ternary complex formation.

1.5.1: Glucose regulation of eIF4F complex formation in pancreatic β-cells

Glucose does not modulate the phosphorylation of eIF4E or the binding of 4E-BP1 to eIF4E in the absence of amino acids (Gilligan et al., 1996). Yet, in the presence of amino acids, glucose induces the phosphorylation of 4E-BP1 on amino acid residues Ser65 and Thr36/45 through the autocrine effect of insulin released in response to increases in glucose concentration (Gomez et al., 2004; Xu et al., 1998). Indeed, the incubation of islets in amino acids and insulin has the same effect on 4E-BP1 phosphorylation as the incubation of islets in amino acids and glucose (Xu et al., 1998). This glucose-stimulated phosphorylation of 4E-BP1 via insulin secretion reduces its

binding to eIF4E and therefore should increase eIF4E availability for formation of the eIF4F complex (Gomez et al., 2004; Xu et al., 1998). However, phosphorylation of 4E-BP1 and subsequent increased availability of eIF4E did not lead to an increase in eIF4F assembly suggesting that this step may not be a major regulator of protein synthesis in the β-cell (Gomez et al., 2004).

In the presence of amino acids, glucose has been shown to also stimulate the phosphorylation of p70 S6 kinase (Gomez et al., 2004), which leads to the up-regulation of translation of a specific subset of mRNAs that contain a tract of polypyrimidines within their 5' UTR (TOP messages). The phosphorylation of 4E-BP1 and p70 S6 kinase is dependent on signalling cascades via the protein kinase mTOR (mammalian target of rapamycin) and is dependent on the presence of amino acids (for review see Proud, 2002). However, inhibition of mTOR by rapamycin has a partial effect on glucose-stimulated protein synthesis in the presence of amino acids and no effect in the absence of amino acids (Gomez et al., 2004). Furthermore, while the absence of amino acids inhibits glucose-stimulated phosphorylation of 4E-BP1 and p70 S6 kinase, glucose stimulated protein synthesis remains unaffected by amino acids (Gomez et al., 2004). This data thus supports the theory that 4E-BP1 and p70 S6 kinase phosphorylation do not play a major role in glucose stimulated protein synthesis in the pancreatic β-cell.

1.5.2: Glucose regulation of ternary complex formation in pancreatic β-cells

The availability of the ternary complex is an important factor in regulating the rate of translation initiation and therefore may be important in regulating glucose-stimulated protein synthesis in the β-cell. In islets glucose increases the activity of eIF2B within the same glucose concentrations that stimulate insulin synthesis (Gilligan et al., 1996). In MIN6 cells, it was found that glucose stimulates the dephosphorylation of eIF2 in parallel with an increase in ternary complex formation and an increase in glucose-stimulated protein synthesis in the presence or absence of amino acids (Gomez et al., 2004). However, while an increase in ternary complex formation is observed in islets, no dephosphorylation of eIF2 is observed in islets (Gilligan et al., 1996; Gomez et al., 2004). Gomez *et al*, 2004 suggest it is likely that dephosphorylation of eIF2 does occur

in islets but that it is masked by phosphorylated eIF2 in non-β-cells or by stressed hypoxic cells at the centre of the islet.

Of the four mammalian serine/threonine eIF2α kinases that have been identified, the PKR-like endoplasmic reticulum eIF2α kinase PERK/PEK appears to play an important role in regulating eIF2α phosphorylation in the pancreatic β-cell (Harding et al., 2001). PERK is highly expressed in the pancreas and is activated in response to ER stress, which occurs when the ER reaches its folding capacity through high rates of protein synthesis (Harding et al., 2001; Harding et al., 2000c; Harding et al., 1999; Shi et al., 1998). PERK is an integral ER membrane protein with its kinase domain on the cytoplasmic side of the ER and its stress response domain in the lumen of the ER (Harding et al., 1999; Shi et al., 1998). In stress-free conditions PERK is bound to lumenal protein BiP; upon ER stress BiP dissociates from PERK, allowing it to oligomerise. After oligomerisation, PERK is activated by trans-autophosphorylation and phosphorylates eIF2α, which reduces the rate of protein synthesis (Bertolotti et al., 2000).

Mutations in the gene that codes for PERK result in Wolcott-Rallison syndrome that is characterised by early infantile type 1 diabetes due to the β-cell's inability to respond to ER stress (Delepine et al., 2000). Interestingly, PERK knockouts result in the same phenotype in mice (Harding et al., 2001). Because, glucose deprivation in the pancreatic β-cell can cause ER stress it was therefore logical to predict that PERK may be responsible for phosphorylating eIF2α and hence regulate ternary complex formation (Harding et al., 2001; Scheuner et al., 2001). However, while the PERK knockout islets had increased levels of insulin synthesis at high glucose, there was no effect on insulin translation at low glucose in islets from PERK knockout islets compared to wild type islets (Harding et al., 2001). Additionally, Gomez *et al*, 2004 showed that phosphorylation of PERK is not affected by glucose concentration and a dominant negative form of PERK had little effect on the phosphorylation of eIF2α at low or high glucose and had no effect on glucose stimulated protein synthesis.

Results from Gomez *et al*, 2004 suggest that an eIF2α kinase other than PERK is responsible for phosphorylation of eIF2α. Meanwhile, mice with deletions in HRI or

PKR do not exhibit symptoms associated with diabetes. However, mGCN2 phosphorylates eIF2α in response to amino acid deprivation (Sood et al., 2000) and the yeast homologue, GCN2 is activated in response to glucose starvation (Yang et al., 2000). It has therefore been suggested that mGCN2 activity may be stimulated by glucose, although, this has yet to be demonstrated in mammalian cells.

Early work showed that β-cell translational elongation was not regulated by glucose. Glucose concentration was shown to have no effect on average islet ribosome transit times (Permutt, 1974) and work by Gilligan *et al* failed to show an increase in dephosphorylation of elongation factor 2 (EF-2) in response to increases in glucose (Gilligan et al., 1996). However, more recently it was demonstrated in the INS-1 derived 832/13 cell line, MIN6 cells and islets that glucose-stimulated protein synthesis is paralleled by an increase in the dephosphorylation of elongation factor 2 (EF-2) (Yan et al., 2003). This dephosphorylation of EF-2 was due to a direct increase in glucose and not an effect of secreted insulin. Furthermore, dephosphorylation of EF-2 appeared to occur through an increase in the activity of protein phosphatase 2A (PP2A) rather than the inhibition of a kinase (Yan et al., 2003).

1.6: Secretory Protein Synthesis in pancreatic β-cells

While there is a two-fold increase in general β-cell protein synthesis in response to glucose there is a larger increase in the synthesis of a number of specific β-cell proteins, including insulin. Some of these proteins have been identified and are synthesised in parallel with insulin (Guest et al., 1991). In fact an increased glucose concentration resulted in at least a two-fold increase in the synthesis of more than 240 secretory granule polypeptides and the synthetic rate of 60 of these was increased by 10 to 30 fold (Guest et al., 1991). In contrast to the secretory membrane fraction, the synthesis of only 8 out of 160 proteins in the soluble fraction was increased by 10-30 fold in response to stimulation by glucose. Specific examples of proteins synthesised in parallel with insulin include prohormone convertases PC2 and PC3 (Alarcon et al., 1993; Guest et al., 1991; Martin et al., 1994; Rhodes and Alarcon, 1994) synaptic vesicle associated membrane protein, syntaxin-1 (Nagamatsu et al., 1997), the secretory granule membrane protein (SGM) 110 (Grimaldi et al., 1987) and the secretory granule protein, chromagranin A (Guest et al., 1989). However, other proteins found in the insulin secretory granule are not regulated in response to glucose, for example, carboxypeptidase H (CPH) (Guest et al., 1989). It is likely that this rapid up-regulation of β-cell proteins in response to glucose is important in maintaining the correct response to changes in plasma glucose levels. Indeed, inhibition of translation in islets by cycloheximide inhibits insulin secretion in response to glucose (Garcia et al., 2001). Therefore, deviation from the normal synthesis of these proteins may result in the malfunction of storage or secretion of insulin and symptoms associated with type II diabetes.

1.7: Post-transcriptional regulation of insulin synthesis

Upon an increase in glucose concentration from low (2.8mM glucose) to high (15.3mM glucose), islets incorporate 8-20 times as much radio-labelled amino acid into immunoprecipitated insulin (Alarcon et al., 1993; Itoh and Okamoto, 1980; Permutt and Kipnis, 1972a; Permutt and Kipnis, 1972b). Permutt *et al*, 1972b also showed that the transcription inhibitor, actinomycin D has little effect on insulin synthesis in the first 45 minutes of incubation in high glucose, suggesting that this increase in PI synthesis is due to post-transcriptional regulation. Later, Itoh *et al*, 1978 and 1980 used both *in vitro* translation of purified islet mRNA and Northern blotting to quantify and show that the amounts of PPI mRNA in islets incubated at high or low glucose concentrations did not vary. These experiments suggest that PI synthesis is regulated at a post-transcriptional level. Indeed, the β-cell has been shown to regulate PI synthesis at the level of mRNA stability, initiation and elongation of translation and SRP arrest (Tillmar et al., 2002; Welsh et al., 1986) but the extent to which each process contributes to the synthesis of PI is disputed.

1.7.1: Initiation

Subcellular fractionation of islets of Langerhans and Northern blot analysis has shown that cytosolic 'free' PPI mRNA that is not associated with ribosomes is recruited onto polysomes either found in the cytosol or associated with the ER, suggesting an increase in the rate of initiation of PI (Itoh and Okamoto, 1980; Welsh et al., 1986; Welsh et al., 1991; Welsh et al., 1987). However, the increase in recruitment of ribosomes onto free PPI mRNA is variable, most likely due to the variability in isolating the islets. Indeed, free PPI mRNA makes up 23-62% of total PPI mRNA at low glucose concentrations and 5-46% of total PPI mRNA at high glucose concentrations and the recruitment of ribosomes onto PPI mRNA accounts for 20-41% of total PPI mRNA that is free at low glucose onto polysomes at high glucose (Itoh and Okamoto, 1980; Welsh et al., 1986; Welsh et al., 1991; Welsh et al., 1987).

Welsh *et al*, 1986 used sucrose sedimentation gradients and Northern blotting to show a shift of free PPI mRNA at low glucose into heavier sedimenting fractions, representing polysomes, at high glucose, indicative of an increase in the rate of initiation (Welsh et

al., 1986). This contradicts Jahr *et al*, 1980 who showed that the amount of ribosome-associated PPI mRNA is the same at low and high glucose in islets, suggesting that PI synthesis is not regulated at the level of initiation of translation. Interestingly, Jahr *et al*, 1980 added cycloheximide five minutes before lysis to prevent ribosomal run-off. Cycloheximide does not appear to have been added to any of the studies previously mentioned, which observe large recruitment of free PPI mRNA onto polysomes at high glucose and perhaps these results should be treated with some caution. (Itoh and Okamoto, 1980; Welsh et al., 1986; Welsh et al., 1991; Welsh et al., 1987). However, Jahr *et al*, 1980 quantified PPI mRNA associated with polysomes by immunoprecipitation of PI nascent chains that were associated with radio-labelled PPI mRNA. In this case a large amount of completed PI would have been immunoprecipitated, possibly masking any changes. Furthermore, this method does not separate out the heavy and light polysomes and only identifies shifts of free PPI into mono/polysomal fractions.

Lomedico *et al*, 1977 *in vitro* translated poly(A) containing RNA from bovine pancreas to show that changes in Mg^{2+} or K^+ concentrations or addition of the initiation inhibitor, aurintricarboxyic acid (ATA) had more effect on PI synthesis than total protein synthesis. In support of these results, Pipeleers *et al*, 1973b showed *in vivo* that PI synthesis is more sensitive than total protein synthesis to increases and decreases in carbohydrate and salt concentrations. Lomedico *et al*, 1977 suggest that in accordance with the Lodish model (Lodish, 1974), the sensitivity of PI to changes in the translation system is due to PI translating less efficiently than other mRNAs. However, experiments by Wanatabe *et al*, 1982 showed that inhibiting initiation or elongation had the same effect on the relative sensitivity of both PI and total protein synthesis at low or high glucose. This suggests that there is no difference in the relative initiation efficiencies between PI and non-PI protein synthesis. Therefore, Wanatabe *et al*, 1982 propose that increases in initiation are global and do not specifically enhance PI synthesis. Recently, glucose-stimulated increases in global rates of initiation of protein synthesis have been demonstrated through polysome analysis of MIN6 cells (Gomez et al., 2004), but a comparison between recruitment of ribosomes onto PPI or other mRNAs has yet to be investigated.

1.7.2: Recruitment of PPI mRNA to the ER

Subcellular fractionation studies have demonstrated that glucose stimulates the recruitment of PPI and 7S SRP RNA to the ER, the site of PI synthesis (Itoh and Okamoto, 1980; Welsh et al., 1986; Welsh et al., 1991; Welsh et al., 1987). Indeed, there is an increase of 12-18% of total PPI mRNA associated with the ER at high glucose compared to low glucose (Itoh and Okamoto, 1980; Welsh et al., 1986; Welsh et al., 1991; Welsh et al., 1987).

Although it has been shown that glucose stimulates the recruitment of PPI mRNA to the ER, the mechanism of this recruitment is unknown. However, because SRP 7S RNA is recruited to the ER to a similar extent to that of PPI mRNA, it has been suggested that SRP may regulate the recruitment of PPI mRNA to the ER. Indeed, it has been shown *in vitro* that there is an increase in translational pausing at low glucose after approximately 70 amino acids have been synthesised (Wolin and Walter, 1988) and as subcellular fractionation showed increased co-sedimentation of SRP 7S RNA with cytosolic ribosome-associated PPI mRNA at low glucose, it was suggested that this pause was due to SRP causing SRP arrest (Welsh et al., 1986). Welsh *et al*, 1986 investigated the effect of the SRP receptor on PI synthesis by incubating disrupted islets that had been incubated at low or high glucose and *in vitro* translating them in the presence of $[^{125}I]$-tyrosine. In these conditions PI synthesis was only due to the translation of pre-initiated ribosomes. Interestingly, the addition of SRP receptor to the *in vitro* translation reaction mixture increased PI synthesis by only 40% with islets incubated at low glucose, while it more than doubled PI synthesis with islets incubated at high glucose (Welsh et al., 1986). This led to the proposal that at low glucose concentrations SRP binds to PPI RNCs but is unable to interact with the SRP receptor at the ER (Welsh et al., 1986). At high glucose concentrations this blockage is relieved, thereby allowing recruitment of PPI mRNA to the ER and PI synthesis to occur. However, this hypothesis is yet to be proven.

It could be argued that the increase in PPI mRNA associated with the ER is due to the increased rate of initiation, therefore enabling more PPI mRNA ribosome-nascent chain complexes to bind SRP and be targeted to the ER. However, Welsh *et al*, 1991 later showed that the non-hydrolysable analogue of GTP, GTP-γ-[S] increases the ratio of

ER-bound mRNA to cytoplasmic mRNAs in a similar manner to glucose. Interestingly, the GTP/GDP ratio in the pancreatic beta cell is much lower than in most other cell types (Hoenig and Matschinsky, 1987). Furthermore, glucose has been found to increase the GTP/GDP ratio from 2:1, where the SRP receptor will predominantly bind GDP and be inactive, to a ratio of 4:1 (Hoenig and Matschinsky, 1987), where the SRP receptor will predominantly bind GTP and be active. Welsh *et al*, 1991 therefore proposed that glucose might regulate the GTP/GDP ratio in order to enhance recruitment of PPI mRNA to the ER and therefore enhance PI synthesis.

Itoh *et al*, 1980 argue that an increase of 12-18% of total PPI mRNA associated with the ER at high glucose compared to low glucose is surprisingly small considering there is up to a ten-fold increase in PI synthesis. Therefore, they propose that further regulation of PI synthesis occurs at the endoplasmic reticulum membranes. Interestingly, expression profiling of β-cells to identify genes up-regulated in response to high glucose showed the largest functional cluster of glucose-responsive β-cell genes to be part of the early secretory pathway and the regulated secretory pathway (Webb et al., 2000). Of particular interest was that the majority of these were involved in ER function, the most dramatic of which was the α-subunit of the SRP receptor (SR), which showed a 20-fold increase upon stimulation of β-cells with high glucose. These results suggest that regulation of the ER is important in β-cell function, although further regulation of PI synthesis at the ER has yet to be demonstrated (Webb et al., 2000).

1.7.3: Elongation

Cycloheximide can be used to slow elongation and make it the rate-limiting step. Under these conditions the rate of protein synthesis is dependent on the rate of elongation or the availability of mRNA, but not the rate of initiation (Watanabe, 1982; Welsh et al., 1986). Interestingly, in the presence of cycloheximide, glucose specifically stimulated the synthesis of PI but not total protein between 0 and 5.6mM (Welsh et al., 1986). Because initiation was not rate-limiting, this increase in PI synthesis was through a glucose-stimulated increase in the rate of elongation and/or a release of PPI mRNA from a non-translatable pool, although which of these it is has not been determined (Watanabe, 1982; Welsh et al., 1986).

1.7.4: The 5' and 3' Untranslated regions of PPI mRNA

Although the mechanism of glucose-regulated PI synthesis is poorly understood, it is likely that the 5' and 3' UTRs play an important role. Indeed the importance of the 5' and 3' UTRs in glucose-stimulated PPI translation has recently been reported (Wicksteed et al., 2001). It has been predicted that the 5' UTR of rat PPI II mRNA contains a stem loop structure that is similar to those predicted in other mammalian PPI mRNAs (Knight and Docherty, 1992; Wicksteed et al., 2001). Additionally the 5' UTR of rat PPI II mRNA is required for glucose stimulation of PPI mRNA translation (Wicksteed et al., 2001). Conversely, the same study shows that the 3'-UTR appears to suppress glucose induced PI synthesis. However, the 5' and 3'-UTRs work co-operatively to increase glucose stimulated PI synthesis and it has been proposed that interaction between the 5' and 3' UTRs at high glucose alleviates the 3' UTR's suppression of PPI synthesis (Wicksteed et al., 2001).

1.7.5: mRNA stability

Welsh *et al*, 1985 showed that glucose specifically stabilises PPI mRNA so that its half-life increases from 29 hours at low glucose to 77 hours at high glucose. More recently, the 3' UTR has been shown to stabilise PPI mRNA in a β-cell specific manner (Wicksteed et al., 2001). In fact, it has been shown that the 3'-UTR contains a polypyrimidine rich sequence, which specifically binds polypyrimidine tract binding (PTB) protein in β-cells incubated at high glucose for one hour (Tillmar et al., 2002). Furthermore, mutation of the PTB binding site of the PPI 3'-UTR fused to a reporter gene resulted in destabilisation of the mRNA. PTB plays an important role in polyadenylation, RNA localisation and translation, and may therefore play a key role in regulating PI synthesis in response to glucose.

Recently it has been shown that in addition to PPI, PTB binds and stabilises PC2 and PC3 but not CPH mRNAs (Knoch et al., 2004). Furthermore in transfected INS-1 cells, synthesis of firefly luciferase is increased and stimulated by glucose over a two hour period in constructs carrying the 5' and 3' UTRs of PC2 and a 50% knockdown of PTB reduces PC2, PC3 and insulin synthesis but not CPH synthesis (Knoch et al., 2004). It

has therefore been suggested that PTB stabilise specific mRNAs at high glucose concentrations.

24 hour incubation in high glucose stimulates PTB mRNA synthesis by 5-fold in MIN6 cells (Webb et al., 2000), suggesting that its synthesis may be important in maintaining the glucose-responsive state of the β-cell. However, protein expression did not vary over one hour suggesting that either post-translational modifications of PTB may be necessary for short-term regulation of PPI mRNA stability or that PTB is not required for acute increases in PI synthesis over one hour (Tillmar et al., 2002). Indeed, the binding of PTB to the 3' UTR of PPI mRNA is inhibited by rapamycin. However, rapamycin does not inhibit glucose-stimulated increases in PI synthesis (TP Herbert, unpublished observations). Therefore, regulation of the stability of PPI mRNA may not be important in the short-term regulation of PI synthesis. However, even though PTB may not be important in the acute regulation of PI synthesis, it is the first trans-acting factor found to bind PPI mRNA. Moreover, it is extremely likely that other trans-acting factors bind PPI mRNA and facilitate its translation.

1.7.6: Splice Variants of PPI mRNA

Recently a PPI splice variant mRNA has been discovered in human and mouse islets (Minn et al., 2004; Minn et al., 2005b; Shalev et al., 2002a). In humans the splice variant is generated from a cryptic splice site within the first intron and results in the first 26 base pairs of the first intron to be included in the mRNA (Shalev et al., 2002a), although in mice the whole intron is included in the insulin II mRNA splice variant (Minn et al., 2004). Interestingly, these splice variants are translated more efficiently than the wild-type mRNAs in both *in vitro* and *in vivo* systems suggesting that alternative splicing of PPI mRNA may play a role in the translational regulation of PI synthesis (Minn et al., 2004; Shalev et al., 2002a). Comparison of the secondary structures of the splice variant mRNAs with the native mRNAs suggested that cis-acting structures within the 5'UTR were responsible for the increased translation efficiency of the splice variant mRNAs (Minn et al., 2004; Shalev et al., 2002a). Furthermore, the splice variant/native RNA ratio was increased by 15-fold in islets incubated at high glucose for 70 hours and was also increased in different mouse diabetic and insulin resistant models (Minn et al., 2005b). This suggests that expression of the splice variant

may be required to compensate for increased insulin demands in cases such as hyperglycaemia and insulin resistance.

In summary glucose has been shown to increase mRNA stability and certain splice variants, initiation of translation, and recruitment of PPI mRNA to the ER. In addition it has been suggested that PI synthesis is regulated through a glucose-stimulated increase in elongation of translation, however, direct evidence for this has not yet been provided. It is clear that the role that each of these stages plays in the precise mechanism for regulating PI synthesis is poorly understood and requires further work.

1.8: Metabolic Signals for Glucose Induced Proinsulin Synthesis

While the signalling pathways that lead to an increase in insulin secretion have been relatively well characterised (reviewed in Campbell et al., 1982; Prentki et al., 1997; Rutter, 2001) those that lead to an increase in PI synthesis are comparatively unknown.

In the case of insulin secretion, the pancreatic beta cell takes up glucose, which is then phosphorylated to glucose-6-phosphate by hexokinase. Pyruvate is produced through glycolysis and is taken up by the mitochondria for the Krebs cycle. Generation of ATP through the Krebs cycle and oxidative phosphorylation results in an increase in the ATP/ADP ratios within the β-cell. This increase in ATP causes closure of ATP-dependent K^+ channels, which results in depolarisation of the plasma membrane and opening of voltage-gated calcium channels. An influx of Ca^{2+} activates protein kinase cascades, finally leading to the secretion of insulin (Prentki et al., 1997). To ensure replenishment of insulin stores there is a concomitant increase in glucose-stimulated PI synthesis. However, the metabolic signals that mediate this are poorly understood. Many techniques have demonstrated the uncoupling of insulin secretion from insulin synthesis. Firstly, the threshold for an increase in insulin secretion (4-6mM) is higher than that for insulin synthesis (2-4mM) (Ashcroft, 1980). Additionally, ionic variations differentially effect insulin synthesis and secretion. For example, an increase in intracellular calcium levels is only required to trigger insulin secretion and conversely an omission in Mg^{2+} ions in the media will attenuate PI synthesis but not secretion (Lin and Haist, 1973; Pipeleers et al., 1973a; Pipeleers et al., 1973b).

Despite the ability to uncouple insulin synthesis and secretion, earlier pathways partaking in the metabolism of glucose link the two processes. Indeed, while glucose and mannose both stimulate insulin synthesis and secretion, the non-metabolizable sugar galactose is ineffective for either processes (Parry and Taylor, 1966). Mannoheptulose, which inhibits phosphorylation of the sugar, inhibits PI synthesis and secretion (Ashcroft et al., 1978; Pipeleers et al., 1973a). Furthermore, in MIN6 cells. pyruvate stimulates insulin synthesis and secretion, suggesting mitochondrial metabolism is required for both processes (Skelly et al., 1998). In addition to the requirement for mitochondrial metabolism, both PI synthesis and insulin secretion requires anaplerosis (generation of Krebs cycle intermediates) to occur (Prentki, 1996).

However, glucose-stimulated insulin secretion but not PI synthesis can be attributed to elevations in cytosolic long chain fatty acyl-CoA (Bollheimer et al., 1998; Katahira et al., 2001; Skelly et al., 1998). This suggests that the metabolic signals that instigate PI synthesis branch away from insulin secretion upstream of any increase in cytosolic fatty acyl CoA (Skelly et al., 1998).

Decreasing ATP levels through addition of oxidative phosphorylation inhibitors results in a decrease in general protein synthesis but not a specific decrease in PI synthesis (Alarcon et al., 2002), suggesting ATP is not responsible for a specific increase in PI synthesis. Recently, succinate or succinyl-coA has been identified as a potential candidate for acting as a stimulus-coupling secondary signal for glucose-stimulated PI synthesis (Alarcon et al., 2002). Succinic acid methyl ester stimulates PI synthesis but not insulin secretion and malonic acid methyl ester, an inhibitor of succinate dehydrogenase, which catalyses the conversion of succinate to fumerate inhibits PI synthesis. Therefore, it has been proposed that the increase in glycolysis and the Krebs cycle due to high glucose concentrations results in an accumulation in succinate in the mitochondria. The succinate is then transported into the cytosol and converted to succinyl co-A where it can act as a secondary signal for increasing PI synthesis (Alarcon et al., 2002). In support of this theory succinyl CoA levels are increased in glucose stimulated islets (Liang and Matschinsky, 1991).

1.9: Transcriptional regulation of proinsulin synthesis

The role of transcription in the short-term regulation of glucose stimulated PI synthesis is unclear. Initial work suggested that islets incubated in high glucose concentrations for less than four hours have little variation in the amounts of PPI mRNA levels suggesting that insulin synthesis is primarily glucose-regulated at the level of translation. (Itoh and Okamoto, 1980; Welsh et al., 1985). However, it was shown that PPI mRNA levels are increased in response to glucose in situations such as prolonged exposure to high glucose (>4 hours) and refeeding after periods of starvation (Brunstedt and Chan, 1982; Giddings et al., 1982; Jahr et al., 1980a). This increase in PPI mRNA is due to increased transcription (Nielsen et al., 1985) and also an increase in the stability of mRNA at high glucose concentrations (Tillmar et al., 2002; Welsh et al., 1985).

More recently short-term regulation of insulin gene transcription has been demonstrated in rat islets and a hamster insulinoma cell line (Leibiger et al., 1998). This activation of transcription occurs within 30 minutes and has been shown to contribute to 50% of PI synthesis. This work and previous studies suggest that the increase in transcription is triggered through the feedback of secreted insulin on the beta cell and not directly through stimulation by glucose. (da Silva Xavier et al., 2000; Leibiger et al., 2001; Leibiger et al., 1998; Leibiger et al., 2002; Leibiger et al., 2000; Wu et al., 1999; Xu and Rothenberg, 1998). However, other work has shown that insulin has either no effect or a negative effect on transcription (Leibiger et al., 2002; Wicksteed et al., 2001).

The variations in response to insulin and transcription of PPI mRNA maybe due to different experimental conditions, for example the type of exposure to insulin. Secretion of insulin occurs in short pulses, which may be to ensure effective response from the target tissues and prevent insulin resistance (Porksen, 2002). Indeed loss of pulsatile release has been associated with type two diabetes (Porksen, 2002). Therefore, experiments in which cells have had long exposure to insulin, eg tissue culture cells, may result in insulin-resistance. Despite the controversy, autocrine insulin feedback and transcription of PPI appears to play an important role in beta cell function. In fact, recently glucose-stimulated up-regulation of PI transcription was found to be necessary

for adequate replenishment of insulin stores in the case of chronically high glucose levels (Leibowitz et al., 2002).

Chapter 2: Materials and Methods

2.1: General Reagents

Unless stated all chemicals were of analytical grade and were routinely purchased from Sigma or Fisher chemicals

Products for molecular biology were routinely purchased from Promega, Sigma, New England Biolabs or Gibco BRL.

Bacterial cell culture reagents were from Oxoid.

2.2: Mammalian Cell Culture

Cell lines used were the human embryonic kidney cell line, HEK293, and the mouse insulinoma cell line MIN6 (provided by Prof Jun-Ichi Miyazaki, Division of Stem Cell Regulation Research, G6 Osaka University Medical School, Japan), a pancreatic β-cell line that is responsive to physiological changes in glucose concentrations (0.5-20mM).

2.2.1: Maintenance of Cell Lines

HEK293 cells were used at approximately 80% confluence and were grown in full Dulbecco's Modified Eagle's Medium (DMEM) containing 25mM glucose supplemented with 10% heat-inactivated foetal calf serum (FCS), 100µg/ml streptomycin and 100units/ml penicillin sulphate, equilibrated with 5% CO_2, 95% air at 37°C.

MIN6 cells were used at approximately 80% confluence between passages 16 to 28. MIN6 cells were grown in full MIN6 media consisting of DMEM containing 25mM glucose supplemented with 15% heat-inactivated FCS, 100µg/ml streptomycin, 100units/ml penicillin sulphate and 75µM β-mercaptoethanol, equilibrated with 5% CO_2, 95% air at 37°C.

80% confluent cells were washed in 1x phosphate buffered saline (PBS) and dispersed with 1% trypsin/EDTA. Dispersed MIN6 cells were split 1:3 and dispersed 293 cells were split 1:5 to 1:10, depending on requirements.

2.2.2: Calcium Phosphate Mediated DNA Transfection

Cells were split to 20-30% confluence at least 4 hours prior to transfection. For a plate with an $80cm^2$ surface area, a solution containing $10\mu g$ DNA and 244mM $CaCl_2$ in a final volume of $500\mu l$ was prepared. This solution was added slowly to $500\mu l$ 2x HEPES buffered saline (HBS), mixing gently on addition. The $DNA/CaCl_2/HBS$ mixture was then added directly to the cells by dropping slowly and evenly onto the medium. After a 16-24 hour incubation at 37°C/5% CO_2, the media was removed, the cells were washed with 1x PBS, fresh, warm complete media was added to the cells and incubation was resumed for a further 24-60 hours.

2.2.3: Lipofectamine Mediated Transfection

Lipofectamine mediated transfections were carried out using Lipofectamine 2000 (Invitrogen). 24 hours prior to transfection, cells were split to 20% confluence. $2.5\mu g$ of DNA was used to transfect one 35mm tissue culture dish. $7\mu l$ of lipofectamine and $175\mu l$ DMEM (no supplements) were placed in one tube and $2.5\mu g$ DNA with $175\mu l$ DMEM (no supplements) were placed in a second tube. Both tubes were incubated for 5 minutes at room temperature. The DNA mixture was added to the lipofectamine mixture and incubated at room temperature for 20 minutes to allow DNA-lipofectamine complexes to form. The DNA-liopfectamine complexes were then added to the cells, which were incubating in full MIN6 media minus antibiotics. The cells were incubated for 4 hours at 37°C/5% CO_2. After incubation the cells were washed twice with PBS and incubated for 24-48 hours in full MIN6 media.

2.3: Bacterial Methods

2.3.1: Culture Media and Supplements

Luria broth (LB)

1% (w/v) tryptone

0.5% (w/v) yeast extract

1% (w/v) NaCl

1.5% (w/v) agar (for solid LB only)

SOC media

2% (w/v) bacto-tryptone

0.5% (w/v) yeast extract

10mM NaCl

2.5mM KCl

10mM MgCl2

10mM MgSO4

20mM glucose

Bacterial expression lysis buffer

20mM Tris pH8

1mM EDTA

200mM NaCl

10% glycerol

0.5% NP-40

1mM DTT

1mM phenylmethylsulfonyl fluoride (PMSF)

2μg/ml leupeptin

1mM benzamidine-HCl

1μg/ml pepstatin

Ampicillin

Final concentration, 100μg/ml

Kanamycin

Final concentration, 50µg/ml

Tetracycline

Final concentration, 100µg/ml

Streptomycin

Final concentration, 30µg/ml

2.3.2: Plasmids

Plasmid	Resistance	Company
pGEX-4T3	Ampicillin	Pharmacia Biotech
pGEM-3ZF	Ampicillin	Promega
pSP64 poly(A)	Ampicillin	Promega
pEGFP-C1	Kanamycin	Promega
pShuttle CMV	Kanamycin	Kind gift from He TC (He et al., 1998)
pAdeasy-1	Ampicillin	Kind gift from He TC (He et al., 1998)
pDsRED2-ER	Kanamycin	Clontech

2.3.3: Bacterial Strains

Strain	Resistance	Company/Ref
XL10 gold	Tetracycline and chloramphenicol	Stratagene
BL21 (DE3)		Novagen
BJ5183		Kind gift from He TC (He et al., 1998)
SCS110		Stratagene

2.3.4: Preparation of competent cells

CaCl₂ Competent Cells

An overnight bacterial culture was grown up at 37°C in 5ml LB supplemented with the appropriate antibiotic. 1ml of this fresh culture was used to inoculate 200ml LB medium and was grown to A_{600} of 0.5. The culture was cooled on ice for five minutes then pelleted by centrifugation at 3200g for 15 minutes at 4°C. The cell pellet was resuspended in 100ml ice-cold 100mM $MgCl_2$ and incubated on ice for 10 minutes. The cells were then repelleted, resuspended in 100ml ice cold $CaCl_2$ and incubated on ice for 90-120 minutes. The cells were again re-pelleted and resuspended in 10ml ice-cold 100mM $CaCl_2$/15% glycerol. The competent cells were finally snap-frozen in a dry ice/ethanol bath and aliquots were stored indefinitely at –80°C.

Electro-competent Cells

An overnight bacterial culture was grown up at 37°C in 10ml LB supplemented with the appropriate antibiotic. 1ml of this fresh culture was used to inoculate 1000ml LB medium and was grown to A_{600} of 0.8. The culture was cooled on ice for 30 minutes and then cells were pelleted by centrifugation at 2600g at 4°C for 10 min. The cell pellet was washed by resuspending in 1000 ml of sterilized, ice-cold 10% glycerol (v/v) and centrifuged at 2500 g for 30 min. The cells were washed again and repelleted. The supernatant was removed apart from 2.5ml, which was used to resuspend the pellet. The competent cells were snap-frozen in a dry ice/ethanol bath. Aliquots were stored indefinitely at –80°C.

2.3.5: Transformation of Competent Cells

CaCl₂ Competent Cells

100μl of $CaCl_2$ competent cells were defrosted on ice and then added to 100ng DNA. The cells and DNA were gently mixed and left on ice for 30 minutes. The cells were then heat shocked at 42°C for 1.5 minutes, then left on ice for a further 2 minutes. Ampicillin-resistant transformed cells were directly plated onto LB-Amp plates. Kanamycin-resistant transformed cells were recovered in 500μl of LB by shaking at 37°C for 1 hour and then plated onto LB-Kan plates. Plates were incubated overnight at 37°C.

Electro-competent Cells

20μl of electro-competent cells were defrosted on ice, mixed with 100ng of plasmid DNA and incubated on ice for 30-60 seconds. The mixture of cells and DNA was transferred to a cold electroporator cuvette, which was then placed in the chilled safety chamber of the E. Coli pulsar (Biorad). Electroporation was performed in 100μl cuvettes at 1800 volts. The cells were resuspended in 1ml SOC medium and recovered by shaking for 30 minutes at 37°C. The transformed cells were then plated on selective medium.

2.3.6: Expression of GST-fusion proteins

BL21 cells containing the pGEX-4T3 plasmid with the gene of interest were cultured overnight in 5-10ml LB-AMP at 37°C with shaking. The overnight culture was then diluted 1/10 into LB-AMP and grown for 1-2 hours until A_{600} reached 0.6-0.8. The cells were cooled on ice for fifteen minutes and a sample was taken for later analysis (pre-induction). Expression of the protein of interest was optimised by inducing at varying concentrations of IPTG (0.5mM-1mM), and at varying temperatures (20°C-37°C). Samples of the induced culture were taken at different time points (2-3 hours). Cells from each sample were pelleted and resuspended in 4X sample buffer for immediate SDS-PAGE analysis.

For large-scale expression and purification of GST fusion proteins, protein expression was performed in the optimum conditions, determined as above. After induction of protein expression by IPTG, cells were pelleted at 4000g for 15 minutes at 4°C. Cells were then resuspended in 3ml of bacterial expression lysis buffer per 100ml of culture. 0.5μg of lysozyme was added per ml of culture to the cells in lysis buffer and then incubated on ice for 30 minutes. Cells were then sonicated with MSE soniprep and cell debris was pelleted at 12000g to leave the GST-fusion protein in the supernatant.

2.3.7: Binding GST-fusion protein to glutathione sepharose 4B beads

The protein of interest was expressed as described above. 100μl of 50% slurry of glutathione sepharose 4B beads were bound to GST-fusion protein isolated from 500ml

of culture as described in the manufacturer's protocol (Amersham Pharmacia Biotech). The protein bound to beads was used immediately or stored in 1x storage solution (1xPBS, 50% glycerol and 1mM benzamidine-HCl, 0.1mM PMSF, 1μg/ml each of leupeptin and pepstatin) at –20°C for a maximum of 1 week.

2.4: Molecular Biology Techniques

2.4.1: Buffers and Reagents

TE

10mM Tris

1mM EDTA pH8

TAE

40mM tris-acetate

1mM EDTA pH8

DNA loading buffer

50% glycerol

0.1M EDTA

1% (w/v) SDS

1mg/ml bromophenol blue

1mg/ml xylene cyanol

Primers were synthesised by MWG biotech:

Primer name	Sequence 5'-3'
PGEM-R-451	CAC ATG TTC TTT CCT GCG TTA TCC CC
PPI-2xMS2-F	CAG CCC GGG ATC CAA CAT GAG GAT CAC CCA TGT CAG CTG GTC GAC TCT AGA AAA CAT GAG GAT CAC CCA TGT TCC GGA AGG GGC AGG TGA CCT TC
PPI-8MS2F	CGA AGA TCT AGC CCT AAG TGA CCA GCT
PPI-8MS2R	GCG GTT AAC GCT CTT TCA AAG GTT TTA

8MS2 F	GCC TGT ACA GGA GGC CCG GGA TCC AAC
8MS2 R	CTG TGT ACA ACC TGC CCC TTC CGG AAC
Fluc-8MS2F	CGA AGA TCT CAT GGA AGA CGC CAA AAA C
Fluc-8MS2R	GCG GTT AAC TTA CAC GGC GAT CTT TCC
PPI-SDM1-903F	CAG AGC TGG TTT AGT GAA CCG TTA GAG ATC TAG CCC TAA GTG AC
PPI-SDM1-903R	GTC ACT TAG GGC TAG ATC TCT AAC GGT TCA CTA AAC CAG CTC TG
PPI-SDM2-903F	CAG AGC TGG TTT AGT GAA CCG TAG CCC TAA GTG ACC AGC TAC AG
PPI-SDM2-903R	CTG TAG CTG GTC ACT TAG GGC TAC GGT TCA CTA AAC CAG CTC TG
PShut-seq874F	AGG CGT GTA CGG TGG GAG
PShut-seq1168R	GAA ATT TGT GAT GCT ATT GC
8MS2HindIIIF	GCC AAG CTT GGA GGC CCG GGA TCC AAC
8MS2HindIIIR	CTG AAG CTT ACC TGC CCC TTC CGG AAC
8MS2HpaIF	GCC GTT AAC GGA GGC CCG GGA TCC AAC
8MS2HpaIR	CTG GTT AAC ACC TGC CCC TTC CGG AAC
Fluc-8MS2F	CGA AGA TCT CAT GGA AGA CGC CAA AAA C
MS2-EXF	CGA GGA TCC ATG GCT TCT AAC TTT ACT CAG
MS2-EXR	GCA CTC GAG TTA GTA GAT GCC GGA GTT TGC

2.4.2: Preparation of plasmid DNA from bacterial culture

Plasmid DNA was prepared from 5ml overnight cultures using gene elute plasmid miniprep kit (Sigma) or from 100ml cultures using wizard plus maxiprep kits (Promega).

2.4.3: Ethanol Precipitation of DNA

DNA was precipitated by the addition of 0.3M sodium acetate pH5.2 (final concentration) and 2 volumes ice-cold ethanol, followed by incubation on ice for 30 minutes. The precipitated DNA was pelleted by centrifugation at 16000g for 10

minutes at 4°C. The pellet was washed in 75% ethanol, dried under vacuum and dissolved in an appropriate volume of de-ionised water or tris-EDTA pH8.

2.4.4: Phenol/Chloroform extraction of DNA

An equal volume of phenol was added to the DNA-containing solution and vortexed. The mixture was centrifuged at 4000rpm for 20 minutes at 20°C. The upper aqueous phase was removed and added to an equal volume of phenol:chloroform (1:1). The mixture was vortexed until an emulsion was reached and then centrifuged at 16000g for 5 minutes at 20°C. The upper aqueous phase was removed and the DNA was ethanol precipitated from this solution as described above.

2.4.5: Agarose gel electrophoresis

Agarose (0.7%-1.5% w/v) was dissolved in TAE and supplemented with 0.1μg/ml ethidium bromide. Agarose gels were run horizontally immersed in 1X TAE at 100volts for 45 minutes.

2.4.6: Gel isolation of DNA fragments

DNA fragments were run on a 1% TAE agarose gel and visualised with ethidium bromide staining. The required fragment was identified by size using a 1kb or 100bp DNA marker (NEB) and excised from the gel. DNA was isolated from the gel using the Geneclean II kit (Anachem). Briefly, the gel was melted in 3 volumes of NaI at 55°C. 6μl of glassmilk was added to the melted gel/NaI mixture and incubated at room temperature for 5 minutes to allow the glassmilk to bind the DNA fragments. The glassmilk was pelleted by centrifugation at 16000g for 30 seconds and the pellet was washed three times in new wash solution. The pellet was dried and resuspended in water to elute the DNA.

2.4.7: Restriction enzyme digest

DNA was digested with 2.5-20units of restriction enzyme (NEB) according to manufacturer's instructions. Double digests were carried out together when possible or sequentially when reaction conditions varied.

2.4.8: Alkaline Phosphate treatment of DNA

Calf intestinal alkaline phosphatase (CIAP, Promega) was used to dephosphorylate restricted cloning vectors to prevent re-ligation. The restriction digest reaction mix was increased to a volume of 40μl and 1μl CIAP was added. The reaction mix was incubated for 30 minutes at 37°C then CIAP was heat inactivated at 85°C for 15 minutes.

2.4.9: Ligation of DNA

Insert DNA was ligated into 50ng of vector DNA in a 6:1 ratio using T4 DNA ligase (Promega) in a total volume of 10μl following manufacturer's instructions.

2.4.10: Amplification of DNA by PCR

Pfu polymerase (Promega) and specific oligonucleotides were used to amplify specific sequences of DNA. A 50μl reaction mix included: 1μl of DNA (100ng), 5μl 10X reaction buffer, 1μl dNTP mix (final concentration, 0.25mM each), 50pmol forward primer, 50pmol reverse primer and 0.5μl pfu polymerase (1.25 units). Cycles varied according to the Tm of the oligos and the length of DNA to be amplified. Generally, there was an initial denaturing period at 95°C for 2 minutes followed by thirty cycles of denaturing at 95°C for 35 seconds, annealing at a temperture determined by the Tm of the oligos for 30 seconds, and an extension period at 72°C for one minute for every 1kb to be amplified. Finally there was a five minute extension time at 72°C and then the reaction mixture was kept at 4°C.

10μl of PCR product was analysed on an agarose gel.

2.4.11: PCR Mutagenesis

Pfu turbo DNA polymerase (Stratagene) was used to delete DNA sequences within plasmids. A 50µl reaction mixture was set up containing 1µl template DNA (5-50ng), 5µl Pfu cloned 10X buffer, 125ng of forward primer, 125ng of reverse primer, 5µl dNTP mix (final concentration, 0.25mM of each) and 1µl of Pfu turbo DNA polymerase. Cycles varied according to the length of DNA to be amplified. Generally, there was an initial denaturing period at 95°C for 2 minutes followed by 18 cycles of denaturing at 95°C for 35 seconds, annealing 55°C for 1 minute, and an extension period at 68°C for two minutes for every 1kb to be amplified. Finally there was a five minute extension time at 68°C and then the reaction mixture was kept at 4°C. Methylated non-mutated parental DNA template was digested by the incubation of the PCR product with 1µl of DpnI for 1 hour at 37°C. 1µl-2.5µl of PCR product was then transformed into XL10 gold.

2.4.12: Sequencing of DNA

Sequencing of DNA was carried out by Lark technologies using silver service primer extension.

2.5: RNA techniques

2.5.1: Buffers and Reagents

10X MOPS
0.2M MOPS
50mM sodium acetate
10mM EDTA

Denaturing RNA sample loading buffer
62.5% deionised formamide
1.14M formaldehyde
1.25 X MOPS

0.114mM EDTA

1mg/ml bromophenol blue

1mg/ml xylene cyanol

50µg/ml ethidium bromide

5% (v/v) glycerol

SSC

3M NaCl

0.3M Na citrate

Church-Gilbert

0.5M NaHPO4 pH7.2

1mM EDTA

7% (w/v) SDS

2.5.2: Purification of RNA using Tri-reagent

RNA sample was added to an equal volume of Tri-reagent (Sigma) and vortexed. 100µl
of chlorobromopropane was added for every 500µl of Tri-reagent used and the mixture
was vortexed for 15 seconds. The mixture was centrifuged at 12000g for 15 minutes to
separate a lower organic phase containing DNA, a protein interphase and an upper
aqueous phase containing RNA. The upper aqueous layer was removed and RNA was
precipitated by the addition of an equal volume of isopropanol and sodium acetate
(0.3M final concentration). RNA was pelleted by centrifugation at 16000g for 10
minutes. RNA pellets were then washed in 75% (v/v) ethanol, dried under vacuum and
resuspended in an appropriate quantity of water.

2.5.3: Purification of RNA using guanidine hydrochloride

1 volume of RNA sample was added to 3 volumes of 8M guanidine hydrochloride,
0.1M sodium acetate and vortexed. An equal volume of ethanol was added and RNA
was precipitated at -80°C overnight. RNA was pelleted by centrifugation at 12000g for

15 minutes. RNA pellets were then washed in 75% ethanol, dried under vacuum and resuspended in an appropriate quantity of water.

2.5.4: Lithium chloride precipitation of RNA

RNA pellets were resuspended in H_2O and added to an equal volume of 5M LiCl. RNA was precipitated overnight at -80°C and then pelleted by centrifugation at 12000g for 15 minutes. RNA pellets were then washed in 75% ethanol, dried under vacuum, resuspended in an appropriate quantity of water.

2.5.5: Northern Blot Analysis

Denaturing RNA loading buffer was added to RNA samples in a 1:5 ratio and samples were heated at 65°C for ten minutes and snap cooled on ice for 2 minutes prior to loading. 1g of agarose was dissolved in 73.5ml dH_2O by boiling and was supplemented with 10ml of 10X MOPS and 16ml of formaldehyde (37%). Gels were run horizontally immersed in 1X MOPS at 80volts for one to two hours. RNA was visualised on a UV illuminator.

The gel was rinsed in dH_2O, soaked in 0.05M NaOH for 20 minutes and finally soaked in 20X SSC for 30 minutes. The gel was blotted by capillary action onto Hybond-N nylon membrane (Amersham) according to manufacturer's instructions. The membrane was dried at room temperature and RNA was fixed to the membrane by UV crosslinking for 4 minutes or baking at 80°C for two hours. While exposing to UV, the 28S and 18S bands were marked on the edge of the membrane to act as size markers for probed messages. The membrane was pre-hybridised in Church-Gilbert solution supplemented with 60µg/ml denatured salmon sperm DNA for 1 hour at 65°C in a rotating oven. Labelled probes were generated from cDNA specific for the appropriate RNA. 40ng of cDNA fragment in 23µl volume was denatured by boiling for 5 minutes at 100°C and snap-cooled on ice for 2 minutes. The labelling reaction was set up by the addition of 8µl OLB labelling 5X buffer (Promega), 8µl dATP/dGTP/dTTP (2.5mM each), 1µl BSA (10mg/ml), 1µl DNA polymerase klenow fragment (Promega) and 5µl [^{32}P]-CTP (3000ci/mmol, Amersham) and incubated for 1 hour at room temperature.

The labelling reaction was then spun through a G50 column (Amersham Pharmacia Biotech) to remove unincorporated [^{32}P]-CTP. The probe was boiled for five minutes and 20μl was added to the pre-hybridisation solution and membrane. The probe was hybridised to the membrane at 65°C, overnight. Remaining probe was stored at –20^{0}C and used within 2 weeks.

The membrane was washed twice in 2X SSC, 0.1% (w/v) SDS at room temperature for 15 minutes followed by a wash in 0.2X SSC, 0.1% SDS (w/v) at 60°C for 15 minutes. X-ray film was exposed to the membrane for 1 hour to 1 week at -80°C.

2.5.6: Reverse Transcription

cDNA was generated from Tri-reagent-isolated total RNA using reverse transcriptase according to the manufacturer's instructions (Stratagene).

2.6: Protein techniques

2.6.1: Buffers, Reagents and Antibodies

SDS PAGE running buffer
1X tris-glycine buffer
1% (w/v) SDS

Laemmli sample buffer (4X)
0.25M Tris pH6.8
4% (w/v) SDS
40% (v/v) glycerol
10% (v/v) β-mercaptoethanol
20μg/ml bromophenol blue

Coomassie blue stain
45% (v/v) methanol
10% (v/v) acetic acid glacial

0.625g coomassie blue R

Destain/fixing solution

50% (v/v) methanol

10% (v/v) acetic acid

Transfer Buffer

1X tris-glycine buffer

1% (w/v) SDS

20% (v/v) methanol

PBS-Tween

1X PBS

0.1% (v/v) tween

Anode buffer for SDS-Tricine gels

0.2M tris-HCl pH8.9

Cathode buffer for SDS-tricine gels

0.1M tris

0.1M tricine pH8.25

0.1% (w/v) SDS

Gel buffer for SDS-Tricine gels

3M tris-HCl pH8.45

0.3% (w/v) SDS

MIN6 lysis Buffer

1% (v/v) triton

10mM β-glycerophosphate

50mM tris-HCl pH7.5

1mM EDTA

1mM EGTA

1mM sodium orthovanadate

1mM benzamidine-HCl

0.2mM phenylmethylsulfonyl fluoride

1µg/ml leupeptin

1µg/ml pepstatin

0.1% (v/v) β-mercaptoethanol

50mM sodium fluoride

RIPA buffer

50mM Tris HCl pH8

150 mM NaCl

1% NP-40

0.5% (w/v) sodium Deoxycholate

0.1% (w/v) SDS

Antibodies

Anti-eIF2α, anti-eIF4GI, anti-eIF4A and anti-polyA binding protein (PABP) antibodies were gifts from Chris Proud (Dundee University), Simon Morley (Sussex University), H.Trachsel (Bern University) and Amelia Nieto (Centro Nacional de Biotecnología Cantoblanco, Madrid) respectively. Anti-Erk2 antiserum was purchased from New England Biolabs. Anti-proinsulin (bovine) was purchased from Sigma. Anti-SRP54 and anti-CPH was purchased from Beckton-Dickenson. Anti-PC2 was a kind gift from Chris Rhodes (Seattle). Anti-GFP was purchased from Molecular Probes.

Standard SDS PAGE

Solution	12.5% SDS-PAGE running gel	20% SDS-PAGE running gel	Stacking gel
40% acrylamide	3.15ml	4.85ml	1.24ml
2% bis-acrylamide	0.5ml	0.8ml	0.65ml
1.5M Tris-HCl, pH8.8	2.5ml	2.5ml	-
1.0M Tris-HCl pH6.8	-	-	1.25ml
H_2O	3.7ml	1.7ml	6.7ml

10% SDS	0.1ml	0.1ml	0.1ml
TEMED	5μl	5μl	10μl
10% APS	50μl	50μl	50μl

2.6.2: SDS PAGE

Running gels were prepared with the acrylamide percentage depending on the range of molecular weights to be analysed. Running gels were poured between two glass plates and allowed to set and then the stacking gel was poured and allowed to set. 4X sample buffer was added to the protein sample and boiled at 100°C for 3 minutes to denature the samples. The gel was run vertically in SDS PAGE running buffer at 180 volts for 1 hour until the bromophenol blue had reached the bottom of the gel. Broad-range pre-stained protein molecular weight markers (NEB) were run alongside samples.

2.6.3: Bradford assay

The Bradford protein assay was used to determine protein content of cell lysates. Dye reagent (Bio-rad) was diluted with water 1/5. 10μl of protein sample was mixed with 1ml of diluted Bradford reagent and incubated for 5 minutes at room temperature. The A_{595} of the reaction mixture was measured and protein content of unknowns was determined by performing linear regression with BSA protein standards ranging from 0mg/ml to 20mg/ml.

2.6.4: Coomassie Staining of proteins run by SDS PAGE

SDS-PAGE gels were shaken in coomassie blue stain for 30 minutes at room temperature. The coomassie was then removed and the gel was placed in destain solution overnight. The gel was rinsed in water and rehydrated in 5% glycerol for 15 minutes and dried under vacuum at 80°C for two hours.

2.6.5: Western Blot Analysis

Protein samples were run on SDS PAGE as described above and then transferred onto Immobilin-P membrane (Millipore) using the trans-blot semi-try transfer cell (Bio-rad).

The membrane was blocked in 5% milk PBS-tween for one hour at room temperature, followed by an overnight incubation at 4°C in the specific antibody in 5% milk PBS-tween. Antibody concentrations were adjusted according to manufacturer's instructions. The membrane was washed twice for 15 minutes in PBS-tween and then incubated in 3.3μl of secondary antibody (NEB) added to 10ml of 5% milk PBS-Tween for 1 hour at room temperature. The membrane was washed three times for 15 minutes with PBS-tween. Enhanced chemi-illuminescence using ECL reagent (Amersham Pharmacia Biotech) detected the proteins of interest.

2.6.6: Trichloroacetic acid precipitation of proteins

5μl of cell lysate was spotted onto a 1cm^2 piece of filter paper, placed into 200ml 5% (w/v) TCA with a pinch of unlabelled methionine and boiled for 2 minutes. The liquid was discarded and replaced with 200ml 5% TCA and boiled again for 2 minutes. The liquid was discarded again and the papers were rinsed in 5% TCA followed by 100% ethanol. The papers were dried at 80°C for 20 minutes.

2.6.7: Immunoprecipitation

5μl of antibody was coupled to 25μl of Protein G Sepharose per immunoprecipitation for 1 hour at room temperature. The bound antibody/protein G complexes were washed in 1ml MIN6 lysis buffer then added to [^{35}S]-Methionine labelled MIN6 protein lysates or *in vitro* translations (final volume of 250μl made up with MIN6 lysis buffer) and rotated for 2 hours at room temperature unless otherwise stated. The beads were washed three times in MIN6 lysis buffer and the bound proteins finally eluted in Laemmli sample buffer prior to being separated by SDS-PAGE. CPH immunoprecipitations were performed by the same technique but replaced MIN6 lysis buffer with RIPA buffer.

2.7: Biochemical techniques

2.7.1: Buffers and solutions

Sucrose gradient solutions

Sucrose (amount dependent on percentage required)

20mM HEPES pH7.6

2mM $MgCl_2$

130mM KCl

1mg/ml heparin

1mg/ml cycloheximide

1mM dithiothreitol (DTT)

Low salt polysome buffer

20mM HEPES pH7.6

2mM $MgCl_2$

130mM KCl

1mg/ml heparin

1mg/ml cycloheximide

2mM DTT

1mM benzamidine-HCl

0.2mM PMSF

1µg/ml leupeptin

1µg/ml pepstatin

High salt polysome buffer

20mM HEPES pH7.6

15mM $MgCl_2$

300mM KCl

1mg/ml heparin

1mg/ml cycloheximide

2mM DTT

1mM benzamidine-HCl

0.2mM PMSF

1µg/ml leupeptin

1µg/ml pepstatin

Hypertonic lysis buffer

250mM sucrose

250mM KCl

10mM MgCl$_2$

10mM tris-HCl pH7.5

1mM EDTA

2mM DTT

1mg/ml RNAsin

1mM benzamidine-HCl

0.2mM PMSF

1µg/ml leupeptin

1µg/ml pepstatin

0.1mg/ml cycoheximide

1X Tris/Magnesium/Potassium (TMK) buffer

100mM Tris Hcl pH8

10mM MgOAc

80mM KCl

1mg/ml heparin

1µl/ml RNAguard

Pull-down lysis buffer

20mM HEPES pH7.5

10mM MgCl

130mM KCl

10% (v/v) glycerol

1mg/ml heparin

100µg/ml cycloheximide

1% (v/v) triton

1mM DTT

1µl/ml RNAguard

1mM benzamidine-HCl

0.2mM phenylmethylsulfonyl fluoride

1µg/ml leupeptin

1µg/ml pepstatin

Elution buffer

20mM HEPES pH7.6

1µl/ml RNAguard

1mM benzamidine-HCl

0.2mM phenylmethylsulfonyl fluoride

1µg/ml leupeptin

1µg/ml pepstatin

1mg/ml heparin

Potassium/HEPES/Magnesium (KHM) buffer

25mM potassium HEPES pH 7.2

130mM potassium acetate

5mM magnesium acetate

1mM dithiothreitol

1µl/ml RNAguard

1mg/ml heparin

2.7.2: Liquid Scintillation Counting of radioactive-labelled samples

[^{35}S]-methionine labelled protein samples were TCA precipitated onto filter paper as described above. The dried papers were placed into vials, 3ml of emulsifier safe liquid scintillation fluid (Packard biotech) was added and counts per minute (cpm) were measured with a Packard scintillation counter.

[^{32}P]-CTP samples were spotted onto 1cm^2 of filter paper, placed in vials and counted with the Packard scintillation counter.

2.7.3: Sucrose Gradients

Gradients were made in Sorvall 12ml polyallomer centrifuge tubes with a 500μl 60% (w/v) sucrose cushion at the bottom. Sucrose gradients were made by the sequential layering and freezing of sucrose gradient solutions of decreasing sucrose concentrations (eg for 7-47% sucrose gradients, solutions of 47%, 39%, 31%, 23%, 15% and 7% (w/v) were added). Prior to use sucrose gradients were defrosted at 4°C overnight or at room temperature for 3 hours.

Cycloheximide was added to cells ten minutes prior to lysis to a final concentration of 100μg/ml. Cells were scraped into high salt polysome buffer supplemented with 1% Triton (unless otherwise specified), vortexed briefly and centrifuged at 16000g for 10 minutes to pellet cell debris and unlysed cells. Lysates were layered onto the top of each gradient and centrifuged at 39 000rpm for 2 hours at 4°C in a Sorvall TH64.I rotor. The gradients were then fractionated using the ISCO gradient fractionator. 65% sucrose solution was pumped to the bottom of the gradient, which displaced the gradient solution upwards and pumped it through a UV absorbance monitor measuring absorbance at 254nM. RNA was precipitated overnight from 1ml fractions at −80°C by the addition of 3ml of 8M guanidine HCl and 4ml of ethanol.

2.7.4: Subcellular fractionation of cell lysates

In all protocols, cycloheximide was added to cells ten minutes prior to lysis to a final concentration of 100μg/ml.

Consecutive centrifugation method
Cell lysates were fractionated using an adaptation of the protocol from Frey *et al* (Frey et al., 2001). After incubation as described in the figure legends, cells were scraped into 1.5ml hypertonic lysis buffer and homogenised with 12 strokes in a dounce homogeniser. The homogenate was centrifuged at 1200g for 2 minutes at 4°C to pellet

unlysed cells and nuclei. The lysate was consecutively centrifuged at 6000g for 20 minutes at 4°C (to pellet membranes) followed by centrifugation at 18000g for 20 minutes at 4°C and then at 200000g for 40 minutes at 4°C (to pellet ribosomes). The pellets were resuspended in polysome buffer. The pellets and final supernatant were analysed by western blotting or RNA was precipitated with the addition of three volumes of 8M guanidine HCl and four volumes of ethanol.

Permeablisation of cells method

Cells were washed in PBS containing cycloheximide, removed from the plate by trypsin-EDTA (Invitrogen) supplemented with cycloheximide and resuspended in 4ml of high salt polysome buffer. Cells were then pelleted at 250g for 2 minutes at 4°C and were then resuspended in 1ml of high salt polysome buffer. Digitonin (Calbiochem) was added to a final concentration of 80µg/ml and cells were incubated on ice for 5 minutes. Membranes were then pelleted at 250g for 3 minutes. The pellet and supernatant were analysed by western blotting or RNA was isolated using Tri-reagent.

2.7.5: mRNA-MS2 binding protein pull-down assay

MS2-GST glutathione sepharose 4B beads were washed twice in 1ml of TMK buffer and resuspended so as to give 50% slurry of beads. RNA samples (either purified RNA or cell lysates) were incubated with 5µl of 50% slurry per 6cm plate of MIN6 cells on a rotator at 4°C for 25 minutes. The beads were then washed three times with 1ml of TMK buffer.

2.7.6: *In vitro* transcription

All *in vitro* transcriptions were carried out using Riboprobe® *in vitro* transcription system (Promega) and T7 RNA polymerase.

2.7.7: Poly(A) mRNA Selection

Poly(A) mRNA was selected using poly(A) select kit (Promega).

2.7.8: *In vitro* translation

Rabbit reticulocyte lysates (Promega) were either used as provided or were centrifuged twice at 200000g for 20 minutes at 4°C to give a post-ribosomal rabbit reticulocyte lysate. Membranes for *in vitro* translation were isolated as described for subcellular fractionation and were then washed twice in 500µl of KHM buffer and resuspended in 20µl of KHM buffer. 4µl of membranes or 1µg of RNA was used in each *in vitro* translation reaction. *In vitro* translation reactions were incubated for 1 hour at 30°C in the following reaction mix:

Rabbit reticulocyte lysate (+/- ribosomes):	14µl
Amino acid mix (- methionine):	0.4µl
[^{35}S]-methionine:	3µl
RNAguard	0.8µl
RNA (1µg or 4µl of membranes)	
Total Volume:	20µl

2.8: Virus techniques

2.8.1: Preparation of viral stocks

Adenoviruses were synthesised using the Adeasy system (figure 2.1), (He et al., 1998) and all adenoviruses used in this study were made from pShuttle CMV vectors containing the gene of interest. To synthesise the adenovirus backbone vector containing the gene of interest, E.Coli, BJ5183 cells were co-transformed by electroporation with 1µg of kanamycin resistant pshuttle vector that was linearised by digestion with PmeI and 0.1µg of ampicillin resistant adenoviral backbone vector, pAdeasy-1. Within the BJ5183 cells, pAdeasy-1 and pShuttle CMV recombined to form the kanamycin resistant pAdeasy 1 recombinant that contained the gene of interest. Digestion with PacI identified positive recombinants, which resulted in a 3.5kb or 4Kb fragment. The recombinants were then transformed into E.Coli, XL10 gold, which resulted in a better yield of plasmid. Approximately 2.5µg of recombinant vector was

linearised with PacI to make linear adenoviral genome, which was then purified by ethanol precipitation and transfected by calcium phosphate transfection into one T-25 flask of 293 cells.
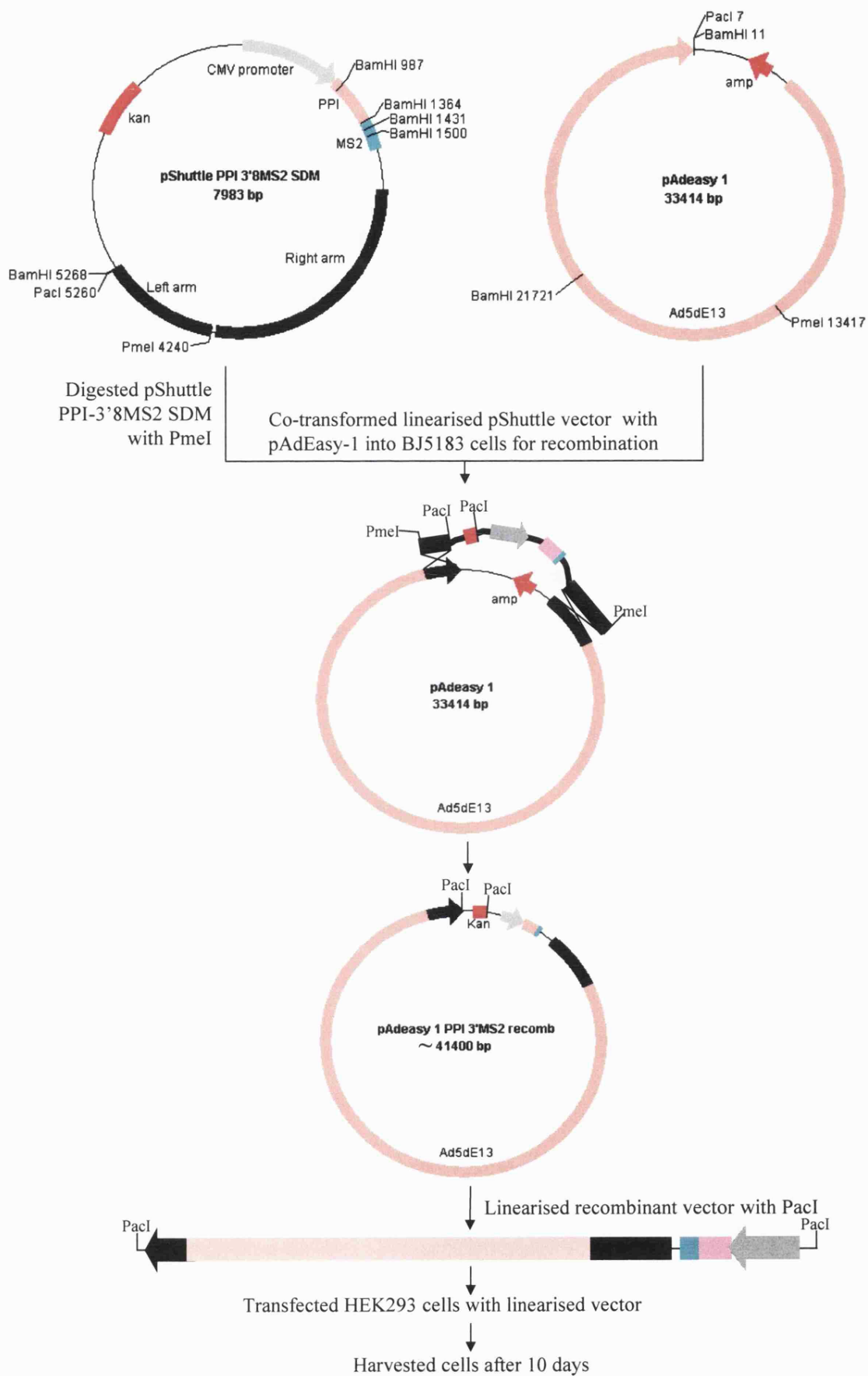
Figure 2.1: Synthesis of viruses (adapted from He et al 1998 PNAS)

2.8.2: Harvesting virus from 293 cells

The viruses were ready for harvesting 7 to 10 days after the transfection of the recombinant adenoviral plasmids. Cells were washed off the flasks, transferred to 50ml conical tubes and pelleted at 3000g for 5minutes. The pellets were resuspended in 2ml 1X PBS, frozen in a dry ice/ethanol bath then thawed in a 37°C water bath and vortexed vigourously. This freeze/thaw/vortex cycle was repeated 3 more times to lyse the cells. The samples were spun again at 3000g for 5 minutes to pellet cell debris and the viral supernatant was stored at -80°C.

2.8.3: Producing high titre virus stocks

90% of the viral supernatant was used to re-infect one confluent T-25 flask of 293 cells. When GFP was present, transfections and viral productions were monitored by GFP expression. After approximately 3-5 days post-infection, when a third to half of the cells had detached from the flask, the virus was harvested by four cycles of freeze/thaw/vortex as described above. The virus supernatant from one T-25 flask was used to infect two T-75 flasks and the virus supernatant from one T-75 flask was used to infect four T-75 flasks. Finally high titre virus was produced when the virus supernatant from four T-75 flasks was used to infect 20 T-75 flasks.

2.8.4: Infection of target cells with high titre virus

100μl high titre virus in 1ml DMEM -FCS was added per 6cm plate of cells. Cells were incubated for one hour at 37°C, 3ml of MIN6 DMEM was added and the cells were incubated for 24-48 hours.

2.9: Quantification of bands

All quantification of blots was performed using ImageJ (downloaded from http://rsb.info.nih.gov/ij/)

2.10: Microscopy

All images were obtained with the Olympus IX70 confocal microscope and were analysed with Olympus fluoview software.

2.11: Microarray Analysis

2.11.1: Preparation of cRNA samples and hybridisation to microarrays

Biotin-labelled cRNA was prepared from total RNA as described previously (GeneChip expression analysis technical manual at www.affymetrix.com) and in chapter 5. Biotin-labelled cRNA for experiment 1 was hybridised to MOE 430A oligonucleotide microarrays at the Microarray facility, University of Leicester. Biotin-labelled cRNA for experiment 2 was hybridised to MOE 430A oligonucleotide microarrays at the MRC microarray facility, University of Cambridge.

2.11.2: Data analysis and criteria for gene selection

Data was analysed using MicroArray Suite 5 (MAS5, Affymetrix) and dChip (www.dchip.org) software.

MAS5

Arrays were normalised using all probe sets to a target signal of 50. Genes showing changes in expression were selected by the following criteria: 1) Exclusion of genes with absent calls in both baseline and experimental arrays; 2) Exclusion of genes with no change call between baseline and experimental arrays and 3) A threshold of 1.5 fold or 2 fold change in expression levels in each of the experiments. Further analysis was carried out using Microsoft Excel.

DChip

Arrays were normalised using the invariant set method. Genes showing changes in expression were selected by the following criteria: 1) Exclusion of genes with a change of less than 100 between baseline and experimental arrays and 2) A threshold of 1.5 fold or 2 fold change in expression levels in each of the experiments within the 90% confidence interval.

Chapter 3: Investigation Into Glucose-Stimulated Proinsulin Synthesis In Pancreatic β-Cells

3.1: Introduction

Upon stimulation of the pancreatic β-cell with glucose there is a 10-20 fold increase of proinsulin (PI) synthesis within 60 minutes (Grimaldi et al., 1987; Guest et al., 1991; Itoh and Okamoto, 1980). This increase occurs in the absence of any change in preproinsulin (PPI) mRNA abundance (Itoh and Okamoto, 1980), or in the presence of the transcription inhibitor; actinomycin D (Alarcon et al., 1993; Permutt and Kipnis, 1972a; Tillmar et al., 2002). Therefore, glucose stimulated PI synthesis is regulated at the post-transcriptional level, likely through an increase in the rate of protein synthesis. Indeed, it has been variously reported that PI synthesis is post-transcriptionally regulated by glucose through changes in the rate of translational initiation and elongation, signal recognition particle arrest and mRNA stability (Tillmar et al., 2002; Watanabe, 1982; Welsh et al., 1986). Interestingly, it has been shown that the synthesis of a number of other secretory proteins is translationally up-regulated in parallel with PI in response to glucose (Guest et al., 1991). These include prohormone converatses, PC2 and PC3 but not the enzyme carboxypeptidase H, all of which are involved in the processing of PI to form insulin (Alarcon et al., 1993; Guest et al., 1989; Martin et al., 1994; Rhodes and Alarcon, 1994).

Previous studies show that initiation plays a key role in the regulation of PPI mRNA translation in response to glucose. Subcellular fractionation of islets of Langerhans shows the recruitment of cytosolic 'free' PPI mRNA onto polysomes, suggesting an increase in the rate of de novo initiation of translation (Itoh and Okamoto, 1980; Welsh et al., 1986; Welsh et al., 1991; Welsh et al., 1987). This increase of polysomal PPI mRNA accounts for the recruitment of 15-38% of total PPI mRNA onto polysomes at high glucose. Although the mechanism of regulating the rate of initiation is poorly understood, it is likely that the 5' and 3' UTRs play an important role by working together co-operatively to increase glucose stimulated PI synthesis (Wicksteed et al., 2001). The 3' UTR acts to stabilise PPI mRNA in a β-cell specific manner. In fact, it has been shown that the 3'-UTR contains a polypyrimidine rich sequence, which

specifically binds polypyrimidine tract binding (PTB) protein in β-cells at high glucose (Tillmar et al., 2002). PTB plays an important role in polyadenylation, RNA localisation and translation, and may therefore play a key role in regulating PI synthesis in response to glucose.

mRNAs encoding secretory proteins, such as PPI, CPH and PC2 are recruited co-translationally from a cytoplasmic pool to the rough endoplasmic reticulum (ER) to ensure polypeptide translocation across the ER and entry into the secretory pathway (Palade, 1975). In islets, glucose was shown to stimulate the recruitment of PPI mRNA onto the ER the site of PI synthesis (Itoh and Okamoto, 1980; Welsh et al., 1986; Welsh et al., 1991; Welsh et al., 1987). These data showed that approximately 50% more PPI mRNA is found associated with the ER at high glucose compared to at low glucose (Itoh and Okamoto, 1980; Welsh et al., 1986; Welsh et al., 1991; Welsh et al., 1987). Furthermore, Welsh *et al*, 1986 showed that these changes in PPI distribution were accompanied by an increase in the amount of SRP 7S RNA associated with the membranes. However, this small increase in ER-associated PPI mRNA does not appear sufficient to explain the large increases in PI synthesis in response to glucose. Itoh *et al*, 1980 therefore suggest that PI synthesis may be regulated at the ER, most likely through an increase in the rate of elongation. Yet, Welsh *et al*, 1986 suggest that PPI synthesis is stimulated by glucose through a combination of a non-specific increase in de novo initiation, a specific recruitment of PPI mRNA to the ER and an increase in the rate of elongation. They suggest this combination of events in response to an increase in glucose concentration would be sufficient to stimulate a large increase in PI synthesis.

3.1.1: Aims

The precise mechanism of how glucose stimulates an increase in PI synthesis is poorly understood and remains to be accounted for. Therefore, the aim of this chapter is to further investigate the mechanism of translational regulation of PI synthesis in response to glucose.

3.2: Results

3.2.1: Polysome analysis of MIN6 cells incubated in low or high glucose concentrations

To investigate which steps may be important in regulation of PI synthesis in response to changes in glucose concentration, polysome analysis of MIN6 cells incubated in low or high glucose was carried out by sucrose sedimentation gradient centrifugation.

Optimisation of conditions for polysome analysis

Initially, the optimum conditions for polysome analysis were determined by varying the concentrations of triton and salt. Polysome analysis of MIN6 cells was carried out using low salt (130mM KCl and 2mM MgCl₂) polysome buffer supplemented with either 0.1% or 1% Triton (figure 3.1a). MIN6 cells were incubated in MIN6 media (see materials and methods section 2.2.1) and 0.1mg/ml of cycloheximide (final concentration) was added to cells 10 minutes prior to lysis to prevent ribosomal run-off. Cells were vortexted for 10 seconds and centrifuged at 12000g for 10 minutes to pellet the nuclei and unlysed cells. The supernatants containing the cell lysates were layered onto 7-47% sucrose gradients, which were centrifuged at 39000rpm for two hours at 4°C. Gradients were subsequently fractionated and the absorbance was measured continuously at 254nm to give polysome profiles of MIN6 cells lysed in 0.1% or 1% triton (figure 3.1a). Varying the concentration of triton between 0.1% and 1% had no effect on the polysome profiles of MIN6 cells (figure 3.1a), therefore, all future experiments with MIN6 cells were carried out using 1% Triton to ensure full lysis of MIN6 cells and maximum yield of RNA.

Work has shown that some mRNAs are associated with the cytoskeleton and that lysing cells with low salt polysome buffer may not dissociate these mRNAs (Biegel and Pachter, 1992). If these mRNAs remain associated with the cytoskeleton they may be pelleted in the 12000g spins, which are required to pellet nuclei and unlysed cells, resulting in a disproportionate population of mRNAs. However, the presence of high salt has been shown to dissociate mRNAs that are associated with the cytoskeleton (Hesketh and Pryme, 1991). However, on the other hand, high salt may cause the dissociation of protein, which may effect the sedimentation properties of specific mRNAs. Therefore, to test the effect of changes in salt concentration on MIN6

Figure 3.1: Optimisation of conditions for polysome analysis MIN6 cells were incubated in DMEM (a) or were pre-incubated in KRB containing 2mM glucose for 1h followed by incubation in KRB containing 2mM or 20mM glucose for a further hour (b and c). 0.1mg/ml (final concentration) of cycloheximide was added cells 10 minutes prior to lysis to prevent ribosomal run-off. Cells were lysed in low salt (a and c) or high salt (b) polysome buffer supplemented with 1% or 0.1% Triton and the lysates layered onto 7 - 47% sucrose gradients containing the appropriate salt concentrations for the lysis buffer used. The gradients were then centrifuged at 39000rpm at 4^0C for 2h and fractionated from top (fraction 1) to bottom (fraction 10) using the ISCO gradient fractionator. Absorbance of gradients was measured continually at 254nm to give polysome profiles. RNA was isolated from 10, 1ml fractions and run on 1% (w/v) agarose formaldehyde gel (b and c only). RNA was then transferred onto nylon membrane and probed for PPI mRNA. These results are representative of three separate experiments.

a) Triton

0.1% triton

1% triton

b) High salt

2mM glucose

20mM glucose

40S
60/
80S
polysomes

PPI →

Fraction number

c) Low salt

2mM glucose

20mM glucose

40S
60/
80S
polysomes

PPI →

Fraction number
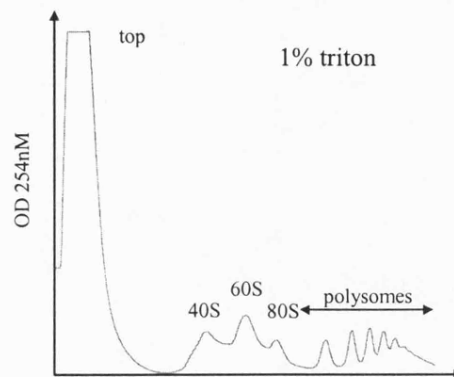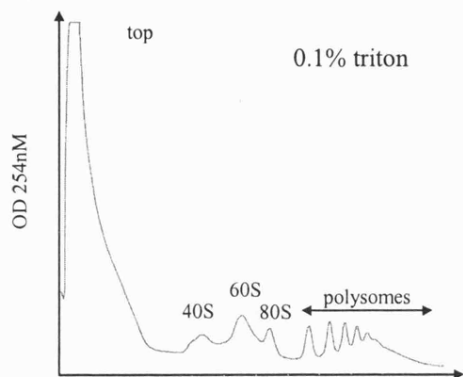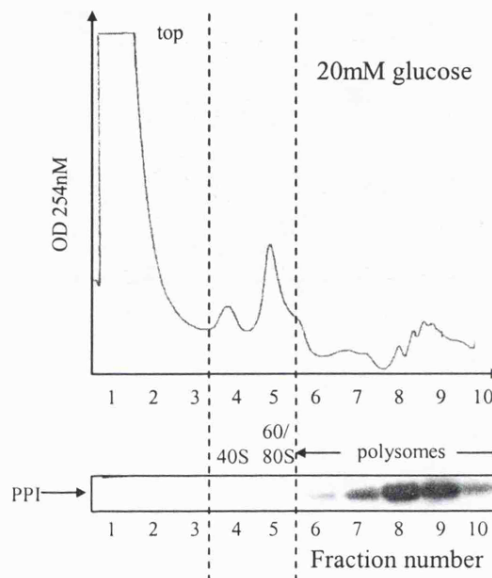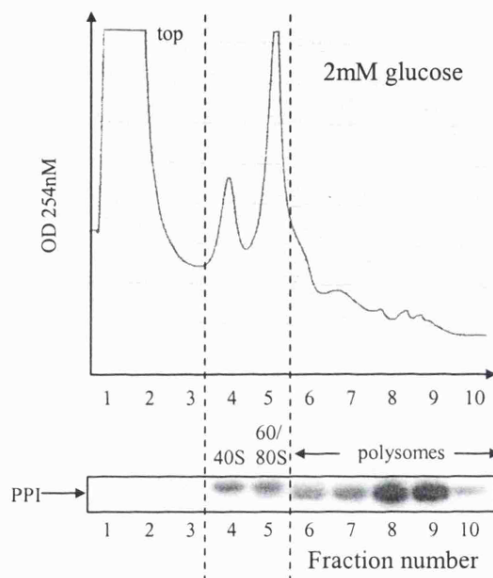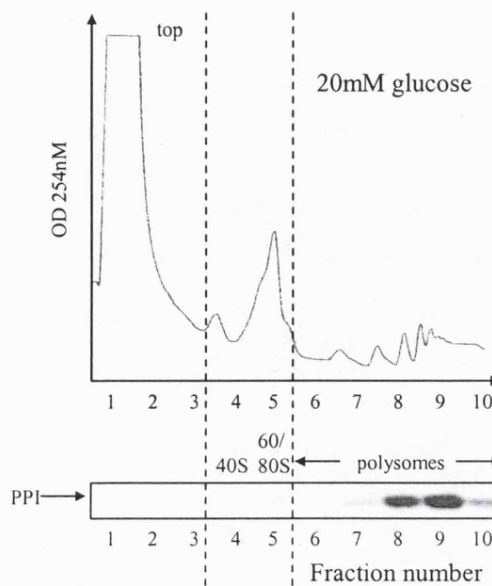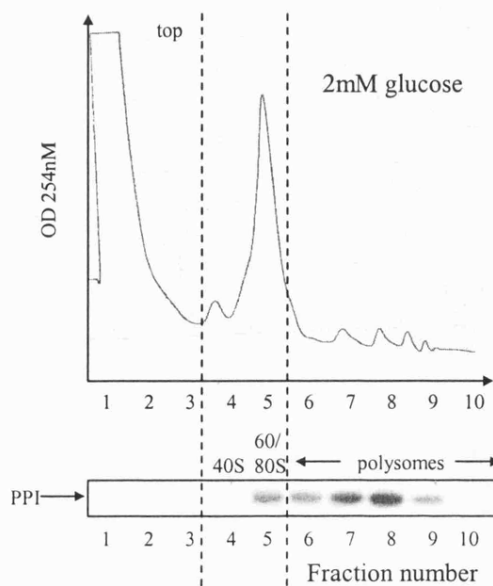
polysome profiles and the distribution of mRNAs, polysome analysis was carried out in MIN6 cells that were lysed in either low salt (130mM KCl and 2mM MgCl$_2$) or high salt (300mM KCl, 10mM MgCl$_2$) polysome buffer by the method described for figure 3.1a. Cells were incubated in KRB containing 2mM glucose for one hour and then further incubated for one hour in KRB containing 2mM or 20mM glucose. Polysome analysis at high salt concentration resulted in a small increase in polysomes compared to those lysed in low salt polysome buffer (figure 3.1b). It is likely that this change in the shape of the profile is due to increased salt concentration causing the dissociation of mRNAs from the cytoskeleton. However, changing the salt concentration had no effect on the sedimentation of PPI within the gradient. Therefore, to ensure maximum recovery of mRNAs, high salt concentrations were used in all subsequent experiments, unless noted otherwise.

Glucose stimulates the recruitment of ribosomes onto PPI mRNA

Having established the optimum conditions for polysome analysis, the sedimentation of specific mRNAs in MIN6 cells was determined by polysome analysis. MIN6 cells were incubated in KRB containing 2mM or 20mM glucose and lysed in high salt polysome buffer supplemented with 1% triton (figure 3.2). Absorbance profiles of the gradients show that an increase in the glucose concentration from 2mM to 20mM results in a large decrease in the 60S/80S peak and an increase in the polysome peaks. This indicates that glucose stimulates the movement of ribosomes onto mRNAs and therefore suggests that glucose stimulates an increase in the global rate of initiation. The results of this study are similar to those reported previously (Gomez et al., 2004). Each gradient was fractionated into 20 fractions, RNA was isolated from each fraction, run on a formaldehyde gel and stained with ethidium bromide. The distribution of specific mRNAs was determined by Northern blot analysis (figure 3.2). All of PPI mRNA isolated from MIN6 cells incubated at either low or high glucose co-sedimented with monosomes or polysomes. Surprisingly, no PPI mRNA sedimented at the top of the gradient, where free mRNA is expected to sediment. There was a small but significant shift of PPI mRNA onto heavier polysomes at high glucose, indicative of a recruitment of ribosomes onto PPI mRNA. Glucose also simulated the recruitment of ribosomes onto S7, CPH, PC2 and actin mRNAs, indicating an increase in the rate of initiation for these mRNAs as well as for PPI mRNA. No free mRNA encoding secretory proteins
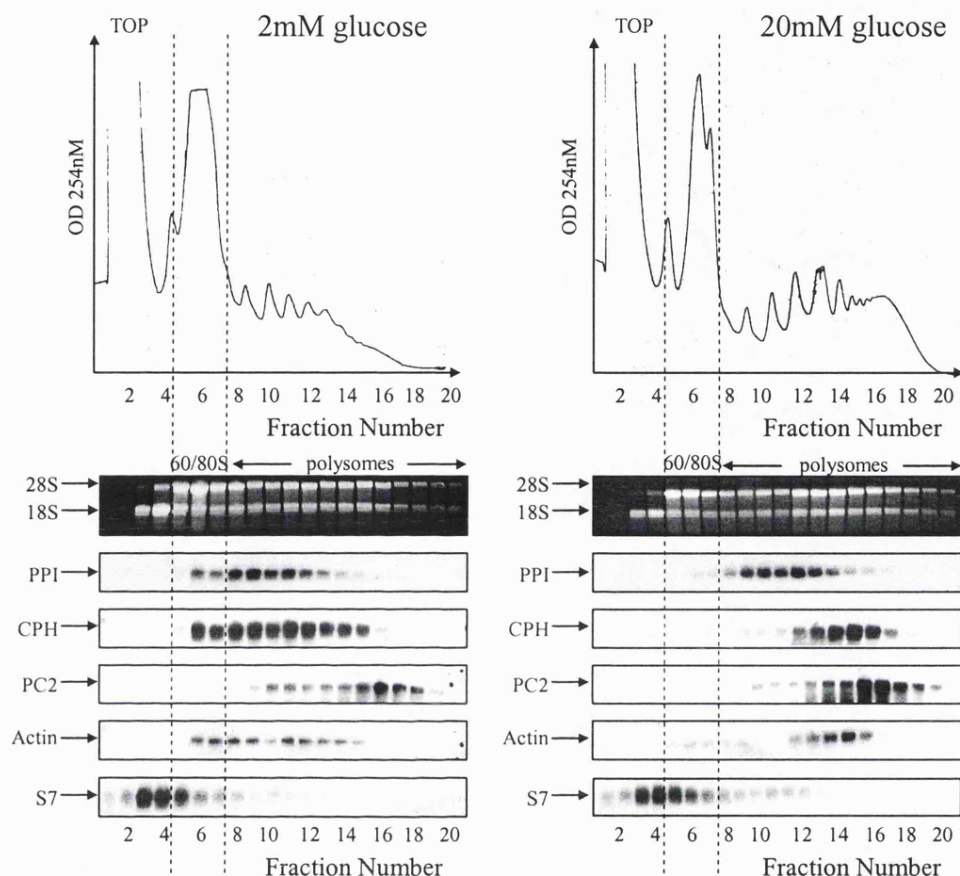
Figure 3.2: Glucose stimulates an increase in the rate of re-initiation on PPI mRNA. MIN6 cells were pre-incubated in KRB containing 2mM glucose for 1h followed by incubation in KRB containing 2mM or 20mM glucose for a further hour. 0.1mg/ml (final concentration) of cycloheximide was added to the cells 10 minutes prior to lysis to prevent ribosomal run-off. Cells were lysed and the lysates layered onto 7 - 47% sucrose gradients. The gradients were then centrifuged at 39000rpm at 4°C for 2h and fractionated from top (fraction 1) to bottom (fraction 20) using the ISCO gradient fractionator. Absorbance of the gradients was measured continually at 254nm to give polysome profiles. RNA was isolated from 20, 1ml fractions and run on 1% agarose formaldehyde gel. RNA then was transferred onto nylon membrane and probed for specific mRNAs as shown. These results are representative of three separate experiments.

CPH and PC2 or cytosolic protein actin was observed at low or high glucose concentrations. However, S7 mRNA, a 5' tract oligopyrimidine (TOP) mRNA that is also translated in the cytosol, sedimented near the top of the gradient indicating that this mRNA was likely to be free.

To establish that the sedimentation properties of PPI mRNA were due to the association of the PPI mRNA to the ribosomes, polysome analysis was carried out in the presence of 15mM EDTA and the absence of Mg^{2+} (Figure 3.3). EDTA chelates Mg^{2+}, which causes the dissociation of ribosomes from RNA but does not generally disrupt non-ribosomal RNA-protein complexes (mRNPs) (Calzone et al., 1982). The presence of EDTA and absence of Mg^{2+} dissociated the polysomes to 40S and 60S ribosomal subunits (figure 3.3). Furthermore, both PPI and actin mRNAs sedimented at the top of the gradient, suggesting that their co-sedimentation with polysomes further down the gradient in the absence of EDTA is due to the association of ribosomes (figure 3.2).

Summary

These results suggest that PI synthesis is not regulated by an increase in de novo initiation of translation, i.e. the recruitment of ribosomes onto free PPI mRNA. Rather, they suggest that glucose stimulates the recruitment of ribosomes onto mRNA associated with one or more ribosomes. This increase is relatively small and affected all mRNAs tested. Thus, it is unlikely that the increase in ribosomes associated with PPI mRNA accounts for the reported specific increase in PI synthesis in response to high glucose concentration (Itoh and Okamoto, 1980).

Glucose stimulates the recruitment of ribosomes onto PPI mRNA both in the cytosol and at the ER

Polysome analysis of MIN6 cells showed that all PPI mRNA is associated with ribosomes at both low and high glucose and that glucose stimulates a small but significant shift of PPI mRNA onto heavier polysomes (figure 3.2). However, it is possible that the recruitment of ribosomes onto ER-associated PPI mRNA is partially
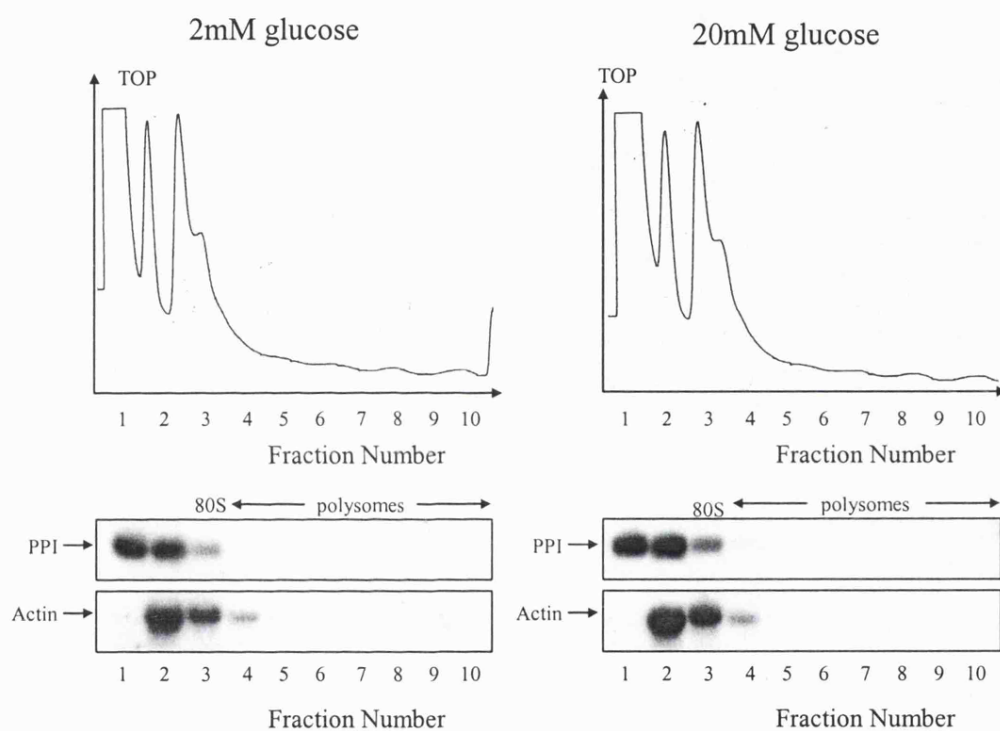
Figure 3.3: EDTA dissociates ribosomes from PPI and actin mRNA. Cells were treated and fractionated as described for figure 3.2, except MgCl$_2$ was excluded and 15mM EDTA was included in the lysis buffer and the sucrose gradients to dissociate the ribosomes. These results are representative of two separate experiments.

concealed by a population of non-translating ribosome-associated cytosolic PPI mRNA. To analyse the distribution of PPI mRNA in the cytosolic and membrane fractions, MIN6 cells that had been incubated in low or high glucose were lysed in hypertonic lysis buffer and the membrane fraction was separated from the cytosolic fraction by centrifugation at 6000g for 20 minutes. The pellet containing the membranes was then resuspended in polysome buffer supplemented with 1-% (w/v) Triton-X-100. Subsequently, the resuspended membranes and the supernatant containing the cytosolic fraction were centrifuged through a sucrose sedimentation gradient.

Polysome profiles of membrane bound mRNAs isolated from MIN6 cells incubated at low or high glucose concentrations showed that an increase in glucose stimulates an increase in the number of polysomes (figure 3.4). Each gradient was fractionated into 10 fractions and, RNA was collected from each fraction and used for Northern blot analysis for PPI, PC2 and CPH mRNAs. An increase in glucose concentration stimulated a small shift of membrane-associated PPI, PC2 and CPH mRNAs onto heavier polysomes (figure 3.4). Because this shift was observed with all secretory mRNAs tested, it is likely that glucose stimulates the recruitment of ribosomes onto all mRNAs encoding secretory proteins.

Polysome profiles of the cytosolic fraction showed that glucose stimulated a decrease in the 80S peak and a small increase in the polysome peaks (figure 3.5). Furthermore, Northern blot analysis showed that a large proportion of mRNAs encoding secretory proteins were found in the cytosol associated with ribosomes and no 'free' PPI, PC2 or CPH mRNAs were detected in the cytosol at low or high glucose (figure 3.5). Although, there was a relatively large shift of the cytosol-translated actin mRNA onto heavier polysomes at high glucose, there was only a small shift of PPI, CPH or PC2 mRNAs onto heavier polysomes at high glucose. This relatively small shift of ribosomes onto mRNAs encoding secretory proteins was most likely due to the glucose-stimulated recruitment of these heavier ribosome-associated mRNAs from the cytosol to the ER, resulting in loss of these mRNAs from the cytosolic fraction. Indeed, the amount of membrane-associated PPI mRNA is increased at high glucose (figure 3.4), probably due to the recruitment of ribosome-associated PPI mRNA to the ER from the cytosol.
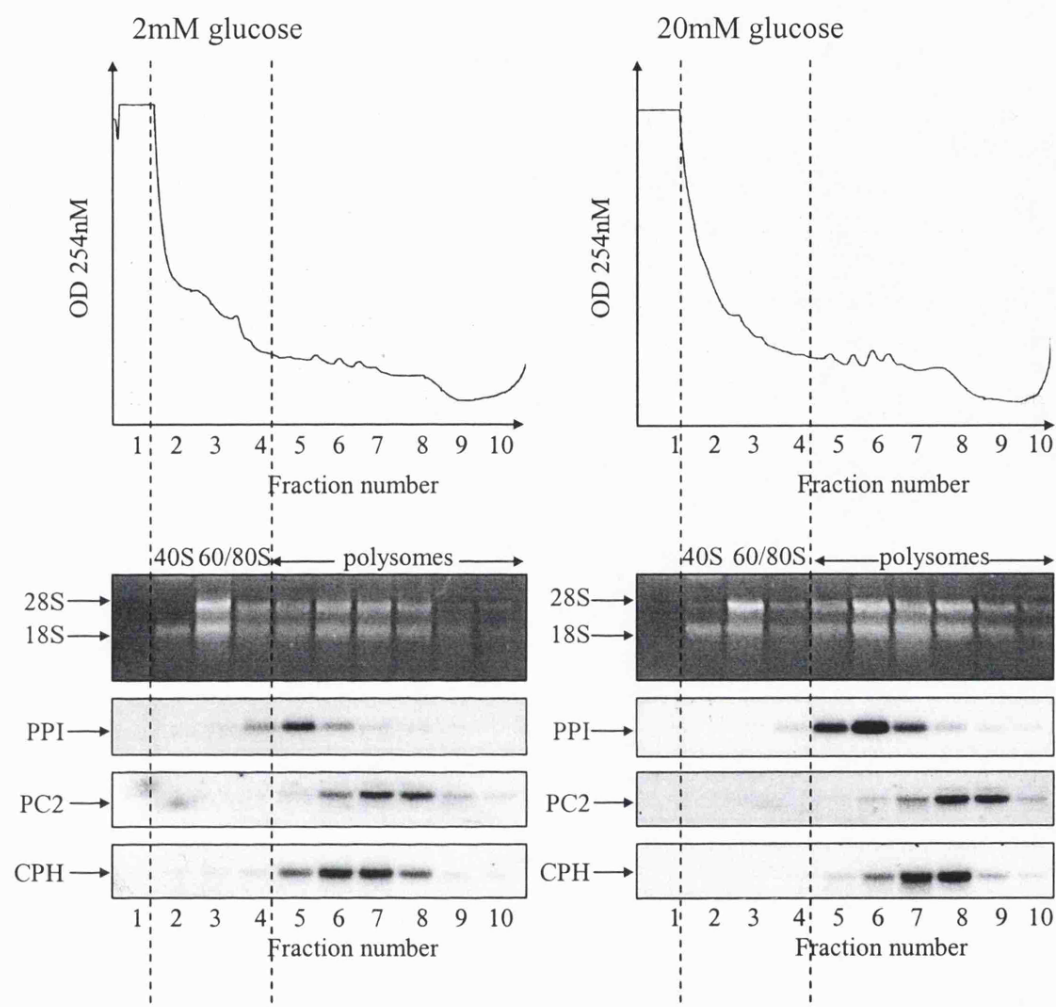
Figure 3.4: Glucose stimulates the recruitment of ribosomes onto membrane-bound preproinsulin mRNA. MIN6 cells were pre-incubated in KRB containing 2mM glucose for 1h followed by incubation in KRB containing 2mM or 20mM glucose for a further hour. 0.1mg/ml (final concentration) of cycloheximide was added to the cells 10min prior to lysis to prevent ribosomal run-off. Cells were then lysed and the membranes were pelleted by centrifugation at 6000g for 20 minutes. The membranes were then resuspended in high salt polysome buffer supplemented with 1-% Triton, layered onto 20-50% sucrose gradients and centrifuged at 39000rpm at 4°C for 2h. Gradients were fractionated from top (fraction 1) to bottom (fraction 10) using the ISCO gradient fractionator. RNA was isolated from 10, 1ml fractions and run on 1% agarose formaldehyde gel, then transferred onto nylon membrane and probed for specific mRNAs as shown. These results are representative of three separate experiments.
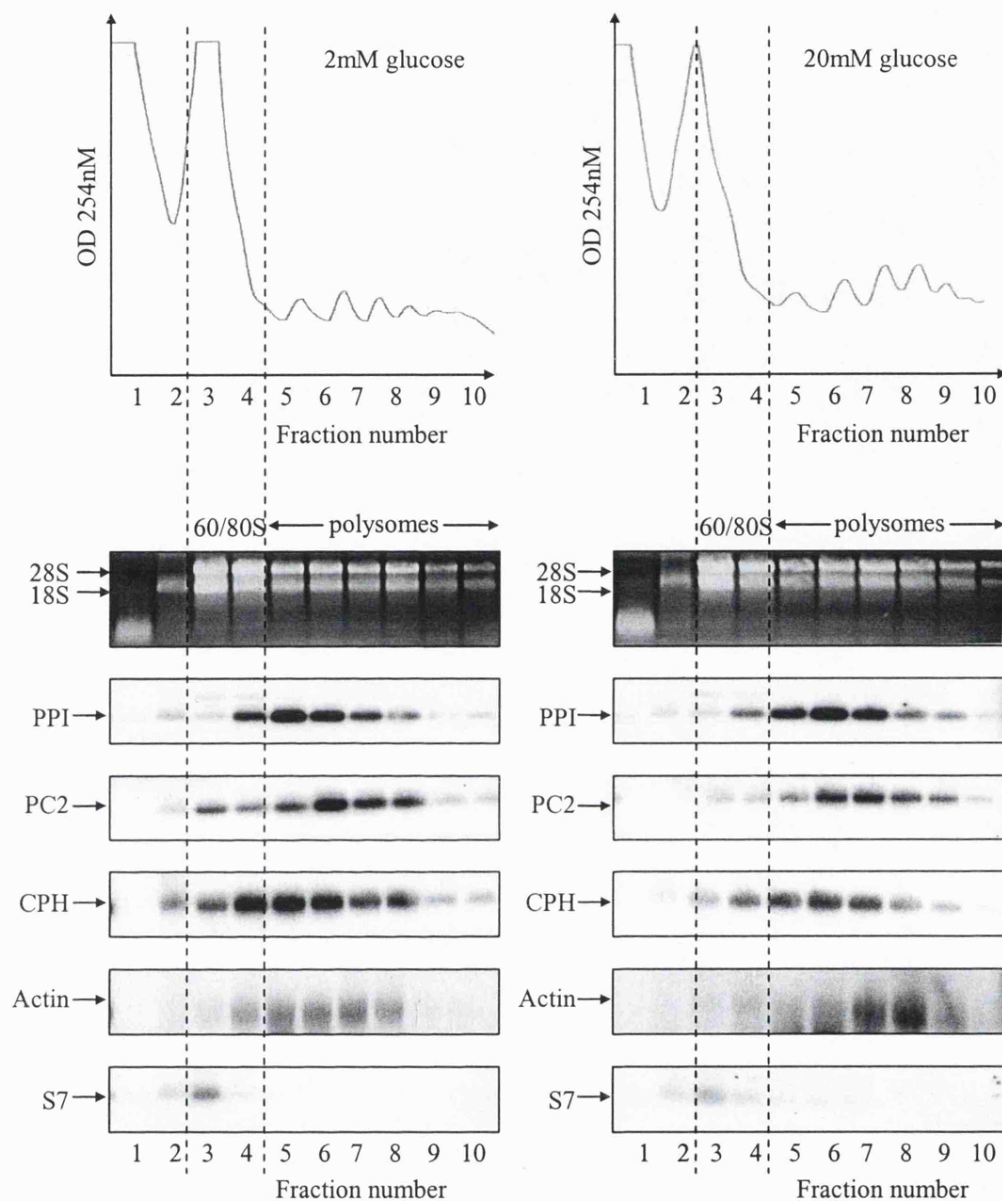
Figure 3.5: Glucose stimulates the recruitment of ribosomes onto cytosolic mRNAs. MIN6 cells were pre-incubated in KRB containing 2mM glucose for 1h followed by incubation in KRB containing 2mM or 20mM glucose for a further hour. 0.1mg/ml (final concentration) of cycloheximide was added to the cells 10min prior to lysis to prevent ribosomal run-off. Cells were then lysed and the membranes were pelleted by centrifugation at 6000g for 20 minutes. The supernatant containing the cytosolic fraction was layered onto 20-50% sucrose gradients and centrifuged at 39000rpm at 4°C for 2h. Gradients were fractionated from top (fraction 1) to bottom (fraction 10) using the ISCO gradient fractionator. RNA was isolated from 10, 1ml fractions and run on 1% agarose formaldehyde gel and then transferred onto nylon membrane and probed for specific mRNAs as shown. These results are representative of three separate experiments.

Summary

Polysome analysis of the ER and cytosolic fractions isolated from MIN6 cells incubated at low or high glucose confirms findings of polysome analysis in whole cell extracts. There is an increase in the rate of initiation, as recruitment of ribosome-associated PPI mRNA onto heavier polysomes is observed at high glucose concentrations both at the ER and in the cytosol. As this recruitment is also observed with all of the other mRNAs tested, it is probably not a mechanism specific to PI synthesis (figure 3.4 and 3.5). However, although there is a pool of mRNAs encoding secretory proteins in the cytosol, they are all associated with ribosomes at both low and high glucose and no free mRNA encoding secretory proteins is observed, suggesting that glucose cannot stimulate an increase in de-novo initiation (figure 3.4 and 3.5). Furthermore, at high glucose there appears to be a loss of secretory protein mRNAs from the cytosolic fraction and a gain of secretory protein mRNAs in the membrane fraction, suggesting that glucose stimulates the recruitment of secretory protein mRNAs to the ER.

In the absence of cycloheximide, ribosomal run-off results in free PPI mRNA at low but not at high glucose concentrations

It has previously been reported that glucose stimulates a recruitment of ribosomes onto 'free' PPI mRNA, i.e. an increase in the rate of de-novo initiation of PI synthesis (Itoh and Okamoto, 1980; Welsh et al., 1986; Welsh et al., 1991; Welsh et al., 1987). However, my results provide evidence to show that PPI mRNA is already associated with ribosomes at both low and high glucose and therefore glucose cannot stimulate de novo initiation (figures 3.2, 3.4 and 3.5). One explanation for these differences is that previous studies did not add cycloheximide to the cells prior to lysis, a step included in this work to prevent ribosomal run-off. Omission of cycloheximide may result in ribosomal run-off and a large pool of 'free' mRNA. In order to investigate the effects of cycloheximide, sucrose sedimentation centrifugation was carried out in MIN6 cells incubated in KRB supplemented with 2mM or 20mM glucose in the presence and absence of both cycloheximide (figure 3.6a and b).

Figure 3.6: Effect of the translation initiation inhibitor, pactamycin and the elongation inhibitor, cycloheximide on polysome profiles, ribosomal RNA and mRNA distribution across a 7-47% sucrose gradient for MIN6 cells incubated in 2mM or 20mM glucose. Polysome analysis was carried out in MIN6 cells as described in figure 3.2 with the addition of translation inhibitors 10 minutes prior to lysis as follows: a) 0.1mg/ml cycloheximide; b) no pre-treatment of cells; c) 0.1μg/ml pactamycin; d) 0.1mg/ml cycloheximide and 0.1μg/ml pactamycin. Cycloheximide was included in the lysis buffer in a), c) and d) but not in b). These results are representative of at least two separate experiments.

a) 0.1mg/ml cycloheximide
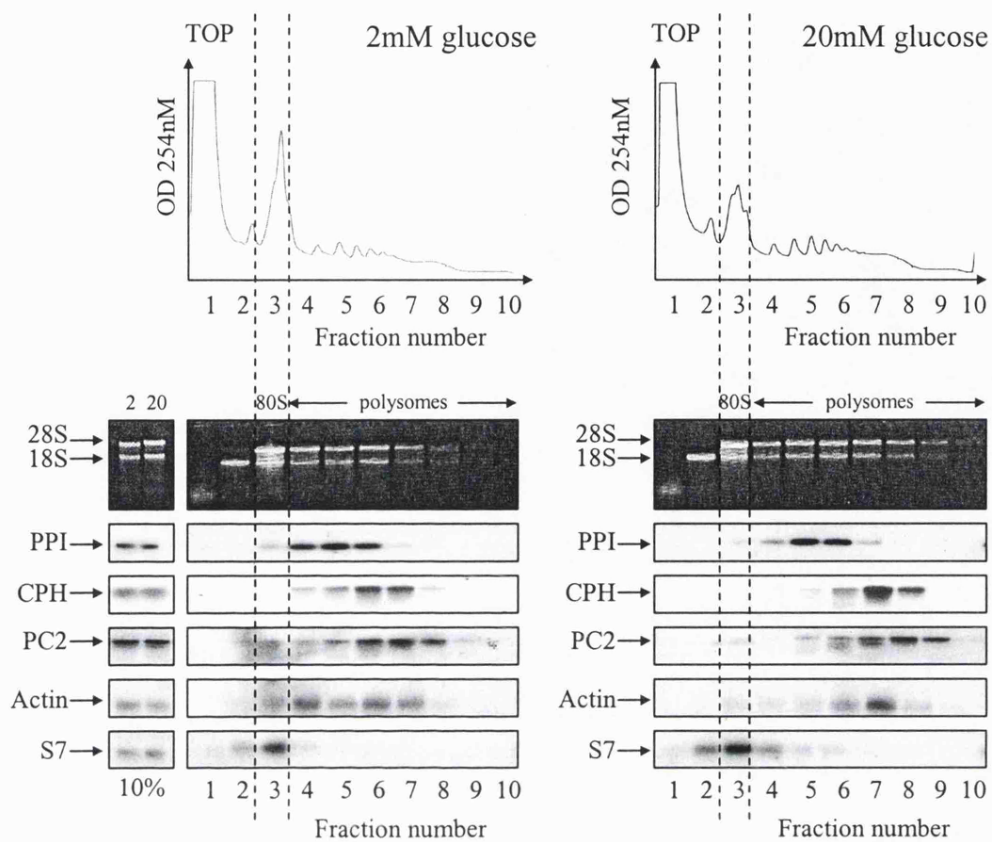
b) No preincubation

106
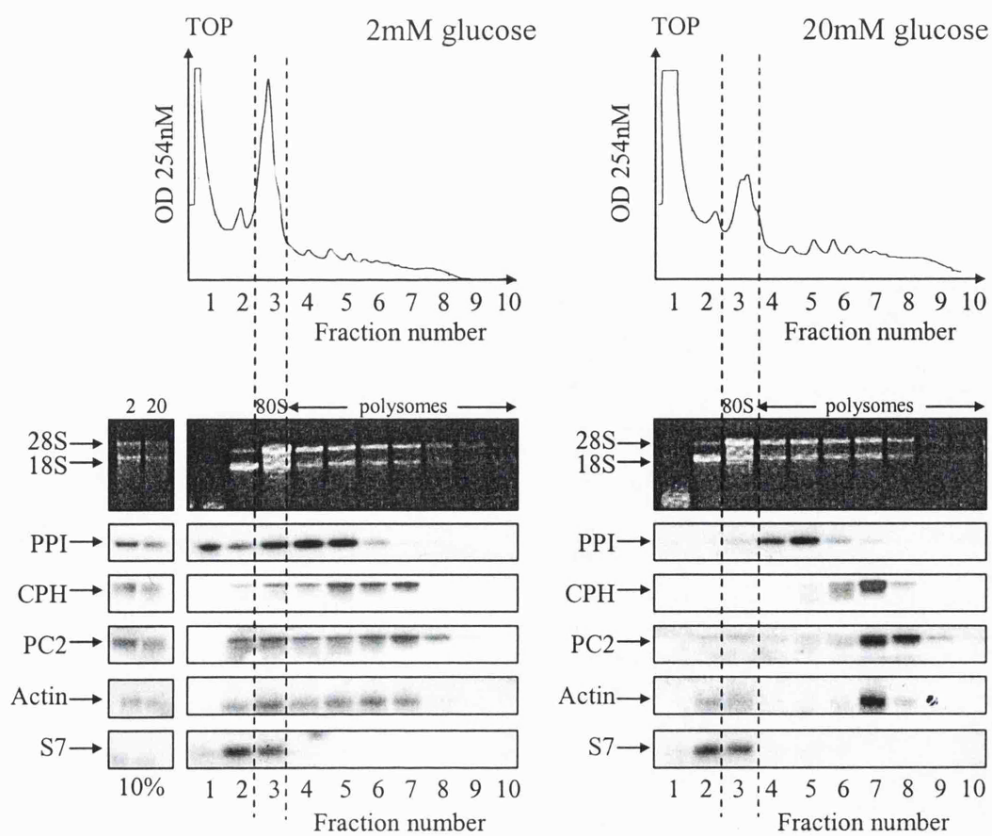
c) 0.1µg/ml pactamycin
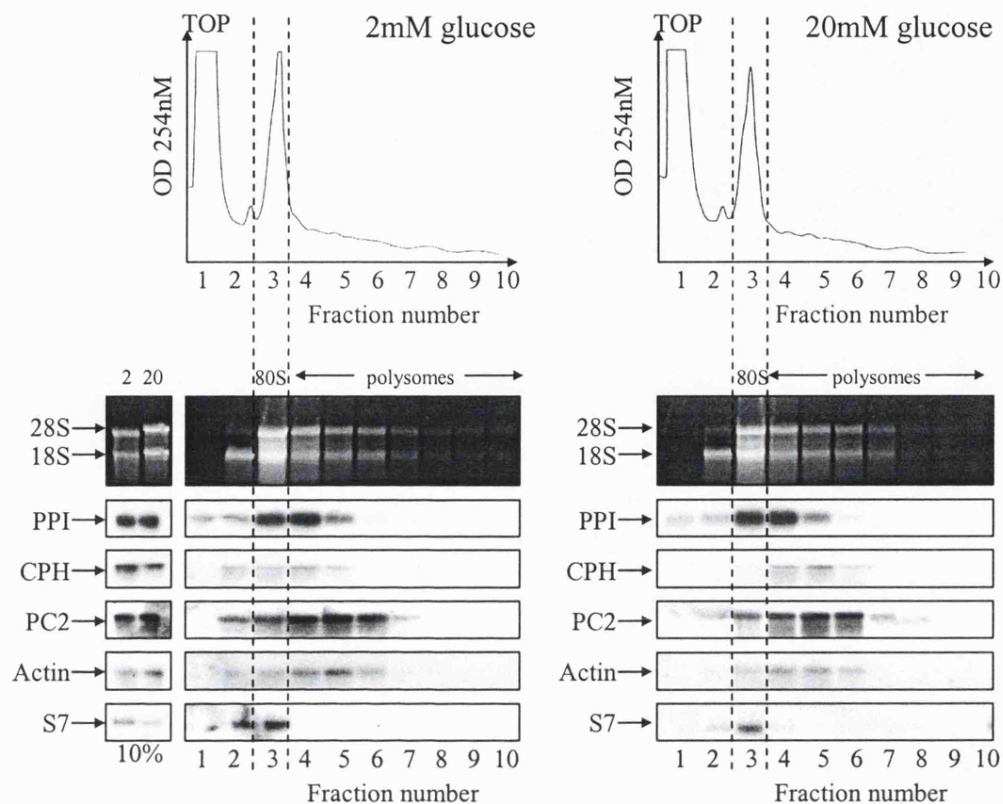
d) 0.1µg/ml pactamycin, 0.1mg/ml cycloheximide
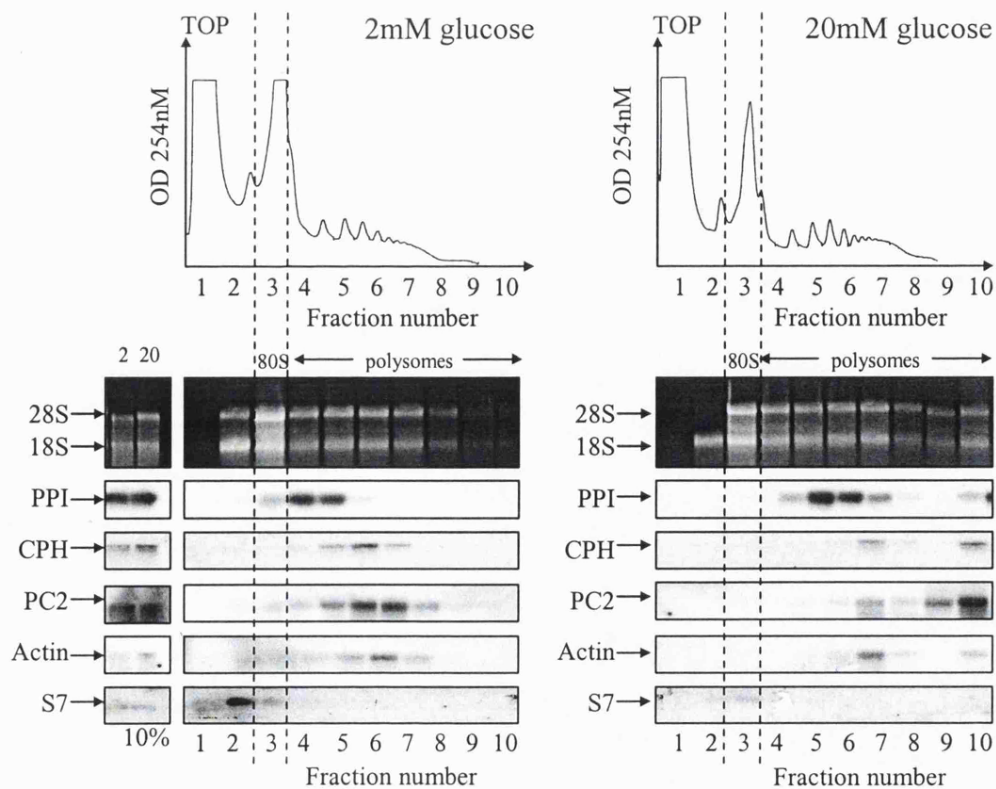
In the presence of cycloheximide, neither free PPI, PC2, CPH nor actin mRNA is observed at either low or high glucose, although a small amount of S7 mRNA does sediment at the top of the gradient at both low and high glucose. (figure 3.2 and 3.6a). However, when cycloheximide is omitted from the protocol, a proportion of PPI mRNA sediments at the top of the gradient at low glucose (figure 3.6b). At high glucose, very little PPI mRNA sediments at the top of the gradient, although PPI mRNA is associated with lighter polysomes than gradients carried out in the presence of cycloheximide (figure 3.6b and 3.6a). The sedimentation profiles for PPI mRNA presented in the absence of cycloheximide are similar to previously reported data that was provided as evidence for glucose-stimulated recruitment of ribosomes onto 'free' PPI mRNA. Additionally, at low glucose, in the absence of cycloheximide, CPH, PC2 and actin mRNAs co-sedimented with lighter polysomes than in the presence of cycloheximide (figure 3.6b). Meanwhile, at high glucose, in the absence of cycloheximide; CPH, PC2 and actin mRNAs sedimented at similar positions as in the presence of cycloheximide (figure 3.6b and 3.6a). Therefore, in the absence of cycloheximide, ribosomal run-off is more pronounced at low glucose than at high glucose concentrations for all mRNAs analysed.

As it has previously been reported that glucose stimulates elongation in islets of Langerhans (Welsh et al., 1986), more ribosomal run-off would be expected at high glucose than at low glucose, resulting in increased amount of free PPI, PC2, CPH and actin mRNAs at high glucose but not necessarily at low glucose. One possibility for this apparent contradiction is that glucose stimulates an increase in ribosome recruitment onto these mRNAs (i.e. at high glucose the loading of ribosomes onto mRNAs counteracts ribosomal run-off). To investigate this possibility the gradients were repeated with a 10-minute incubation in pactamycin prior to cell lysis. Pactamycin is an initiation inhibitor that prevents 80S formation and formation of the di-peptide bond and therefore prevents ribosomal recruitment onto mRNA (figure 3.6c). Under these conditions, the majority of PPI, PC2, CPH and actin mRNAs co-sediment with monosomes and disomes at both low and high glucose presumably due to a combination of the inhibition of 80S formation and di-peptide bond formation. Because ribosome run-off has occurred in the presence of the initiation inhibitor, it can be assumed that it occurs in its absence (see figure 3.6 b and c). Therefore, it is likely that

at high glucose and in the absence of inhibitors, the loading of ribosomes is compensating for the ribosomal run-off.

Because cycloheximide only inhibits elongation, it is likely that ribosomes are still able to initiate. Therefore, when cycloheximide is added to cells 10 minutes prior to lysis, ribosomes can initiate but cannot elongate. This may result in the accumulation of new initiated ribosomes onto formerly free mRNAs, resulting in the shift of free mRNA into the monosome fraction during the 10-minute incubation in cycloheximide. However, in the presence of cycloheximide, only a very small amount of PPI mRNA co-sediments with monosomes at low glucose compared to the amount co-sedimenting with polysomes; therefore it is likely that all PPI mRNA is monosomal/polysomal at both low and high glucose. In order to confirm this, gradients were carried out in the presence of cycloheximide and pactamycin, so that both initiation and elongation were inhibited, thereby preventing ribosomal run-off and initiation of new ribosomes (figure 3.6d). In the presence of cycloheximide and pactamycin a similar sedimentation profile is generated for PPI, PC2, CPH, actin and S7 mRNAs at both low and high glucose to that generated in the presence of cycloheximide alone (figure 3.6d compared to figure 3.6a).

To determine whether ribosomal run-off was taking place before or during cell lysis, MIN6 cells that were incubated in low or high glucose concentrations were lysed without a pre-incubation in cycloheximide, in the presence or absence of cycloheximide in the lysis buffer. In the total absence of cycloheximide (no preincubation, no cycloheximide in the lysis buffer), ribosomal run-off was observed at low glucose concentrations but not at high glucose (figure 3.7a) as was previously observed (figure 3.6b). Furthermore, ribosomal run-off was still observed at low glucose when cycloheximide was present in the lysis buffer, but there was no preincubation in cycloheximide.

Summary
The results of these experiments indicate that ribosomal run-off occurs with all mRNAs in the absence of cycloheximide at both low and high glucose. However, at high glucose, the higher global rate of initiation compensates for this ribosomal run-off, therefore less free mRNA is observed at high glucose compared to at low glucose.

Figure 3.7: Ribosomes run-off PPI mRNA immediately after the removal of cells from the incubator. MIN6 cells were incubated in KRB containing 2mM glucose for 1 hour and then incubated in KRB containing 2mM or 20mM glucose for 1 hour. Cycloheximide was not added to the cells prior to lysis. Cells were then lysed in high salt polysome buffer that contained cycloheximide (a) or were lysed in high salt buffer that did not contain cycloheximide (b) and polysome analysis was carried out on as described in figure 3.2. These results are representative of two separate experiments.

a)- CHX preincubation + CHX lysis buffer
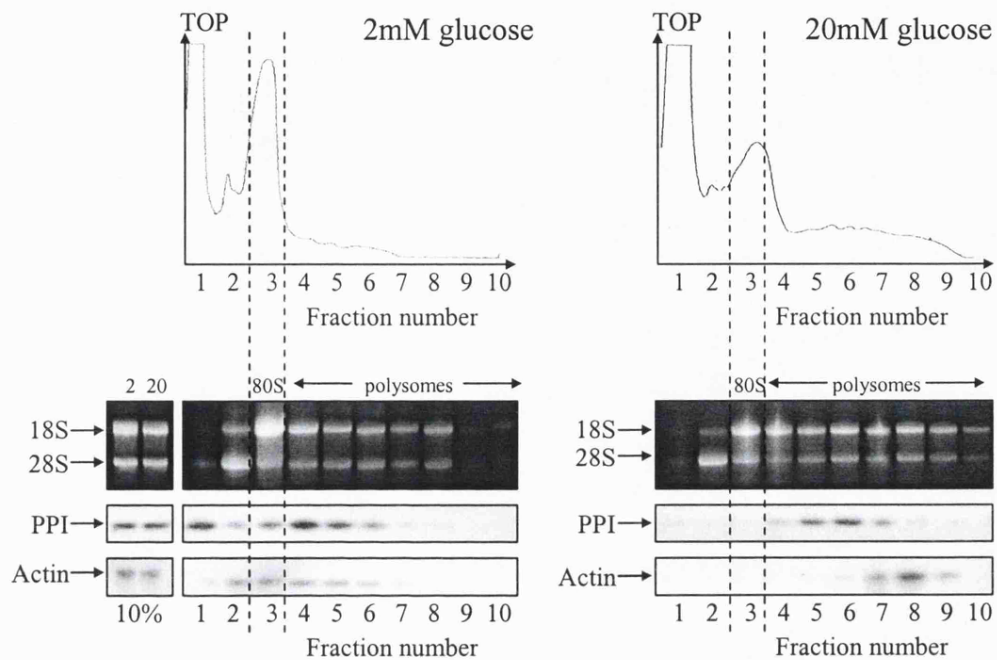
b)- CHX preincubation - CHX lysis buffer

111
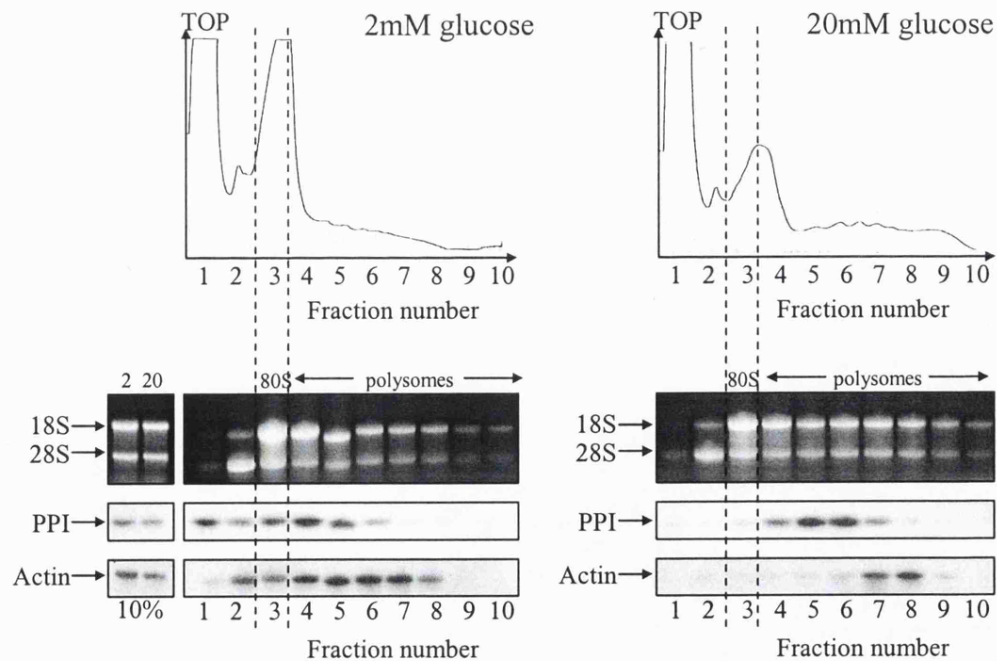
Polysome analysis in the presence of puromycin

At low glucose concentrations the majority of mRNA encoding secretory proteins is associated with ribosomes and a large proportion of these mRNAs are found in the cytosol (figure 3.2, 3.3, 3.4, 3.5). However, as this mRNA is only translated at the ER, what is the translation status of this cytosolic mRNA at low glucose? Because PI is a secretory protein, this cytosolic PPI mRNA that sediments with monosomes/polysomes may be SRP arrested. Indeed, it has been shown *in vitro* that there is an increase in translational pausing around nucleotide 200 and it is likely that this pause is due to SRP causing SRP arrest (Wolin and Walter, 1993). If ribosomes stack up behind the SRP-arrested ribosome, the ribosome centres can be as little as 28 nucleotides apart, suggesting that up to 7 ribosomes can be bound to an SRP arrested PPI mRNA (Wolin and Walter, 1988).

In order to investigate whether mRNAs at low glucose concentrations are actively translating polysome analysis was carried out in the presence of puromycin, a translation inhibitor that is incorporated into nascent polypeptide chains, resulting in premature termination of polypeptide synthesis (Pestka, 1974; Roy and Wonderlin, 2003; Skogerson and Moldave, 1968). Upon high salt conditions, such as during cell lysis, these terminated ribosomes dissociate from the mRNA (Pestka, 1974; Roy and Wonderlin, 2003; Skogerson and Moldave, 1968). Therefore, actively translating mRNAs can be identified from non-translating mRNAs by their premature termination and release of their ribosomes upon treatment with puromycin and lysis with high salt concentrations.

In the presence of puromycin (200µM, final concentration), at both low and high glucose, the 80S peak is larger and the polysomes are decreased in comparison with the control profiles (figure 3.8a and b). However, there are still some polysome peaks in the presence of puromycin, suggesting that ribosomes are still attached to some mRNAs. Interestingly, Northern blots for PPI and actin show that at low glucose some of the PPI and actin mRNAs are released from ribosomes and sediment at the top of the gradient. However, significant amounts of PPI and actin mRNAs are still ribosome-associated at low glucose. Surprisingly, at high glucose the majority of PPI and actin mRNAs are associated with more than one ribosome and no free PPI mRNA is observed. These results suggest that, in the presence of puromycin, more ribosomes

a) + puromycin
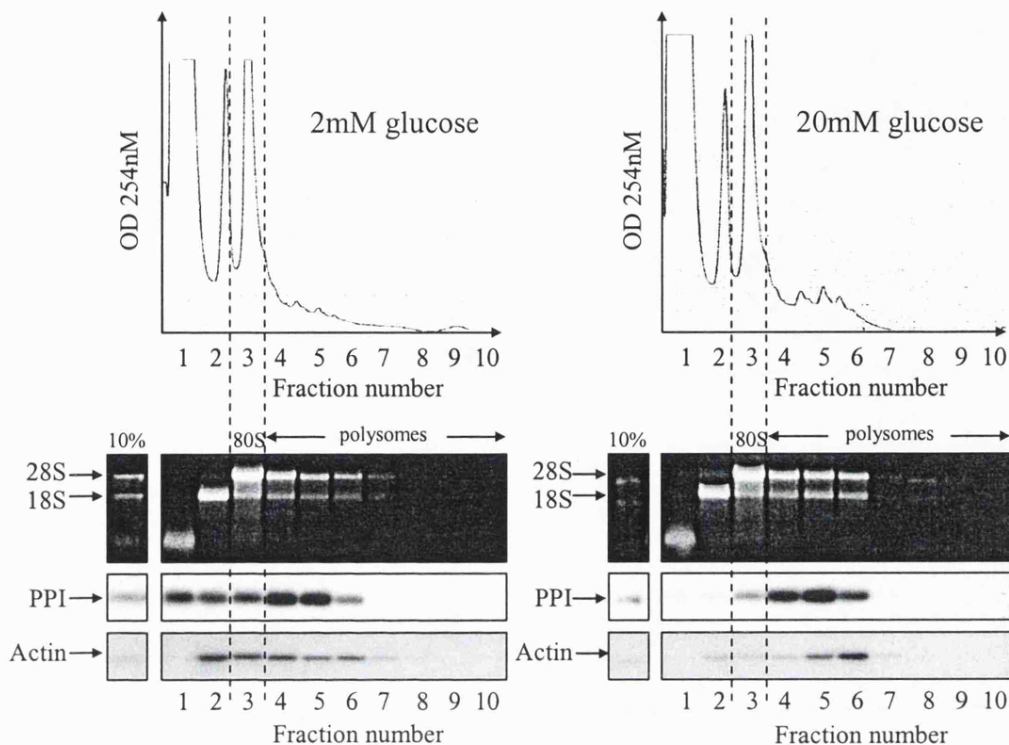
b) -puromycin
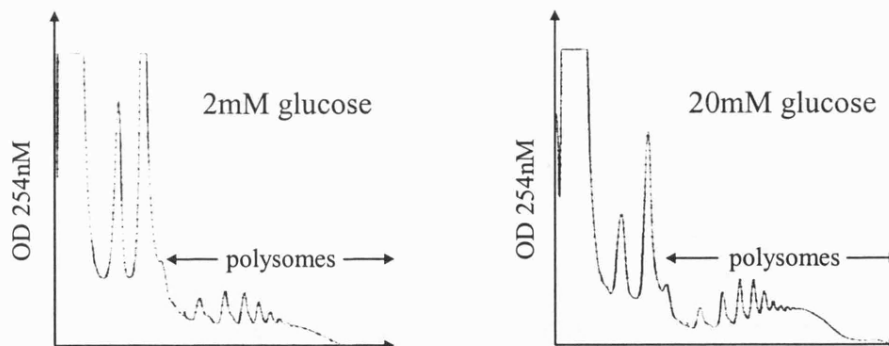
Figure 3.8: Puromycin causes run-off of some, but not all, ribosomes from mRNAs. MIN6 cells were pre-incubated in KRB containing 2mM glucose for 1h followed by incubation in KRB containing 2mM or 20mM glucose for a further hour. 200μM (final concentration) of puromycin was added to the cells 10min prior to lysis to terminate actively translating ribosomes. Cells were lysed and the lysates layered onto 20 - 50% sucrose gradients. The gradients were then centrifuged at 39000rpm at 4°C for 2h and fractionated from top (fraction 1) to bottom (fraction 10) using the ISCO gradient fractionator. Absorbance of the gradients was measured continually at 254nm to give polysome profiles. RNA was isolated from 10, 1ml fractions and run on 1-% agarose, formaldehyde gel. RNA was transferred onto nylon membrane and probed for specific mRNAs as shown. These results are representative of two separate experiments.

113

terminate prematurely at low glucose than at high glucose, implying that there are more actively translating ribosomes at low glucose than at high glucose. However, other more plausible explanations for these results are possible. Indeed, one possibility is that ribosomes may stack up behind the puromycin-stalled ribosome and these stalled ribosomes are unable to incorporate puromycin themselves. Therefore, when cells are lysed and subjected to high salt, ribosomes that have incorporated puromycin into their nascent chains dissociate and those stacked up behind remain associated to the mRNA. Because initiation is increased at high glucose, more ribosomes can stack up, therefore mRNAs at high glucose are associated with more ribosomes than mRNAs at low glucose concentrations.

3.2.2: Conclusions: Polysome analysis of MIN6 cells incubated in low or high glucose concentrations

In conclusion, polysome analysis of MIN6 cells has shown that there is no free PPI mRNA at neither low nor high glucose concentrations (figure 3.2, 3.4 and 3.5). Furthermore, it appears that free PPI mRNA observed in earlier work (Itoh and Okamoto, 1980; Welsh et al., 1986; Welsh et al., 1991; Welsh et al., 1987) is most likely due to ribosomal run-off, as in the absence of cycloheximide, free PPI mRNA was observed at low but not at high glucose concentrations (figure 3.6). Although glucose did not stimulate de novo initiation, glucose did stimulate initiation of ribosomes onto ribosome-associated PPI mRNA in both the ER and cytosolic fractions (figure 3.2, 3.4 and 3.5). Moreover, the glucose-stimulated increase in initiation and increased ribosomal run-off at low glucose was also observed with mRNAs encoding the secretory proteins, PC2 and CPH and mRNAs encoding the cytosolic proteins, actin and S7, suggesting that these regulatory mechanisms apply to all mRNAs (figures 3.2, 3.4, 3.5 and 3.6). Surprisingly, polysome analysis in the presence of puromycin only resulted in the release of ribosomes from PPI and actin mRNAs at low glucose but not at high glucose concentrations (figure 3.8).

3.2.3: Subcellular fractionation of MIN6 cells incubated in low or high glucose concentrations

Glucose stimulates selective recruitment of PPI mRNA to the ER: consecutive centrifugation method

Polysome analysis of the cytosolic and ER fractions of MIN6 cells appeared to show increased PPI mRNA associated with the ER and a decrease in cytosolic PPI mRNA at high glucose (figure 3.4 and 3.5), suggesting that there is a glucose-stimulated recruitment of PPI mRNA to the ER. To further investigate the recruitment of β-cell mRNAs to the ER, the subcellular distribution of mRNAs encoding secretory proteins and cytosolic proteins was determined.

Subcellular distribution of mRNA in MIN6 cells

MIN6 cells were pre-incubated for one hour in KRB containing 2mM glucose and then incubated for one hour in KRB containing 2mM or 20mM glucose. The cells were then lysed and fractionated by consecutive centrifugation (figure 3.9a) at 6000g, 18000g and 200000g to yield a P6 fraction enriched with the ER membranes and its associated mRNAs, a P200 fraction containing mono/polysomal cytosolic mRNA/mRNPs and a S200 fraction containing 'free' mRNA i.e. mRNA with neither mRNA nor protein bound. The 18000g spin was required to remove any residual ER membranes from the sample. RNA was isolated from each fraction and Northern blot analysis was used to determine the location of specific mRNAs (figure 3.9b).

Subcellular fractionation of MIN6 cells shows that at low glucose 51% of PPI mRNA (average over 4 experiments, standard deviation (SD) =11.43) is present in the cytosol and is associated with ribosomes (P200, figure 3.9b). Meanwhile 49% (SD=11.01) of PPI mRNA is associated with the membranes at low glucose (P6). Conversely, at 20mM glucose the majority of PPI mRNA (73%, SD=11.05) is associated with the membranes (P6), with the remainder (26%, SD=11.36) associated with ribosomes in the cytosol (P200). The recruitment of PPI mRNA to the ER at high glucose amounts to almost a 187 fold increase (SD=55.82) in membrane-associated PPI mRNA (figure 3.9c). Additionally, very little 'free' PPI mRNA was observed in the S200 fraction at either low or high glucose. A small amount of ribosomal RNA is also observed in the S200 fraction, due to carry over from the P200 fraction.

Figure 3.9: Glucose stimulates the recruitment of mRNAs encoding secretory membrane proteins to the ER-*Subcellular fractionation using consecutive* **centrifugation.** MIN6 cells were pre-incubated in KRB containing 2mM glucose for 1hour followed by incubation in KRB containing 2mM or 20mM glucose for a further hour. 0.1mg/ml (final concentration) of cycloheximide was added to the cells 10min prior to lysis to prevent ribosomal run-off. a) Cells were lysed in hypertonic lysis buffer and fractionated by consecutive centrifugation resulting in the membrane fraction (P6), polysome fraction (P200) and a supernatant fraction containing free mRNAs (S200). b) Isolated RNA from each fraction was run on a 1% agarose, formaldehyde gel, then transferred onto nylon membrane and probed for PPI, PC2, CPH, actin and S7 mRNAs. c) The relative amounts of PPI, PC2 and CPH mRNAs associated with the membranes were determined by densitometry and the mean % increase and the standard error of the mean in membrane-associated mRNA at high glucose was calculated. These results are representative of four separate experiments.

a)

Homogenate

1200g, 2 minutes

Pellet. Nuclei — Supernatant

6000g, 20minutes

Pellet (P6)
Membrane-bound
polysomes — Supernatant

18000g, 20minutes
200000g,20minutes

Pellet (P200)
Mono/polysomes — Supernatant (S200)
Free cytosolic mRNA

b)

	10%	P6	P18	P200	S200
mM glucose	2 20	2 20	2 20	2 20	2 20

28S →
18S →

PPI →
PC2 →
CPH →
Actin →
S7 →
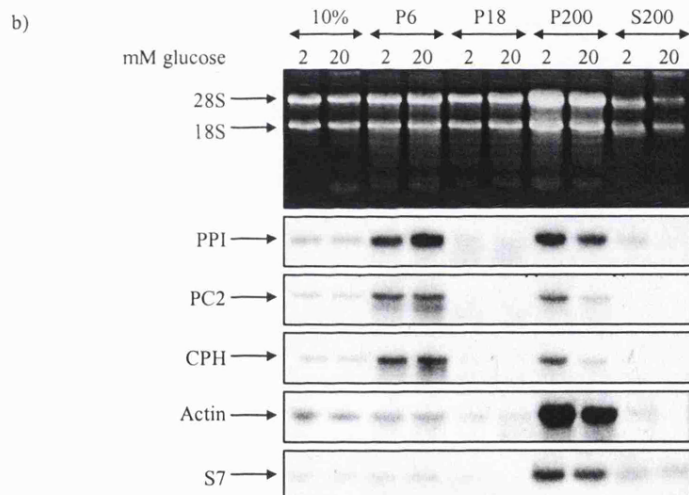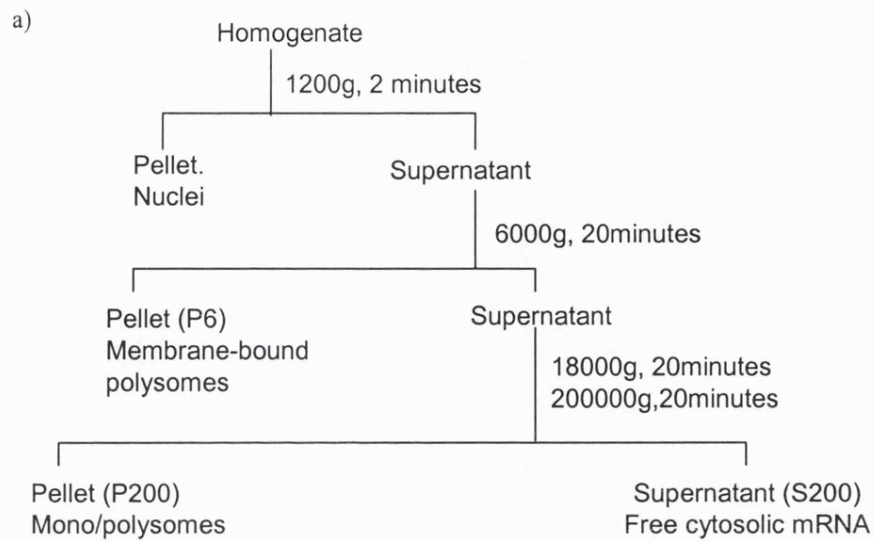
c)   % increase in membrane-associated mRNA in response to increased glucose
concentration

% increase

250
200
150
100
50
0

PPI   CPH   PC2

mRNA

117
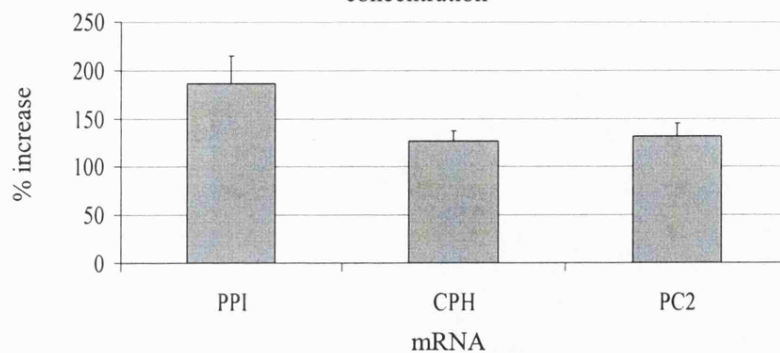
In order to ascertain whether other secretory protein mRNAs were recruited to the ER, Northern blot analysis was carried out for CPH and PC2 mRNAs (figure 3.9b). In contrast to PPI, the majority of CPH and PC2 mRNAs are present in the membrane fraction (P6) at both low and high glucose (figure 3.9b). At low glucose 71% (average over 4 experiments, SD =11.15) of CPH and 52.5% (SD=17.61) of PC2 mRNAs were found associated with the membrane fraction (P6) and at high glucose 85% (SD=6.84) of CPH and 70% (SD=9.88) of PC2 were found associated with the membrane fraction. Therefore, glucose stimulated only a 127% (SD=20.28) increase in CPH mRNA associated with the ER and a 132% (SD=26.26) increase in PC2 mRNA associated with the ER (figure 3.9c).

The distribution of cytosolic-translated mRNAs encoding actin and ribosomal protein S7 was also investigated to determine the efficiency of the subcellular fractionation procedure. The majority of both actin and S7 were found associated with ribosomes within the cytosol (P200) at both low and high glucose (P6, figure 3.9b).

Subcellular fractionation of MIN6 cells in the presence of EDTA

To confirm that PPI mRNA was associated with ribosomes, subcellular fractionation was repeated in the presence of 15mM EDTA and the absence of Mg^{2+} (Figure 3.10). In the presence of EDTA, the majority of PPI mRNA was found free in the cytosol (S200), suggesting that the sedimentation of PPI in the presence of Mg^{2+} and absence of EDTA is due to the association of ribosomes (figures 3.10 and 3.9). Although the presence of EDTA resulted in the majority of PPI in the S200 fraction, significant amounts of actin, PC2 and CPH dissociated from the membranes but were still pelleted in the 200000g spin. This may indicate that these mRNAs were sedimenting as mRNPs (figure 3.10).

Subcellular distribution of proteins important in initiation of translation and protein targeting to the ER

I have shown that glucose stimulates the recruitment of mRNAs encoding secretory proteins to the ER. As the recruitment of secretory proteins to the ER is mediated by SRP, the subcellular distribution of the 54Kda subunit of SRP (SRP54) was also determined by Western blotting (figure 3.11). The majority of SRP54 was found in the

Figure 3.10: Effect of EDTA on glucose stimulated recruitment of mRNAs encoding secretory membrane proteins to the ER-*Subcellular fractionation using consecutive centrifugation.*** Cells were treated and fractionated as described for figure 3.9, except MgCl₂ was excluded and 15mM EDTA was included in the lysis buffer. These results are representative of two separate experiments.

Figure 3.11: Glucose does not appear to stimulate the recruitment of initiation factors or SRP54 to the ER-*Subcellular fractionation using consecutive centrifugation.*** MIN6 cells were pre-incubated in KRB containing 2mM glucose for 1 hour followed by incubation in KRB containing 2mM or 20mM glucose for a further hour. 0.1mg/ml (final concentration) of cycloheximide was added to the cells 10min prior to lysis to prevent ribosomal run-off. Cells were fractionated by consecutive centrifugation (as shown in figure 3.10a) resulting in the membrane fraction (P6), polysome fraction (P200) and a supernatant fraction containing free mRNAs (S200). 8% of the pellets and 1% of the supernatants were run on 12.5% SDS-PAGE and subjected to immunoblotting with specific antibodies. Detection was by enhanced chemiluminescence. These results are representative of three separate experiments.

free in the cytosol and did not appear to be bound to ribosomes or RNA. No consistent redistribution of SRP54 to the ER was observed in MIN6 cells.

Because poly (A) binding protein (PABP) is important in regulating initiation of translation, possibly through aiding the circularisation of mRNAs, it is possible that glucose stimulates the redistribution of this protein to the ER to enhance translation of secretory proteins. However, subcellular fractionation of PABP showed that it was present in all fractions and that the amount present in each fraction does not vary between low and high glucose (figure 3.11). In addition to PABP, the subcellular distribution of the initiation factors: eIF2, eIF4G and eIF4A were also investigated. Like SRP54, the majorities of these initiation factors were found free in the cytosol (S200) and there were no observed recruitment of these factors to the ER (figure 3.11). The subcellular fractionation of phosphorylated eIF2 also showed the majority free in the cytosol. In agreement with previous work from our laboratory, eIF2 was more phosphorylated in cells incubated at low glucose compared to at high glucose (Gomez *et al* 2003).

To further determine the efficacy of the subcellular fractionation procedure, protein samples from each fraction were retained for SDS-PAGE and Western blotted using antibodies against the ER-lumenal protein, calreticulin and Erk2, which is primarily a cytosolic protein. Calreticulin was only found in the ER fraction (P6) confirming that the ER were pelleted at 6000g and were not broken in the subcellular fractionation procedure, which would have resulted in the release of calreticulin into the cytosol (S200) (figure 3.11). Erk2 was only detected in the cytosol (S200), which confirms that the ER-enriched fraction did not contain unlysed cells (figure 3.11).

Summary

Using subcellular fractionation of MIN6 cells incubated in low or high glucose concentrations; I have shown that PPI mRNA is recruited to the ER at high glucose concentrations (figure 3.9b). Furthermore, mRNAs encoding secretory proteins, CPH and PC2 are also recruited to the ER at high glucose. However, the increase in CPH and PC2 mRNA associated with the ER at high glucose concentrations are less than for PPI mRNA, as the majority of CPH and PC2 mRNA is already associated with the membranes at low glucose concentrations. Subcellular fractionation of proteins showed

that glucose did not stimulate the recruitment of SRP54, PABP, eIF4G, eIF4A or eIF2 to the ER (figure 3.11).

Glucose stimulates selective recruitment of PPI mRNA to the ER: permeablisation of cells method

Because of the importance of the subcellular fractionation results in understanding the mechanism of PI synthesis, subcellular fractionation was repeated using an alternative technique. Digitonin was used to permeablise MIN6 cells, the cytosol was washed out to leave the ER and its associated mRNAs with the permeablised cells (see materials and methods, section 2.7.4). This technique has already been used to successfully separate cytosolic mRNAs from ER bound mRNAs (Seiser and Nicchitta, 2000).

Optimisation of digitonin concentration for permeablisation of cells

In order to identify the optimum concentration of digitonin required for permeablisation, MIN6 cells were permeablised using a range of digitonin concentrations from 40μg/ml to 160μg/ml (figure 3.12a). RNA was isolated from both the cytosol and permeablised cell fractions and used for Northern blot analysis. PPI mRNA was found both in the pelleted permeablised cell fraction (containing the ER membranes) and in the supernatant (containing the cytosol); whereas actin mRNA was found solely in the cytosolic fraction, indicating that the cytosol and cytosolic mRNAs were efficiently washed out of the cells.

A sample from each fraction was run on SDS-PAGE and antibodies for calreticulin and Erk2 were used to ensure that the subcellular fractionation procedure had worked efficiently. The majority of calreticulin was found in the permeablised cell fraction, confirming that the ER membranes were pelleted with the permeablised cells, while the majority of Erk2 was found in the supernatant confirming that cytosolic proteins were washed out with the cytosol (figure 3.12b). A longer exposure of the Erk2 Western blot showed a small amount in the membrane fraction when 40μg/ml of digitonin was used (figure 3.12b), which was presumably due to a small number of unpermeablised cells. It was therefore decided that a concentration of 80μg/ml of digitonin would be used for future digitonin permablisation experiments.
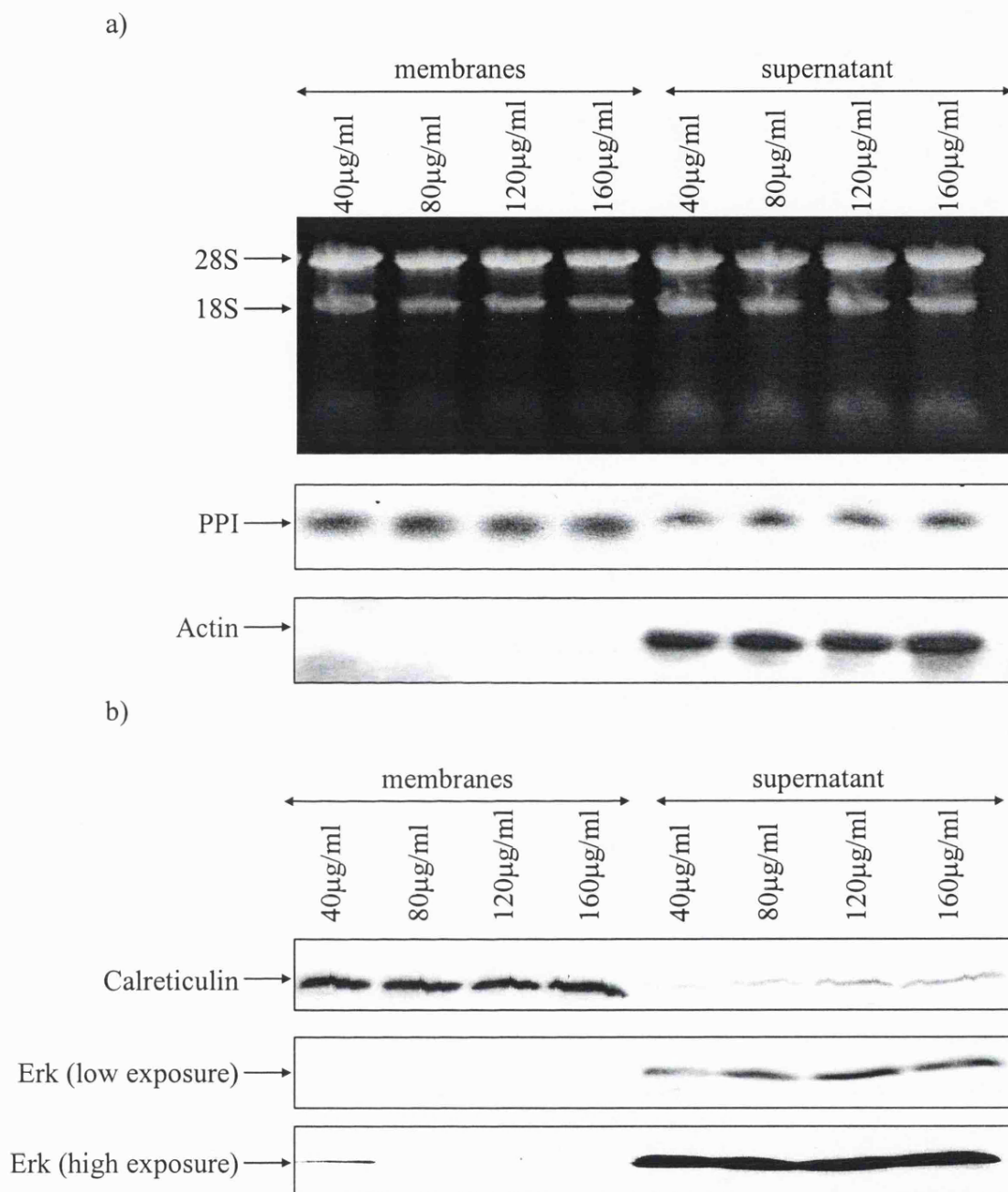
Figure 3.12: Optimisation of digitonin concentration for subcellular fractionation using cell permeablisation method. MIN6 cells were incubated in DMEM. 0.1mg/ml (final concentration) of cycloheximide was added to the cells 10 minutes prior to lysis to prevent ribosomal run-off. Cells were permeablised with 40 -160µg/ml digitonin and pelleted. a) RNA was isolated from the supernatant, containing the cytoplasm, and from the pellet, which includes the membranes. RNA from both fractions were run on 1% agarose formaldehyde gel, transferred onto nylon membrane and probed for PPI and actin mRNAs. b) Protein samples from each fraction were run on 12.5% SDS PAGE and subjected to immunoblotting with Erk2 and calreticulin antibodies. Detection was by enhanced chemiluminescence.
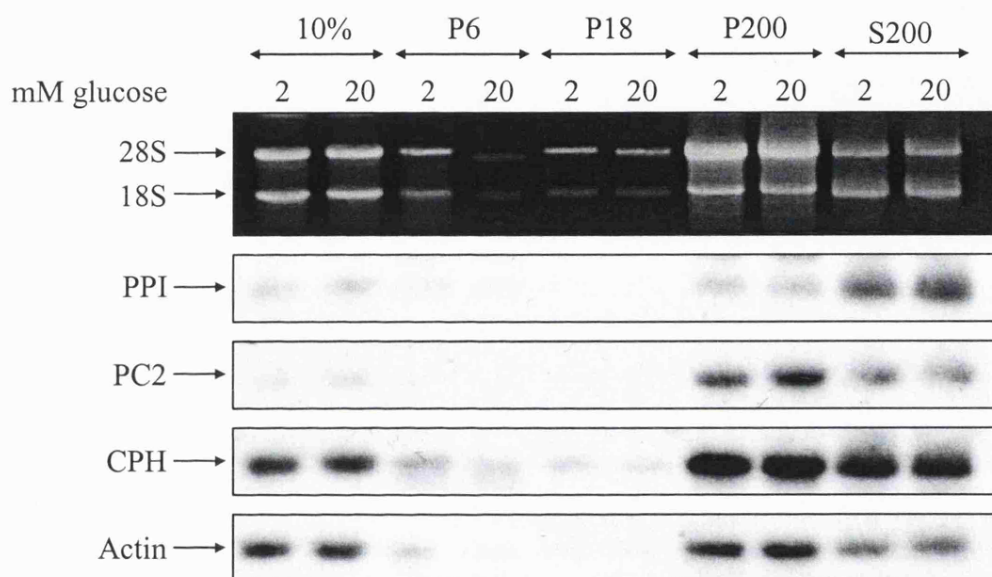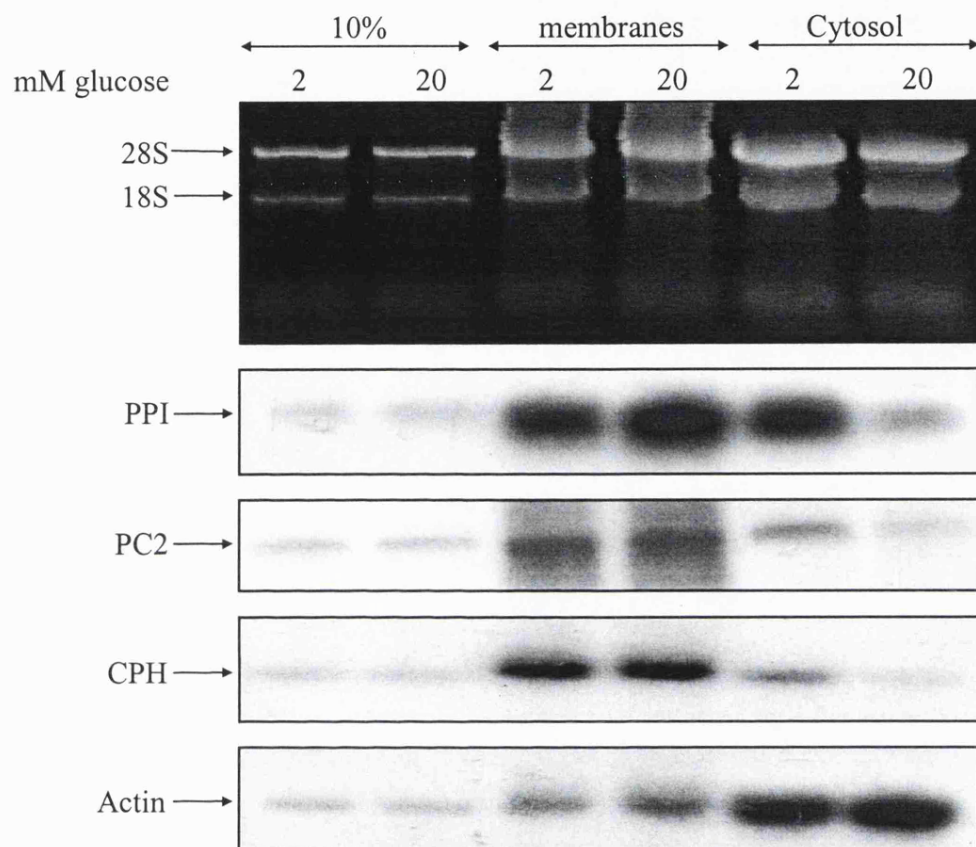
Figure 3.13: Glucose stimulates the recruitment of mRNAs encoding secretory membrane proteins to the ER- *Subcellular fractionation using digitonin.* MIN6 cells were pre-incubated in KRB containing 2mM glucose for 1 hour followed by incubation in KRB containing 2mM or 20mM glucose for a further hour. 0.1mg/ml (final concentration) of cycloheximide was added to the cells 10 minutes prior to lysis to prevent ribosomal run-off. Cells were permeablised with 80μg/ml digitonin and pelleted. RNA was isolated from the supernatant, containing the cytoplasm, and from the pellet, which includes the membranes. RNA from both fractions were run on 1% agarose formaldehyde gel, transferred onto nylon membrane and probed for specific mRNAs. These results are representative of three separate experiments.

Subcellular distribution of mRNA in MIN6 cells using digitonin

MIN6 cells were pre-incubated in KRB containing 2mM glucose for one hour followed by a one hour incubation in KRB containing 2mM or 20mM glucose, then fractionated using the digitonin method (see materials and methods). At low glucose concentrations, 48% of PPI mRNA is located with the membrane fraction and 52% of PPI mRNA with the cytosolic fraction. However, at high glucose concentration the majority of PPI mRNA is located on the ER membranes (73%) (figure 3.13). There is clearly a recruitment of PPI mRNA from the cytosol at low glucose to the membranes at high glucose. In contrast, the majority of PC2 (61% and 75% at low and high glucose respectively) and CPH (59% and 72% at low and high glucose respectively) mRNAs are located in the membrane fraction, thus glucose stimulates only a small recruitment of PC2 and CPH mRNAs to the ER (figure 3.13). Actin was used as a control to confirm that cytosolic-translated mRNAs were not found in the membrane fraction.

Subcellular distribution of proteins important in initiation of translation and protein targeting to the ER

The distribution of SRP54, PABP and the initiation factors eIF4G, eIF2 and eIF4A was also investigated (figure 3.14). The cytosolic samples for SRP54, PABP and eIF4G subcellular fractionation analysis were also subjected to a spin at 200000g for 20 minutes at 4°C to pellet mRNAs that were associated with ribosomes (figure 3.14a). At both low and high glucose the majority of SRP54, eIF4G, eIF2 and eIF4A were found in the cytosolic fractions. The 200000g spin also showed that the majority of SRP54 and eIF4G was found free in the cytosol (S200). Furthermore, glucose did not stimulate a redistribution of any of these proteins. The majority of PABP was found free in the supernatant but a significant amount was also found in the P200 fraction and presumably was associated with mRNAs that have ribosomes bound. An even smaller amount of PABP was also found associated with the membranes. Western blotting for Erk2 and calreticulin confirmed the efficiency of the subcellular fractionation procedure.
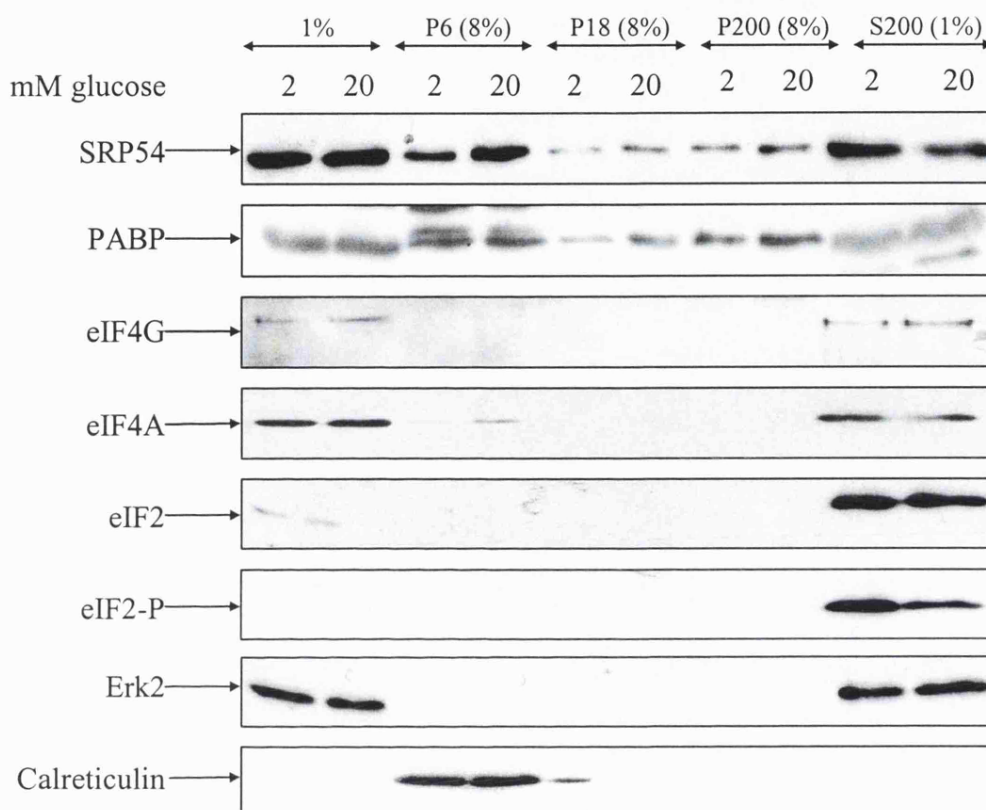
a)

b)
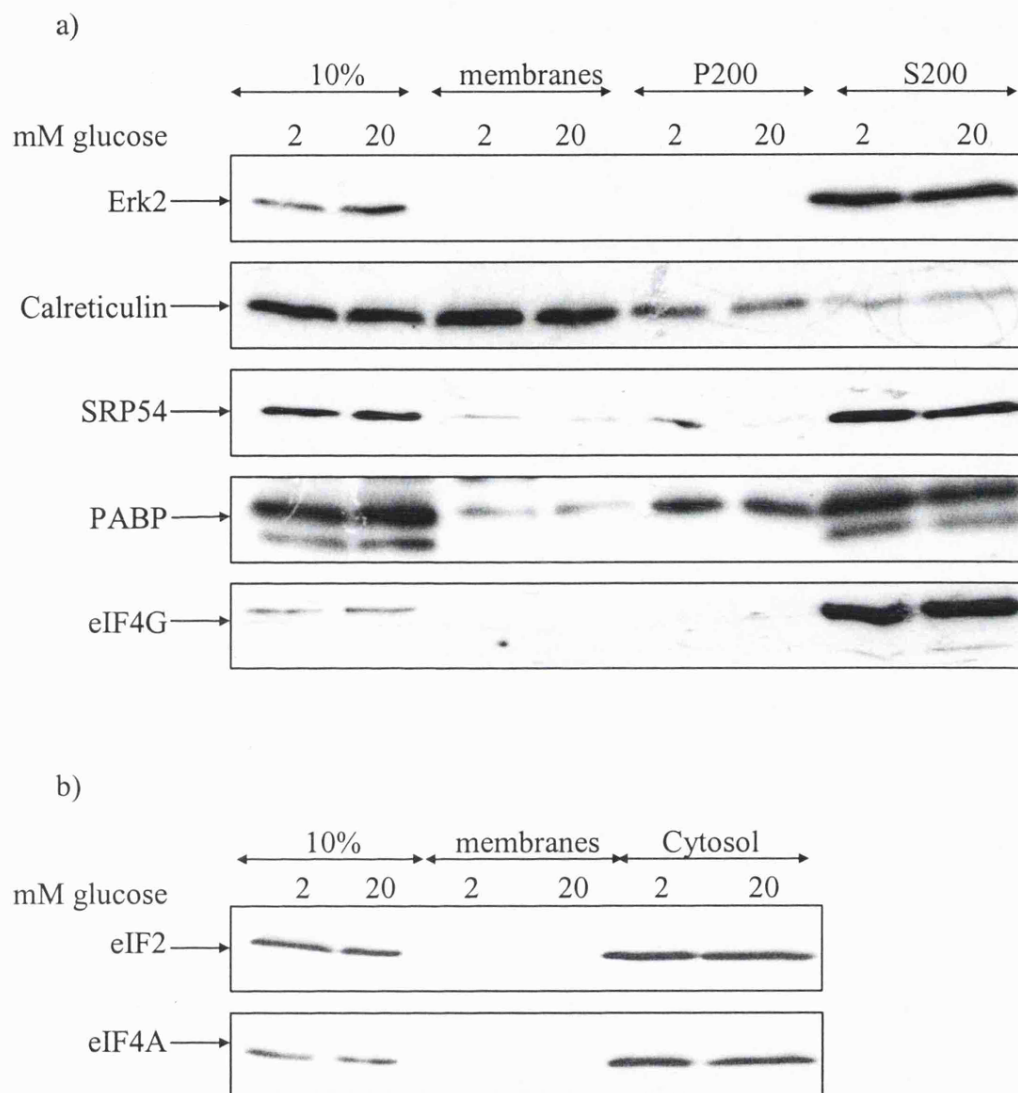
Figure 3.14: Glucose does not appear to stimulate the recruitment of initiation factors or SRP54 to the ER- *Subcellular fractionation using digitonin.* MIN6 cells were pre-incubated in KRB containing 2mM glucose for 1 hour followed by incubation in KRB containing 2mM or 20mM glucose for a further hour. 0.1mg/ml (final concentration) of cycloheximide was added to the cells 10 minutes prior to lysis to prevent ribosomal run-off. Cells were permeablised with 80μg/ml digitonin and pelleted. Protein samples from each fraction were run on 12.5% SDS PAGE and subjected to immunoblotting with Erk2 and calreticulin antibodies. Detection was by enhanced chemiluminescence. These results are representative of three separate experiments.

3.2.4: Conclusions: Subcellular fractionation of MIN6 cells

Using two alternative subcellular fractionation procedures evidence has been provided to show that: 1) it is likely glucose stimulates a recruitment of all mRNAs encoding secretory proteins to the ER; 2) low glucose concentrations selectively inhibit the recruitment of PPI mRNA to the ER and; 3) glucose stimulates the recruitment of PPI mRNA to the ER.

3.2.5: Ribosomal run-off occurs at the ER at low glucose but not at high glucose concentrations.

In the absence of cycloheximide, polysome analysis of MIN6 cells showed that ribosomal run-off occurred at low glucose, resulting in a significant amount of free PPI mRNA (figure 3.6). However, only a small amount of ribosomal run-off occurred in MIN6 cells that were incubated at high glucose and there was no free PPI mRNA. In order to confirm these previous results, subcellular fractionation was repeated with cycloheximide omitted from the protocol.

MIN6 cells were incubated in KRB supplemented with 2mM or 20mM glucose and fractionated in the absence of cycloheximide using the consecutive centrifugation method. In the absence of cycloheximide, at low glucose, the majority of PPI mRNA is in the cytosol, either as free mRNA (S200) or as monosomes/polysomes (P200) and very little is bound to the ER (P6) (figure 3.15). Meanwhile, at high glucose, the majority of PPI mRNA is associated with the ER with a smaller proportion associated with ribosomes in the cytosol and a very small amount is free in the cytosol. Ribosomes also ran off actin and CPH mRNAs but not to the same extent as PPI mRNA, as a smaller proportion of these mRNAs are found in the free pool (S200).

Summary
Subcellular fractionation in the absence of cycloheximide confirmed that more ribosomal run-off occurs at low glucose than at high glucose. Furthermore, subcellular fractionation showed that the ribosomal run-off resulted in a reduction in the amount of PPI mRNA associated with the membranes at low glucose but not at high glucose.
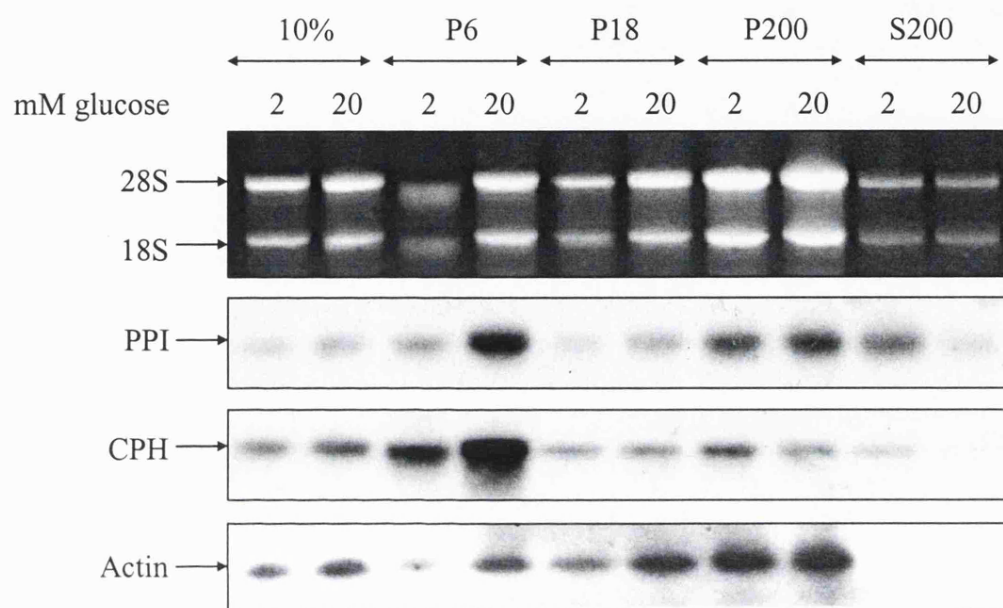
Figure 3.15: Subcellular distribution of MIN6 preproinsulin mRNA in the absence of cycloheximide MIN6 cells were pre-incubated in KRB containing 2mM glucose for one hour followed by incubation in KRB containing 2mM or 20mM glucose for another hour. Cycloheximide was not added to the cells prior to lysis and was not present in the lysis buffer. Lysates were fractionated by consecutive centrifugation at 6000g, 18000g and 200000g resulting in the membrane fraction (P6), polysomal fractions (P18 and P200) and a supernatant containing free mRNAs (S200). RNA was isolated from each fraction and run on a 1% agarose formaldehyde gel. Ribosomal RNA from the pellets and the supernatants was visualised by ethidium bromide staining. RNA was then transferred onto nylon membrane and probed for PPI, PC2, CPH, actin and S7 mRNA. These results are representative of two separate experiments.

3.2.6: PPI mRNA is tightly associated with the membranes and actively translating at both low and high glucose concentrations

A significant proportion of PPI mRNA is associated with the membranes at low and high glucose (figures 3.9 and 3.13). However, it is unknown as to whether this mRNA is associated with the SRP receptor or the translocon. Indeed, it has been proposed that further regulation of PI synthesis may occur at the ER membranes (Itoh and Okamoto, 1980; Welsh et al., 1986; Welsh et al., 1991; Welsh et al., 1987). One way that PI synthesis may be regulated at the ER is by the sequestering of PPI ribosome nascent chain complexes (RNCs) at the SRP receptor at low glucose until high glucose stimulates its transport to the translocon.

PPI mRNA is tightly associated with the membranes at both low and high glucose concentrations

Actively translating RNCs, which have inserted their nascent chains into the translocon are resistant to high salt washes (500mM KCl); whereas RNCs which have not inserted their nascent chains into the translocon (and are therefore unlikely to be translating) can be washed off the ER membranes with high salt buffers (Wolin and Walter, 1993). Therefore, to investigate the association of PPI RNCs with the ER membranes, the membranes were isolated (permeablisation of cells method) from MIN6 cells incubated at 2mM or 20mM glucose concentration using low salt (130mM KCl) polysome buffer and consecutively washed with polysome buffer containing increasing concentrations of KCl (250mM and 500mM KCl, figure 3.16a). After the salt washes, the membranes were pelleted. RNA was isolated from the salt washes, the salt washed membranes and the cytosolic supernatant fraction (S6) and used for Northern blot analysis. Both salt washes resulted in the release of the same amount of PPI mRNA from membranes isolated at low glucose or high glucose (figure 3.16b). This suggests that the quantity of PPI mRNA loosely associated with the membranes is the same in cells incubated in low or high glucose conditions and therefore transfer of PI RNCs to the translocon from the SRP receptor is unlikely to be regulated by glucose.

Figure 3.16: PPI mRNA is associated with the translocon at high and low glucose – cell permeablisation method. MIN6 cells were pre-incubated in KRB containing 2mM glucose for 1 hour followed by incubation in KRB containing 2mM or 20mM glucose for a further hour. 0.1mg/ml (final concentration) of cycloheximide was added to the cells 10 minutes prior to lysis to prevent ribosomal run-off. Cells were then lysed and fractionated by the digitonin cell permeablisation method (using low salt polysome buffer containing 130mM KCl) resulting in a membrane fraction and a cytosolic fraction. The membrane fraction was consecutively washed with polysome buffer containing 250mM KCl (250mM wash) and 500mM KCl (500mM wash). b) RNA was isolated from each fraction and run on a 1% agarose, formaldehyde gel. Ribosomal RNA from the pellets and the supernatants was visualised by ethidium bromide staining. RNA was then transferred onto nylon membrane and probed for PPI and mRNA. c) Protein samples from each fraction were run on 12.5% SDS PAGE and subjected to immunoblotting with specific antibodies. Detection was by enhanced chemiluminescence. These results are representative of three separate experiments.

a)

Cells
|
Digitonin + low salt buffer, 250g, 3 minutes

Pellet   Supernatant (S6)
(Permeablised cells)

250mM K⁺ wash

Pellet (P6)   Supernatant (250 wash)

500mM K⁺ wash

Pellet (membranes)   Supernatant (500 wash)

b)

c)

131
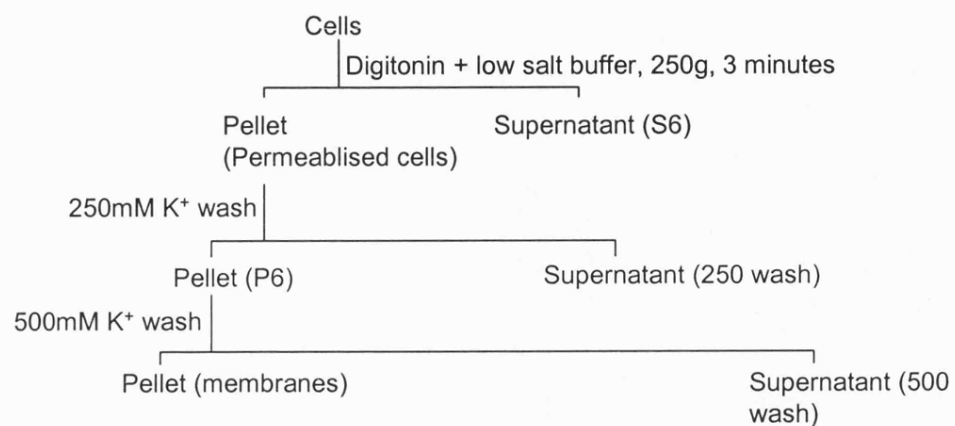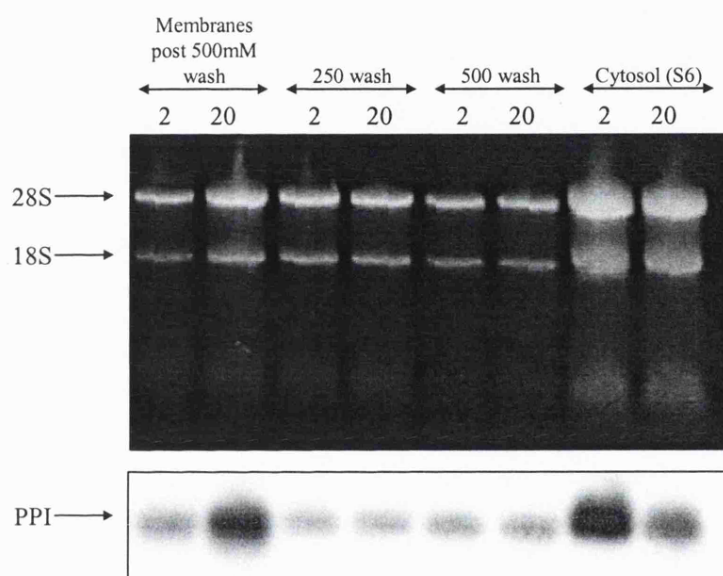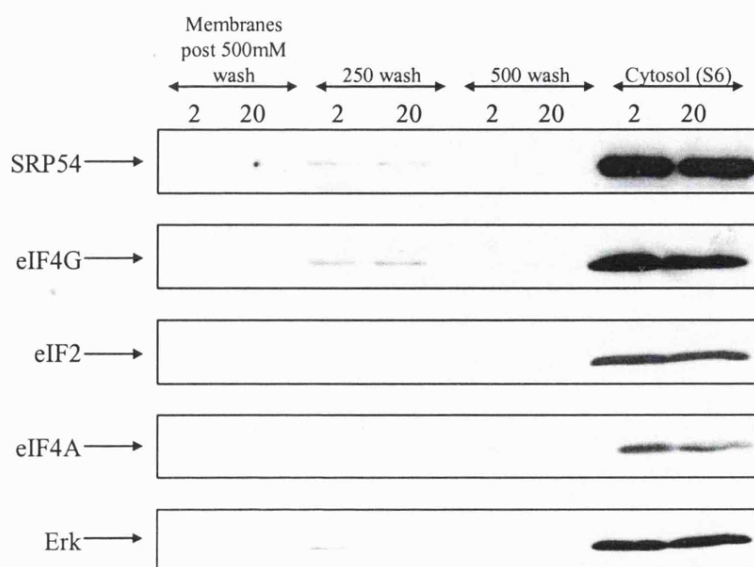
Western blot analysis confirmed the efficiency of the subcellular fractionation and confirmed that the majority of SRP54, eIF4G, eIF4A, eIF2 and erk are in the post-membrane fractions (figure 3.16c).

Summary
High salt washes of membranes did not result in a differential loss of PPI mRNA from the ER, suggesting that transfer of mRNA from the SRP receptor to the translocon is not regulated by glucose.

PPI mRNA that is associated with the ER is actively translating at low and high glucose
The majority of PI RNCs are tightly associated with the translocon (figure 3.16), however, it is unknown if ER-associated PPI mRNA is actively translating at both low and high glucose concentrations. In order to investigate whether ER-associated PPI mRNA is actively translating, subcellular fractionation was carried out in the presence of puromycin. MIN6 cells were incubated in low or high glucose and treated with puromycin 10 minutes prior to lysis to a final concentration of 200μM. The lysates were fractionated by the consecutive centrifugation method, RNA was isolated from each fraction and used to probe for PPI, CPH and actin mRNAs by northern blotting. In the presence of puromycin the majority of PPI and CPH mRNA was released from the ER (P6) at both low and high glucose and was found in the cytosol still associated with ribosomes (P200) (figure 3.17a). This suggests ER-associated PPI and CPH RNCs were actively translating. Western blotting showed that puromycin had no effect on the subcellular distribution of SRP54, despite the release of PPI and CPH ribosome-nascent chain complexes from the ER, suggesting that SRP binding to the ER is not reliant on the signal sequence (figure 3.17b).

3.2.7: Conclusions: Association of PPI mRNA with the membranes
Salt washes of the ER membranes showed that the association of PPI or CPH RNCs with the ER membranes did not differ in MIN6 cells incubated in low or high glucose concentrations (figure 3.16). Furthermore, the majority of ER-associated CPH and PPI mRNAs are actively translating at low and high glucose (figure 3.17). This data therefore suggests that regulation of PI synthesis does not occur through regulating the association of PPI RNCs with the ER or through inhibition of PI synthesis at the ER.
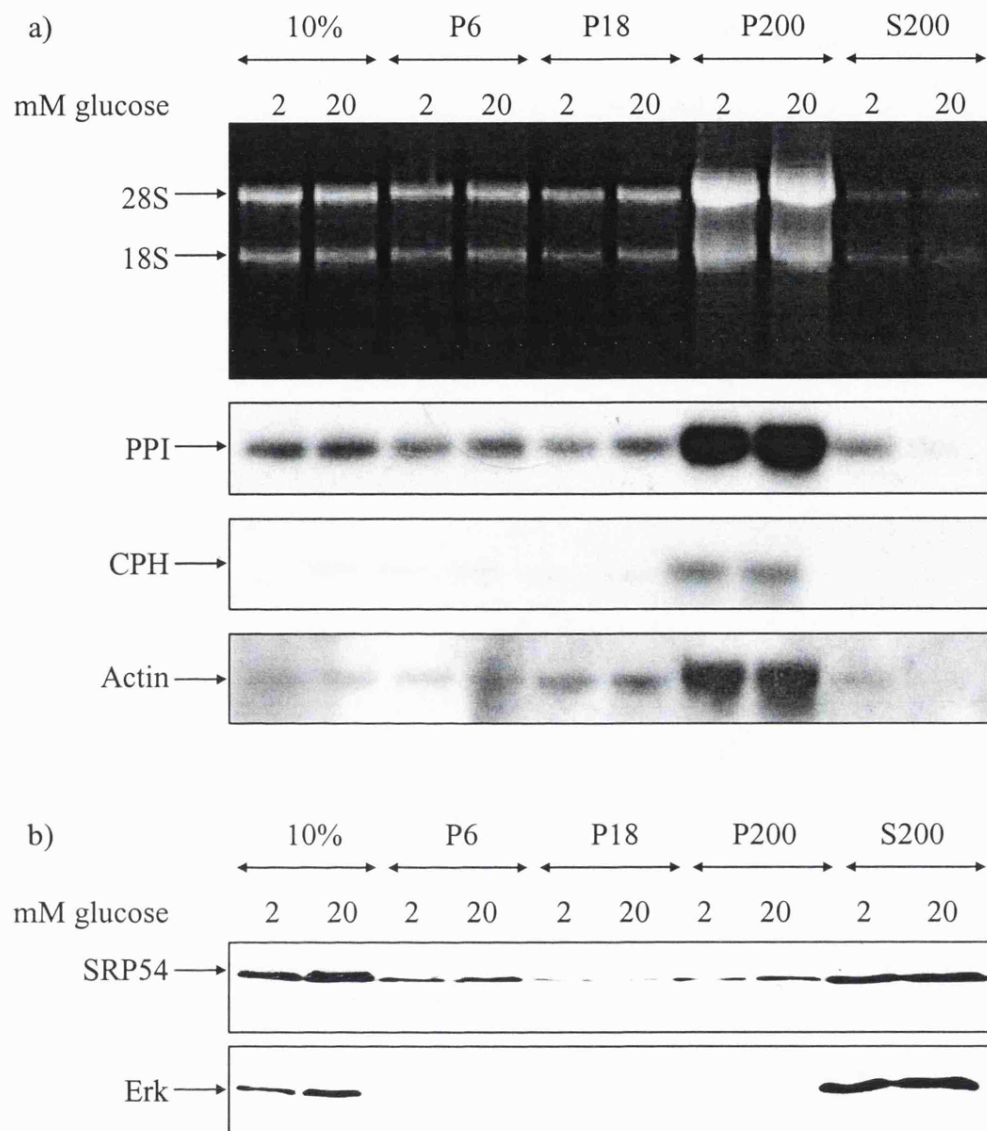
Figure 3.17: PPI mRNA that is associated with the membrane is actively translating at low and high glucose. MIN6 cells were pre-incubated in KRB containing 2mM glucose for 1 hour followed by incubation in KRB containing 2mM or 20mM glucose for a further hour. 200μM (final concentration) of puromycin was added to the cells 10min prior to lysis to terminate actively translating ribosomes. Cells were fractionated by consecutive centrifugation resulting in the membrane fraction (P6), polysome fraction (P200) and a supernatant fraction containing free mRNAs (S200). a) Isolated RNA from each fraction was run on a 1-% agarose, formaldehyde gel, then transferred onto nylon membrane and probed for PPI, CPH and actin mRNAs. b) 8% of the pellets and 1% of the supernatants were run on 12.5% SDS-PAGE and subjected to immunoblotting with SRP54 and Erk antibodies. Detection was by enhanced chemiluminescence. These results are representative of two separate experiments.

3.2.8: Glucose stimulated recruitment of PPI mRNA to the ER is important in glucose stimulated proinsulin synthesis

The work carried out so far shows that PPI mRNA is recruited to the ER in response to an increase in glucose concentrations (figures 3.9 and 3.13). In order to investigate the significance of the recruitment of PPI mRNA to the ER as a mechanism for regulating PI synthesis, [^{35}S]-methionine incorporation into MIN6 cells (*in vivo*) was compared with *in vitro* translations of the ER membranes (*in situ*) and *in vitro* translations of mRNA purified from the ER membranes (*in vitro*).

Optimisation of conditions for rabbit reticulocyte lysate (RRL) translation reactions

Removing cycloheximide from the membranes for in situ translations

For *in situ* translations in RRL, membranes were isolated in the presence of cycloheximide from MIN6 cells incubated in low or high glucose by the consecutive centrifugation method. However, cycloheximide used to prevent ribosomal run-off during the membrane isolation method may not dissociate from the ribosome-nascent chain complex and therefore could continue to inhibit translational elongation in the RRL. In order to remove cycloheximide from the membranes, the membranes were washed twice in buffer that did not contain cycloheximide, before they were added to the RRL.

Before proceeding further, to ensure that cycloheximide could be washed off cells and therefore presumably the membranes, [^{35}S]-methionine incorporation was compared between cells that were incubated in cycloheximide that was then washed off and cells that were incubated in cycloheximide and cells that were not incubated in cycloheximide. After MIN6 cells were incubated in KRB supplemented with 20mM glucose for one hour they were treated as follows: 1) Cells were incubated in KRB containing 20mM glucose and [^{35}S]-methionine for 30 minutes; 2) cells were incubated in KRB supplemented with 20mM glucose, [^{35}S]-methionine and 0.1mg/ml cycloheximide (final concentration) for 30 minutes; 3) Cells were incubated for 10 minutes in KRB supplemented with 20mM glucose and 0.1mg/ml of cycloheximide (final concentration). After 10 minutes incubation in cycloheximide, cells were washed twice in KRB supplemented with 20mM glucose and incubated in KRB containing 20mM glucose and [^{35}S]-methionine for 30 minutes. Cells were lysed after their

respective incubations and [^{35}S]-methionine incorporation was measured by TCA precipitation and liquid scintillation counting. [^{35}S]-methionine incorporation into cells that were incubated in cycloheximide (method 2 and 3) were found as a percentage of [^{35}S]-methionine incorporation into cells that were not incubated in cycloheximide (method 1).

The addition of cycloheximide for the whole 30-minute incubation with [^{35}S]-methionine (method 2) reduced [^{35}S]-methionine incorporation to 5% of the control (method 1) (figure 3.18). Meanwhile, cells that had been incubated in cycloheximide that was subsequently washed out (method 3) incorporated almost exactly the same amount of [^{35}S]-methionine as cells that had never been incubated in cycloheximide (method 1). Because cells in which cycloheximide was added and then washed off were able to incorporate almost exactly the same amount of [^{35}S]-methionine as control cells, it was likely that cycloheximide would easily be washed off isolated membranes. Therefore, in order for *in situ* translations to occur, isolated membranes were washed twice with KHM buffer (see materials and methods) to remove the cycloheximide and finally resuspended in KHM buffer for addition to RRL.

Optimisation of in situ translation reactions

Membranes from a 10cm plate of MIN6 cells were resuspended in KHM buffer to a final volume of 30μl. In order to optimise the amount of membranes used, 1 - 3μl of resuspended membranes were added to whole RRL or ribosome-depleted RRL (figure 3.19). After the *in situ* translation reaction, the membranes were pelleted and the pelleted membranes and supernatants containing the RRL were run on a 20% SDS-PAGE (figure 3.19a and 3.19b respectively). Very little [^{35}S]-methionine incorporation was observed in the supernatant fraction compared to the membrane fraction (figure 3.19b compared to figure 3.19a) confirming that the majority of *in situ*-translated proteins were translated into the ER lumen. Furthermore, as the presence or absence of ribosomes in the RRL had no effect on the *in situ* translation (figure 3.19a), it is likely that the synthesis of these proteins was directed by ribosomes endogenous to the ER fraction.
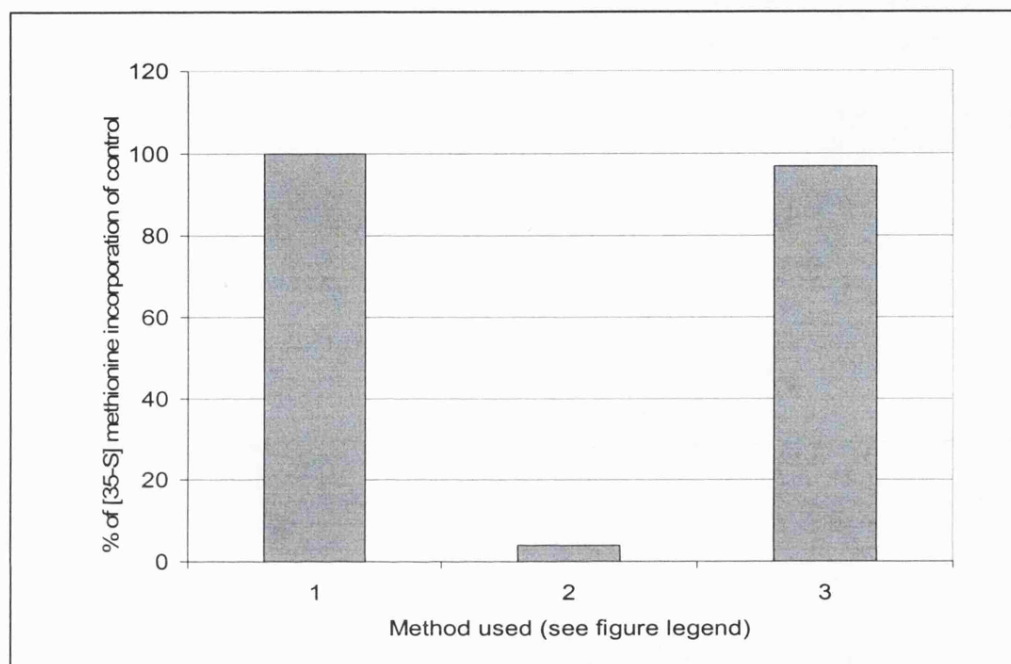
Figure 3.18: Cycloheximide can be added to cells and then washed out, with no future effect on [^{35}-S] methionine incorporation. MIN6 cells were incubated in KRB containing 20mM glucose for one hour. Cells were treated as follows: Method 1) [^{35}-S]-methionine was added to cells for 30 minutes. 2) [^{35}-S]-methionine and 0.1mg/ml of cycloheximide (final concentration) was added to cells for 30 minutes. 3) 0.1mg/ml of cycloheximide (final concentration) was added to cells for 10 minutes. The media was removed and cells were washed twice in KRB containing 20mM glucose. [^{35}-S]-methionine was then added for 30 minutes. Cells were lysed in MIN6 lysis buffer and [^{35}-S]-methionine incorporation was calculated by TCA precipitations. This is representative of one experiment.

136

Figure 3.19: Optimisation of the conditions for *in situ* translations of membranes isolated from MIN6 cells. MIN6 cells were pre-incubated in KRB containing 2mM glucose for 1 hour followed by incubation in KRB containing 2mM or 20mM glucose for a further hour. 0.1mg/ml (final concentration) of cycloheximide was added to the cells 10 minutes prior to lysis to prevent ribosomal run-off. Membranes were isolated by consecutive centrifugation as described in figure 3.9 and washed twice with KHM buffer. 1-3μl of re-suspended membranes were translated in either ribosome-depleted rabbit reticulocyte lysate (RRL) or full RRL for one hour at 30°C. a) After translation membranes were pelleted at 13000g for 10 minutes, re-suspended in 1X Laemelli's buffer and resolved on 20% SDS-PAGE gels. b) Supernatants resulting from the pelleting of in situ translated membranes were also resolved on 20% SDS-PAGE gels. c) *In vitro* translations were carried out in the absence of endogenous mRNA and in the presence of control luciferase mRNA and resolved on 20% SDS-PAGE. These results are representative of three separate experiments.

a)

b)

c)

138
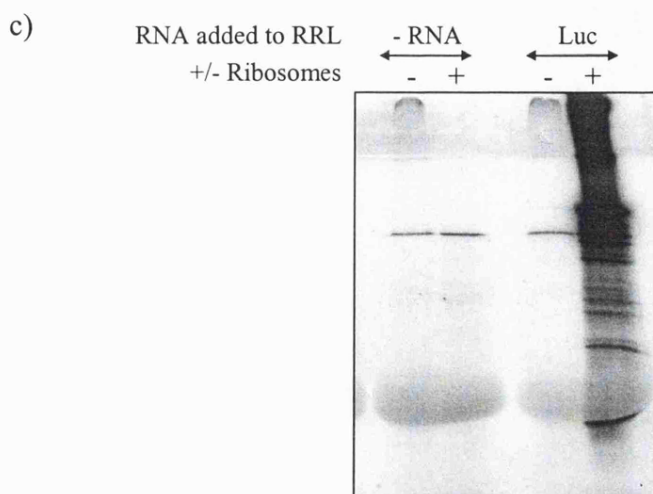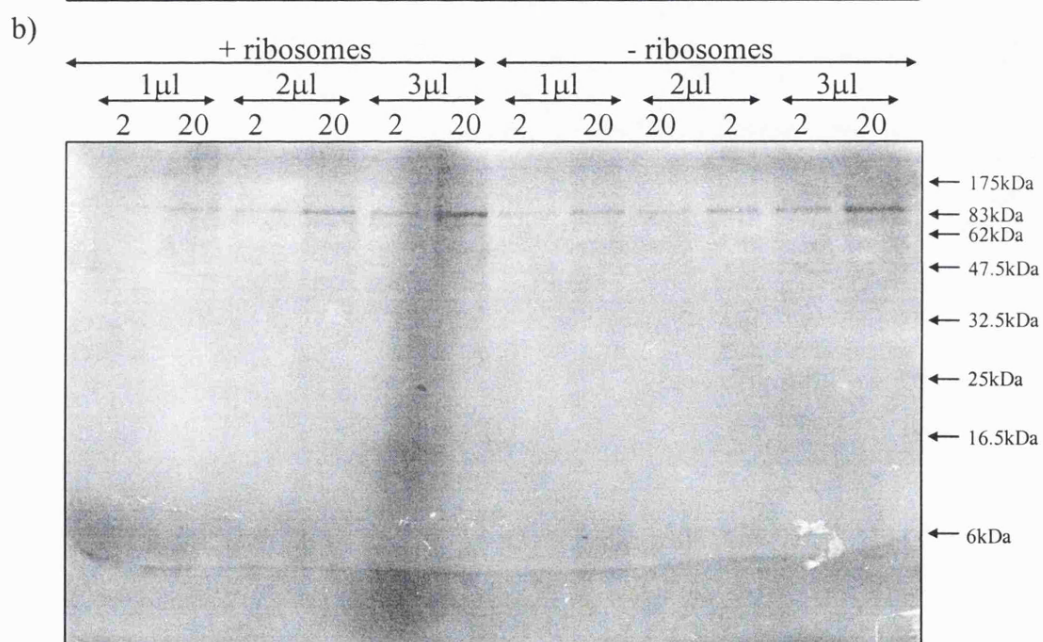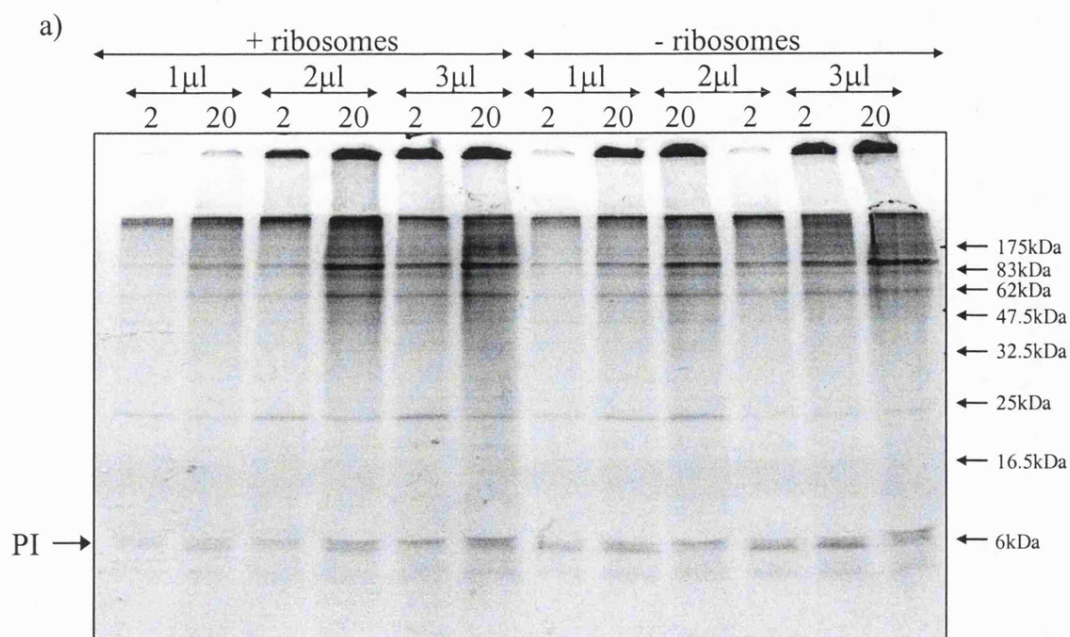
For control experiments, whole RRL and ribosome-depleted RRL were incubated in the absence of exogenous mRNA or in the presence of luciferase mRNA (figure 3.19c). In the absence of ribosomes, luciferase RNA was not translated. As translation of luciferase will only take place in the presence of ribosomes, this confirms that the ribosomes were efficiently depleted from the RRL and that ribosomes endogenous to the ER must be responsible for the translation products in the ribosome-depleted reactions shown in figure 3.19a. No translation products were observed when whole RRL or ribosome-depleted RRL were incubated without the addition of mRNA or membranes (figure 3.19c), thereby confirming that the products shown in figure 3.19a are due to the addition of the membranes to the RRL.

Because the quantity of membranes used in the RRL reaction had no effect on the quality of the *in situ* translation reactions (figure 3.19a), future *in situ* translation reactions used 3μl of membranes per reaction, so as to ensure maximum [^{35}S]-methionine incorporation into protein.

In vitro translation of RNA isolated from the membranes

Initial attempts at translating RNA purified from membranes in RRL failed (*in vitro* translations). This was possibly due to the large amount of ribosomal RNA that was present within the sample. Therefore mRNA was isolated from total RNA using the poly(A) tract isolation system. *In vitro* translation of 20μg of total RNA resulted in no translation products, whereas *in vitro* translation of poly(A) mRNA isolated from 1-4μg of total RNA resulted in increasing amounts of translation products (figure 3.20).

Glucose stimulated recruitment of PPI mRNA to the ER is important in glucose stimulated PI synthesis

MIN6 cells were pre-incubated in KRB supplemented with 2mM glucose for 1 hour, followed by a 1 hour incubation in KRB supplemented with 2mM or 20mM glucose. The membranes were then isolated by the consecutive centrifugation method and *in situ* translated in RRL.

a)
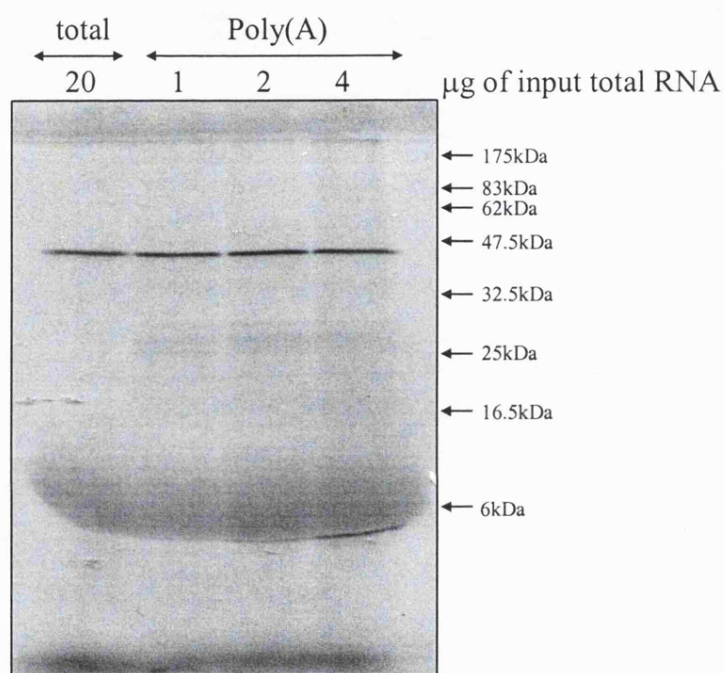
Figure 3.20: Optimisation of the conditions for *in vitro* translations of RNA isolated from MIN6 cells. RNA was purified from the membranes that were isolated by consecutive centrifugation as described in figure 3.9 and resuspended in 40µl. 20µg of total RNA was retained for *in vitro* translation. Poly(A) mRNA was purified from the remaining 20µl using mRNA selection poly(A) tract isolation system II (Promega) and the equivalent of 1, 2 and 4µg of total input RNA was used for *in vitro* translation of poly(A) mRNA. 1/10th of *in vitro* translations were resolved on 20% SDS-PAGE.

In situ translations of membranes extracted from MIN6 cells incubated at high glucose incorporated significantly more [^{35}S]-methionine into both PI and other proteins than those extracted from cells incubated at low glucose (figure 3.21a). However, although these data show that glucose stimulates translation of PI synthesis at the ER, they do not demonstrate whether the observed glucose-stimulated increase in PI synthesis is solely due to an increase in the amount of PPI mRNA associated with the ER membranes or if there is additional regulation at the ER membranes.

In order to determine the importance of glucose-stimulated recruitment of PPI mRNA to the ER in regulating PI synthesis, mRNA was isolated from membrane fractions extracted from MIN6 cells incubated at low or high glucose and translated *in vitro* in RRL in the presence of [^{35}S]-methionine. PI was then immunoprecipitated from the *in vitro* translation reactions and run on a 20% SDS-PAGE alongside 10% of the total reaction (figure 3.21b). RRL reactions using mRNA purified from the membranes of cells incubated in high glucose incorporated significantly more [^{35}S]-methionine into PI than RRL reactions using mRNA purified from the membranes of cells incubated in low glucose concentrations (figure 3.21b). Moreover, this increase in PI synthesis is similar to that observed in the *in situ* translation reactions (figure 3.21a), suggesting that further regulation of PI synthesis did not take place at the membranes in the *in situ* translations.

In situ and *in vitro* translations of membrane mRNA isolated from MIN6 cells suggest that the glucose-stimulated recruitment of PPI mRNA to the membrane is important in regulating PI synthesis (figure 3.21a and b). However, it has already been shown that glucose stimulates the rate of initiation (figure 3.2) and glucose may well regulate PI synthesis through additional mechanisms. To determine the importance of glucose-stimulated recruitment of PI mRNA to the ER in the overall picture of PI synthesis, [^{35}S]-methionine incorporation into MIN6 cells (*in vivo* translations) was investigated and compared to the rates of PI synthesis from the *in situ* and *in vitro* translation reactions. MIN6 cells were incubated in KRB containing low or high glucose concentrations in the presence of [^{35}S]-methionine. PI was then immunoprecipitated from the MIN6 cell extracts, run on SDS-PAGE and detected by autoradiography (figure 3.21c). *In vivo*, MIN6 cells that had been incubated in high glucose incorporated more [^{35}S]-methionine into PI than those incubated in low glucose. Furthermore, the

Figure 3.21: The recruitment of preproinsulin mRNA onto the membranes and/or regulation at the ER membranes at high glucose plays a significant role in glucose stimulated protein synthesis. MIN6 cells were pre-incubated in KRB containing 2mM glucose for 1 hour followed by incubation in KRB containing 2mM or 20mM glucose for a further hour. 0.1mg/ml (final concentration) of cycloheximide was added to the cells 10 minutes prior to lysis to prevent ribosomal run-off. a) Membranes were isolated by consecutive centrifugation as described in figure 3.9 and washed twice with KHM buffer. 3μl of re-suspended membranes were translated in either ribosome-depleted rabbit reticulocyte lysate (RRL) or full RRL for one hour at 30°C. After translation membranes were pelleted at 13000g for 10 minutes, re-suspended in 1X Laemelli's buffer and resolved on 20% SDS-PAGE gels. b) Tri-reagent was used to purify RNA from the membranes that were isolated by consecutive centrifugation as described in figure 3.9. Poly (A) RNA was purified from the total RNA and *in vitro* translated as described for (a). PI was immunoprecipitated from the rest of the *in vitro* translation reactions and resolved on 20% SDS-PAGE alongside 1/10th of the *in vitro* translation reaction. c) MIN6 cells were lysed in MIN6 lysis buffer. ci) a sample of the lysates was run on a SDS polyacrylamide gel and the proteins were visualised by autoradiography. cii) PI was immunoprecipitated from the lysates and resolved on 20% SDS-PAGE. These results are representative of three separate experiments.

a) *In situ* translation
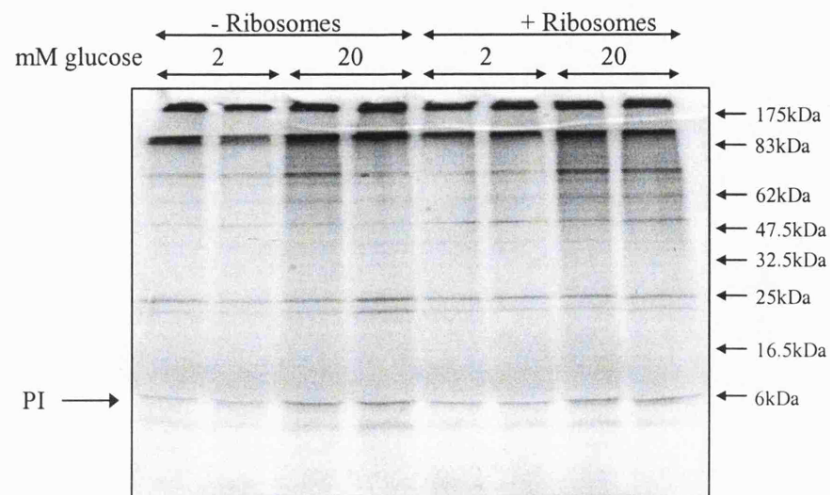
b) *In vitro* translation
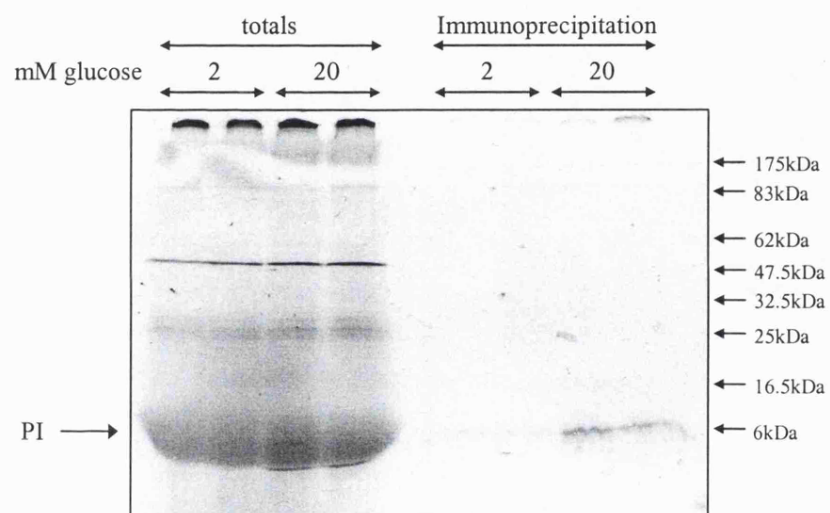
c) *In vivo* translation
i) totals
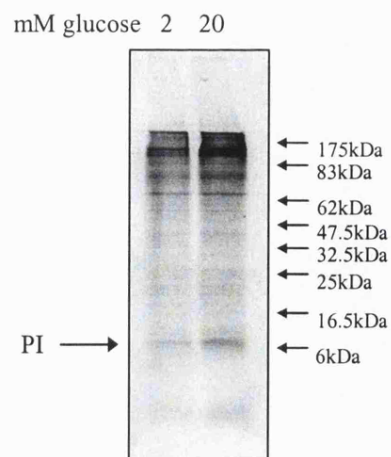
ii) Immunoprecipitation

143
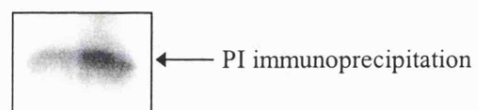
glucose-stimulated increase in [^{35}S]-methionine incorporation *in vivo* is larger than the increase observed *in situ*.

3.2.9: Conclusions: Glucose stimulated recruitment of PPI mRNA to the ER is important in glucose-stimulated proinsulin synthesis

Taken together these results show that glucose-stimulated recruitment of PPI mRNA to the ER is an important step in the regulation of PI synthesis. However, additional glucose-regulated mechanisms, for example an increase in the rate of initiation of translation, also play an important role in contributing to glucose-regulated PI synthesis.

3.2.10: Investigation of glucose stimulated proinsulin synthesis in islets of Langerhans

I have shown in MIN6 cells that glucose stimulates a recruitment of ribosomes onto mRNAs that are already associated with ribosomes. Furthermore, this increase in initiation is a global effect that is most likely observed with all mRNAs. In addition to an increase in the rate of initiation, this work has shown that glucose stimulates the recruitment of PPI mRNA to the ER at high glucose, which is an important step in glucose-stimulated PI synthesis. However, because MIN6 cells are a β-cell line it could be argued that it is more physiologically relevant to study the primary cells. Therefore polysome analysis and subcellular fractionation was repeated in islets of Langerhans that were isolated from female Wistar rats.

Islets were pre-incubated in KRB containing 2mM glucose for two hours followed by a one-hour incubation in KRB containing 2mM or 20mM glucose. Islets were lysed in high salt polysome buffer supplemented with 1% triton and underwent sucrose sedimentation gradient centrifugation. However, because of the low yield of protein and RNA obtained from islets clear polysome profiles were not produced. The gradients were fractionated, RNA was isolated from each fraction and run on a formaldehyde gel. The distribution of PPI mRNA across the gradient was determined by Northern blot analysis (figure 3.22ai). At both low and high glucose all PPI mRNA

Figure 3.22: Glucose stimulated proinsulin synthesis in islets of Langerhans. Islets were pre-incubated in KRB containing 2mM glucose for 2h followed by incubation in KRB containing 2mM or 20mM glucose for a further hour. 0.1mg/ml (final concentration) of cycloheximide was added to the cells 10min prior to lysis to prevent ribosomal run-off. b) Cells were then lysed in high salt polysome buffer supplemented with 1% triton and the lysates were layered onto 20-50% sucrose gradients and centrifuged at 39000rpm at 4°C for 2 hours. Gradients were fractionated from top (fraction 1) to bottom (fraction 10) using the ISCO gradient fractionator. RNA was isolated from 10, 1ml fractions and run on 1-% agarose, formaldehyde gel. RNA was then transferred onto nylon membrane and probed for PPI mRNA. ii) Cells were treated and fractionated as described for i) except 15mM EDTA was included in the lysis buffer and the sucrose gradients to dissociate the ribosomes but leave intact mRNPs. b) Cells were fractionated by consecutive centrifugation as described in figure 3.9a. i) RNA was isolated from each fraction was run on a 1% agarose formaldehyde gel, then transferred onto nylon membrane and probed for PPI mRNA; ii) Protein samples were run on 12.5% SDS-PAGE and subjected to immunoblotting with Erk2, calreticulin and SRP54 antibodies. Detection was by enhanced chemiluminescence. These results are representative of three separate experiments.

a) Polysome analysis

i)

ii)

b) Subcellular fractionation

i)

ii)
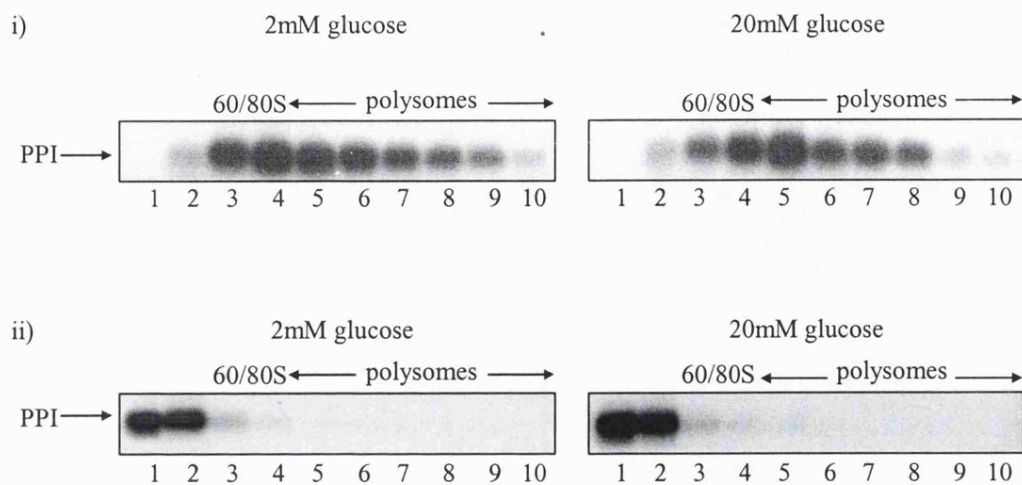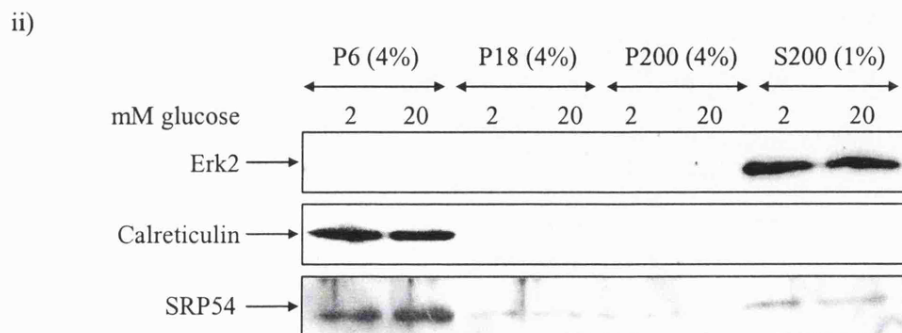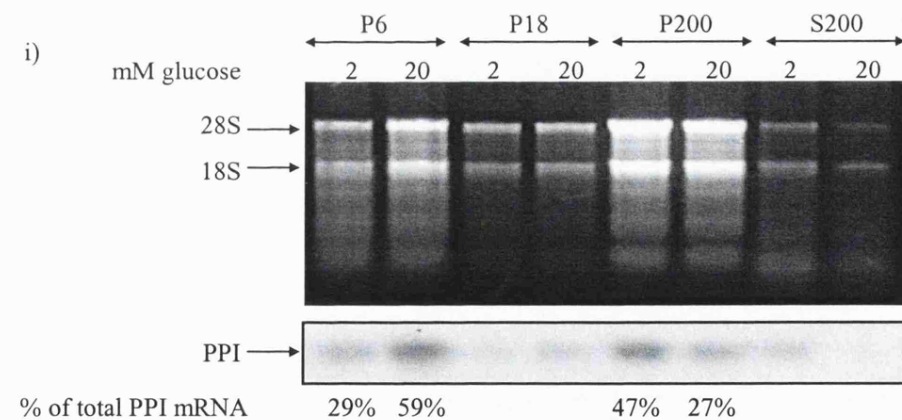
sediments with either monosomes or polysomes and there is no 'free' PPI mRNA. Upon an increase in glucose concentration there is a small but significant shift of PPI mRNA onto heavier polysomes. In the presence of EDTA all PPI mRNA is found at the top of the gradient, confirming that the sedimented PPI is due to bound ribosomes (figure 3.22aii).

Polysome analysis of islets confirmed the results in MIN6 cells that PPI mRNA is not free and that there is a recruitment of ribosomes onto ribosome-associated PPI mRNA. In order to investigate recruitment of PPI mRNA to the ER, islets of Langerhans were incubated in low or high glucose concentrations as above and fractionated by consecutive centrifugation. The location of PPI mRNA within each fraction was determined by Northern blot analysis. At low glucose a large amount (47%, mean of three experiments, SD=15.2) of PPI mRNA is associated with ribosomes in the cytosol (P200) with only 29% (SD=10.09) associated with the ER membranes (P6, figure 3.22bi). Conversely, at high glucose the majority (59%, SD=14.34) of PPI mRNA is associated with the ER (P6) with only 27% (SD=11.84) associated with ribosomes in the cytosol (P200). This change in PPI mRNA adds up to an approximate 200% (SD=25.3) increase in PPI mRNA associated with the ER at high glucose. Very little PPI mRNA is observed free in the cytosol (S200) and the little that there is may well be due to carry over from the P200 fraction as a small amount of ribosomal RNA is also observed in the S200 fraction.

The effectiveness of the subcellular fractionation technique was confirmed by Western blot analysis of protein samples for the ER marker, calreticulin and cytosolic marker, Erk2 (Figure 3.22bii). Calreticulin was found solely associated with the membranes (P6) and Erk2 was found solely in the cytosol (S200). The distribution of SRP54 within islets was also investigated (figure 3.22aii). In this case the amount loaded in the P6, P18 and P200 fractions was proportionally four times more than the amount loaded in the S200 fraction. Therefore, approximately 50% of SRP54 is present on the membranes and 50% in the cytosol at both low and high glucose concentrations.

These results in islets confirm results in MIN6 cells that there is neither a large pool of 'free' PPI mRNA nor a perceivable increase in the rate of de novo initiation on the PPI-mRNA in response to glucose. Furthermore, glucose does stimulate the recruitment of

ribosomes onto ribosome-associated PPI mRNA i.e. an increase in the rate of initiation and glucose stimulates an increase in the recruitment of PPI mRNA to the ER.

3.3: Discussion

Glucose stimulates a 10 to 20 fold increase in PI synthesis within 60 minutes in pancreatic β-cells (Grimaldi et al., 1987; Guest et al., 1989; Itoh and Okamoto, 1980). This glucose stimulated increase in PI synthesis is primarily regulated at a post-transcriptional level, most likely through an increase in the rate of protein synthesis (Alarcon et al., 1993; Itoh and Okamoto, 1980; Permutt and Kipnis, 1972a). However, the mechanism for glucose-regulated PI synthesis and secretory granule protein synthesis is poorly understood. Therefore, this present study investigates the mechanism of PI synthesis in the pancreatic β-cell.

3.3.1: Glucose stimulates the rate of initiation but not the rate of de-novo initiation in pancreatic β-cells

Sucrose sedimentation gradients of lysates from MIN6 cells and islets incubated in low or high glucose concentrations showed that no PPI mRNA sedimented at the top of the gradient, where free PPI mRNA is expected to sediment (figure 3.2 and 3.22ai). This finding was supported by subcellular fractionation of MIN6 cells and islets, which showed that all of PPI mRNA was associated with ribosomes (figure 3.9, 3.13 and 3.22bi).

Although glucose did not stimulate the recruitment of ribosomes onto free PPI mRNA (de-novo initiation), polysome analysis of MIN6 cell lysates showed that glucose did stimulate the recruitment of ribosomes onto ribosome-associated PPI mRNA (figure 3.2), indicative of an increase in the rate of initiation. Polysome analysis of MIN6 cells also showed that an increase in the rate of initiation but not in the rate of de-novo initiation also occurred for mRNAs encoding secretory proteins, CPH and PC2 and for mRNAs encoding cytosolic proteins; actin and S7 (figure 3.2). Furthermore, this recruitment of ribosomes onto ribosome-associated mRNAs encoding PI, CPH and PC2 was observed in the cytosolic (figure 3.5) and membrane fractions (figure 3.4), indicative of an increase in the rate of initiation in the cytosol and at the ER. As glucose stimulated the recruitment of ribosomes onto all of the mRNAs tested, it is likely that glucose stimulates increases in the rate of initiation for the majority of mRNAs.

Interestingly, previous work has shown that the 5' and 3' UTRs of PPI mRNA act co-operatively to increase PI synthesis in response to increases in glucose concentration (Wicksteed et al., 2001). Therefore the observed glucose-stimulated increase in the rate of initiation (figure 3.2) could be via an increase in the rate of ribosome-reycling from the 3'UTR to the 5'UTR.

Polysome analysis of MIN6 cells showed that glucose does not stimulate the recruitment of ribosomes onto free PPI mRNA, i.e. an increase in the rate of de novo initiation (figure 3.2). This contradicts previous reports that show a pool of free PPI mRNA at low glucose (23-62%) that is recruited onto ribosomes at high glucose, likely through an increase in the rate of de novo initiation (Itoh and Okamoto, 1980; Welsh et al., 1986; Welsh et al., 1991; Welsh et al., 1987). However, these studies should be treated with caution since they failed to use cycloheximide to prevent ribosomal run-off. Indeed, I demonstrate that subcellular fractionation and polysome analysis in the absence of cycloheximide resulted in a pool of free PPI mRNA for cells incubated at low glucose, and that this pool most likely results from ribosomal run-off (figures 3.6 and 3.15). Furthermore, as ribosomal run-off still occurs when cycloheximide is not added to cells prior to lysis but is included in the lysis buffer (figure 3.7), ribosomal run-off most likely occurs post-incubation during the lysis procedure.

As it has previously been reported that glucose stimulates elongation in islets (Welsh 1986), more ribosomal run-off would be expected at high glucose than at low glucose. The increased rate of ribosomal run-off at high glucose would therefore result in increased amount of free PPI, PC2, CPH and actin mRNAs at high glucose but not necessarily at low glucose. However, I showed that in the absence of cycloheximide, there is an increased amount of free PPI mRNA at low glucose compared to at high glucose (figure 3.6 and 3.15). One possibility for the increased amount of ribosomal run-off at low glucose compared to at high glucose is that ribosomal run-off occurs at both low and high glucose concentrations but that the glucose-stimulated increase in ribosome recruitment onto these mRNAs (figure 3.2) counteracts ribosomal run-off at high glucose. Indeed, ribosomal run-off was observed at both low and high glucose in the presence of the initiation inhibitor, pactamycin (figure 3.7), therefore, it can be assumed that, in the absence of pactamycin, ribosomes will run off the mRNA at both glucose concentrations. Thus it is likely that at high glucose concentrations, an

increased rate of ribosome recruitment onto ribosome-associated PPI mRNA is compensating for the ribosomal run-off.

The small increase in the rate of initiation is potentially enough to compensate for ribosomal run-off at high glucose. However, there is a large amount of run-off at low glucose compared to high glucose (figure 3.6b) while polysome analysis in the presence of cycloheximide (figure 3.2 and 3.6a) shows that glucose only stimulates a small increase in the rate of initiation. The most likely explanation is that because less ribosomes are associated with PPI mRNA at low glucose than at high glucose (figure 3.2), a larger proportion of PPI mRNA becomes free at low glucose. In the absence of cycloheximide, it is likely that the cumulative effect of the lower rate of initiation and smaller PPI polysomes result in a significant increase in the amount of ribosomal run-off at low glucose compared to at high glucose concentrations.

3.3.2: Glucose stimulates the recruitment of secretory protein mRNAs to the ER

In MIN6 cells and islets, glucose stimulated a recruitment of cytosolic ribosome-bound PPI mRNA at low glucose onto the ER at high glucose (figures 3.9, 3.13 and 3.22b). Furthermore, *in situ* translations of the membranes isolated from MIN6 cells and *in vitro* translations of mRNA isolated from the membranes of MIN6 cells showed that the glucose stimulated recruitment of PPI mRNA to the ER results in approximately a two-fold increase in PI synthesis (figure 3.21a and 3.21b). Therefore, from these data I can conclude that the observed recruitment of PPI mRNA to the ER plays a significant role in glucose-stimulated PI synthesis.

Additionally, in MIN6 cells, glucose also stimulated the recruitment of secretory protein mRNAs, CPH and PC2 to the ER (figure 3.9 and 3.13). It has been reported that the synthesis of a large number of secretory granule proteins is increased upon glucose stimulation (Guest et al., 1991). Therefore, it is likely that the majority of mRNAs encoding secretory granule proteins are recruited to the ER in response to high glucose concentrations. Microarray analysis using mRNA isolated from the membranes of MIN6 cells incubated in low or high glucose concentrations could be used to identify mRNAs that are recruited to the ER at high glucose concentrations. Indeed, cDNA

microarrays have already been used to identify ER-associated mRNAs in Jurkat cells (Lerner et al., 2003).

Previous work has shown that glucose increased the ratio of GTP to GDP from 2:1 to 4:1 (Hoenig and Matschinsky, 1987). It has been suggested that this increase will allow the SRP receptor to switch from its inactive GDP-bound state to its active GTP-bound state (Welsh et al., 1986). Moreover, the non-hydrolysable analogue of GTP, GTP-γ-[S] stimulated recruitment of PPI mRNA to the ER in a similar manner to glucose (Welsh et al., 1991). Furthermore, the addition of SRP receptor to homogenates isolated from islets incubated in high glucose more than doubled PI synthesis, while the addition of SRP receptor to homogenates isolated from islets incubated in low glucose only increased PI synthesis by 40% (Welsh et al., 1986). These results suggest that glucose may regulate SRP binding to the SRP receptor through the regulation of their GTP cycles. If glucose does regulate the GTP cycles of SRP and the SRP receptor, it is likely that this has an effect on all secretory protein mRNAs and may be the mechanism for glucose-stimulated recruitment of these mRNAs to the ER. However, in this study I did not observe a consistent glucose-stimulated recruitment of SRP54 to the ER (figures 3.9 and 3.13).

Importantly, glucose had a greater stimulatory effect on the recruitment of PPI mRNA to the ER than CPH or PC2 mRNAs (glucose stimulates a 2 fold increase in PPI mRNA associated with the ER compared to a 1.3 fold increase in CPH and PC2 mRNAs, figure 3.9). This increased recruitment of PPI mRNA to the ER, compared to CPH and PC2 mRNAs may reflect differences in the rates of initiation of these different mRNAs. Indeed, polysome analysis of PPI and PC2 mRNAs shows that PPI mRNA is has smaller polysomes than PC2 mRNA at low glucose concentrations (figure 3.2). Alternatively, glucose may differentially regulate the translocation of PPI, CPH and PC2 mRNAs to the ER, perhaps through differences in the signal peptides of these mRNAs.

Interestingly, at low glucose, a higher proportion of PC2 (55%) and CPH (60%) mRNAs were associated with the ER compared to PPI (46%) mRNA. This suggests that at low glucose, a specific mechanism is preventing PPI mRNA from being recruited to the ER. How PPI mRNA is prevented from interacting with the ER is unclear.

Interestingly, rat PPI mRNA has numerous pause sites and translational pausing on PPI mRNA has been observed *in vitro* in the absence of SRP (Wolin and Walter, 1988). Therefore, at low glucose concentrations, PI synthesis may specifically pause at one of these sites, thereby specifically preventing it from being recruited to the ER.

The proportion of PPI mRNA at the ER at low glucose maybe smaller than that for CPH and PC2 mRNAs because PPI mRNA is a shorter mRNA. The shorter PPI mRNA will probably spend less time translating at the ER than the longer PC2 and CPH mRNAs, resulting in higher turnover of PPI mRNA and comparatively more cytosolic PPI mRNA than PC2 or CPH mRNAs.

3.3.3: Glucose does not regulate proinsulin synthesis at the ER

In situ and *in vitro* translations of MIN6 cells incubated in low or high glucose showed that the recruitment of PPI mRNA to the ER is an important step in glucose-stimulated PI synthesis (figure 3.21a and b). However, *in vivo* translations showed a larger increase in glucose-stimulated PI synthesis than the *in situ* or *in vitro* translations, suggesting that additional regulatory mechanisms are required (figure 3.21). Indeed, this chapter has already shown that glucose stimulates initiation of PPI translation (figure 3.2). A previous study, which observed only a small recruitment of PPI mRNA to the ER suggested that PI synthesis may be further regulated at the ER (Itoh and Okamoto, 1980). However, I have provided evidence to show that the majority of ER-associated PPI mRNA is tightly associated with the membranes and is actively translating at both low and high glucose concentrations (figure 3.16 and 3.17). This suggests that the transfer of the PPI ribosome-nascent chain complex from the SRP receptor to the translocon is not regulated by glucose.

3.3.4: Final conclusions

This work has shown that PI synthesis is not regulated through an increase in de novo initiation as all PPI mRNA is ribosome-bound at both low and high glucose concentrations (figure 3.2, 3.9, 3.13, 3.22). However, glucose does stimulate the recruitment of ribosomes onto ribosome-associated PPI mRNA, which is indicative of an increase in the rate of initiation of translation. In addition to an increase in the rate of

initiation of translation for PI, glucose also stimulated the recruitment of ribosomes onto all other mRNAs tested, suggesting that glucose stimulates an increase in the overall rate of initiation of translation. Indeed, work from the laboratory has shown in MIN6 cells that glucose stimulates the dephosphorylation of eIF2 in parallel with an increase in ternary complex formation and an increase in glucose-stimulated protein synthesis (Gomez et al., 2004).

Glucose also stimulated the recruitment of PPI, CPH and PC2 mRNAs to the ER (figure 3.9 and 3.13), therefore it is likely that glucose stimulates the recruitment of all secretory proteins to the ER. Moreover, glucose stimulated the specific recruitment of PPI mRNA to the ER over other secretory protein mRNAs and this may be an important mechanism for the specific up-regulation of proinsulin synthesis.

Chapter 4: Identification of PPI mRNA-binding proteins and the localisation of PPI mRNA in MIN6 cells

4.1: Introduction

Glucose stimulates a two-fold increase in total protein synthesis as well as specifically stimulating a 10 to 20 fold increase in PI synthesis within 60 minutes (Grimaldi et al., 1987; Guest et al., 1989; Itoh and Okamoto, 1980). At present, however, the mechanism(s) of proinsulin synthesis are poorly understood. I have previously demonstrated that stimulation with glucose causes the recruitment of ribosomes onto ribosome-associated PPI mRNA (i.e. an increase in the rate of initiation, figure 3.2). Importantly, I have also shown that there is a redistribution of PPI, PC2 and CPH mRNAs from the cytosol at low glucose to the ER at high glucose (figures 3.9 and 3.13). In addition to a general glucose-stimulated recruitment of secretory protein mRNAs to the ER, the association of PPI mRNA with the ER appears to be specifically regulated by glucose. At low glucose concentrations only 46% of PPI mRNA is associated with the ER while, 59% of CPH and 61% of PC2 mRNAs are associated with the ER at low glucose concentrations (figure 3.9). This data suggests that PPI mRNA is specifically inhibited from associating with the ER and two possible explanations for this exist: 1) mRNA binding proteins may prevent PPI mRNA from associating with the ER through a number of possible mechanisms; 2) PPI mRNA may be localised to specific sub-cellular compartment, thus preventing it from being targeted to the ER.

4.1.1: Regulation of translation through mRNA binding proteins

mRNA binding proteins are often associated with the 5' UTR or 3' UTR of mRNAs and have been shown to regulate translation. A well-documented example of the role of UTRs as regulatory elements is in the regulated expression of both the transferrin receptor and ferritin in response to changes in cellular iron levels (reviewed in Ponka et al., 1998). The transferrin receptor is responsible for uptake of iron into the cell, while ferritin mRNA is responsible for detoxifying and storing cellular iron. Transferrin mRNA has 5 iron regulatory elements (IRE) in the 3' UTR. In the absence of iron, trans-acting factors bind the IRE and prevent transferrin mRNA from degradation by

ribonucleases. In the presence of iron, these factors dissociate, which results in destabilisation of transferrin mRNA. The destabilsation of transferrin mRNA at high levels of cellular iron results in a decrease in transferrin mRNA synthesis and therefore a decrease in iron uptake into the cell. In contrast to the transferrin mRNA, where the IRE regulate mRNA stability via the 3'UTR, ferritin mRNA IRE regulate translation through the 5'UTR. At low cellular iron levels IRP binds IRE and represses translation. However, in the presence of iron, IRP dissociates and allows translation of ferritin mRNA, which increases synthesis of ferritin and storage of iron. Additionally in the absence of IRP, the 5' UTR IRE of ferritin enhances binding of initiation factors to ferritin mRNA.

4.1.2: Regulation of proinsulin synthesis through mRNA binding proteins and localisation of mRNA

Interestingly, the 5'UTR of rat PPI mRNA contains a conserved, predicted stem loop structure and specific protein interactions have been observed with [^{32}P]-labelled RNA probes corresponding to sequences from this region (Knight and Docherty, 1992). More recently, the 5' and 3' untranslated regions of PPI mRNA have been shown to be required for glucose stimulated PI synthesis, possibly through the binding of specific proteins and/or the regulation of PPI RNA localisation (Wicksteed et al., 2001).

Polypyrimidine tract binding protein (PTB) has been shown to bind PPI mRNA and influence its expression. PTB binds to the 3' UTR of PPI mRNA and regulates the long-term stability of PPI mRNA (Tillmar et al., 2002). It is likely that other proteins bind PPI mRNA to regulate its expression of PI in response to changes in glucose concentrations and the identification of these proteins will certainly help to understand the mechanism of glucose-stimulated PI synthesis.

4.1.3: Localisation of mRNA

As one molecule of mRNA can translate many protein molecules, the localisation of mRNA to specific subcellular compartments provides an energy-efficient mechanism for the localisation of proteins. This localised protein synthesis also ensures high concentrations of protein in areas of the cell where they are required and excludes

proteins from areas where they may be detrimental, for example, the mis-localisation of Drosophila nanos or oskar mRNA results in severe developmental abnormalities (Ephrussi et al., 1991; Gavis and Lehmann, 1992).

Localisation of an mRNA is usually dependent on its 3'UTR and the trans-acting factors that bind to elements within the 3'UTR and promote active transport of the mRNA (St Johnston, 2005). Localisation signals vary from the very simple to the very complex. The simplest example of a localisation signal is the 11-nucleotide A2RE element in MBP mRNA that is recognised and bound by hnRNPA2 protein (Ainger et al., 1997; Hoek et al., 1998; Munro et al., 1999). This binding of hnRNPA2 to the A2RE is necessary for the localisation of MBP mRNA to the oligodendrocyte processes. Meanwhile, Drosophila bicoid mRNA contains a localisation element that is more than 600 nucleotides long and contains 5 stem loops (Brunel and Ehresmann, 2004; MacDonald, 1990; Macdonald and Struhl, 1988). This complex structure is required to localise bicoid mRNA to the anterior of the oocyte.

To ensure that proteins are not mis-localised, many localised mRNAs are also under translational control. A well-characterised example is the localisation and the translational regulation of Drosophila oskar mRNA in oocytes. Both the localisation of *Drosophila* oskar mRNA and translational regulation of oskar protein synthesis are mediated by the 3'-UTR of oskar mRNA (reviwed in Lipshitz and Smibert, 2000). To prevent the mis-localisation of oskar protein, the translation of oskar mRNA is repressed until it is localised to the posterior pole. This repression is mediated by trans-acting factors Bruno and HRP48 that bind the 3'UTR. Interestingly, recent work showed that Bruno represses translation of oskar by recruiting CUP protein that subsequently binds eIF4E, thereby inhibiting translation (Nakamura et al., 2004; Wilhelm et al., 2003). Once the oskar mRNA is localised to the posterior pole, its translation is activated through elements in the 5'UTR. The activation of translation also requires trans-acting factors such as vasa, which is believed to promote ternary complex formation (Carrera et al., 2000).

Similar mechanisms to those described above may localise PPI mRNA to specific sub-cellular compartments, thus preventing it from being targeted to the ER.

4.1.4: Aims

The objectives of this chapter are to: 1) identify proteins that are associated with PPI mRNA at low and high glucose concentrations and 2) determine the localisation of PPI mRNA at low and high glucose.

4.2: Results

4.2.1: MS2 binding protein tagging system

To identify proteins that bind PPI-mRNA *in vivo* and to visualise PPI mRNA in MIN6 cells, the MS2 tagging system was used. The MS2 tagging system exploits MS2 protein, which forms the capsid of MS2 bacteriophage and binds specifically and tightly to a small RNA hairpin (Peabody, 1993). MS2 protein bound to an immobilised support has been used to isolate mRNAs containing MS2 binding sites (Bardwell and Wickens, 1990) and to label mRNAs containing MS2 binding sites with MS2 fused to EGFP for visualisation by microscopy (Rook et al., 2000).

4.3: Results I: Identification of PPI mRNA-binding proteins

4.3.1: Generation of recombinant viruses

To purify PPI mRNA-protein complexes, a series of recombinant adenoviruses were generated, which expressed PPI or firefly luciferase (Fluc, control) mRNAs that contained eight copies of the stem-loop, MS2 binding site. When designing the constructs for making viruses, it was important to consider the location of the MS2 binding sites and their effect on the regulation of PI synthesis. Because the 5' and 3' UTRs are believed to be important in regulating translation of PI (Wicksteed et al., 2001), the MS2 binding sites were initially inserted into the centre of the coding region for PPI mRNA and Fluc mRNA, generating adenoviruses, AdPPI-8MS2 and AdFluc-8MS2 (figure 4.1a and b respectively). This ensured that the binding of MS2 protein to the mRNA did not interfere with the regulation of PI synthesis. However, because the binding of ribosomes to the coding region of PPI and Fluc mRNAs may inhibit the interaction of MS2 with its binding sites within PPI and Fluc mRNA, additional constructs were designed to contain eight MS2 binding sites after the 3'UTR of PPI and Fluc mRNAs, generating viruses AdPPI-3'8MS2 and AdFluc-3'8MS2 (figure 4.1c and d respectively).

159

a) PPI-8MS2

b) Fluc-8MS2

c) PPI-3'8MS2

d) Fluc-3'8MS2

e) GST-MS2

f) EGFP-MS2-NLS
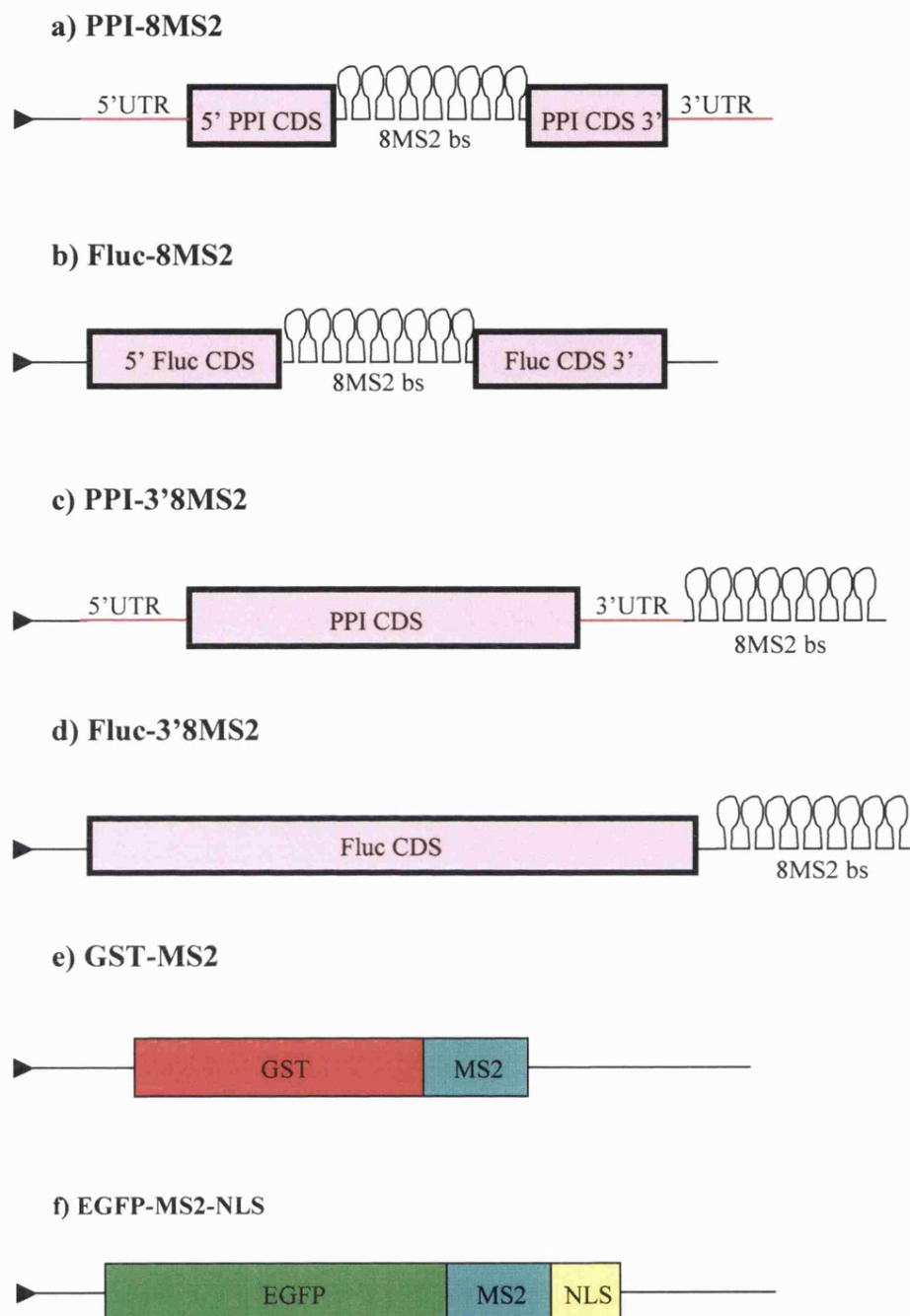
Figure 4.1: Constructs for the expression of specific mRNAs and MS2 fusion proteins: Expression of mRNA in mammalian cells was driven by the CMV promoter and generated mRNAs encoding PPI or Fluc with eight copies of the MS2 binding site (a-d). Expression of the MS2-GST fusion protein in E.Coli was driven by the tac promoter (e). Expression of EGFP-MS2-NLS protein in mammalian cells was driven by the CMV promoter and generated MS2 protein fused to EGFP and a nuclear localisation signal (f). Constructs (a-d) and (f) were used to make adenoviruses for infecting and expressing in MIN6 cells.

4.3.2: Strategy for the identification of PPI mRNA-binding proteins

Two techniques were used to purify Fluc-8MS2, PPI-8MS2, Fluc-3'8MS2 or PPI-3'8MS2 mRNA-protein complexes from MIN6 cells:

1) MS2 was expressed as a glutathione-S-transferase (GST) fusion protein (MS2-GST, figure 4.1e) and covalently bound to glutathione sepharose 4B beads. To affinity-purify specific mRNAs containing the MS2 recognition sequence, these beads were incubated with cell lysates or total RNA from MIN6 cells that were infected with AdPPI-8MS2, AdPPI-3'8MS2, AdFluc-8MS2 or AdFluc-3'8MS2.

2) MIN6 cells were co-infected with AdPPI-8MS2, AdPPI-3'8MS2, AdFluc-8MS2 or AdFluc-3'8MS2 and adenovirus expressing MS2 protein fused to enhanced green fluorescent protein and three copies of a consensus nuclear localisation signal (AdEGFP-MS2-NLS, figure 4.1f). When the viruses were expressed, EGFP-MS2-NLS bound to the MS2 binding sites within PPI or Fluc mRNA, while any unbound EGFP-MS2-NLS localised to the nucleus (figure 4.2). After infection, cells were lysed and PPI-8MS2 mRNA was pulled down by immunoprecipitation of EGFP-MS2-NLS with anti-GFP antibody.

4.3.3: Expression of Adenoviruses

To confirm the expression of PPI-8MS2, PPI-3'8MS2, Fluc-8MS2 and Fluc-3'8MS2 mRNAs in infected cells, total RNA was isolated from MIN6 cells that were infected with the respective adenoviruses for 48 hours, as described in materials and methods. The isolated total RNA was then run on an agarose formaldehyde gel and rRNA was identified by ethidium bromide staining. RNA was then transferred onto nylon membrane and mRNAs containing the 8MS2 binding sites were identified by probing for the 8MS2 binding sites. Northern blot analysis with the 8MS2 probe showed that mock infected cells did not contain mRNA with the MS2 binding sites (figure 4.3). However, Northern blot analysis of RNA isolated from cells that were infected with AdPPI-8MS2 or AdPPI-3'8MS2 showed a band below the 18S rRNA marker, the
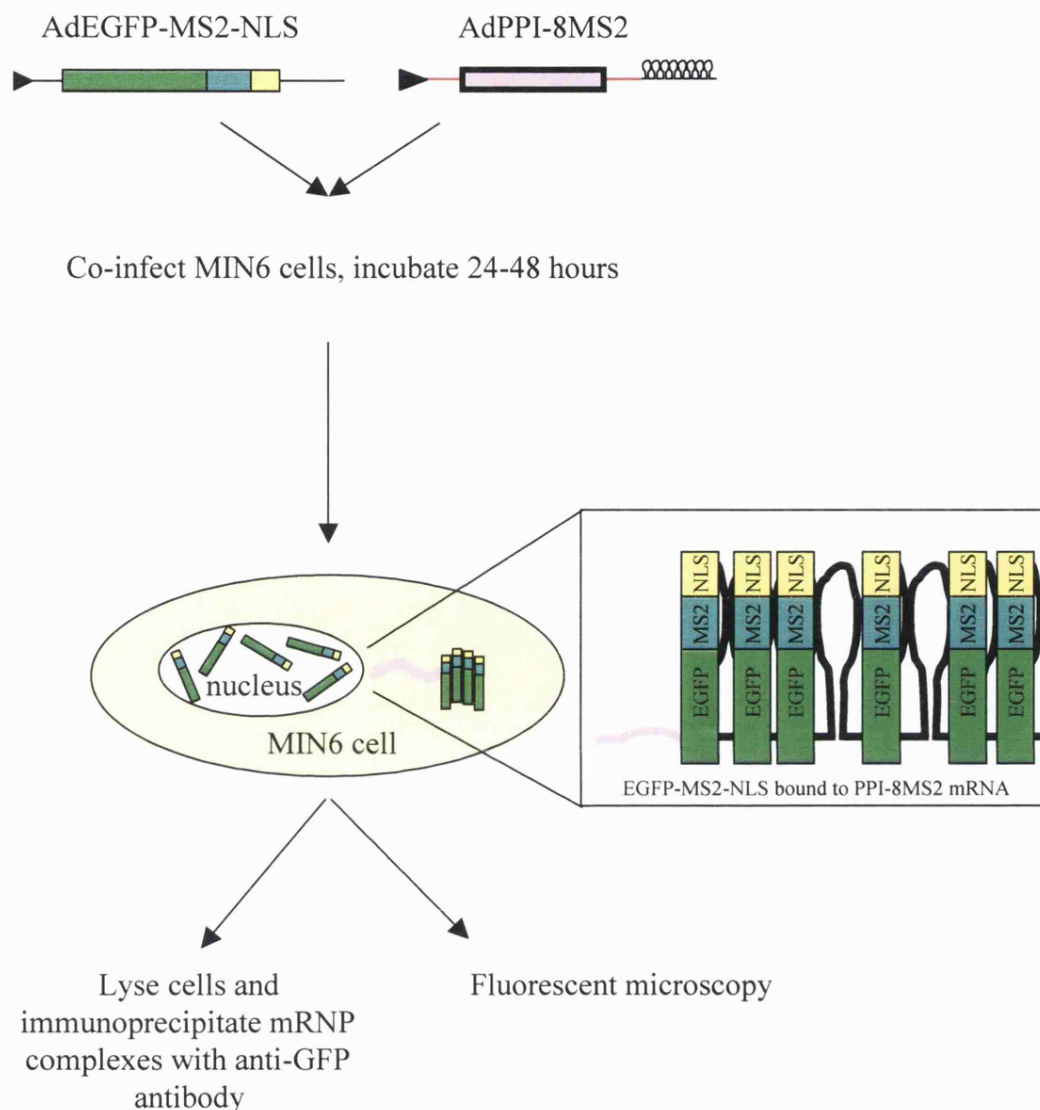
Figure 4.2: Schematic diagram of MS2 protein binding to mRNA
Cells are infected with virus expressing mRNA containing eight MS2 binding sites and virus expressing MS2 protein fused to EGFP and a nuclear localisation signal. After expression of both viruses, EGFP binds to the MS2 binding sites within the mRNA. Unbound EGFP-MS2-NLS remains in the nucleus, while the bound EGFP-MS2-NLS localises with the mature mRNA in the cytosol. Live cells can be visualised with fluorescent microscopy or cells are lysed and anti-GFP antibody can be used to immunoprecipitate mRNP complexes.
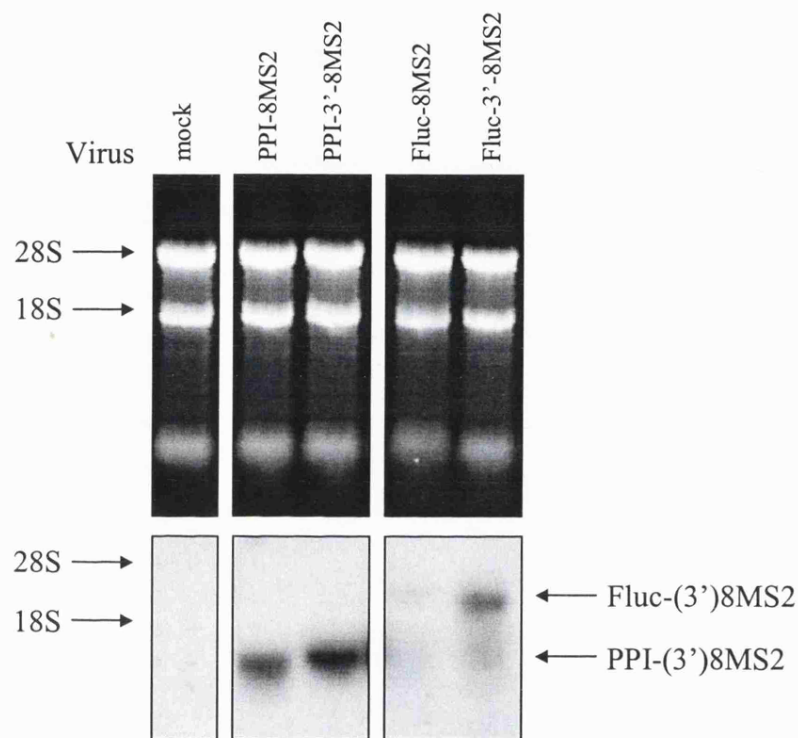
Figure 4.3: Northern blot analysis confirms expression of PPI-8MS2, Fluc-8MS2, PPI-3'8MS2 and Fluc-3'8MS2 mRNAs

MIN6 cells were mock-infected or were infected with virus expressing PPI-8MS2, Fluc-8MS2, PPI-3'8MS2 or Fluc-3'8MS2 mRNAs. Cells were harvested in tri-reagent to isolate total RNA. Total RNA was run on a 1% agarose, formaldehyde gel and visualised by ethidium bromide staining. Total RNA was then transferred onto nylon membrane. Northern blot analysis with a probe specific for the 8MS2 binding sites probed for mRNAs specifically containing the 8MS2 sequence. These results are representative of three separate experiments.

correct size for PPI-8MS2 mRNA. Northern blot analysis of RNA isolated from cells that were infected with AdFluc-3'8MS2 and AdFluc-8MS2 showed a band between the 18S and 28S rRNA markers, which was the expected migration point for Fluc-8MS2 mRNA.

To confirm the expression of the EGFP-MS2-NLS mRNA, MIN6 cells were infected with AdEGFP-MS2-NLS. Total RNA was purified from the cells using Tri-reagent and then run on an agarose formaldehyde gel. Expression of EGFP-MS2-NLS mRNA was confirmed by Northern blot analysis using a probe made from GFP cDNA (figure 4.4a). To confirm the expression of EGFP-MS2-NLS protein, Western blots were carried out with anti-GFP antibody on MIN6 cells lysates from cells infected with AdEGFP-MS2-NLS and/or AdPPI-3'8MS2 (figure 4.4b). EGFP-MS2-NLS protein appears to be clipped and the clipping is reduced when MIN6 cells are also infected with AdPPI-3'8MS2. To confirm that EGFP-MS2-NLS protein could be visualised, MIN6 cells were infected with AdEGFP-MS2-NLS and were excited with a laser emitting wavelength at 488nm (figure 4.5c). Fluorescent microscopy of AdEGFP-MS2-NLS-infected cells also confirmed that EGFP-MS2-NLS protein was localised to the nucleus (figure 4.4c).

4.3.4: Expression of MS2-GST and binding to glutathione Sepharose 4B beads

The bacterial expression of MS2-GST from pGEX-4T3-MS2 was initially tested to find the optimal conditions for expression. BL21 cells transformed with pGEX-4T3-MS2 were cultured overnight in 10ml LB-AMP at 37°C with shaking. The overnight culture was then diluted 1/10 into LB-AMP and grown for 1-2 hours until A_{600} reached 0.6-0.8. The cells were cooled on ice for fifteen minutes and a 100µl sample was pelleted and resuspended in 4X sample buffer for SDS-PAGE analysis (pre-induction). Expression of MS2-GST was induced at varying concentrations of IPTG (0.5mM-1mM), and at varying temperatures (30°C-37°C). 100µl samples of the induced culture were taken at different time points (2-3 hours). Cells from each sample were then pelleted and resuspended in 4X sample buffer for SDS PAGE analysis (post-induction). To determine the optimal conditions for expression of MS2-GST, the pre-induction and

Figure 4.4: Expression of EGFP-MS2-NLS mRNA and protein

a) MIN6 cells were mock-infected or were infected with AdEGFP-MS2-NLS. Cells were harvested in Tri-reagent to isolate total RNA. Total RNA was run on a 1% agarose, formaldehyde gel and visualised by ethidium bromide staining. Total RNA was then transferred onto nylon membrane. Northern blot analysis was carried out with a probe specific for the EGFP sequence. b) MIN6 cells were mock-infected or were infected with AdEGFP-MS2-NLS, AdPPI-3'8MS2 or were co-infected with AdEGFP-MS2-NLS and AdPPI-3'8MS2. Cells were lysed in MIN6 lysis buffer and cell debris was pelleted by centrifugation at 12000g for 10 minutes at 4°C. 20µg of protein was run on a 12.5% SDS-PAGE, transferred onto nitrocellulose membrane and subjected to Western blotting with anti-GFP antibody. Detection was by enhanced chemilluminescence. c) MIN6 cells were infected with AdEGFP-MS2-NLS. Live cells were then visualised with a confocal microscope in bright field to give whole cell images or were excited with a laser emitting light at 488nm to fluoresce EGFP. The bright field and fluorescent images were overlaid to show the localisation of the EGFP. These results are representative of two separate experiments.

a) Northern blot

Virus: mock, AdEGFP-MS2-NLS

28S →
18S →

28S →
18S →
← EGFP-MS2-NLS

b) Western blot

| virus | AdPPI 3'8MS2 | - | + | + | - |
| | AdEGFP-MS2-NLS | - | - | + | + |

← 175KDa
← 83KDa
← 62KDa
← 47.5KDa

EGFP-MS2-NLS →
← 32.5KDa

← 25KDa

Clipped EGFP-MS2-NLS →
← 16.5KDa

c) Confocal microscopy

Bright field   488nm   overlay

166
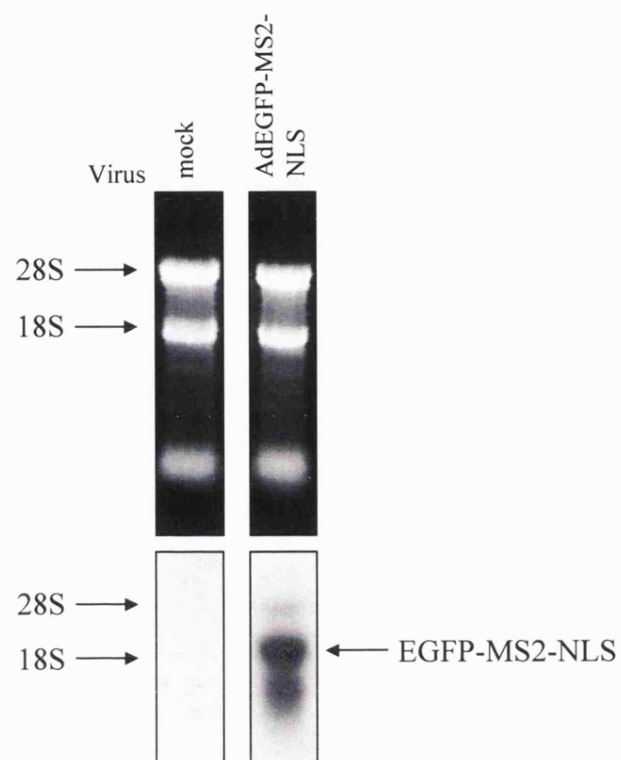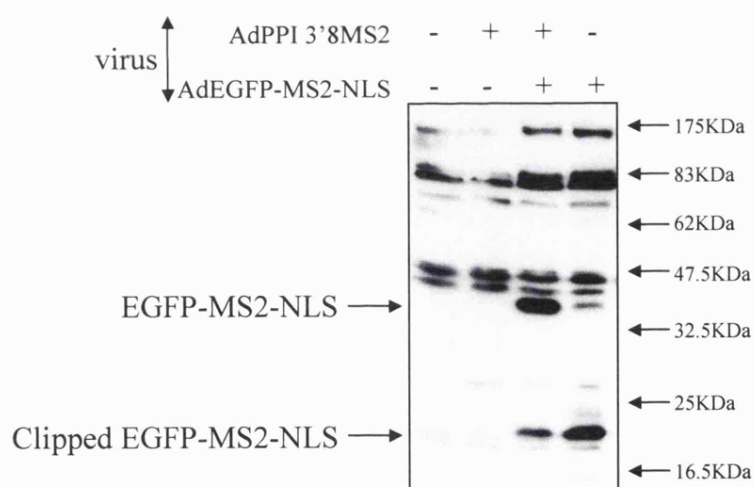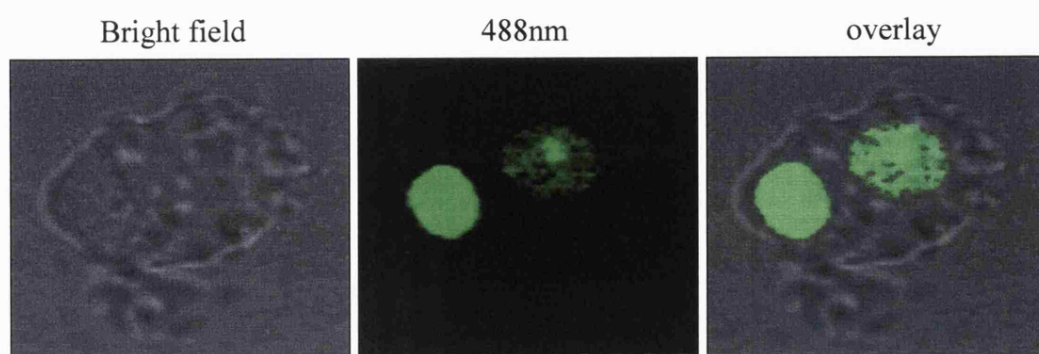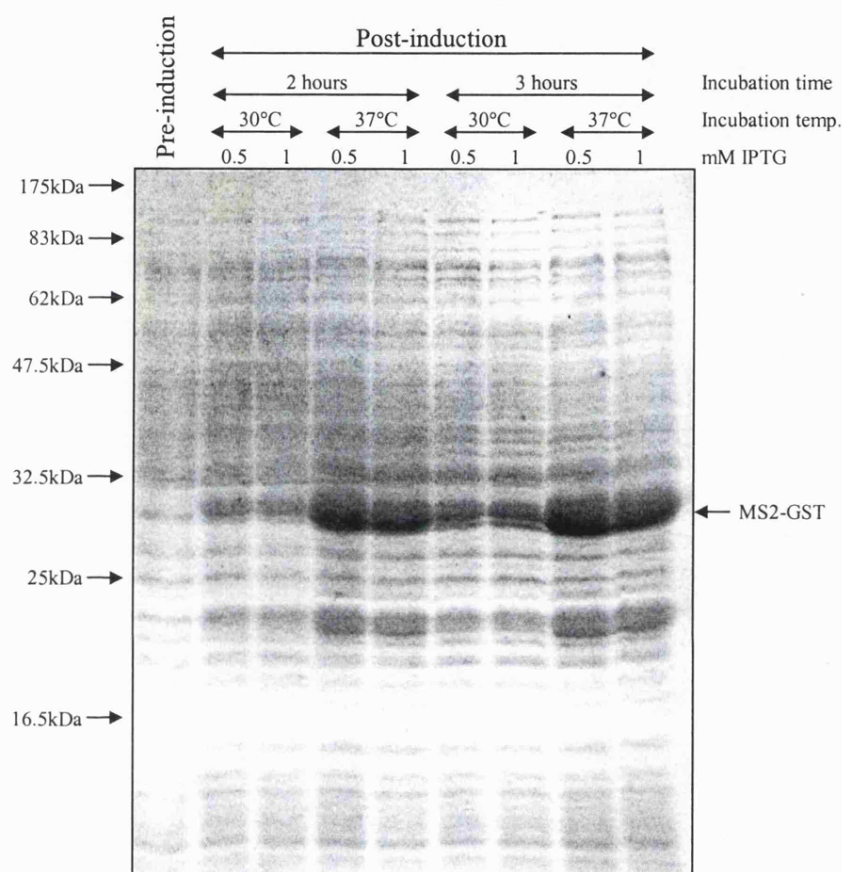
Figure 4.5: Optimisation of MS2-GST expression

An overnight culture of BL21 cells that were transformed with pGEX-4T3-MS2 was diluted 1/10 into LB-AMP and grown for one-two hours until A_{600} reached 0.6-0.8. The cells were cooled on ice for fifteen minutes and a 100μl sample was removed, pelleted and the pellet was resuspended in 1X sample buffer (pre-induction). Expression of MS2-GST was optimised by inducing expression at varying concentrations of IPTG (0.5mM-1mM), and at varying temperatures (30°C-37°C). Samples of the induced culture were taken at different time points (2-3hours). Cells from each sample were pelleted, resuspended in 4X sample buffer and run on 12.5% SDS-PAGE. The gel was stained with coomassie blue for 30 minutes and destained overnight. These results are representative of two separate experiments.

post-induction samples were run on a 12.5% SDS-PAGE and stained with coomassie blue. The coomassie staining showed that the addition of IPTG induced the synthesis of a protein running just below the 32.5kDa marker, and it is likely that this protein is MS2-GST (figure 4.5). Furthermore, maximum synthesis was obtained when expression was induced at a concentration of 0.5mM IPTG at 37°C for 3 hours. Therefore, in future experiments, expression of MS2-GST were induced using these conditions.

To bind MS2-GST to glutathione sepharose 4B beads, expression of MS2-GST was induced in 100ml of LB-ampicillin by 0.5mM IPTG at 37°C for 3 hours. Expressed MS2-GST fusion protein was purified and bound to glutathione sepharose 4B beads as described in materials and methods. 100μl samples of cells were taken pre-induction and post-induction and were run on a 12.5% SDS-PAGE alongside 10μg and 20μg samples of the lysate before and after binding to beads, the washes after binding to the beads and 2.5μl and 5μl of beads. Coomassie staining of the gel showed that a large amount of MS2-GST was bound to the beads (figure 4.6).

4.3.5: Pull-downs of PPI or Fluc mRNA

Before identifying the proteins that were associated with PPI mRNA it was necessary to determine whether mRNAs containing MS2 binding sites could be specifically pulled out of the lysates. Therefore, the ideal conditions for pulling out mRNA with 8MS2 binding sites were determined by using AdPPI-8MS2 and AdFluc-8MS2, which had the 8MS2 binding sites in the middle of the coding sequence or by using AdPPI-3'8MS2 and AdFluc-3'8MS2, which had the 8MS2 binding sites at the 3' end of the 3'UTR. Both the MS2-GST pull-down method and the immunoprecipitation with anti-GFP method were used for both sets of viruses.

Pull-downs of PPI-8MS2 mRNA and Fluc-8MS2 mRNA: MS2-GST pull-downs

MIN6 cells were infected with AdPPI-8MS2 or AdFluc-8MS2, or were mock-infected for the control. Cells were lysed and 10% of the lysate was retained, while the remaining cell lysates were rotated with MS2-GST beads for 30 minutes at 4°C. After rotation with the cell lysates, the beads were pelleted, washed and resuspended in Tri-reagent and the supernatant (lysate after binding) was added to an equal volume of Tri-
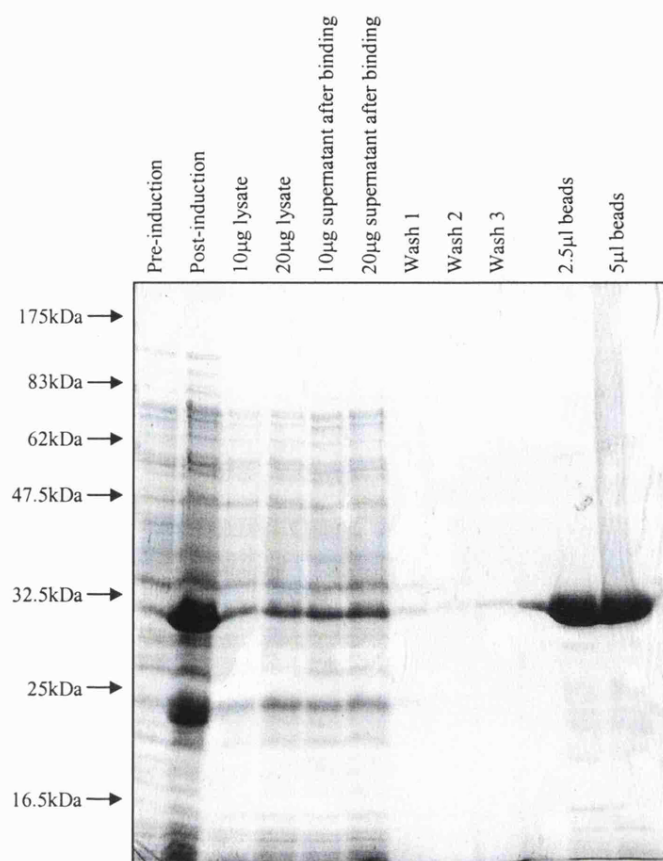
Figure 4.6: Expression of MS2-GST and binding to glutathione sepharose 4B beads

1ml of an overnight culture of BL21 cells that were transformed with pGEX4T3 was added to 100ml of LB-AMP and grown for one-two hours until A_{600} reached 0.6-0.8. The cells were cooled on ice for fifteen minutes and a 100μl sample was removed, pelleted and the pellet was resuspended in 1X sample buffer (pre-induction). IPTG was added to the cells to a final concentration of 0.5mM and the cells were shaken at 37°C for 3hours. A 100μl sample was removed, pelleted and the pellet was resuspended in 1X sample buffer (post-induction). The remaining cells were pelleted at 4000g for 15minutes at 4°C. Cells were resuspended in 3ml of bacterial expression lysis buffer and 50μg of lysozyme was added to the cells in lysis buffer, which were then incubated on ice for 30 minutes. Cells were sonicated with MSE soniprep and cell debris was pelleted at 12000g to leave the supernatant (cell lysate). 30μg of cell lysate was retained and added to 4X sample buffer. The lysate was rotated with 50μl of glutathione sepharose 4B beads (100μl of 50% slurry) for one hour at 4°C and then washed 3 times in binding buffer. 20μl of each wash was retained and added to 4X sample buffer. The beads were finally resuspended in 100μl of 1x storage solution (1xPBS, 50% glycerol and 1mM benzamidine-HCl, 0.1mM phenylmethylsulfonyl fluoride, 1μg/ml each of leupeptin and pepstatin). 4X sample buffer was added to 2.5μl and 5μl of the 50% slurry of beads. The samples from the pre-induction, post-induction, lysate before binding, lysate after binding, washes and the beads were run on a 12.5% SDS-PAGE. The gel was stained with coomassie blue for 30 minutes and destained overnight. These results are representative of three separate experiments.

169

reagent. RNA isolated from 10% of the original lysate, the supernatant and the beads was run on an agarose formaldehyde gel. A high exposure of the ethidium bromide stained gel showed that while the majority of rRNA remained in the supernatant, a small amount was associated with the beads in both the control and infected cells, suggesting that this association of ribosomes was not due to the specific binding of MS2 protein to ribosome-bound mRNAs containing MS2 binding sites (figure 4.7). Furthermore, Northern blot analysis showed that while expression of PPI-8MS2 mRNA and Fluc-8MS2 mRNA was high, neither Fluc-8MS2 mRNA nor PPI-8MS2 mRNA were pulled out of the lysate by the MS2-GST glutathione sepharose 4B beads.

Pull-downs of PPI-8MS2 and Fluc-8MS2: Anti-EGFP immunoprecipitation

Neither Fluc-8MS2 nor PPI-8MS2 mRNA were pulled out of cell lysates using MS2 fused to GST that was bound to glutathione sepharose 4B beads (figure 4.7). One possibility for this is that the MS2 binding site is inaccessible due to the binding of ribosomes and proteins to the mRNA. Therefore, to overcome this potential problem, a second method was used whereby MIN6 cells were co-infected with AdEGFP-MS2-NLS and AdPPI-8MS2 or AdFluc-8MS2. In this way, when PPI-8MS2 or Fluc-8MS2 mRNAs were transcribed, EGFP-MS2-NLS could potentially bind the MS2 binding sites within PPI-8MS2 or Fluc-8MS2 mRNA, before they became coated in ribosomes and proteins.

MIN6 cells were mock-infected or were co-infected with AdEGFP-MS2-NLS and AdPPI-8MS2 or AdFluc-8MS2 or were just infected with AdEGFP-MS2-NLS. After infection, cells were lysed in subcellular fractionation lysis buffer, homogenised and centrifuged to pellet cell debris and nuclei, which should contain unbound EGFP-MS2-NLS protein due to the nuclear localisation signal. 10% of the initial lysate was retained, while the remaining lysate was rotated for 1 hour at 4°C with anti-GFP antibody that had been coupled to protein G sepharose beads. The beads were pelleted and the supernatant (lysate after binding) was added to an equal volume of Tri-reagent. After washing, the beads were finally resuspended in Tri-reagent. RNA isolated from 10% of the initial lysate, 10% of the supernatant and all of the beads was run on an agarose, formaldehyde gel. Ethidium bromide staining of the gel showed that the majority of rRNA remained in the supernatant (figure 4.8). The high exposure of ethidium bromide staining showed that a small amount of rRNA was associated with

Figure 4.7: Pull-downs of PPI-8MS2 and Fluc-8MS2 mRNAs from cell lysates with MS2-GST bound to glutathione sepharose beads

MIN6 cells were mock-infected or were infected with AdPPI-8MS2 or AdFluc-8MS2. After 48 hour infection, cells were lysed with 500μl of pull-down lysis buffer, the cell debris was pelleted at 12000g for 10 minutes at 4°C and 10% of the cell lysate was added to tri-reagent. The remaining cell lysates (450μl) were rotated with 5μl of MS2-GST beads for 30 minutes at 4°C. After rotation, the beads were pelleted by centrifugation at 2000g for 1 minute at 4°C. The supernatant (lysate after binding) was added to an equal volume of tri-reagent. The beads were then washed three times in pull-down lysis buffer then finally resuspended in 750μl of tri-reagent. RNA isolated from the 10% of lysate, the supernatant and the beads was run on an agarose formaldehyde gel and rRNA was stained with ethidium bromide. RNA was then transferred to nylon membrane and probed for mRNAs containing the sequence for 8MS2 binding sites. These results are representative of two separate experiments.
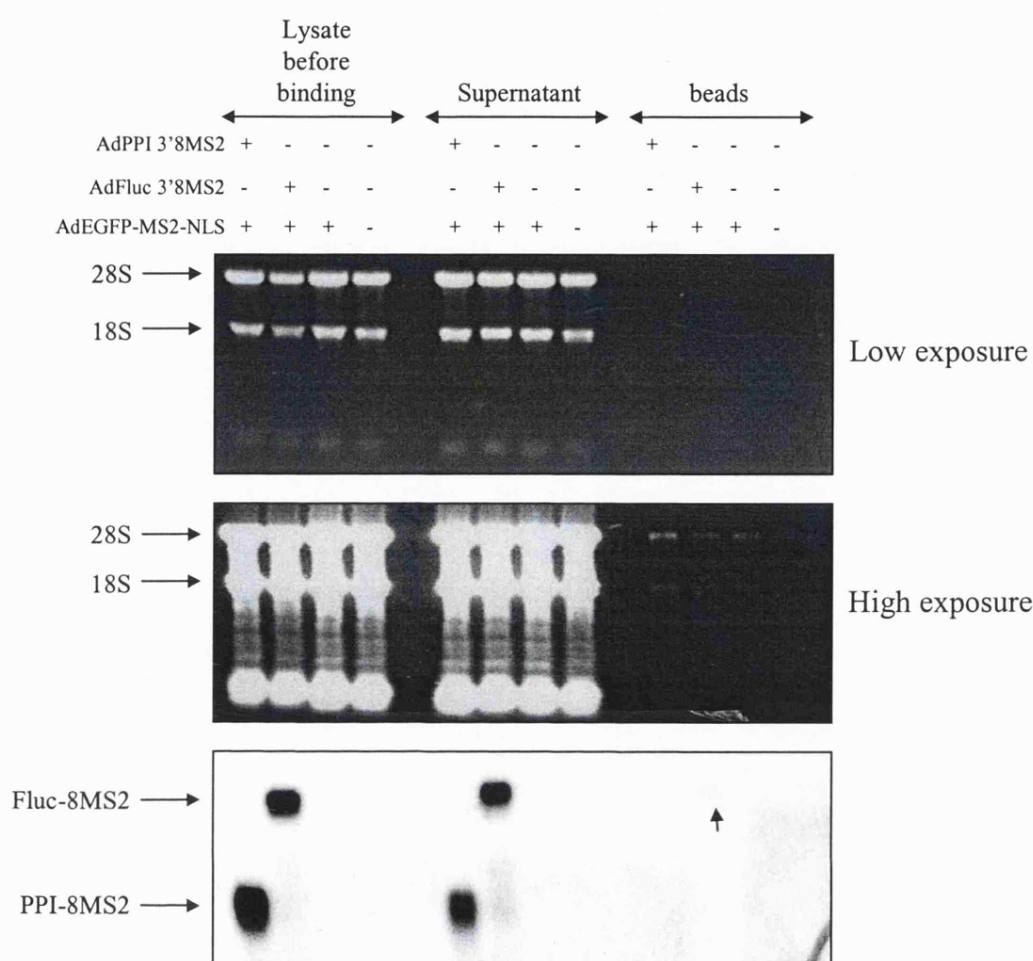
Figure 4.8: Co-immunoprecipitations of PPI-8MS2 and Fluc-8MS2 mRNAs with EGFP-MS2-NLS protein using anti-GFP antibody

MIN6 cells were mock-infected or were co-infected with AdEGFP-MS2-NLS and AdPPI-8MS2 or AdFluc-8MS2 mRNAs or were just infected with AdEGFP-MS2-NLS. Cells were lysed in 375μl of subcellular fractionation lysis buffer, homogenised and centrifuged to pellet cell debris and nuclei, which should contain unbound EGFP-MS2-NLS protein due to the nuclear localisation signal. 10% of the lysate was retained and added to tri-reagent. An equal volume of subcellular fractionation buffer supplemented with 2% triton was added to the remaining lysate to make a final concentration of 1% triton. The lysate was then rotated for 1 hour at 4°C with anti-GFP antibody that had been coupled to protein G sepharose beads. The beads were pelleted and the supernatant was added to an equal volume of tri-reagent. The beads were then washed 3 times with 1ml of subcellular fractionation lysis buffer supplemented with 1% triton and then finally resuspended in tri-reagent. RNA was isolated from 10% of the initial lysate, 10% of the supernatant and all of the beads and was run on an agarose, formaldehyde gel. Ethidium bromide stained the rRNA and the total RNA was transferred onto nylon membrane and probed for mRNAs containing the sequence for 8MS2 binding sites. These results are representative of two separate experiments.

172

beads, although because this occurred with both the control and infected cells, it was unlikely that this rRNA co-immunoprecipitated with mRNAs containing MS2 binding sites. Northern blot analysis for the MS2 binding sites showed that all of PPI-8MS2 mRNA and the majority of Fluc-8MS2 mRNA remained in the supernatant and was not immunoprecipitated. However, a very small amount of Fluc-8MS2 did appear to co-immunoprecipitate with EGFP-MS2-NLS (marked with arrow).

Summary

In vitro binding assays with MS2-GST were unable to pull-down PPI-8MS2 or Fluc-8MS2 mRNAs (figure 4.7). By immunoprecipitating EGFP-MS2-NLS from cells infected with AdEGFP-MS2-NLS and AdPPI-8MS2 or AdFluc-8MS2 mRNAs, very small amounts of Fluc-8MS2 mRNA but not PPI-8MS2 mRNA were co-immunoprecipitated (figure 4.8). As mentioned earlier, by placing the 8MS2 binding sites in the coding region of PPI or Fluc mRNA, there is a risk that ribosomes bound to the coding region may inhibit EGFP-MS2-NLS from binding to the MS2 binding sites within the mRNA.

Pull-downs of PPI-3'8MS2 and Fluc-3'8MS2: MS2-GST pull-downs

To prevent ribosomes from inhibiting EGFP-MS2-NLS binding to its binding sites within PPI-8MS2 and Fluc-8MS2 mRNAs, the MS2 binding sites were placed after 3'UTR of PPI and Fluc. Initially, to determine whether MS2-GST would pull down PPI-3'8MS2 or Fluc-3'8MS2 mRNAs, MS2-GST pull-downs were carried out on total RNA isolated from control, mock-infected MIN6 cells or MIN6 cells that were infected with AdPPI-3'8MS2 or AdFluc-3'8MS2 (figure 4.9). Total RNA was isolated from MIN6 cells using Tri-reagent and resuspended in TMK buffer (100mM Tris Hcl pH8, 10mM MgOAc, 80mM KCl, 1mg/ml heparin, 1µl/ml RNAguard) and 10% was removed for analysis. MS2-GST glutathione sepharose 4B beads were then added to each RNA sample and the samples were rotated at 4°C for 30 minutes. The beads were pelleted, washed and finally, to remove residual protein, both the beads and the supernatant (total RNA after binding) were added to Tri-reagent for RNA isolation. RNA isolated from the lysate before binding (10%), the supernatant and the beads was then run on a 1% agarose, formaldehyde gel, which was stained with ethidium bromide. A significant amount of degraded rRNA was found associated with beads in the mock-infected cells as well as in MIN6 cells that were infected with AdFluc-3'8MS2 or
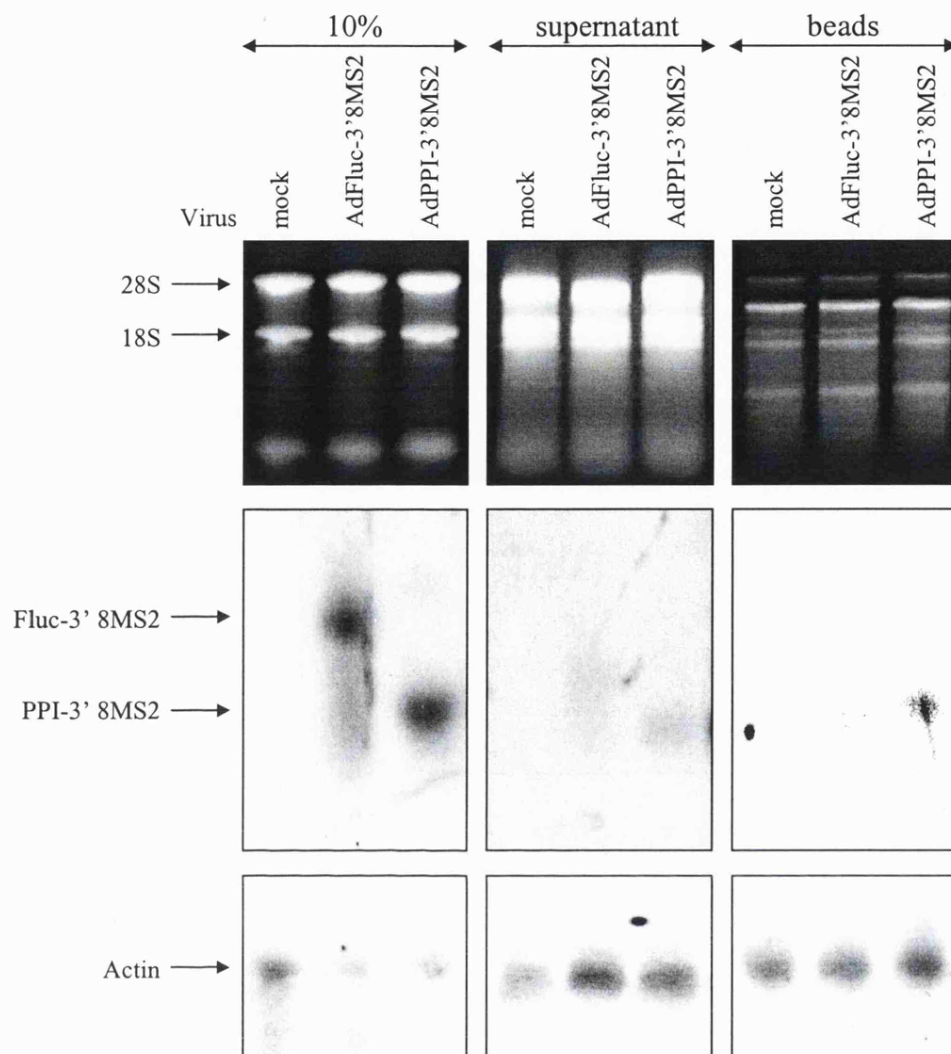
Figure 4.9: Pull-downs of PPI-3'8MS2 and Fluc-3'8MS2 mRNAs from a solution of total MIN6 RNA using MS2-GST bound to glutathione sepharose beads

MIN6 cells were infected with AdPPI-3'8MS2 or AdFluc-3'8MS2 mRNAs or were mock infected. Cells were harvested in 1ml of tri-reagent and total RNA isolated from a 6cm plate of MIN6 cells was resuspended in 90μl of water. 10% of the total RNA was removed for analysis and 5X TMK buffer was added to the remaining RNA to make a final solution of RNA in 1X TMK buffer (100mM Tris Hcl pH8, 10mM MgOAc, 80mM KCl, 1mg/ml heparin, 1μl/ml RNAguard). 5μl of glutathione sepharose 4B beads coupled to MS2-GST were then added to each RNA sample and the samples were rotated at 4°C for 30 minutes. The beads were then washed 3 times in 1ml of TMK buffer and finally resuspended in 750μl of tri-reagent for RNA isolation. Isolated RNA from the initial lysate, the supernatant (total RNA after binding) and the beads was run on a 1% agarose, formaldehyde gel and stained with ethidium bromide. Total RNA was then transferred onto nylon membrane and probed for mRNAs containing the sequence for the 8MS2 binding sites and actin mRNA.

174

AdPPI-3'8MS2 (figure 4.9). Furthermore, although Northern blot analysis showed that both Fluc-3'8MS2 and PPI-3'8MS2 mRNAs were pulled down, probing with an actin probe showed the presence of actin mRNA on the beads in all samples (figure 4.9). This result suggests that MS2 does not specifically pull out PPI-3'8MS2 or Fluc-3'8MS2 mRNAs.

Although MS2 protein fused to GST did not pull out PPI-3'8MS2 or Fluc-3'8MS2 mRNAs from a solution of total RNA, the large amount of rRNA may have inhibited the interaction beTween MS2 and its binding sites. Therefore, to see if PPI-3'8MS2 mRNA could be pulled out of MIN6 cell lysates using MS2 fused to GST, the MS2 binding protein pull-down assay was carried out on cell lysates from mock infected MIN6 cells or MIN6 cells infected with AdPPI-3'8MS2. MIN6 cells were lysed in pull-down MIN6 lysis buffer (20mM HEPES pH7.5, 10mM MgCl, 130mM KCl, 10% glycerol, 1mg/ml heparin, 100µg/ml cycloheximide, 1% triton, 1mM DTT, 1µl/ml RNAguard). Cell lysates from the mock infected or infected cells were then added to MS2-GST beads and the samples were rotated at 4°C for 30 minutes. RNA was isolated from 10% of the original lysate, the supernatant (lysate after binding) and the beads and run on a 1% agarose formaldehyde gel. Ethidium bromide staining of the gel showed that rRNA was pulled down in both mock infected MIN6 cells and MIN6 cells infected with AdPPI-3'8MS2 (figure 4.10), suggesting that this rRNA is not due to the specific binding of mRNAs containing the MS2 binding sites. Furthermore, while Northern blot analysis with a cDNA probe containing the MS2 binding sites showed that PPI-3'8MS2 mRNA was pulled down, actin was also shown to be associated with the beads in mock-infected cells and infected cells, suggesting that MS2-GST did not specifically pull-down PPI-3'8MS2 mRNA.

Summary
This data showed that MS2-GST bound to glutathione sepharose 4B beads was unable to pull-down mRNA that contained MS2 binding sites either in the centre of the coding region or at the 3' end of PPI or Fluc.
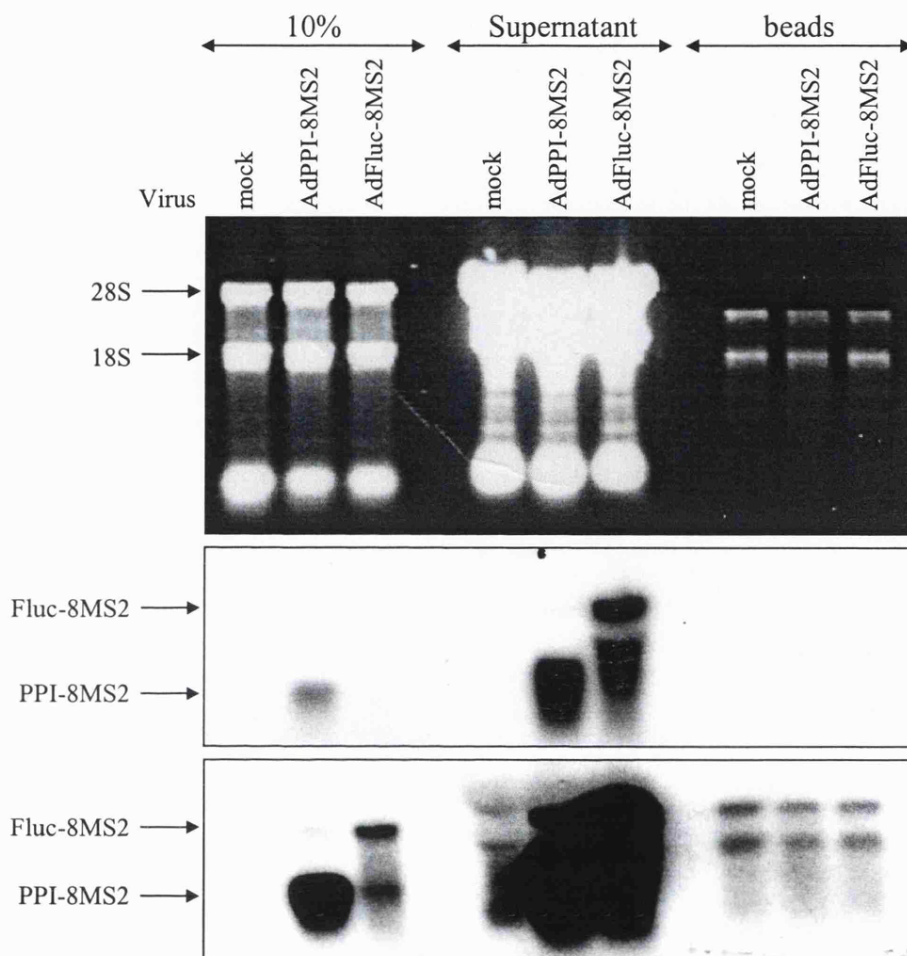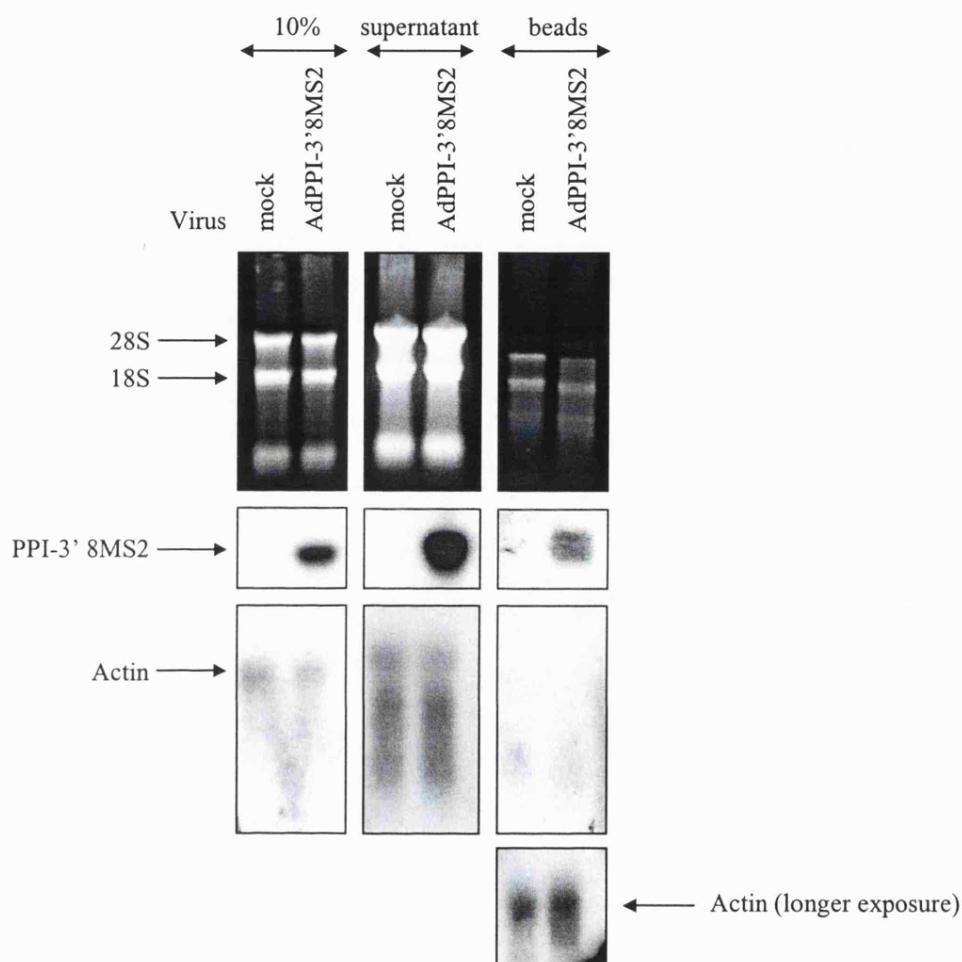
Figure 4.10: Pull-downs of PPI-3'8MS2 mRNA from cell lysates using MS2-GST bound to glutathione sepharose beads

MIN6 cells were mock-infected or were infected with AdPPI-3'8MS2. Cells were then lysed in 150μl of pull-down MIN6 lysis buffer (20mM HEPES pH7.5, 10mM MgCl, 130mM KCl, 10% glycerol, 1mg/ml heparin, 100μg/ml cycloheximide, 1% triton, 1mM DTT, 1μl/ml RNAguard), vortexed briefly and cell debris was pelleted by centrifugation at 12000g for 10 minutes at 4°C. 10% of the original lysate was retained, while the remaining cell lysates from the mock infected or infected cells were added to 5μl of glutathione sepharose 4B beads coupled to MS2-GST and rotated at 4°C for 30 minutes. RNA was then isolated from 10% of the original lysate, the supernatant (lysate after binding) and from the beads and run on a 1% agarose formaldehyde gel. Total RNA was transferred onto nylon membrane and probed for mRNAs containing the sequence for the 8MS2 binding sites and actin mRNA. These results are representative of two separate experiments.

176

Pull-downs of PPI-3'8MS2 and Fluc-3'8MS2: Pull-downs by immunoprecipitation of
EGFP

Although PPI-8MS2 mRNA was not pulled down when EGFP-MS2-NLS was immunoprecipitated using anti-GFP antibody, a very small amount of Fluc-8MS2 did co-immunoprecipitate with EGFP-MS2-NLS (figure 4.8). Therefore, to see if placing the 8MS2 binding sites at the 3' end of PPI and Fluc mRNAs improved their co-immunoprecipitation with EGFP-MS2-NLS, the same experiment was repeated in MIN6 cells that were co-infected with AdPPI-3'8MS2 or AdFluc-3'8MS2 and AdEGFP-MS2-NLS (figure 4.11). Cells were lysed and immunoprecipitations were carried out as described for MIN6 cells that were infected with AdPPI-8MS2 and AdFluc-8MS2 (figure 4.8). As extra controls MIN6 cells were also infected only with AdFluc-3'8MS2, AdPPI-3'8MS2 or AdEGFP-MS2-NLS and samples were also taken for protein analysis as well as RNA analysis (figure 4.11 and 4.12). Ethidium bromide staining of RNA isolated from the beads after immunoprecipitation shows that very little rRNA co-immunoprecipitated with control cells or infected cells (figure 4.11a and b). Interestingly, probing for the 8MS2 binding sites by Northern blot analysis showed that the amounts of both PPI-3'8MS2 mRNA and Fluc-3'8MS2 mRNA dramatically decreased when MIN6 cells were co-infected with AdEGFP-MS2-NLS compared to when these viruses were infected alone (figure 4.11a and b). This decrease in mRNA levels is observed in the 10% samples, which were taken before immunoprecipitation as well as in the supernatant and therefore cannot be due to mRNA degradation during the incubation with the antibody. Importantly, probing for the 8MS2 binding sites also showed that PPI-3'8MS2 and Fluc-3'8MS2 mRNAs both bound to the beads (figure 4.12a and b). Neither PPI-3'8MS2 nor Fluc-3'8MS2 mRNAs were pulled out when cells were only infected with Ad PPI-3'8MS2 or AdFluc-3'8MS2 and were not infected with AdEGFP-MS2-NLS, suggesting that the co-immunoprecipitation of these mRNAs with EGFP-MS2-NLS protein was specific and through EGFP-MS2-NLS. Furthermore, Northern blot analysis for actin showed the presence of actin in the 10% samples and in the supernatant after binding but not with the beads, further confirming that PPI-3'8MS2 and Fluc-3'8MS2 mRNAs specifically co-immunoprecipitated with EGFP.

To confirm that EGFP-MS2-NLS was immunoprecipitated, protein samples of the pellet (containing nuclei and cell debris), the lysate (before immunoprecipitation), the

Figure 4.11: Co-immunoprecipitations of PPI-3'8MS2 and Fluc-3'8MS2 mRNAs with EGFP-MS2-NLS using anti-GFP antibody. RNA analysis.

MIN6 cells were infected with AdPPI-8MS2 (a) or AdFluc-8MS2 (b) and AdEGFP-MS2-NLS as shown. Cells were lysed in subcellular fractionation lysis buffer, homogenised and centrifuged to pellet cell debris and nuclei, which should contain unbound EGFP-MS2-NLS due to the nuclear localisation signal. 10% of the lysate was retained and added to Tri-reagent. An equal volume of subcellular fractionation buffer supplemented with 2% triton was added to the remaining lysate to make a final concentration of 1% triton. The lysate was then rotated for 1 hour at 4°C with anti-GFP antibody that had been coupled to protein G sepharose beads. The beads were pelleted and the supernatant was added to an equal volume of Tri-reagent. The beads were then washed 3 times with 1ml of subcellular fractionation lysis buffer supplemented with 1-% triton and then finally resuspended in Tri-reagent. RNA isolated from 10% of the initial lysate (10%), the supernatant (lysate after binding) and the beads was run on a 1% agarose, formaldehyde gel. rRNA was stained with ethidium bromide and the RNA was then transferred onto nylon membrane and probed for mRNAs containing the sequence for 8MS2 binding sites and actin mRNA. These results are representative of three separate experiments.
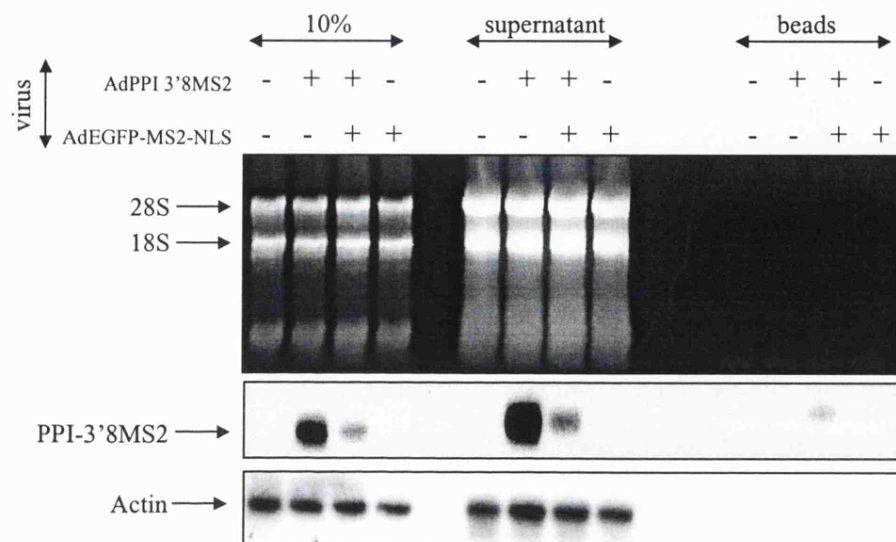
a) AdPPI-3'8MS2
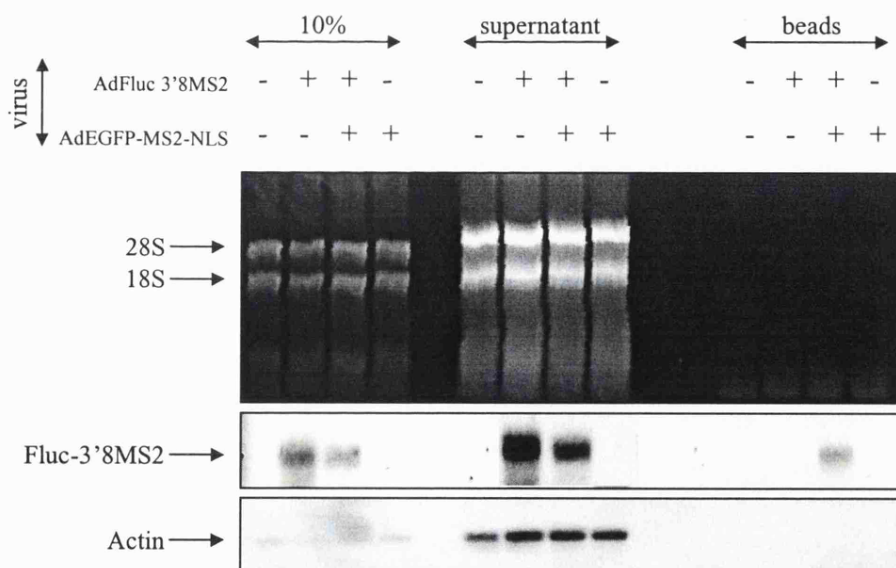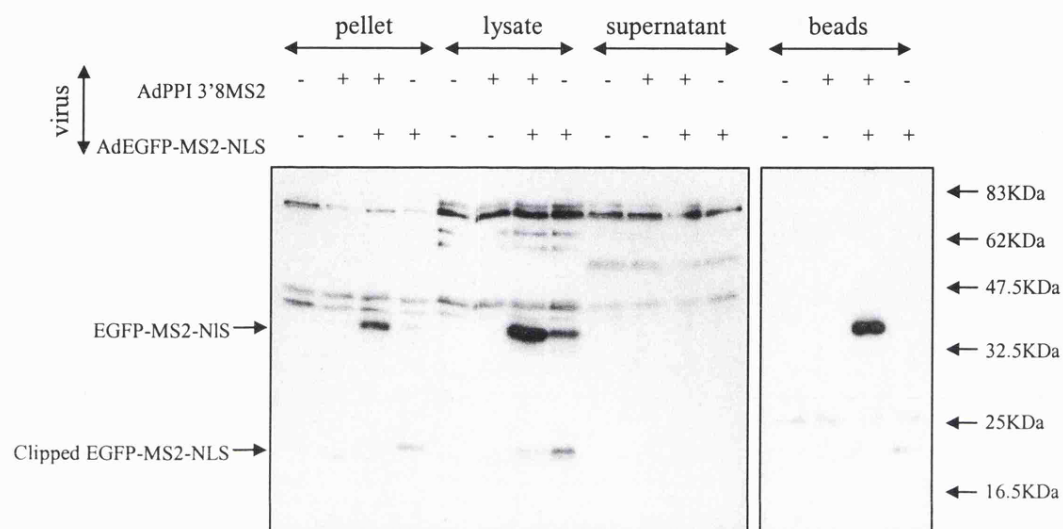
b) AdFluc-3'8MS2

Figure 4.12: Co-immunoprecipitations of PPI-3'8MS2 and Fluc-3'8MS2 mRNAs with EGFP-MS2-NLS using anti-GFP antibody. Protein analysis. Samples from figure 4.11a were retained for protein analysis. 10% of the pellet, containing cell debris and nuclei was run on 12.5% SDS-PAGE alongside equivalent amounts of the lysate before binding, the supernatant (lysate after binding) and the beads. Protein was transferred onto nitrocellulose membrane and subjected to Western blotting with anti-GFP antibody. Western blots of the pellet, the lysate and the supernatant were probed with anti-rabbit secondary antibody, while Western blots of the beads were probed with anti-protein A secondary antibody. Detection was by enhanced chemilluminescence.

supernatant (lysate after immunoprecipitation) and the beads were run on 12.5% SDS-PAGE and then transferred onto nitrocellulose membrane. The presence of EGFP-MS2-NLS was determined by Western Blot analysis with anti-GFP antibody. EGFP-MS2-NLS was observed in the pellet and 10% fractions in cells infected with AdEGFP-MS2-NLS (figure 4.12). As described earlier, EGFP-MS2-NLS appears to undergo clipping and interestingly, this clipping is reduced when MIN6 cells are also infected with AdPPI-3'8MS2 (figure 4.12). Therefore, while a large amount of EGFP-MS2-NLS immunoprecipitated in the presence of AdPPI-3'8MS2, only a small amount immunoprecipitated in its absence.

Although both Fluc-3'8MS2 and PPI-3'8MS2 mRNAs co-immunoprecipitated with EGFP-MS2-NLS, a large proportion (more than 50%) of both Fluc-3'MS2 and PPI-3'MS2 mRNAs remained in the supernatant after binding (figure 4.11a and b). A possible reason why only a small fraction of PPI-3'8MS2 and Fluc-3'8MS2 mRNAs co-immunoprecipitated with EGFP-MS2-NLS is that only a small proportion of the bound EGFP-MS2-NLS is immunoprecipitated from the lysate. Indeed, Western blotting with anti-GFP antibody showed that a large amount of EGFP-MS2-NLS was present in the lysate and was not pelleted with the nuclei (figure 4.12). As fluorescence microscopy of MIN6 cells infected with EGFP-MS2-NLS showed the majority of EGFP-MS2-NLS in the nucleus (figure 4.4c), it is likely that the nuclei were partially broken during lysis, allowing release of unbound EGFP-MS2-NLS into the lysate, which may have preferentially immunoprecipitated over bound EGFP-MS2-NLS.

To improve the efficiency of the EGFP-MS2-NLS immunoprecipitation, an additional step was incorporated to remove unbound EGFP-MS2-NLS. MIN6 cells were mock-infected, were infected with AdPPI-3'8MS2, AdFluc-3'8MS2 or AdEGFP-MS2-NLS or were co-infected with AdEGFP-MS2-NLS and AdPPI-3'8MS2 or AdFluc-3'8MS2. Cells were then lysed in low salt polysome buffer supplemented with 1% triton and the nuclei and cell debris were pelleted at 12000g for 10 minutes at 4°C. To separate EGFP-MS2-NLS that was bound to ribosome-associated mRNAs from unbound EGFP-MS2-NLS, the lysate was centrifuged at 200000g for 20 minutes at 4°C (see chapter 3, figure 3.9). The supernatant (S200) containing unbound EGFP-MS2-NLS was retained for protein and RNA analysis while the pellet, which contains ribosome-bound mRNAs,

was resuspended in low salt lysis buffer supplemented with 1% triton. EGFP-MS2-NLS was then immunoprecipated from the resuspended pellet.

RNA was isolated from 10% of the original lysate, the S200 fraction, the supernatant after binding (resuspended P200 fraction, S_{bind}) and the beads. The isolated RNA was then run on a 1% agarose, formaldehyde gel. Ethidium bromide staining of the gels showed that the majority of rRNA was pelleted in the 200000g spin, as the majority of rRNA is found in the supernatant after binding (the resuspended P200 pellet). RNA was then transferred onto nylon membrane and probed for mRNAs containing MS2 binding sites. In agreement with the previous result (figure 4.11), a larger amount of PPI-3'8MS2 and Fluc-3'8MS2 mRNAs were found when the respective viruses were infected alone, compared to when these viruses were co-infected with AdEGFP-MS2-NLS (figure 4.13). Furthermore all of Fluc-3'8MS2 mRNA and the majority of PPI-3'8MS2 mRNA were pelleted in the 200000g spin, as no Fluc-3'8MS2 mRNA and very little PPI-3'8MS2 mRNA was observed in the S200 fraction. In MIN6 cells that were co-infected with AdEGFP-MS2-NLS and AdPPI-3'8MS2 or AdFluc-3'8MS2, a larger amount of Fluc-3'8MS2 mRNA and PPI-3'8MS2 mRNA was found associated with the beads than with the supernatant after binding, suggesting that the majority of these mRNAs were pulled out of the supernatant. Indeed, by separating EGFP-MS2-NLS that was bound to ribosome-associated mRNAs from unbound EGFP-MS2-NLS the proportion of PPI-3'8MS2 and Fluc-3'8MS2 mRNAs that co-immunoprecipitated with EGFP-MS2-NLS was increased (figure 4.11 compared to figure 4.13). Furthermore, the co-immunoprecipitation was specific as no PPI-3'8MS2 nor Fluc-3'8MS2 mRNAs co-immunoprecipitated with EGFP-MS2-NLS in MIN6 cells that were only infected with these viruses and no actin was co-immunoprecipitated, despite large quantities in the supernatant after binding (figure 4.13).

Western blot analysis with anti-GFP antibody of the samples from the cells co-infected with AdPPI-3'8MS2 and AdEGFP-MS2-NLS confirmed that the 200000g spin left the majority of EGFP-MS2-NLS in the supernatant fraction (S200) (figure 4.14). Furthermore, while no EGFP-MS2-NLS was observed in the supernatant after binding (S_{bind}), a small amount of EGFP-MS2-NLS immunoprecipitated in MIN6 cells that were infected with both AdEGFP-MS2-NLS and AdPPI-3'8MS2 but not in MIN6 cells that were infected with only AdEGFP-MS2-NLS. This suggests that the EGFP-MS2-NLS

Figure 4.13: Optimisation of co-immunoprecipitations of PPI-3'8MS2 and Fluc-3'8MS2 mRNAs with GFP-MS2-NLS using anti-GFP antibody. RNA analysis.

MIN6 cells were mock-infected or were infected with viruses expressing PPI-3'8MS2 (a), Fluc-3'8MS2 (b) and/or GFP-MS2-NLS as shown. Cells were then lysed in low salt polysome buffer supplemented with 1% triton and the nuclei and cell debris were pelleted at 12000g for 10 minutes at 4°C. The lysate was centrifuged at 200000g for 20 minutes at 4°C. The supernatant (S200) was retained for protein and RNA analysis while the pellet was resuspended in low salt lysis buffer supplemented with 1% triton. EGFP-MS2-NLS was then immunoprecipitated from the resuspended pellet as described in figure 4.25. RNA was isolated with Tri-reagent from 10% of the initial lysate (10%), the S200 fraction, the lysate after binding (S_{bind}) and the beads and was run on a 1% agarose, formaldehyde gel. Ethidium bromide stained the rRNA and the total RNA was transferred onto nylon membrane and probed for actin mRNA and mRNAs containing the sequence for 8MS2 binding sites. These results are representative of three separate experiments.
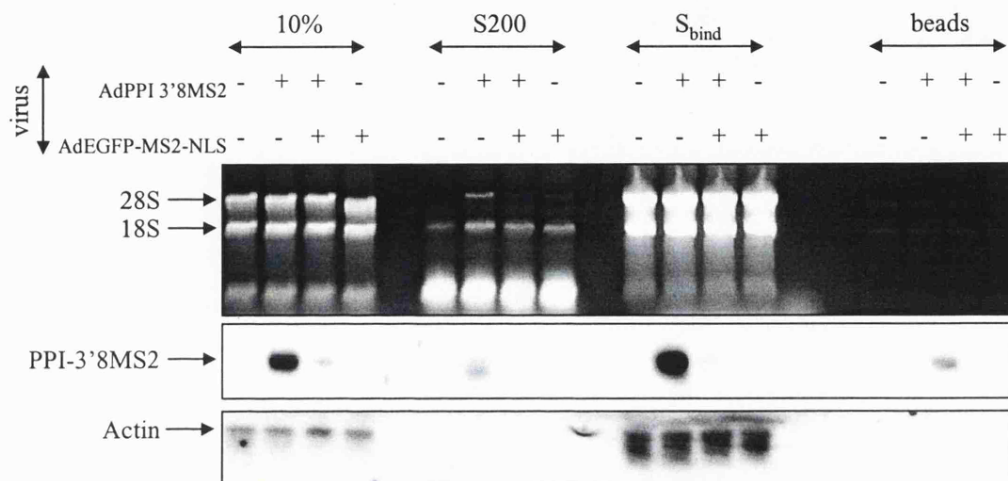
a) AdPPI-3'8MS2
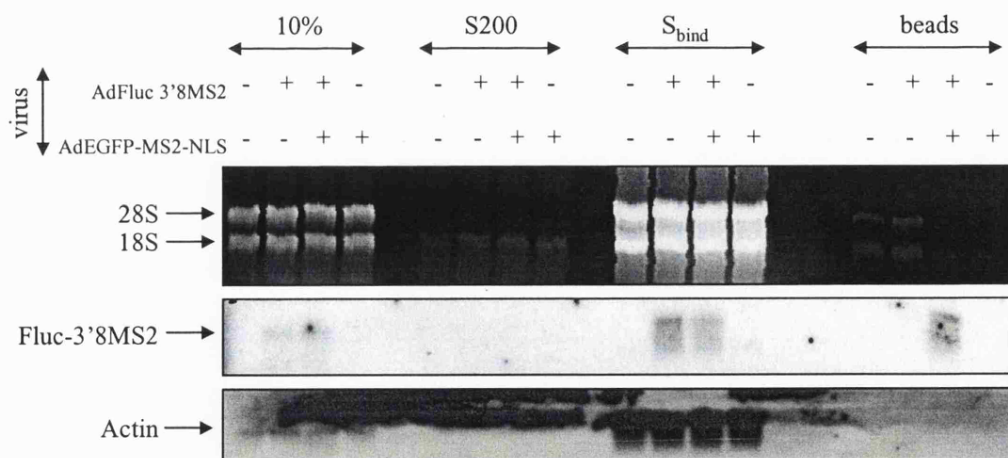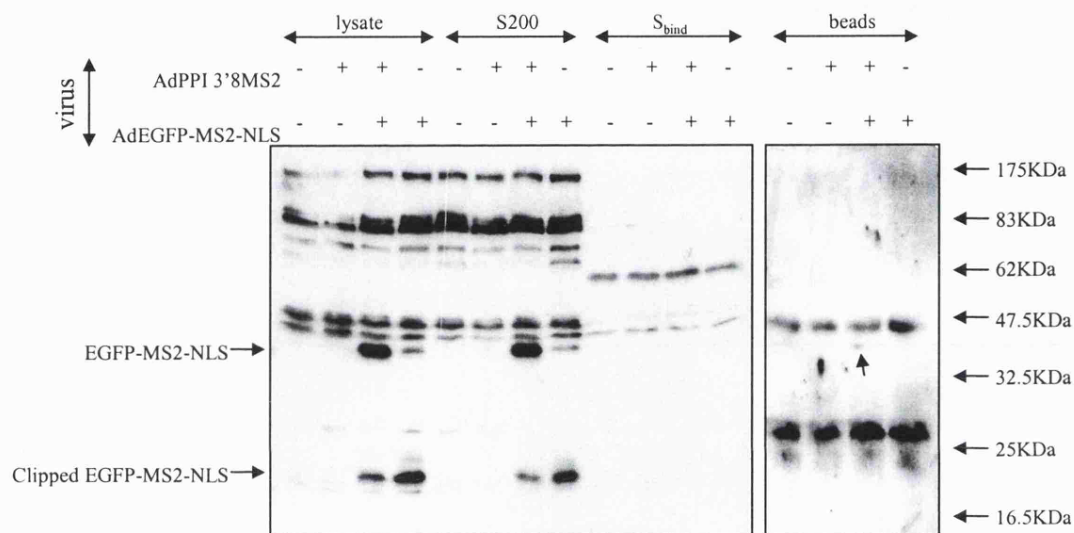
b) AdFluc-3'8MS2

Figure 4.14: Optimisation of co-immunoprecipitations of PPI-3'8MS2 and Fluc-3'8MS2 mRNAs with EGFP-MS2-NLS using anti-GFP antibody. RNA analysis.

Samples from figure 4.13 were retained for protein analysis. 10% of the initial lysate was run on 12.5% SDS-PAGE alongside equivalent amounts of the S200 fraction, the supernatant after binding (S_{bind}) and the beads. Protein was transferred onto nitrocellulose membrane and subjected to Western blotting with anti-GFP antibody. Western blots of the initial lysate, the S200 fraction and the supernatant after binding were probed with anti-rabbit secondary antibody, while Western blots of the beads were probed with anti-protein A secondary antibody. Detection was by enhanced chemiluminescence.

185

was specifically pelleted in the 200000g spin when it was bound to ribosome-associated PPI-3'8MS2 and that this pelleted EGFP-MS2-NLS was immunoprecipitated (figure 4.14).

4.3.6: Conclusions to pull-downs of PPI and Fluc mRNAs:

MS2-GST was unable to bind mRNAs containing the MS2 binding sites irrespective of the positioning of the binding sites or whether the pulldown was using purified mRNA or mRNA in cell lysates. However, by expressing both EGFP-MS2-NLS and mRNA containing the MS2 binding sites and allowing MS2 to bind its binding sites *in vivo* followed by immunoprecipitating for EGFP-MS2-NLS, Fluc-3'8MS2 and PPI-3'8MS2 mRNAs were specifically isolated. PPI-3'8MS2 and Fluc-3'8MS2 mRNAs immunoprecipitated from MIN6 lysates far more efficiently than PPI-8MS2 and Fluc-8MS2 mRNAs (figure 4.11 compared with figure 4.8), was most likely because ribosomes prevented MS2 from binding its binding sites within the coding sequence. By spinning the cells lysates at 200000g and separating bound EGFP-MS2-NLS from unbound EGFP-MS2-NLS, the proportion of PPI-3'8MS2 and Fluc-3'8MS2 mRNAs that co-immunoprecipitated with EGFP-MS2-NLS from the cell lysate was increased. Therefore, future experiments used this method with AdPPI-3'8MS2 and AdFluc-3'8MS2.

4.3.7: Elution of PPI or Fluc mRNA from beads

PPI-3'8MS2 and Fluc-3'8MS2 mRNA were successfully purified from cell lysates. To elute the mRNA-protein complexes from the antibody, the beads were washed in elution buffer supplemented with 800mM $MgCl_2$ and 800mM NaCl. However, neither elution buffer supplemented with 800mM NaCl nor 800mM $MgCl_2$ eluted PPI-3'8MS2 or Fluc-3'8MS2 mRNAs, as all of the mRNA remained associated with the beads (figure 4.15).

4.3.8: Identification of mRNA binding proteins associated with PPI-3'8MS2 and Fluc-3'8MS2 mRNAs

Because elution buffer containing high salt was unable to elute PPI-3'8MS2 or Fluc-3'8MS2 mRNAs (figure 4.15), mRNA-binding proteins that were associated with PPI-

a) 800mM MgCl$_2$ elution

b) 800mM NaI elution
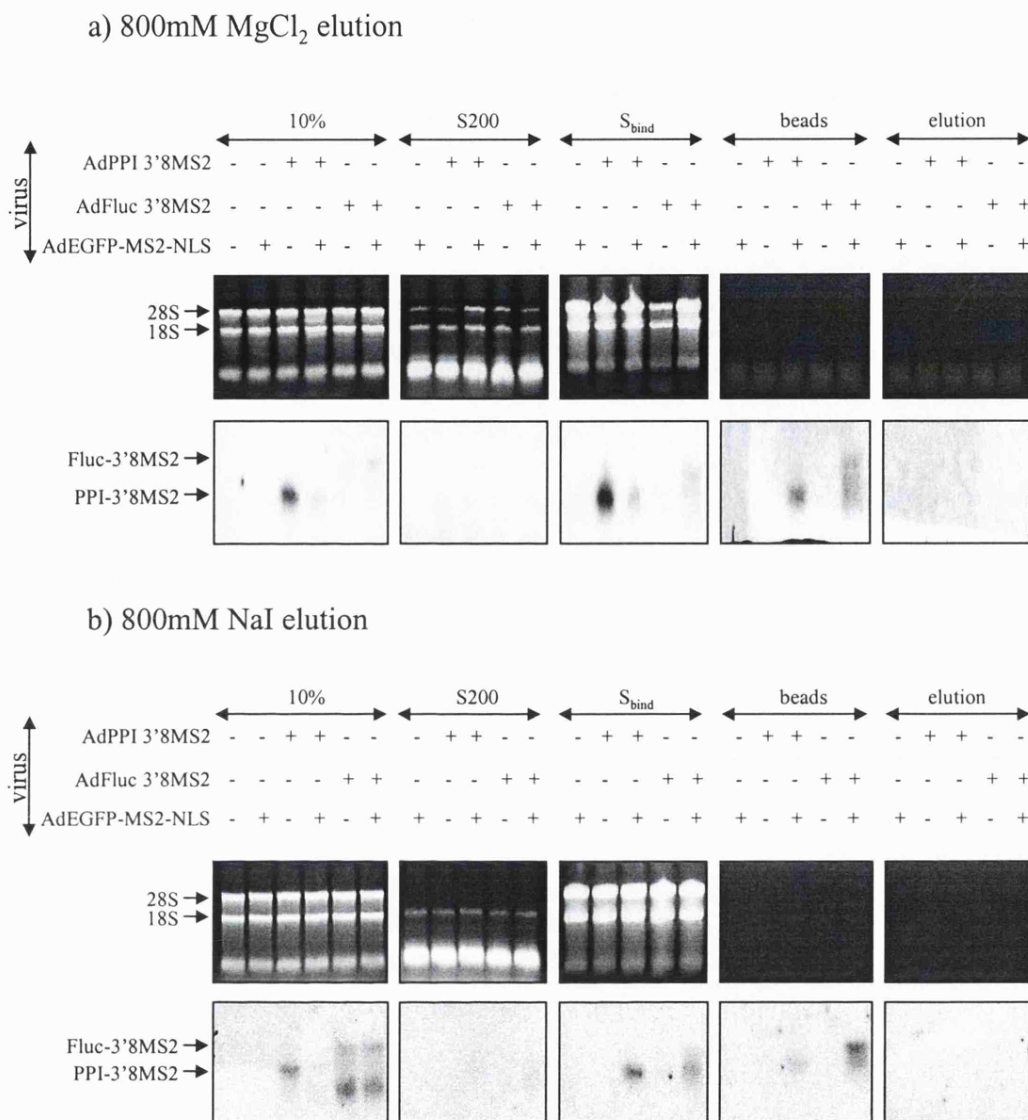
figure 4.15: Eluting RNA from the beads after co-immunoprecipitation with EGFP

MIN6 cells were mock-infected or were infected with viruses expressing PPI-3'8MS2, Fluc-3'8MS2 or EGFP-MS2-NLS as shown. PPI-3'8MS2 or Fluc-3'8MS2 mRNA was pulled out of the cell lysates as described in figure 4.27. After washing, the beads were finally resuspended in elution buffer (20mM HEPES pH7.6, 1mg/ml heparin, 1µl/ml RNAguard, 1mM benzamidine-HCl, 0.2mM phenylmethylsulfonyl fluoride, 1µg/ml leupeptin, 1µg/ml pepstatin) containing 800mM MgCl$_2$ (a) or 800mM NaI (b). The beads were finally pelleted and RNA was isolated from the beads and the supernatant (elution) as well as the supernatant after binding (S$_{bind}$), the S200 fraction and 10% of the initial lysate. The isolated RNA was run on a 1-% agarose formaldehyde gel and rRNA was stained with ethidum bromide. The RNA was then transferred onto nylon membrane and probed for actin mRNA and mRNAs containing the sequence for 8MS2 binding sites.

187

Figure 4.16: [^{35}S]-methionine incorporation into proteins associated with PPI-3'8MS2 and Fluc-3'8MS2 mRNAs

MIN6 cells were infected with virus as shown and after 24 hours of infection were incubated for a further 24 hours in MIN6 -methionine media that was supplemented with [^{35}S]-Methionine. The cells were then pre-incubated in KRB supplemented with 2mM glucose for one hour followed by a one hour incubation in KRB supplemented with 2mM or 20mM glucose. Cells were then lysed in low salt polysome buffer supplemented with 1% triton and PPI-3'8MS2 and Fluc-3'8MS2 mRNAs were co-immunoprecipitated with EGFP-MS2-NLS as described in figure 4.13. The beads were resuspended in 1X sample buffer and 4X sample buffer was added to the supernatant after binding. The supernatants after binding (a) and the beads (b) were then run on 12.5% SDS-PAGE gels, which were then washed twice in fixing solution, soaked for 20 minutes in amplify and dried. Proteins that had incorporated [^{35}S]-methionine were detected by exposure to film.
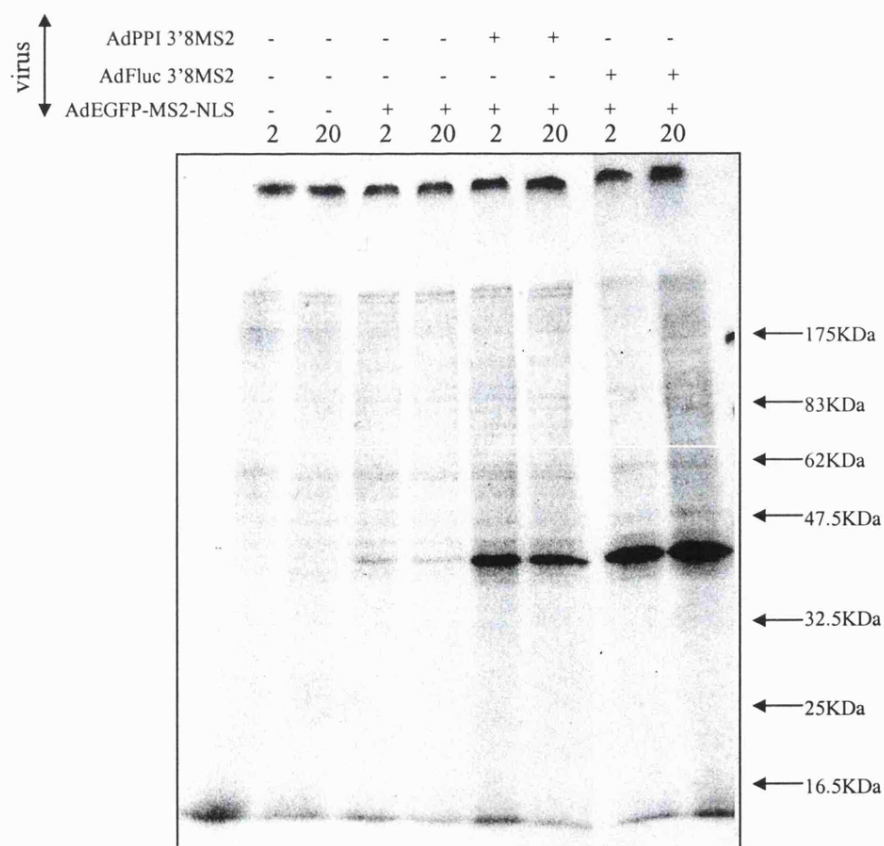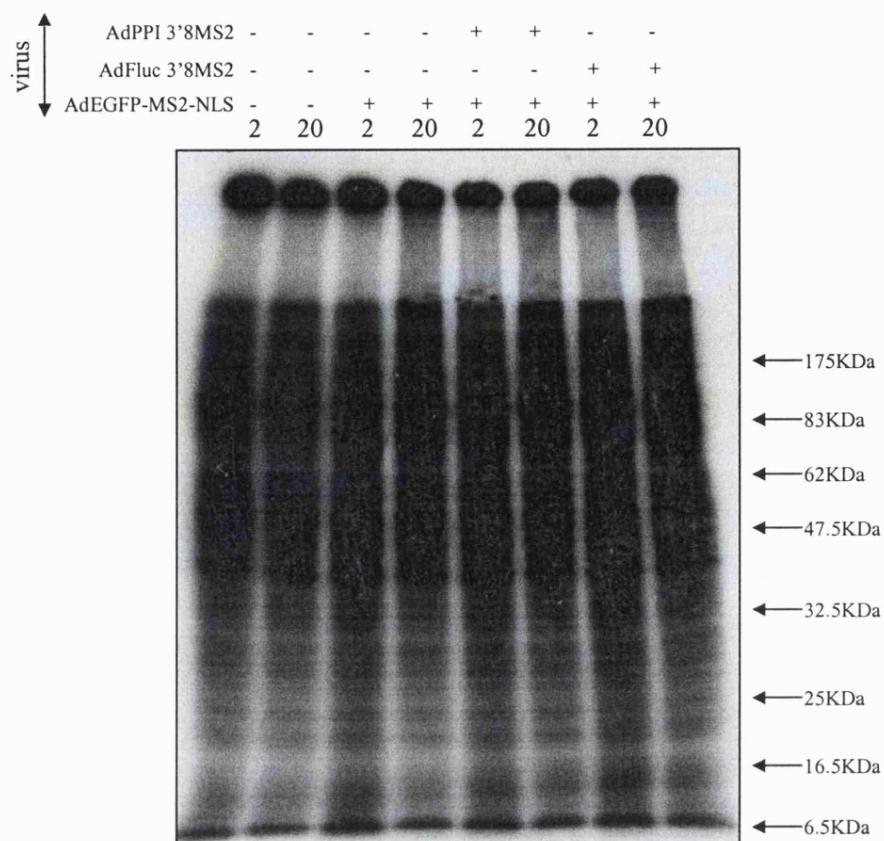
3'8MS2 and Fluc-3'8MS2 were eluted by boiling the beads in 1X sample buffer for 3 minutes. However, as this procedure also elutes a very large quantity of antibody from the beads, silver stained or coomassie stained SDS-PAGE of the elution will likely only identify the substantial amount of anti-GFP antibody and not the smaller quantity of mRNA-binding proteins. Therefore, to identify just the mRNA binding proteins and not the antibody, MIN6 cells were infected with virus as shown (figure 4.16) and then labelled with [^{35}S]-methionine for 24 hours. In this way, [^{35}S]-methionine-labelled proteins that bind to PPI-3'8MS2 or Fluc-3'8MS2 mRNAs *in vivo* can be identified from un-labelled anti-GFP antibody. After 24 hours incubation in [^{35}S]-methionine, the cells were pre-incubated in KRB supplemented with 2mM glucose for one hour followed by a one hour incubation in KRB supplemented with 2mM or 20mM glucose. Cells were then lysed and PPI-3'8MS2 and Fluc-3'8MS2 mRNAs were co-immunoprecipitated with EGFP-MS2-NLS as described in the figure legend to figure 4.13. The beads and supernatant after binding were then run on 12.5% SDS-PAGE gels. Proteins that had incorporated [^{35}S]-methionine were detected by exposure to film.

A large amount of proteins that had incorporated [^{35}S]-methionine were observed in the supernatant after binding (figure 4.16a). One protein that was immunoprecipitated by anti-GFP antibody when MIN6 cells were co-infected with AdEGFP-MS2-NLS and AdPPI-3'8MS2 or AdFluc-3'8MS2 was between 32.5Kda and 47.5Kda and most likely represented EGFP-MS2-NLS (figure 4.16b). Indeed, a band of the same size was observed when MIN6 cells were infected only with virus expressing EGFP-MS2-NLS, however, the quantities were much lower than when MIN6 cells were also infected with virus expressing PPI-3'8MS2 or Fluc-3'8MS2 because the majority of unbound EGFP-MS2-NLS had been separated from bound EGFP-MS2-NLS during the 200000g spin.

Final Conclusions

Although the conditions for purifying PPI-3'8MS2 and Fluc-3'8MS2 mRNAs were optimised so that the majority of PPI-3'8MS2 or Fluc-3'8MS2 mRNAs were isolated from MIN6 cell lysates, I was unable to elute the mRNA or identify proteins that were bound to the mRNA. Potential studies to solve these problems are discussed later.

4.4: Results II: Subcellular localisation of PPI mRNA using fluorescence microscopy

I have shown using biochemical fractionation techniques that PPI mRNA is recruited from the cytosol to the ER at high glucose concentrations (chapter 3, figures 3.9 and 3.13). Therefore, I wanted to see if the redistribution of PPI mRNA to the ER at high glucose could be visualised in living cells, by binding EGFP-MS2-NLS to PPI-3'8MS2 mRNA.

To visualise the localisation of cytosolic PPI-3'8MS2 or Fluc-3'8MS2 mRNA fluorescently, MIN6 cells were co-infected with AdEGFP-MS2-NLS and AdPPI-3'8MS2 or AdFluc-3'8MS2. Upon expression of the viruses, EGFP-MS2-NLS protein bound to the MS2 binding sites within the PPI-3'8MS2 or Fluc-3'8MS2 mRNAs (figure 4.2). Meanwhile, unbound EGFP-MS2-NLS was localised to the nucleus, due to the nuclear localisation signal. After infection, EGFP-MS2-NLS that was bound to cytosolic PPI-3'8MS2 or Fluc-3'8MS2 mRNAs was visualised by confocal laser microscopy. Images of infected live MIN6 cells were taken when the photo multiplier tube (PMT) sensitivity was low (500), medium (600) or high (700). When the PMT is high, the detector absorbs more emitted light and therefore more EGFP is observed. However, while increasing the PMT increases the intensity of true signals, it also increases the intensity of the background.

4.4.1: Visualisation of ER in MIN6 cells

To visualise the localisation of PPI-3'8MS2 mRNA to the ER, the ER needed to be identified. Therefore, the ER was identified by lipofectamine-mediated transfection of MIN6 cells with the construct dsRED-ER, which expresses calreticulin fused to dsRED and an ER retention signal. MIN6 cells were either just transfected with dsRED-ER or were infected with AdEGFP-MS2-NLS for 24 hours (to allow identification of the nucleus) and were then transfected with dsRED-ER. Images of living, transfected MIN6 cells were taken with bright field or during excitation with a wavelength of 543nm (for dsRED) or 488nm (for EGFP). The majority of the cytosol was stained with dsRED-ER, indicating that a large amount of ER is in the cytosol of MIN6 cells

(figure 4.17a). Cells that were transfected with dsRED-ER and were also infected with AdEGFP-MS2-NLS showed distinct barriers between the nucleus and the ER (figure 4.17b).

4.4.2: Visualisation of PPI-3'8MS2 mRNA in MIN6 cells

To determine if EGFP-MS2-NLS co-localised with PPI-3'8MS2 and the ER, MIN6 cells were co-infected with AdEGFP-MS2-NLS and AdPPI-3'8MS2 or were only infected AdEGFP-MS2-NLS. After 24 hours of infection, the cells were then transfected with dsRED-ER. When the PMT was low, and PPI-3'8MS2 mRNA was co-expressed with EGFP-MS2-NLS, all of EGFP-MS2-NLS localised to the nucleus and no EGFP-MS2-NLS co-localised with the ER (figure 4.17c). When the same cells were visualised with a high PMT, EGFP-MS2-NLS was found in the cytosol, suggesting that some EGFP-MS2-NLS was localised to the cytosol, possibly through the binding of PPI-3'8MS2 mRNA. However, at the same high PMT, control cells that were only infected with AdEGFP-MS2-NLS and transfected with dsRED-ER, showed a similar diffuse pattern of EGFP-MS2-NLS in the cytosol. Therefore the cytosolic EGFP-MS2-NLS did not appear to result from the specific binding of EGFP-MS2-NLS to PPI-3'8MS2 mRNA.

The cytosolic EGFP that is observed when PMT is high may be due to a small amount of excitation of dsRED by the laser emitting light at 488nm, which usually excites EGFP. Therefore, to prevent excitation of dsRED-ER by the laser emitting 488nm, MIN6 cells were co-infected with AdEGFP-MS2-NLS and AdPPI-3'8MS2 or AdFluc-3'8MS2, but were not transfected with dsRED-ER. In agreement with figure 4.17c, when PMT was low, all of EGFP-MS2-NLS localised to the nucleus in the presence and absence of PPI-3'8MS2 or Fluc-3'8MS2 mRNAs (figure 4.18). When the PMT was raised to medium or high, a small amount of EGFP-MS2-NLS was observed in the cytosol in both the absence and presence of PPI-3'8MS2 or Fluc-3'8MS2 mRNAs. Therefore, it is likely that the EGFP-MS2-NLS that was observed in the cytosol was due to background fluorescence resulting from the high amounts of nuclear EGFP-MS2-NLS.

Figure 4.17: Localisation of the ER and PPI-3'8MS2 mRNA in MIN6 cells
a) MIN6 cells were transfected with the construct dsRED ER by lipofectamine mediated transfection. Living transfected, MIN6 cells were observed by confocal microscopy under bright field and with a laser emitting a wavelength of 543nm. b) MIN6 cells were infected with AdEGFP-MS2-NLS for 24 hours and then were transfected with dsRED-ER. Live MIN6 cells were observed by confocal microscopy during excitation with a laser emitting a wavelength of 543nm or 488nm. c) MIN6 cells were infected with AdEGFP-MS2-NLS or were co-infected with AdEGFP-MS2-NLS and AdPPI-3'8MS2 mRNA for 24 hours and were then transfected with dsRED-ER. Images of the live MIN6 cells were taken during excitation with a laser emitting a wavelength of 543nm or 488nm. Images were taken when the PMT was set at low (L, 400) or high (H, 700).

a) MIN6 cells transfected with dsRED-ER

Bright field	543nm	overlay
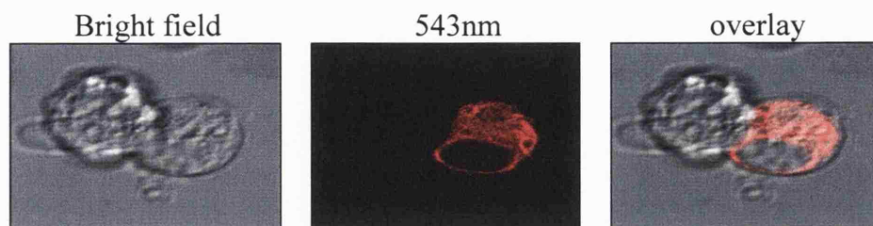
b) MIN6 cells transfected with dsRED-ER and infected with MS2-EGFP

488nm	543nm	overlay
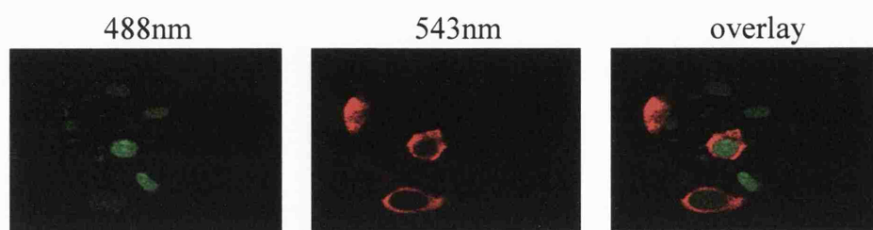
c) MIN6 cells infected with EGFP-MS2-NLS and PPI-3'8MS2 and transfected with dsRED

dsRed-ER	MS2-EGFP	PPI-3'8MS2	PMT	488nm	553nm	overlay
+	+	+	L			
+	+	+	H			
+	+	-	L			
+	+	-	H			
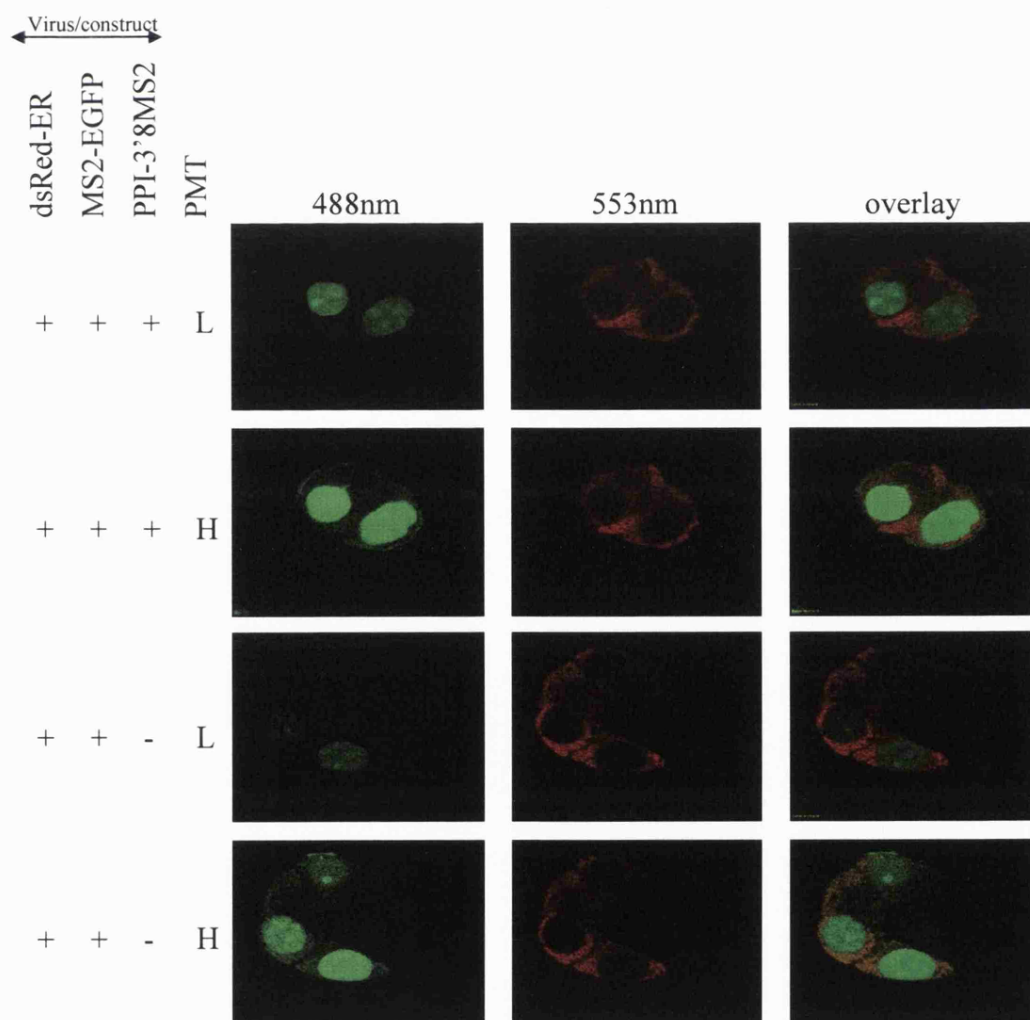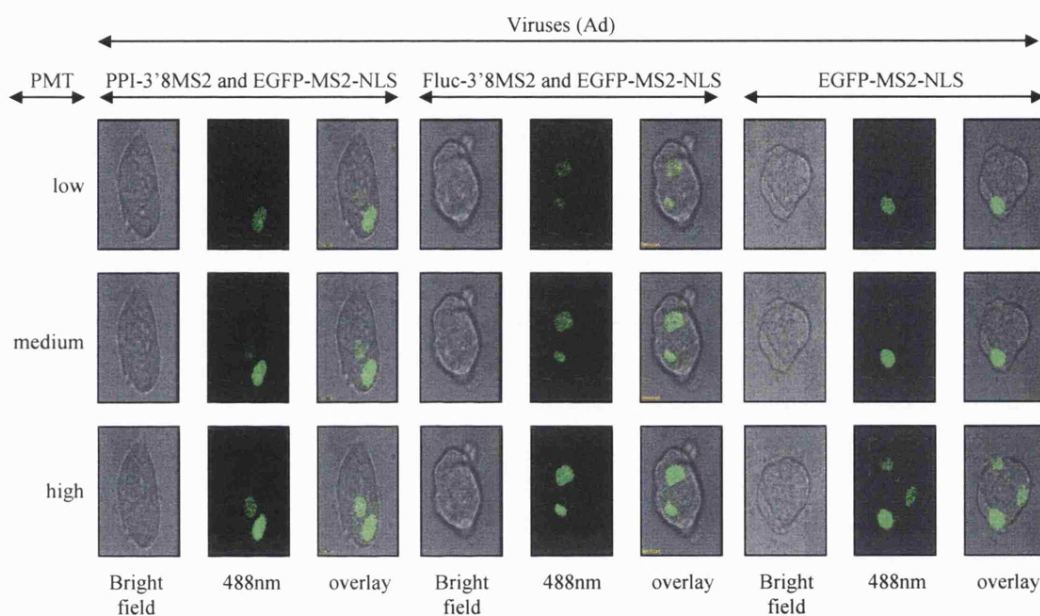
Figure 4.18: EGFP labelling of specific mRNAs in MIN6 cells

MIN6 cells were infected with viruses expressing EGFP-MS2-NLS and/or PPI-3'8MS2 or Fluc-as shown. Images of the live MIN6 cells were taken by confocal microscopy in bright field or during excitation with a laser emitting a wavelength of 488nm with the PMT set at low (500), medium (600) or high (700). These results are representative of three separate experiments.

In summary, due to the background cytosolic EGFP-MS2-NLS, I was unable to visualise mRNAs that contained the MS2 binding sites.

4.5: Discussion

4.5.1: Isolation of PPI mRNA binding proteins

Two techniques were used to isolate PPI mRNA and its associated proteins. 1) MS2-GST was immobilised to glutathione sepharose beads to affinity-purify specific mRNAs containing the MS2 binding sites; and 2) EGFP-MS2-NLS was co-expressed with mRNAs containing the MS2 binding sites and then immunoprecipitated with anti-GFP antibody.

MS2-GST that was immobilised on glutathione sepharose beads was unable to pull down PPI-8MS2 or PPI-3'8MS2 mRNAs (figures 4.7, 4.9 and 4.10). One possibility why MS2-GST may have been unable to pull out PPI-8MS2 or PPI-3'8MS2 mRNA is that MS2 binds its recognition site in mRNA as a dimer (Lago et al., 2001). The immobilisation of MS2-GST on beads may have prevented this dimerisation, thereby inhibiting the binding of MS2-GST to its binding sites within the mRNA.

By co-expressing PPI-3'8MS2 or Fluc-3'8MS2 mRNAs and EGFP-MS2-NLS, both PPI-3'8MS2 and Fluc-3'8MS2 mRNAs were specifically co-immunoprecipitated with EGFP-MS2-NLS (figure 4.11 and 4.13). Furthermore, by separating unbound EGFP-MS2-NLS from EGFP-MS2-NLS that was bound to ribosome-bound mRNAs, the majority of PPI-3'8MS2 or Fluc-3'8MS2 mRNAs were successfully pulled out of MIN6 cell lysate (figure 4.13). Although PPI-3'8MS2 and Fluc-3'8MS2 mRNAs were successfully pulled out of MIN6 cell lysates, I was unable to identify any proteins other than EGFP-MS2-NLS that were specifically bound to the mRNA (figure 4.16). In fact, all of the protein bands other than EGFP-MS2-NLS were observed in both the infected cells and the mock-infected cells. The relatively large amount of EGFP-MS2-NLS compared to other mRNA binding proteins is most likely due to the rapid expression of EGFP-MS2-NLS from the CMV promoter and rapid turnover of EGFP-MS2-NLS in the cell, which will have resulted in high [^{35}S]-methionine incorporation into EGFP-MS2-NLS compared to other proteins.

To detect proteins bound to PPI-3'8MS2 or Fluc-3'8MS2 mRNAs above the amount of background, larger quantities of these mRNAs need to be expressed and isolated. In

this work I showed that the majority of PPI-3'8MS2 or Fluc-3'8MS2 mRNAs co-immunoprecipitated with EGFP-MS2-NLS (figure 4.13), suggesting that the co-immunoprecipitation of these mRNAs with EGFP-MS2-NLS is efficient. Importantly, the amount of PPI-3'8MS2 and Fluc-3'8MS2 mRNAs that were co-expressed with EGFP-MS2-NLS was low, suggesting that the expression of these mRNAs may be the limiting factor in isolating enough mRNA to detect mRNA binding proteins (figure 5.11 and 4.13). One simple way to increase the expression of PPI-3'8MS2 mRNA would be to increase the virus titre. Interestingly, the expression of PPI-3'8MS2 and Fluc-3'8MS2 mRNAs was much higher in MIN6 cells only infected with AdPPI-3'8MS2 or AdFluc-3'8MS2 compared to in MIN6 cells that were also infected with AdEGFP-MS2-NLS (figure 4.11 and 4.13). This may be because AdEGFP-MS2-NLS could competitively inhibit the uptake of AdPPI-3'8MS2 or AdFluc-3'8MS2. Because there is a large excess of unbound EGFP-MS2-NLS protein (figure 4.14), the amount of AdEGFP-MS2-NLS used for infection could be decreased to potentially improve the infectivity and expression of AdPPI-3'8MS2 when these viruses are co-infected with AdEGFP-MS2-NLS into MIN6 cells.

4.5.2: Subcellular localisation of PPI mRNA

The subcellular localisation of PPI-3'8MS2 mRNA could not be visualised by binding EGFP-MS2-NLS to PPI-3'8MS2 mRNA. This was most likely because the background of the unbound EGFP-MS2-NLS in the nucleus was too high to observe the much lower quantities of cytosolic EGFP-MS2-NLS (figure 4.17 and 4.18). Decreasing the amount of AdEGFP-MS2-NLS could decrease the amount of unbound, nuclear EGFP-MS2-NLS and therefore decrease the amount background from the nucleus. Furthermore, as discussed above, by decreasing the amount of AdEGFP-MS2-NLS, the expression of PPI-3'8MS2 mRNA may improve, thereby increasing the proportion of cytosolic mRNA-bound EGFP-MS2-NLS to unbound EGFP-MS2-NLS.

Chapter 5: Identification Of Pancreatic β-Cell Proteins Differentially Regulated By Glucose

5.1: Introduction

Upon increases in glucose concentration from 2.8mM to 16.7mM glucose, islets incorporate twice as much [^{3}H]-leucine into total protein (Permutt, 1974; Permutt and Kipnis, 1972a). This increase in protein synthesis is over only one hour and is independent of new mRNA synthesis, which suggests that in the short term, glucose up-regulates pancreatic β-cell protein synthesis at a post-transcriptional level (Permutt, 1974; Permutt and Kipnis, 1972a).

5.1.1: Short-term incubation of β-cells in high glucose concentrations stimulates the up-regulation of specific β-cell proteins at the translational level

While there is a two-fold increase in general β-cell protein synthesis in response to glucose there is a larger increase in the synthesis of a number of specific β-cell proteins, including PI. In fact, incubation of islets in high glucose concentration for one hour resulted in at least a two-fold increase in the synthesis of more than 240 secretory granule polypeptides and the synthetic rate of 60 of these was increased by 10 to 30 fold (Guest et al., 1991). In contrast to the secretory membrane fraction, the synthesis of only 8 out of 160 proteins in the soluble fraction was increased by 10-30 fold in response to stimulation by glucose. It is likely that the majority of these glucose-regulated proteins are regulated at the post-transcriptional level, as actinomycin D has little effect on protein synthesis rates in islets over one hour (Permutt, 1974; Permutt and Kipnis, 1972a).

While work has shown that the synthesis of more than 240 beta cell proteins increases after only one hour incubation in high glucose, only a small number of these have been identified. Some specific examples of translationally-regulated proteins include PI, prohormone convertases, PC2 and PC3 (Alarcon et al., 1993; Martin et al., 1994; Rhodes and Alarcon, 1994; Skelly et al., 1996), synaptic vesicle associated membrane protein, syntaxin-1(Nagamatsu et al., 1997), the secretory granule membrane protein

SGM 110 (Grimaldi et al., 1987) and the secretory granule protein, chromagranin A (Guest et al., 1989). However, not all proteins found in the insulin secretory granule are regulated in response to glucose, for example, glucose had no effect on the synthesis of carboxypeptidase H in islets or MIN6 cells (Guest et al., 1989; Skelly et al., 1996).

It is likely that the rapid up-regulation of β-cell protein synthesis in response to glucose is important in maintaining the correct response to changes in plasma glucose levels. Indeed, inhibition of translation in islets by cycloheximide inhibits insulin secretion in response to glucose (Garcia et al, 2001). Therefore deviation from the normal synthesis of these proteins may result in malfunctioning storage or secretion of PI and symptoms associated with type II diabetes.

5.1.2: Expression profiling in pancreatic β-cells

To identify glucose-induced changes in β-cell expression, 2-D gel electrophoresis has been performed with [^{35}S]-methionine-labelled proteins synthesised over 4 hours at 10mM glucose in β-cells that had been incubated in 6, 10 or 20mM glucose for 10 days (Ling et al., 1996). Three patterns of protein expression were observed. The first were protein spots that showed a concentration dependent up-regulation of protein synthesis in response to glucose and the second were protein spots that showed a concentration dependent down-regulation of protein synthesis in response to glucose. The third pattern was protein spots that showed an up-regulation from 6mM to10mM glucose and a down regulation from 10mM to 20mM glucose. This analysis exemplified the differential changes in the synthesis of distinct β-cell proteins in response to glucose concentration.

5.1.3: Effect of long term incubations in glucose on the transcriptional profiles of β-cells

To begin to identify proteins that are glucose-regulated in β-cells, Affymetrix microarray analysis has been carried out on MIN6 cells, fluorescence-activated cell sorter (FACS)-purified rat β-cells and human islets that were incubated in low or high glucose for 24 hours (Flamez et al., 2002; Shalev et al., 2002b; Webb et al., 2000; Webb

et al., 2001). In MIN6 cells incubated in 25mM glucose, the expression of 78 genes varied by an average of 2.2 fold or more compared to MIN6 cells incubated in 5.5mM glucose (Webb et al., 2000; Webb et al., 2001). Using similar methods, Flamez *et al*, (2002) showed that the levels of more than 150 transcripts were glucose-regulated when FACS-purified β-cells were incubated in 10mM glucose compared to 3mM glucose (average fold change of 2, over 3 experiments). Both these studies classified the glucose-regulated genes into functional groups and showed that large proportions of these up-regulated genes were involved in secretory and metabolic pathways. Meanwhile, in human islets, an increase in glucose concentration from 1.67mM to 16.7mM glucose resulted in the up-regulation of 14 genes and the down-regulation of 6 genes by an average of more than 1.5 fold (3 experiments, (Shalev et al., 2002b)).

5.1.4: Effect of short term incubations in glucose on the transcriptional profiles of β-cells

cDNA microarray analysis has identified a number of β-cell proteins that are transcriptionally regulated during a 45 minute incubation in low or high glucose. MIN6 cells were incubated in DMEM containing 5mM glucose for 18 hours and were then either harvested immediately or incubated in DMEM containing 25mM glucose for 1 hour (Susini et al., 1998). Glucose activated the expression of 72 genes by more than 1.3 fold and 6 genes by more than 2 fold. While the 78 up-regulated genes were of diverse functions, the majority of genes whose expression changed more than 2 fold were immediate early genes, confirming previous work that glucose activates the expression of immediate early genes such as c-fos (Ohsugi et al., 2004; Susini et al., 1998). This microarray analysis showed that when MIN6 cells were exposed to high glucose for one hour, the majority of increases and decreases in mRNA expression levels were less than 1.5 fold.

5.1.5: Proteomics techniques to identify glucose-regulated proteins

Microarray analysis identifies the up-regulation of gene expression but does not distinguish whether these changes in mRNA levels are paralleled by changes in protein levels. Recently, 2-D gel electrophoresis and mass spectrometry have been used to

identify the differential expression of proteins that are expressed in freshly isolated islets compared to isolated islets that have been incubated in 11mM glucose for 24 hours (Ahmed and Bergsten, 2005). 379 proteins were differentially expressed and of these, 77 distinct proteins were characterised by mass spectrometry. The major functional groups of these 77 proteins were metabolism (25%), cell signalling (20%), cellular defence and molceular chaperones (18%).

<u>5.1.6: Microarray analysis identifies changes in mRNA expression levels</u>

Microarray analysis is a powerful tool for identifying large numbers of genes whose expression changes in response to certain stimuli. Generally, microarray analysis is carried out using cDNA microarrays or high-density synthetic oligonucleotide arrays (for reviews see Duggan et al., 1999; Lipshutz et al., 1999). The advantages of high-density oligonucleotide arrays are that a much lower quantity of RNA is required for the hybridisation to oligonucleotide arrays than for hybridisation to cDNA microarrays. Additionally because oligonucleotide arrays are synthetic, they can contain far more probes than cDNA microarrays, allowing the identification of far more genes.

Affymetrix are the major provider of high-density oligonucleotide arrays. The hybridisation of RNA to Affymetrix microarrays can be split into two stages. First the total RNA is used as a template to make fragmented biotin-labelled cRNA (the labelled target) and second, the fragmented cRNA is hybridised to the array. To prepare the labelled targets for hybridisation to the array, total RNA is reverse transcribed using an oligo-dT primer containing a T7 polymerase promoter to make double stranded cDNA (figure 5.1a). The double stranded cDNA is then transcribed *in vitro* to incorporate biotinylated CTP and UTP and then finally, the biotin-labelled cRNA is fragmented. The biotin-labelled fragmented cRNA from experimental and control conditions are then bound to separate chips (figure 5.1b). The chips are washed, stained with a streptavidin-phycoerythrin conjugate and finally scanned. To determine changes in gene expression, the signals from the baseline array are then compared with the control array.
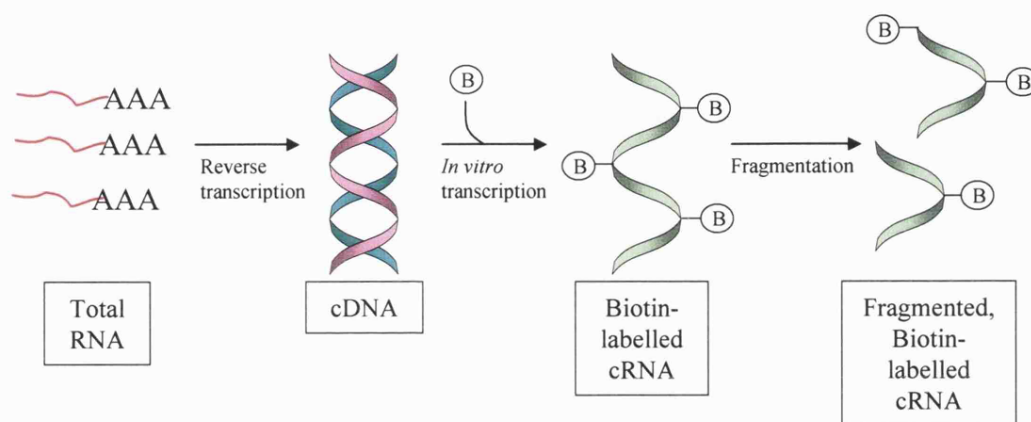
a) Synthesis of fragmented, biotin-labelled cRNA
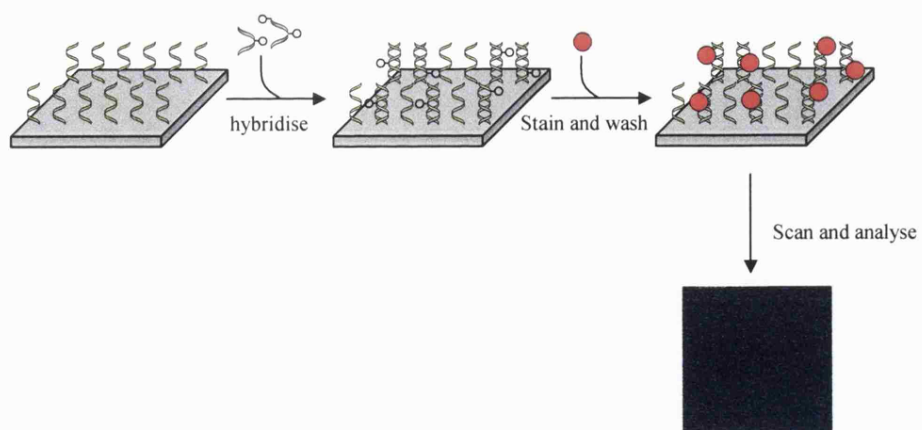
b) Hybridisation of cRNA to arrays

Figure 5.1: Affymetrix Microarray strategy
Adapted from www.affymetrix.com

The majority of microarray expression analyses identify changes in total mRNA levels and therefore identify changes in transcription or mRNA stability. However, to identify translationally regulated proteins, microarray analysis was performed on polysomal mRNAs, which are mRNAs that are associated with ribosomes and therefore likely to be actively translating (Johannes et al., 1999; Mikulits et al., 2000; Schratt et al., 2004). As the recruitment of ribosomes onto mRNA is indicative of an increase in the rate of initiation of translation, mRNAs that redistribute from the non-polysomal fractions into the polysomal fractions are most likely to be translationally regulated. This technique also identifies changes in total mRNA levels, as an increase in total mRNA (polysomal and non-polysomal) in the cell is usually accompanied by an increase in the amount of polysomal mRNA.

5.1.7: Objectives

Although gene expression profiling in β-cells incubated in low versus high glucose concentrations has identified proteins that are transcriptionally regulated in both the long term (24 hours) and the short term (1 hour), the majority of translationally regulated β-cell proteins remain unidentified. Therefore, the objective of this chapter is to use microarray analysis of polysomal mRNAs to identify β-cell proteins that are translationally regulated in response to increases in glucose concentration.

5.2: Methods of Microarray Analysis

5.2.1: Affymetrix Microarray Analysis

In this study, Affymetrix mouse microarrays MOE 430A were used. These arrays contain 22626 probe sets for approximately 14000 genes. Each probe set contains 11 probe pairs, which interrogate for the same gene. The probe pair is made up of a 25-mer oligonucleotide that is complementary to the sequence being interrogated (perfect match) and a 25-mer oligonucleotide that is the same as the perfect match probe, except for a base pair substitution at the 13th position (mis-match).

Once the chips are scanned, analysis can be carried out using a number of different analysis programs. However, in this study, MicroArray Suite 5 (MAS5, Affymetrix) and dChip (www.dchip.org) will be used. Although, both dChip and MAS5 use the intensity values of the hybridised targets to the mismatch and perfect match probes to calculate the expression values, they use different algorithms to establish quality control, normalisation values and expression values. Furthermore, it has been shown that while MAS5 is superior at identifying transcripts whose concentrations are high, dChip is better at identifying changes in transcripts that have lower concentrations (Rajagopalan, 2003). Therefore, the initial analysis was performed with MAS5 and then dChip was used to confirm changes observed in MAS5 and potentially identify any other transcripts that were not identified by MAS5.

5.2.2: MicroArray Suite 5 (MAS5, Affymetrix).

Normalisation of arrays (Data analysis fundamentals manual at www.affymetrix.com)
To correct for differences in the hybridisation, washing and staining efficiencies and therefore, make the arrays comparable, the baseline and experiment arrays were normalised by the scaling method. In all of the MAS5 analysis used in this thesis, all arrays were scaled by 'all probe sets scaling' so that the intensity of each probe set was multiplied by a scale factor to result in a mean intensity of the array at 500.

Calculating expression values

MAS5 uses two different mathematical methods to determine the detection call for a transcript (present or absent) and the signal for a transcript (quantitative measure of abundance).

Detection p value and detection call

The detection p value is used to determine the detection call (present or absent) of a specific transcript. The detection p value is found in two stages. First, each probe pair (prefect match (PM) and mis-match (MM)) within a probe set is given a discrimination value (R):

$$R=(PM-MM)/(PM+MM)$$

The larger the PM intensity is compared to the MM intensity, the closer R is to 1. Each of the R-values for each of the probe pairs within the probe set is assigned a rank depending on how far it is from a user-definable threshold (usually set at 0.015) and the p-value is determined using the One-Sided Wilcoxon's Signed Rank test. User-definable cut-offs are then set so that a large p-value (0.06-1) indicates the absence of a transcript and a small value (default: 0-0.04) indicates the presence of a transcript. Transcripts whose p value is between 0.04 and 0.06 are designated marginal.

Signal algorithm

The quantitative signal value for each probe set is determined using One-step Tukey's Bi-weight Estimate. The signal for each probe pair is determined by subtracting the MM intensity from the PM intensity, and taking the log of this value. Each probe pair is then weighted so that values closer to the median value for a probe set are more heavily weighted than values far from the median value. The weighted values for each probe pair intensity are then used to determine the average signal for the probe set.

Quality Control

Noise, background and scale factors

After analysis of each array, an expression report, which contains all of the quality control data is generated for each array. Large differences in noise values, average background and scale factors suggest large assay variability or sample degradation.

Percentage of present genes

The percentage of genes present is also included in the expression report and depends on a number of factors including: cell type, environmental and biological factors and RNA quality. A low percentage of present genes can be indicative of degraded RNA. Additionally, replicate samples should have similar percentages of genes present.

RNA quality

To check the quality of the RNA sample, the signal for the 3' end of actin and GAPDH are compared with the signal for the 5' end of actin and GAPDH. Because the reverse transcription reaction is carried out using an oligo-dT primer, there may be some 3' bias, especially if the RNA sample is partially degraded or the transcription of cDNA and cRNA is inefficient. To ensure that RNA quality is good, Affymetrix recommend that the 3'/5' ratio should not exceed 3.

Comparison Analysis

MAS5 also uses two difference statistical techniques to determine the change call (increase, decrease or no change) for a transcript and the signal log ratio for a transcript (quantitative difference between two arrays).

Change call

The change call p value is determined by the One-Sided Wilcoxon's Signed Rank test. Values close to 0 indicate an increase in the expression of a transcript in the experimental array, values close to 1 indicate a decrease in the expression of a transcript in the experimental array and values close to 0.5 indicate no change in the expression of a transcript in the experimental array.

Signal log ratio

The signal log ratio is determined by comparing each probe pair on the baseline array to the matching probe pair on the experimental array. The mean of the Log_2 ratio of each probe pair is determined using the One-step Tukey's Biweight method. Therefore to determine fold change of a transcript:

Fold change = $2^{(\text{signal log ratio})}$

5.2.3: DChip (www.dchip.org)

Normalisation of arrays

After scanning the array, Affymetrix software generates the cell files, which contain a single intensity value for every probe. When the cell files are read into dchip, dchip outputs the 'array summary file', which contains the median probe intensity for each array. The median probe intensity is calculated by finding the median value of every 5 probe by 5 probe region on the array and gives a value for the overall brightness of the array. Differences in the median intensities of arrays indicates the need for normalisation.

Ideally normalisation should be calculated using only non-differentially expressed genes. Therefore, to determine the normalisation value, dChip uses an algorithm to find a set of probes whose expression does not change between the arrays to be normalised. This set of probes is known as the invariant set (Schadt et al., 2001). The invariant set method assumes that if the intensities of each probe set are ranked, probes of non-differentially expressed genes will rank in similar positions in the non-normalised and baseline arrays (NB: baseline refers to the array to which all other arrays are normalised). Therefore the invariant set contains probes in which the PM intensity rank differences are small between the non-normalised and the baseline. The invariant set are plotted on a graph of the baseline intensities against the non-normalised intensities and used to calculate a running median normalisation curve. To calculate the normalised values, an imaginary vertical line is drawn through each of the points representing a perfect match or mis match probe. The y-axis value where this line intercepts the normalisation curve is then used as the intensity value for the normalised array (on the x-axis). After normalisation, expression values for each probe set are calculated by the weighted average of PM/MM differences.

Quality Control

To check hybridisation efficiencies and control the quality of the data, dchip cross-references each array with the other arrays to identify any problematic array outliers, which are probe sets whose pattern is different to the consensus pattern of most other arrays. The % of array outliers in each array are provided in the array summary file.

Any array with an array outlier value over 5% should be treated with caution and a warning is given.

5.3: Results

5.3.1: Strategy for the identification of translationally controlled mRNAs

As the recruitment of ribosomes onto mRNA is indicative of an increase in the rate of initiation of translation, mRNAs that redistribute in sucrose gradients from the non-polysomal fractions into the polysomal fractions are most likely translationally regulated. Therefore, to identify translationally-regulated proteins, Affymetrix microarray analysis was used to quantitate and compare the amounts of polysomal mRNAs (mRNAs with more than 3 ribosomes) isolated from MIN6 cells incubated in low (0.5mM) glucose concentrations with polysomal mRNAs isolated from MIN6 cells incubated in high (20mM) glucose concentrations.

MIN6 cells were incubated in KRB supplemented with 0.5mM glucose for 1 hour and then further incubated in KRB supplemented with 0.5mM or 20mM glucose for 1 hour (figure 5.2a). 0.1mg/ml of cycloheximide (final concentration) was added to cells 10 minutes prior to lysis to prevent ribosomal run-off. Cells were lysed in high salt polysome lysis buffer supplemented with 1% triton and then centrifuged at 12000g for 10 minutes to pellet the nuclei and unlysed cells. The supernatants containing the cell lysates were layered onto 7-47% sucrose gradients, which were centrifuged at 39000rpm for two hours at 4°C. Gradients were subsequently fractionated and the absorbance was measured continuously at 254nm to give polysome profiles of MIN6 cells. Absorbance profiles of the gradients show that an increase in the glucose concentration from 0.5mM to 20mM results in a large decrease in the 60S/80S peak and an increase in the polysome peaks (figure 5.2b). This indicates that glucose stimulates the movement of ribosomes onto mRNAs and therefore suggests that glucose stimulates an increase in the global rate of initiation, results similar to those previously reported (figure 3.2 and (Gomez et al., 2004)). Each gradient was fractionated into 20 fractions, RNA was isolated from each fraction and 1/12th was run on a formaldehyde gel, stained with ethidium bromide (figure 5.2c). The polysome profiles and ethidium bromide stained rRNA were used to identify and pool the remaining RNA from fractions representing mRNAs that were associated with more than three ribosomes (designated polysomal mRNAs) and fractions representing mRNAs that were associated with three ribosomes or less (designated non-polysomal mRNAs). Differential amounts of

Figure 5.2: Strategy for the identification of β-cell proteins translationally regulated by glucose

MIN6 cells were pre-incubated in KRB containing 0.5mM glucose for 1 hour followed by incubation in KRB containing 0.5mM or 20mM glucose for a further hour. 0.1mg/ml (final concentration) of cycloheximide was added to the cells 10 minutes prior to lysis to prevent ribosomal run-off. Cells were lysed and the lysates layered onto 7 - 47% sucrose gradients. The gradients were then centrifuged at 39000rpm at 4°C for 2 hours and fractionated from top (fraction 1) to bottom (fraction 20) using the ISCO gradient fractionator. Absorbance of the gradients was measured continually at 254nm to give polysome profiles. RNA was isolated from 20, 1ml fractions and $1/12^{th}$ was run on 1% agarose formaldehyde gel. The remaining $11/12^{th}$ was pooled into polysomal and non-polysomal fractions and the polysomal fractions were used for microarray analysis as described in the results. This is representative of 2 independent experiments.

a

MIN6 cells
0.5mM glucose

MIN6 cells
20mM glucose

b

0.5mM glucose

TOP

OD 254nM

2 4 6 8 10 12 14 16 18 20
60/80S   Fraction Number

20mM glucose

TOP

OD 254nM

2 4 6 8 10 12 14 16 18 20
60/80S   Fraction Number

c

28S →
18S →

5S →

2 4 6 8 10 12 14 16 18 20

non-polysomal mRNA | polysomal mRNA

2 4 6 8 10 12 14 16 18 20

non-polysomal mRNA | polysomal mRNA

d

Affymetrix microarray

Affymetrix microarray

Compare hybridisation intensities to identify fold changes and
glucose-stimulated mRNAs

polysomal mRNAs between low and high glucose concentrations were then identified by Affymetrix microarray analysis (figure 5.2d). Microarray analysis was carried out twice (experiment 1 and experiment 2) using polysomal mRNA isolated from MIN6 cells incubated in 0.5mM glucose or 20mM glucose. Therefore, RNA was hybridised to four different arrays. The synthesis of fragmented cRNA from polysomal RNA and the hybridisation of the cRNA to the arrays were carried out by the Microarray facility at the University of Leicester and the MRC geneservice at the University of Cambridge. Both facilities then provided the cell files for analysis.

To ensure the quality and reproducibility of the hybridisation and normalisation procedures, Affymetrix microarray requires an equal quantity of RNA to be hybridised to the baseline and experimental arrays. However, in this work, because glucose stimulated a large increase in the amount of rRNA in the polysome fractions, the quantity of total RNA will be higher at high glucose than at low glucose concentrations. Therefore, it is important to be aware that by using equal starting quantities of total RNA for the low and high glucose arrays, the only mRNAs that will be identified as being recruited into the polysomal fractions are those that are recruited above the average increase in total RNA.

5.3.2: Quality control of RNA before hybridisation to arrays

To confirm the quality of the initial polysomal RNA samples, 200ng of RNA was run on the Agilent 2100 bioanalyser using the RNA 6000 nanoassay. This produced electrophoretic data with a gel-like image. The electrophoretic data showed two clear peaks for the 18S and 28S rRNA and no smaller fragments (indicative of RNA degradation), thus confirming that the RNA was good quality (figure 5.3a). The yield of the isolated polysomal RNA was then quantified by measuring the absorbance at 260nm. As expected the total RNA was higher in the high glucose samples than the low glucose samples (figure 5.3, table b). Nonetheless, 10μg of total RNA was used for all of the reverse transcription reactions.

After the synthesis of the cRNA, the size distribution of the cRNA was run on the Agilent 2100 bioanalyser using the RNA 6000 nanoassay to assess its quality. Analysis of the cRNA generated from MIN6 polysomal RNA resulted in a wide distribution of

a) Yield of total RNA

sample	Ratio 260/280	Yield (μg) of total RNA
Experiment 1, 0.5mM glucose	1.89	12.7
Experiment 1, 20mM glucose	1.92	35.5
Experiment 2, 0.5mM glucose	1.95	16.94
Experiment 2, 20mM glucose	1.93	30.75

b) Total RNA

0.5mM glucose   20mM glucose
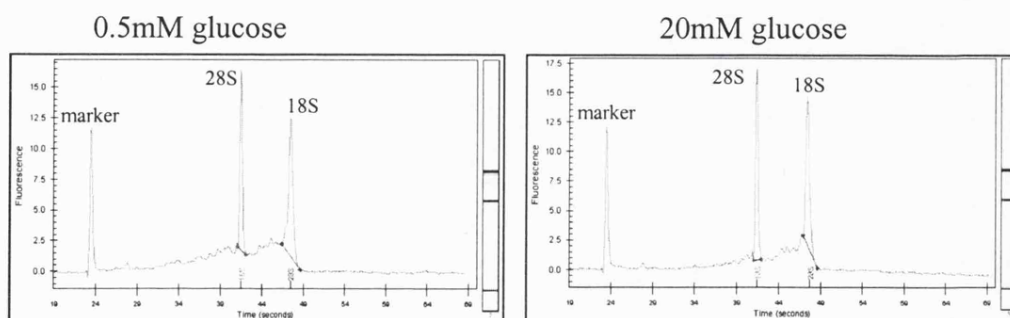
c) Yield of cRNA

Sample	Yield (μg)
Experiment 1, 0.5mM glucose	15.41
Experiment 1, 20mM glucose	15.02
Experiment 2, 0.5mM glucose	11.52
Experiment 2, 20mM glucose	14.07

d) cRNA

0.5mM glucose   20mM glucose
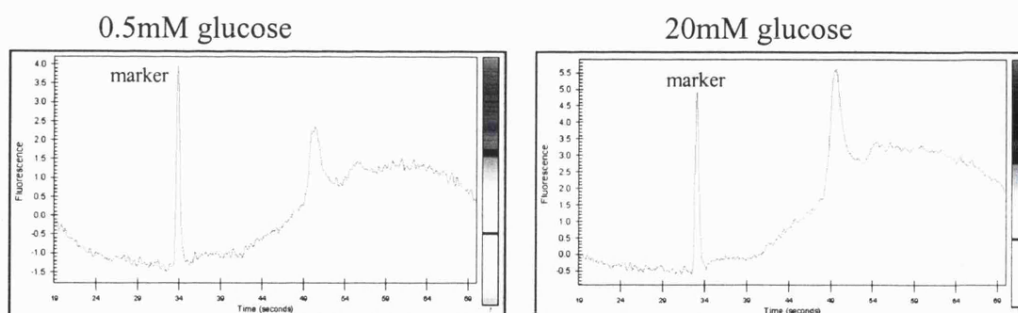
Figure 5.3: Quantity and quality control of total RNA and cRNA
a) The quantity of total polysome RNA was calculated by measuring the OD
at 260nm and the purity of the RNA was calculated by finding the ratio of the
OD at 260nm:OD at 280nm. b) 200ng of total polysomal RNA isolated from
MIN6 cells incubated in 0.5mM or 20mM glucose was run on the Agilent
2100 bioanalyser using the RNA 6000 nanoassay. c) The yield of cRNA was
calculated by measuring the OD at 260nm. d) cRNA was made from 10μg of
total polysomal RNA isolated from MIN6 cells incubated in 0.5mM or 20mM
glucose and 200ng of this cRNA was run on the Agilent 2100 bioanalyser
using the RNA 6000 nanoassay.

products, indicative of efficient *in vitro* transcription reactions (figure 5.3c). The yield of cRNA was then quantified by measuring the absorbance at 260nm (figure 5.3, table d). 15µg and 11.5µg of fragmented cRNA was hybridised to MOE430A arrays for experiment 1 and 2 respectively. The complete microarray data for both experiments analysed in MAS5 and dChip can be found on the CD attached with this thesis.

5.3.3: Analysis of Microarrays Using MAS5

MAS5 Expression Reports

To check the quality of the microarray, expression reports for each array were generated by MAS5. In both experiment 1 and experiment 2, the noise and background values were similar (table 5.1). Furthermore, there was not more than a 3-fold difference in the scale factors between all four arrays. This data therefore confirmed that the hybridisation quality of the arrays was good, thereby meaning that the four arrays were comparable.

To further ensure that the replicate experiments were comparable, the percentage of genes present at low and high glucose in experiment 1 were compared with the percentage of genes present at low and high glucose in experiment 2. The percentage of genes present at low glucose was 46% and 40% for experiments 1 and 2 respectively, while the percentage of genes present at high glucose was 50% and 52% for experiments 1 and 2 respectively (table 5.1). The similarity between the percentage of genes present in the two low glucose samples and the two high glucose samples confirm the reproducibility of the microarray.

To check the quality of the RNA sample, the 3'/5'ratio was found for actin and GAPDH. The 3'/5' ratios for both actin and GAPDH were less than 2.5 for both the low and high glucose arrays in experiment 1, indicative of good quality RNA (table 5.1). However, in experiment 2, the 3'/5' ratios for actin and GAPDH were 18.37 and 16.94 respectively for the low glucose array and 10.16 and 8.43 respectively for the high glucose array. Because the 3'/5' ratios for the arrays for experiment 2 were significantly higher than 3 for both actin and GAPDH, this sample may be of poorer quality. However, since the other quality controls were acceptable for experiment 2, it is likely that the results from these arrays are reliable.

array	noise	Scale factor	Ave back- ground	% probe sets present	% probe sets absent	3'/5' actin	3'/5' GAPD H
0.5mM Exp. 1	2.120	16.407	51.76	46.2	52.3	1.87	1.26
20mM Exp. 1	2.130	11.659	49.72	50.6	48.1	2.49	1.20
0.5mM Exp. 2	2.510	9.872	67.13	40.0	58.5	18.37	16.94
20mM Exp. 2	1.5	6.100	40.44	52	46.5	10.16	8.43

Table 5.1: Quality control data generated by MAS5 expression report
The expression report was generated using MAS5 to ensure the quality of each array.

Identification of genes regulated by glucose using MAS5 data analysis

Experiment 1 and 2 were analysed separately by MAS5. Additional analysis was then carried out in Excel to identify probe sets that changed in both experiments 1 and 2. To identify changes in levels of polysomal mRNAs using MAS5, the following criteria were set: 1) probe sets with absent calls in both baseline (0.5mM glucose) and experimental (20mM glucose) arrays were excluded; 2) probe sets with no change call between baseline and experimental arrays were excluded and 3) a threshold of 1.5 fold or 2 fold change in levels of polysomal mRNAs between low and high glucose concentrations in the two individual experiments.

To determine an overall picture of the effect of glucose on polysomal mRNA levels, a scatter plot was drawn to compare the signal of polysomal mRNA at high glucose versus the signal of polysomal mRNA at low glucose. Each probe set that was plotted was designated a colour that was dependent on whether the detection p value determined the probe set present or absent. Because the detection call (present or absent) and the signals are determined using separate algorithms, some probe sets are designated absent when in fact they have relatively high signals. In this case the high signal is most likely due to a hybridisation to both the PM and MM, hence the absent call. The majority of transcripts are either absent at both 0.5mM and 20mM glucose (yellow) or are present at both 0.5mM and 20mM glucose (red) (figure 5.4). A small number of transcripts are absent at one glucose concentration and then present at the other glucose concentration (blue).

Although the scatter plot analysis demonstrates a large number of glucose responsive β-cell genes, the majority of glucose-responsive genes change by less than 3 fold, as only a small number of probe sets are outside the 3 fold change lines (figure 5.4). In fact, when experiment 1 and experiment 2 were analysed separately, 10.7% of probe sets (approximately 2500) showed an increase or decrease in polysomal mRNAs between 0.5mM and 20mM glucose (table 5.2). The data was then filtered to only include probe sets that changed more than 2 fold. In experiment 1, glucose stimulated a 2 fold or more increase in polysomal mRNA levels for 220 probe sets and a 2 fold or more decrease in polysomal mRNA levels for 301 probe sets. In experiment 2, glucose stimulated a 2 fold or more increase in polysomal mRNA levels for 136 probe sets and a 2-fold decrease in polysomal mRNA levels for 204 probe sets.

a) Experiment 1
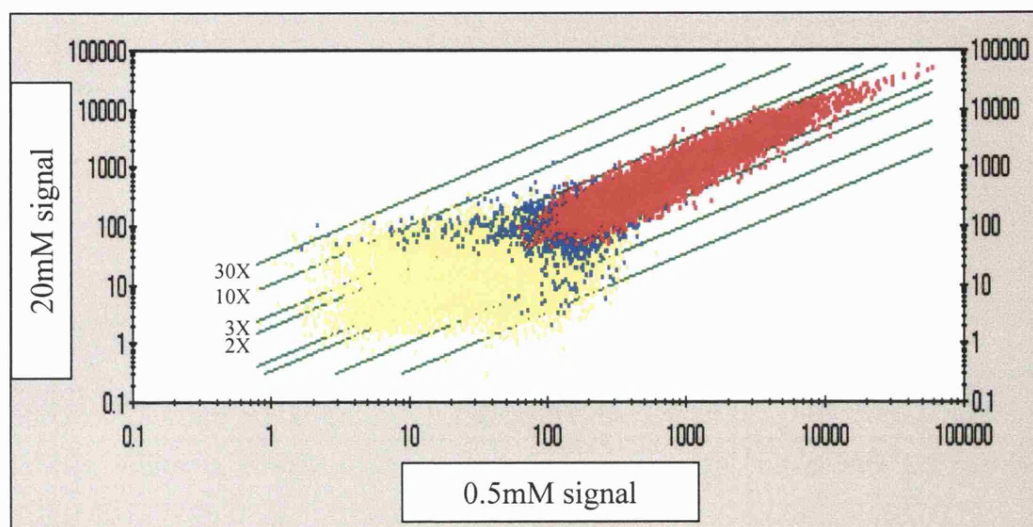
b) Experiment 2
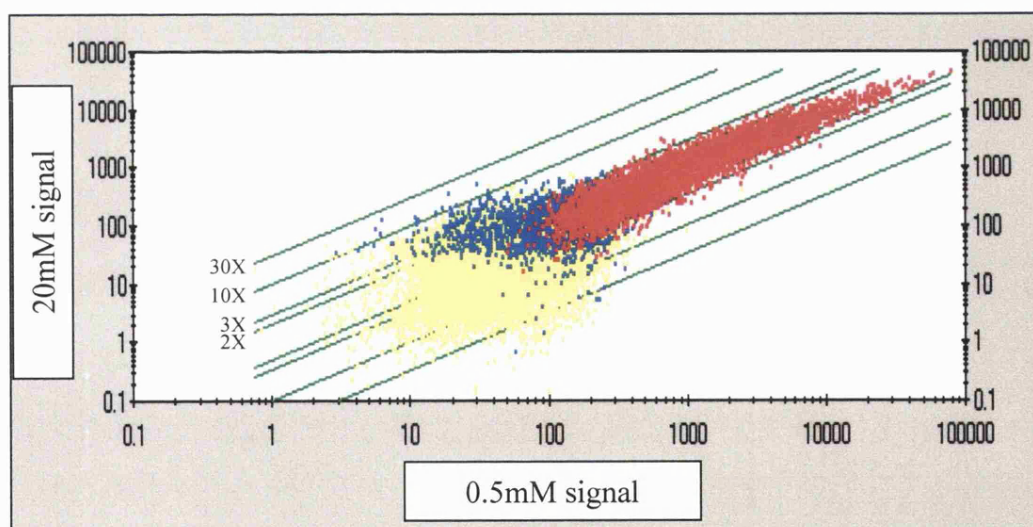
Figure 5.4: Scatter plot analysis of polysomal mRNA levels
To compare polysomal mRNA levels in MIN6 cells incubated in low vs high glucose, the intensity values of each probe set at high glucose (y-axis) was plotted against the intensity value for each probe set at low glucose (x-axis). Probe sets that were designated absent in both arrays are coloured yellow, probe sets that were designated present in both arrays are coloured red and probe sets that were designated absent in one array and present in the other array are coloured blue. The fold change lines parallel to the diagonal identify probe sets in the comparison that change 2-fold, 3-fold, 10-fold and 30-fold. a) Experiment 1, b) Experiment 2.

218

Exp.	% increase	% decrease	% no change	# of probe sets that increase more than 2 fold	# of probe sets that decrease more than 2 fold	# of probe sets that change more than 2 fold
Exp. 1	6.0	4.7	88.1	220	301	521
Exp. 2	6.1	4.6	88.0	136	204	340

Table 5.2: Glucose stimulates a change in 10.7% of genes
The percentage of probe sets whose expression increased or decreased in response to an increase in glucose concentration was calculated in MAS5 separately for experiment 1 and experiment 2. The number of these probe sets that increased or decreased by more than two fold was then calculated from the total number of increases and decreases.

The glucose-stimulated increases and decreases from both experiment 1 and experiment 2 were combined and probe sets that increased or decreased in both experiments were selected by using Excel. Glucose stimulated an increase in polysomal mRNA for over 600 probe sets in both experiments, and a decrease in polysomal mRNA levels for less than 100 probe sets in both experiments (figure 5.5). The data was then filtered so that only probe sets, which had changed in both experiments by more than 1.5 fold, or more than 2 fold, were displayed. An increase in glucose concentration resulted in a 1.5 fold increase in polysomal mRNA levels for 275 probe sets and a 1.5 fold decrease in polysomal mRNA levels for 47 probe sets. Meanwhile, polysomal mRNA levels for 17 probe sets increased by more than 2 fold and polysomal mRNA levels for 22 probe sets decreased by more than 2 fold in response to an increase in glucose concentration. Therefore, out of the 2500 glucose-regulated probe sets in each individual experiment, only 600 changed in both experiments and of these only 322 changed by more than 1.5 fold in both experiments and of these only 39 changed by more than 2 fold in both experiments. The genes encoding polysomal mRNAs that increase or decrease by more than 1.5 fold or 2 fold in response to an increase in glucose are listed along with their Genbank accession numbers in table 5.3 and 5.4.

Glucose responsive genes whose polysomal mRNA levels changed 1.5 fold or more or 2 fold or more in both experiments were functionally classified using NCBI databases (www.ncbi.nlm.nih.gov) according to known cellular functions or sequence similarity to genes of known functions. More than 50% of probe sets that glucose stimulated a 2 fold or more change were important in transcription or metabolism (figure 5.6). Transcription and metabolism were also the two largest functional groups that glucose stimulated a 1.5 fold change or more in polysomal mRNA. Additionally, glucose stimulated a 1.5 fold change in a large number of polysomal mRNAs that express proteins important in translation. Interestingly, while the level of polysomal mRNA for all of the probe sets involved in translation and 91% of probe sets important in metabolism increased 1.5 fold rather than decreased in response to glucose, the level of polysomal mRNAs important in transcription increased 1.5 fold for only 60% of probe sets and the remaining 40% decreased in response to glucose.
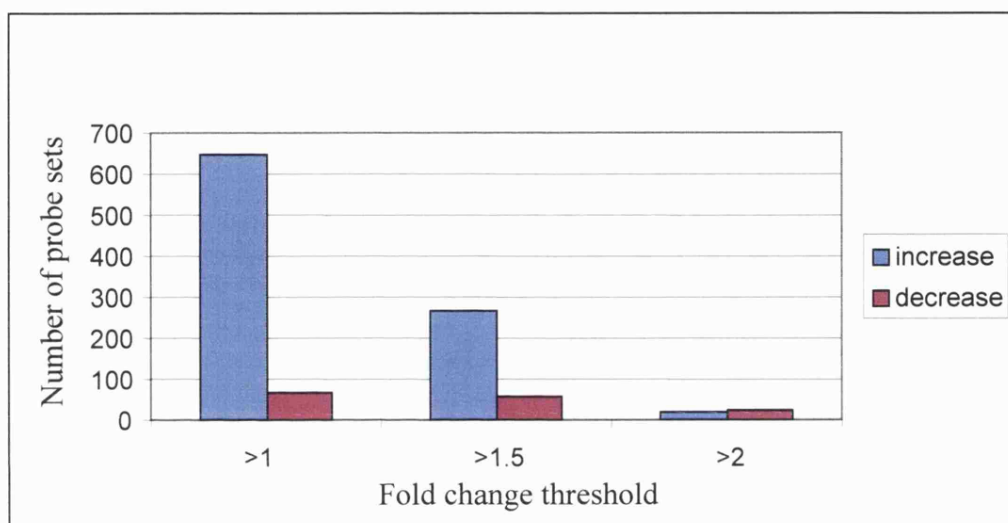
Figure 5.5: Number of probe sets that increased or decreased in individual experiments 1 and 2 in response to glucose stimulation
The total number of probe sets that increased or decreased (i.e. change of more than 1 fold) in both experiment 1 and experiment 2 were plotted with the number of probe sets that increased by more than 1.5 fold and more than 2 fold in both experiment 1 and experiment 2.

Table 5.3: List of polysomal mRNAs whose levels changed by more than 2-fold in response to glucose stimulation (MAS5)

Polysomal mRNAs whose levels were shown to increase or decrease by more than 2 fold in response to 1 hour glucose stimulation are listed. Identity of columns from left to right: gene description, Genbank accession number, fold change in experiment 1 as calculated by MAS5, fold change in experiment 2 as calculated by MAS5, average fold change in experiment 1 and experiment 2.

Gene Description	Accession	Exp 1	Exp 2	Average
Apoptosis, repair, DNA synthesis				
RIKEN cDNA 5830413E08 gene	AK017926	-2.30	-2.83	-2.56
Cell signalling				
Rab acceptor 1 (prenylated)	L40934	2.14	2.64	2.39
RIKEN cDNA 1110011F09 gene	BC016408	2.14	2.46	2.30
calpactin	NM_009112	2.14	2.00	2.07
plexin A2	D86949	-2.00	-2.00	-2.00
suppressor of cytokine signaling 7	AK014988	-2.46	-2.30	-2.38
induced in fatty liver dystrophy 2	BC012955	-2.46	-3.03	-2.75
beta-spectrin 2, non-erythrocytic	BQ174069	-2.64	-2.64	-2.64
Cytoskeletal				
myosin light chain, alkali, nonmuscle	BC026760	2.00	2.14	2.07
Translation				
gene rich cluster, C2f gene	NM_013536	2.64	2.00	2.32
Metabolism and mitochondria				
thioredoxin 2	NM_019913	10.56	6.06	8.31
thioredoxin interacting protein	NM_023719	4.92	2.64	3.78
S-adenosylmethionine decarboxylase 1	NM_009665	2.30	2.00	2.15
cDNA sequence BC003494	BC018194	2.14	2.46	2.30
glutathione peroxidase 4	AF274027	2.00	3.25	2.62
aminolevulinic acid synthase 1	BC022110	-2.00	-2.14	-2.07
potassium inwardly-rectifying channel	NM_008426	-2.30	-2.64	-2.47
mitochondrial carrier homolog 1	AF192558	2.00	2.00	2.00
Unclassified				
clone IMAGE:6398163, mRNA	C88880	2.14	2.46	2.30
clone IMAGE:5358852, mRNA	BI692833	2.00	2.30	2.15
RIKEN cDNA 2700019D07 gene	BM937429	-2.14	-2.00	-2.07
RIKEN cDNA 2610029D06 gene	BB333454	-2.46	-2.00	-2.23
Transcription and splicing				
FBJ osteosarcoma oncogene	AV026617	3.03	2.46	2.75
early growth response 1	NM_007913	2.46	2.00	2.23
amino-terminal enhancer of split	NM_010347	2.30	2.00	2.15
breakpoint cluster region protein 1	NM_011793	2.00	2.14	2.07
deltex 2 homolog (Drosophila)	BB518874	-2.00	-2.14	-2.07
inhibitor of DNA binding 3	NM_008321	-2.00	-2.46	-2.23
zinc finger protein 54	NM_011760	-2.14	-2.83	-2.49
core promoter element binding protein	AV025472	-2.30	-2.00	-2.15
feminization 1 homolog b (C. elegans)	NM_010193	-2.30	-5.66	-3.98
zinc finger protein 93	NM_009567	-2.46	-2.30	-2.38
Jun oncogene	NM_010591	-2.64	-2.83	-2.73
activating transcription factor 4	AV314773	-2.64	-3.73	-3.19
activating transcription factor 4	M94087	-2.83	-3.03	-2.93
zinc finger protein BC027407	BC023090	-3.03	-2.14	-2.59
zinc finger protein 51	BC011183	-3.25	-2.14	-2.70
DNA-damage inducible transcript 3	NM_007837	-3.48	-4.00	-3.74
Jun oncogene	BC002081	-3.73	-4.92	-4.33

Table 5.4: List of polysomal mRNAs whose levels changed by more than 1.5-fold in response to glucose stimulation (MAS5)

Polysomal mRNAs whose levels were shown to increase or decrease by more than 1.5 fold in response to 1 hour glucose stimulation are listed. Identity of columns from left to right: gene description, Genbank accession number, fold change in experiment 1 as calculated by MAS5, fold change in experiment 2 as calculated by MAS5, average fold change in experiment 1 and experiment 2.

Gene description	Accession	Exp 1	Exp 2	Average
Apoptosis, repair, DNA synthesis				
Bcl2-associated X protein	BC018228	1.87	2.14	2.00
histone 1, H3a	NM_013550	1.62	2.14	1.88
histone 1, H2bc	M25487	1.62	2.14	1.88
brain protein 44-like	AV223468	1.62	2.14	1.88
apoptosis related protein	AK002276	2.00	1.74	1.87
H3 histone, family 3A	BI111967	1.87	1.87	1.87
H2A histone family, member X	NM_010436	2.14	1.52	1.83
replication factor C (activator 1) 5	AK011489	1.52	1.74	1.63
brain protein I3	NM_018772	1.62	1.62	1.62
mutS homolog 6 (E. coli)	U42190	-1.74	-1.74	-1.74
DNA-damage-inducible transcript 4	AK017926	-2.30	-2.83	-2.56
Cell Signalling				
Cd27 binding protein	NM_013929	1.62	13.93	7.78
Rab acceptor 1 (prenylated)	L40934	2.14	2.64	2.39
Rab1B	BC016408	2.14	2.46	2.30
serologically defined colon cancer antigen	NM_019990	1.62	2.64	2.13
calpactin	NM_009112	2.14	2.00	2.07
acid phosphatase 1, soluble	NM_021330	1.62	2.46	2.04
deleted in polyposis 1-like 1	AK002562	1.87	2.00	1.93
protein phosphatase 2, regulatory subunit B	BC003979	1.87	1.87	1.87
Down syndrome critical region homolog 5	BF318238	1.87	1.87	1.87
protein phosphatase 1, catalytic subunit	NM_031868	1.87	1.87	1.87
interleukin-1 receptor-associated kinase 1	NM_008363	1.52	2.14	1.83
cyclin I	BC003290	2.00	1.62	1.81
histidine triad nucleotide binding protein	U60001	2.00	1.62	1.81
casein kinase II, beta subunit	NM_009975	1.62	2.00	1.81
Cd27 binding protein	AF033112	2.00	1.52	1.76
BRCA2 and CDKN1A interacting protein	NM_025392	2.00	1.52	1.76
sorting nexin 5	NM_024225	1.87	1.62	1.75
protein phosphatase 1, regulatory	NM_021391	1.62	1.87	1.75
CDC28 protein kinase 1	NM_016904	1.52	1.87	1.69
vascular endothelial growth factor B	U48800	1.52	1.87	1.69
ketoacid dehydrogenase kinase	NM_009739	1.52	1.87	1.69
GDP dissociation inhibitor 3	NM_008112	1.52	1.87	1.69
CDK2 -associated protein 1	AK004852	1.62	1.74	1.68
nephronophthisis 1 (juvenile) homolog	NM_016902	1.62	1.62	1.62
gene rich cluster, C8 gene	BI081061	1.62	1.52	1.57
RAN binding protein 1	L25255	1.62	1.52	1.57
uridine-cytidine kinase 2	NM_030724	1.52	1.62	1.57
cornichon homolog (Drosophila)	AF022811	1.52	1.62	1.57
paternally expressed 3	NM_008817	-1.52	1.74	0.11
cyclin T2	BB426893	-1.87	-1.52	-1.69
plexin A2	D86949	-2.00	-2.00	-2.00
CDC-like kinase	U21209	-1.74	-2.30	-2.02
repetin	AK009453	-2.46	-1.74	-2.10
optic atrophy 1 homolog (human)	NM_133752	-2.46	-1.87	-2.16
suppressor of cytokine signaling 7	AK014988	-2.46	-2.30	-2.38
beta-spectrin 2	BQ174069	-2.64	-2.64	-2.64
induced in fatty liver dystrophy 2	BC012955	-2.46	-3.03	-2.75

225

Gene description	Accession	Exp 1	Exp 2	Average
Cytoskelatal				
dynein, cytoplasmic, light chain 2A	BG791323	2.64	1.74	2.19
human CHMP1.5 protein homolog	BC010524	1.74	2.64	2.19
myosin light chain, alkali, nonmuscle	BC026760	2.00	2.14	2.07
profilin 1	NM_011072	2.46	1.52	1.99
cofilin 1, non-muscle	NM_007687	1.74	2.14	1.94
dynactin 3	NM_016890	2.00	1.74	1.87
tubulin cofactor a	BB559082	1.87	1.52	1.69
Ena-vasodilator stimulated phosphoprotein	AW553781	1.62	1.62	1.62
microtubule-associated protein light chain	NM_026160	1.62	1.52	1.57
t-complex testis expressed 1	BG094946	1.52	1.52	1.52
Translation				
gene rich cluster, C2f gene	NM_013536	2.64	2.00	2.32
ribosomal protein L18	NM_009077	1.87	2.46	2.16
ribosomal protein S16	NM_013647	2.64	1.62	2.13
ribosomal protein L29	AI893877	2.64	1.62	2.13
cold shock domain protein A	AV216648	1.62	2.64	2.13
ribosomal protein L12	NM_009076	2.30	1.74	2.02
ribosomal protein S14	BE368859	2.30	1.74	2.02
ribosomal protein L29	AA690930	2.30	1.74	2.02
ribosomal protein S7	AI414989	2.14	1.87	2.00
ribosomal protein S8	BQ127746	1.87	2.14	2.00
ribosomal protein S2	NM_008503	1.87	2.14	2.00
similar to yeast ribo prot	W11855	2.14	1.74	1.94
acidic ribosomal phosphoprotein PO	NM_007475	2.14	1.74	1.94
ribosomal protein S14	AW548239	2.14	1.74	1.94
ribosomal protein L29	NM_009082	2.14	1.74	1.94
immature colon carcinoma transcript 1	NM_026729	1.87	2.00	1.93
similar to yeast ribo prot	BI900577	2.14	1.62	1.88
ribosomal protein S5	NM_009095	2.14	1.62	1.88
ribosomal protein 10	NM_052835	1.62	2.14	1.88
ribosomal protein L13a	NM_009438	2.00	1.74	1.87
ribosomal protein L10A ·	AK002613	2.14	1.52	1.83
ribosomal protein L35	AV066335	2.14	1.52	1.83
ribosomal protein S13	NM_026533	2.14	1.52	1.83
ribosomal protein L17	BC003896	2.14	1.52	1.83
popeye 3	BF228007	2.00	1.62	1.81
ribosomal protein L28	NM_009081	2.00	1.62	1.81
similar to yeast ribo prot	BI900577	2.00	1.62	1.81
ribosomal protein L18	AU019414	1.87	1.74	1.80
ribosomal protein S18	NM_011296	2.00	1.52	1.76
Finkel-Biskis-Reilly murine sarcoma virus	NM_007990	1.87	1.62	1.75
ribosomal protein L26	NM_009080	1.87	1.62	1.75
ribosomal protein L24	BC002110	1.87	1.52	1.69
ribosomal protein L19	NM_009078	1.87	1.52	1.69
mitochondrial ribosomal protein S24	BF167852	1.62	1.74	1.68
ribosomal protein L7a	NM_013721	1.74	1.52	1.63
DNA segment, Chr 11	BC024944	1.62	1.62	1.62
ribosomal protein S10	NM_025963	1.62	1.62	1.62
ribosomal protein S24	AV206764	1.62	1.52	1.57
ribosomal protein L7	M85235	1.52	1.62	1.57
ribsomal protein L11	NM_025919	1.52	1.52	1.52
ribosomal protein S15	NM_009091	1.52	1.52	1.52
ribosomal protein L27	NM_011289	1.52	1.52	1.52
ribosomal protein L37a	NM_009084	1.52	1.52	1.52
ribosomal protein S7	NM_011300	1.52	1.52	1.52

Gene description	Accession	Exp 1	Exp 2	Average
Metabolism and mitochondria				
thioredoxin 2	NM_019913	10.56	6.06	8.31
thioredoxin interacting protein	NM_023719	4.92	2.64	3.78
lysophospholipase 1	BC013536	3.48	1.87	2.67
glutathione peroxidase 4	AF274027	2.00	3.25	2.62
o-fucosyltransferase 2	BC018194	2.14	2.46	2.30
ubiquinone	NM_025843	2.64	1.74	2.19
peptidyl-prolyl cis/trans isomerase	NM_023371	1.74	2.64	2.19
S-adenosylmethionine decarboxylase 1	NM_009665	2.30	2.00	2.15
fatty acid binding protein 5, epidermal	BC002008	1.74	2.46	2.10
ubiquinone 1 beta subcomplex, 9	W29413	2.30	1.87	2.08
mitochondrial ribosomal protein S18A	NM_026768	1.87	2.30	2.08
ubiquinone 1 beta subcomplex, 9	AV161987	2.64	1.52	2.08
mitochondrial carrier homolog 1	AF192558	2.00	2.00	2.00
general control of amino acid synthesis 1	NM_015740	1.62	2.30	1.96
ATP synthase, F0 complex, subunit c	NM_026468	1.74	2.14	1.94
ATP synthase, F1 complex, delta subunit	BC008273	2.00	1.87	1.93
ATP synthase, F1 complex, O subunit	NM_138597	2.00	1.87	1.93
ATPase, H+ transporting, V1 subunit F	BC016553	1.87	2.00	1.93
ATP synthase, F0 complex, subunit c	NM_007506	2.00	1.74	1.87
ubiquinone 1 beta subcomplex, 5	BC025155	2.00	1.74	1.87
ubiquinone Fe-S protein 5	NM_134104	1.74	2.00	1.87
cytochrome c oxidase, subunit Vb	NM_009942	2.00	1.62	1.81
arsenite transporter, ATP-binding, homolog 1	NM_019652	1.62	2.00	1.81
PC1 inhibitor	AF181560	1.62	2.00	1.81
ubiquinone flavoprotein 2	BI692577	1.74	1.87	1.80
mitochondrial ribosomal protein	NM_026065	1.87	1.74	1.80
translocator inner mitochondrial membrane	AF106620	1.87	1.74	1.80
mitochondrial ribosomal protein L27	NM_053161	1.87	1.74	1.80
deoxyuridine triphosphatase	AF091101	2.00	1.52	1.76
ubiquinone 1 alpha subcomplex, 7	BI558499	2.00	1.52	1.76
ubiquinone 1 beta subcomplex, 7	NM_025843	2.00	1.52	1.76
ferritin heavy chain	BE457668	1.52	2.00	1.76
cytochrome c oxidase, subunit VIIIa	NM_007750	1.52	2.00	1.76
Friedreich ataxia	AV007132	1.87	1.62	1.75
phosphomannomutase 1	BC006809	1.62	1.87	1.75
mitochondrial ribosomal protein L52	AV021593	1.87	1.62	1.75
fractured callus expressed transcript 1	NM_019502	1.87	1.62	1.75
protein O-fucosyltransferase 2	BB699319	1.74	1.74	1.74
SH3-domain GRB2-like B1 (endophilin)	BC024362	1.74	1.74	1.74
deleted in polyposis 1	NM_007874	1.87	1.52	1.69
succinate dehydrogenase complex subunit C	NM_025321	1.52	1.87	1.69
mitochondrial ribosomal protein S12	NM_011885	1.87	1.52	1.69
mitochondrial ribosomal protein 63	AB049958	1.87	1.52	1.69
mitochondrial ribosomal protein L53	BC022162	1.52	1.87	1.69
triosephosphate isomerase	NM_009415	1.62	1.74	1.68
ubiquinol-cytochrome c reductase binding protein	NM_026219	1.62	1.74	1.68
translocator of inner mitochondrial membrane	AF106621	1.74	1.62	1.68
mitochondrial ribosomal protein L51	BC021535	1.74	1.62	1.68
cystatin B	NM_007793	1.74	1.52	1.63
ubiquinol-cytochrome c reductase	AK003966	1.74	1.52	1.63
predicted methyltransferase	BC026936	1.52	1.74	1.63
glycine C-acetyltransferase	NM_013847	1.52	1.74	1.63

Gene description	Accession	Exp 1	Exp 2	Average
Metabolism and mitochondria (continued)				
cytochrome c oxidase, subunit VIIIa	NM_007750	1.52	1.74	1.63
translocase mitochondrial membrane 9 homolog	BF021416	1.74	1.52	1.63
mitochondrial ribosomal protein L10	BC016219	1.52	1.74	1.63
S-adenosylhomocysteine hydrolase	NM_016661	1.62	1.62	1.62
peroxiredoxin 2	NM_011563	1.62	1.62	1.62
supressor of mif two, 3 homolog 1	NM_019929	1.62	1.62	1.62
ubiquinone 1 alpha subcomplex, 6 (B14)	NM_025987	1.62	1.62	1.62
cysteine-rich protein 2	NM_007792	1.62	1.52	1.57
cytochrome c oxidase, subunit Va	NM_007747	1.62	1.52	1.57
ubiquinone Fe-S protein 7	BC013503	1.62	1.52	1.57
ubiquinone 1 alpha subcomplex, 5	NM_026614	1.52	1.62	1.57
mitchondrial ribosomal protein S7	AK012225	1.62	1.52	1.57
differentiation-associated-protein 3	Y17852	1.62	1.52	1.57
mitochondrial ribosomal protein S16	NM_025440	1.62	1.52	1.57
mitochondrial ribosomal protein S15	BB314055	1.52	1.62	1.57
neighbor of Cox4	BQ174254	1.52	1.52	1.52
mitochondrial ribosomal protein L28	NM_024227	1.52	1.52	1.52
stearoyl-Coenzyme A desaturase 2	BB459479	-1.74	2.30	0.28
methyltransferase activity	AK013137	-1.74	-1.74	-1.74
DNA methyltransferase (cytosine-5) 1	BB165431	-1.52	-2.14	-1.83
calcium channel, voltage-dependent	AJ437291	-1.62	-2.14	-1.88
mitochondrial DNA-directed RNA polymerase	AK003792	-2.00	-1.87	-1.93
aminolevulinic acid synthase 1	BC022110	-2.00	-2.14	-2.07
potassium inwardly-rectifying channel	NM_008426	-2.30	-2.64	-2.47
Unclassified				
RIKEN cDNA 1110005A23 gene	AV066677	1.74	4.00	2.87
RIKEN cDNA 2900010M23 gene	NM_026063	3.25	1.87	2.56
nucleophosmin 1	AK005498	1.62	3.25	2.44
Mus musculus, clone IMAGE:6398163, mRNA	C88880	2.14	2.46	2.30
RIKEN cDNA 1700008C22 gene	BB650419	2.46	1.87	2.16
Mus musculus, clone IMAGE:5358852, mRNA	BI692833	2.00	2.30	2.15
DNA segment, Chr 9,	BI692686	2.46	1.74	2.10
cDNA sequence AF155546	BC020013	1.87	2.30	2.08
RIKEN cDNA 1110014C03 gene	BI409239	1.52	2.46	1.99
RIKEN cDNA 2610003B19 gene	AK010307	2.30	1.62	1.96
RNA binding motif protein 3	AY052560	2.14	1.74	1.94
expressed sequence AA959893	NM_133837	1.74	2.14	1.94
RIKEN cDNA 1010001M12 gene	AV048277	1.87	2.00	1.93
RIKEN cDNA 2900064A13 gene	NM_133749	2.14	1.62	1.88
RIKEN cDNA 2310020H20 gene	AK009021	1.62	2.14	1.88
RIKEN cDNA 2810403H05 gene	BC008274	1.62	2.00	1.81
RIKEN cDNA 2410015M20 gene	BQ031065	1.87	1.74	1.80
arginine-rich, mutated in early stage tumors	AK014338	1.74	1.87	1.80
RIKEN cDNA 0610006N12 gene	BG968046	1.74	1.87	1.80
function unknown	NM_080837	2.00	1.52	1.76
expressed sequence AL024210	AU046270	2.00	1.52	1.76
RIKEN cDNA 0910001L24 gene	NM_022419	1.52	2.00	1.76
expressed sequence AL024210	AU046270	1.87	1.62	1.75
RIKEN cDNA 1010001M12 gene	AV048277	1.74	1.74	1.74
RIKEN cDNA 2210016L21 gene	BG076998	1.87	1.52	1.69
RIKEN cDNA 3010033P07 gene	BI456571	1.87	1.52	1.69
RIKEN cDNA 2700060E02 gene	NM_026528	1.87	1.52	1.69
RIKEN cDNA 2010003O02 gene	C78790	1.52	1.87	1.69

Gene description	Accession	Exp 1	Exp 2	Average
Unclassified (continued)				
RIKEN cDNA 5730501N20 gene	BM939903	1.74	1.62	1.68
gene rich cluster, C10 gene	NM_013535	1.74	1.62	1.68
enhancer of rudimentary homolog	BB071632	1.74	1.62	1.68
RIKEN cDNA 1810045K17 gene	AK008280	1.74	1.52	1.63
RIKEN full-length enriched library	BB329157	1.74	1.52	1.63
RIKEN cDNA 5330431N19 gene	BQ031101	1.52	1.74	1.63
hypothetical protein LOC215449	BM242378	1.52	1.74	1.63
carcinoma related gene	NM_033562	1.52	1.74	1.63
RIKEN cDNA 9930116P15 gene	BG071611	1.52	1.74	1.63
hypothetical protein 6720481I12	BB610210	1.62	1.62	1.62
RIKEN cDNA 2900010J23 gene	BI144310	1.62	1.62	1.62
RIKEN cDNA 0610012G03 gene	BC021536	1.62	1.62	1.62
small EDRK-rich factor 2	AA271358	1.62	1.62	1.62
proteolipid protein 2	AK012816	1.62	1.62	1.62
small EDRK-rich factor 2	BB704811	1.62	1.52	1.57
RIKEN cDNA 0710007A14 gene	BC011427	1.52	1.62	1.57
RIKEN cDNA 1810020E01 gene	BB667677	1.52	1.62	1.57
RIKEN cDNA 0610007H07 gene	BC027637	1.52	1.62	1.57
RIKEN cDNA 2210021A15 gene	AK011080	1.52	1.62	1.57
hypothetical protein LOC231887	BI408557	1.52	1.62	1.57
nucleophosmin 1	NM_008722	1.52	1.62	1.57
RIKEN cDNA 1110025I09 gene	BC024620	1.52	1.52	1.52
RIKEN cDNA 2310004N24 gene	AK009156	1.52	1.52	1.52
RIKEN cDNA 5730405M06 gene	AW555798	-1.52	1.87	0.18
RIKEN cDNA 4933432B13 gene	BG081523	-1.52	-1.62	-1.57
RIKEN cDNA A030003E17 gene	BM243780	-1.62	-1.52	-1.57
RIKEN cDNA 2010002H18 gene	AW553435	-1.52	-1.74	-1.63
unclassifiable	BB132473	-1.74	-1.62	-1.68
hypothetical protein LOC223435	BB080177	-1.52	-1.87	-1.69
Similar to synaptic nuclei expressed gene 2	BF582734	-1.52	-2.00	-1.76
RIKEN cDNA 6430543G08 gene	BB317849	-1.62	-2.00	-1.81
RIKEN full-length enriched library,	BE956516	-1.87	-1.87	-1.87
ERIKEN cDNA 2810408B13	BB484975	-2.00	-1.74	-1.87
RIKEN cDNA 1110021E09 gene	AK007374	-2.14	-1.62	-1.88
RIKEN cDNA 1200002M06 gene	BC015303	-2.00	-1.87	-1.93
expressed sequence AA407558	AW536361	-1.62	-2.30	-1.96
RIKEN cDNA 2700019D07 gene	BM937429	-2.14	-2.00	-2.07
RIKEN cDNA 1110018N15 gene	BB739221	-1.74	-2.64	-2.19
RIKEN cDNA 2610029D06 gene	BB333454	-2.46	-2.00	-2.23
Secretion				
Yip1 interacting factor homolog (S. cerevisiae)	BC011117	1.52	2.83	2.17
prefoldin 2	NM_011070	1.87	2.00	1.93
peptidase activity	BC008259	1.87	2.00	1.93
signal recognition particle 14 kDa	NM_009273	2.30	1.52	1.91
clathrin, light polypeptide (Lca)	BF140275	1.52	2.14	1.83
DnaJ (Hsp40) homolog, subfamily D, member 1	NM_025384	2.00	1.62	1.81
prefoldin 5	NM_020031	2.00	1.62	1.81
signal sequence receptor, delta	NM_009279	1.62	1.87	1.75
interaction with t-SNAREs 1B homolog	NM_016800	1.74	1.74	1.74
surfeit gene 4	BF122782	1.74	1.74	1.74
endoplasmic reticulum protein 29	AK013303	1.74	1.62	1.68
STIP1 homology and U-Box containing protein 1	NM_019719	1.74	1.62	1.68

Gene description	Accession	Exp 1	Exp 2	Average
Secretion (continued)				
prefoldin 5	NM_020031	1.62	1.62	1.62
signal recognition particle 14 kDa	NM_009273	1.52	1.62	1.57
surfeit gene 4	AW990392	1.52	1.62	1.57
heat shock protein, 1	C77384	-1.87	1.74	-0.06
karyopherin (importin) alpha 1	AV337732	-1.62	-2.14	-1.88
Transcription and splicing				
FBJ osteosarcoma oncogene	AV026617	3.03	2.46	2.75
early growth response 1	NM_007913	2.46	2.00	2.23
amino-terminal enhancer of split	NM_010347	2.30	2.00	2.15
breakpoint cluster region protein 1	NM_011793	2.00	2.14	2.07
small nuclear ribonucleoprotein D2	BQ043840	2.46	1.62	2.04
breakpoint cluster region protein 1	NM_011793	2.14	1.87	2.00
transcription factor-like 4	AF213670	1.74	2.14	1.94
nascent polypeptide-associated complex	NM_013608	2.00	1.87	1.93
v-maf	BC022952	2.14	1.62	1.88
CREBBP/EP300 inhibitory protein 1	BC010712	1.74	2.00	1.87
zinc finger, HIT domain containing 1	BC026751	1.74	2.00	1.87
Sin3-associated polypeptide 18	BG085340	1.74	2.00	1.87
Sin3-associated polypeptide 18	BC006625	1.87	1.87	1.87
general transcription factor III A	AV173739	1.87	1.87	1.87
U2af1-rs1 region 1	AB076722	2.00	1.62	1.81
ocular development associated gene	BC019449	2.00	1.62	1.81
endothelial differentiation-related factor 1	AB030185	1.87	1.74	1.80
RNA polymerase	BC024419	2.00	1.52	1.76
CREBBP/EP300 inhibitory protein 1	NM_025613	2.00	1.52	1.76
transcription elongation factor B (SIII)	AK019181	2.00	1.52	1.76
RNA polymerase 1-3 (16 kDa subunit)	NM_009087	1.87	1.62	1.75
mediator of RNA polymerase II transcription	NM_026068	1.74	1.74	1.74
high mobility group box 1	NM_010439	1.74	1.74	1.74
eukaryotic translation elongation factor 2	BC007152	1.52	1.87	1.69
COP9 homolog	BE853265	1.74	1.52	1.63
U6 snRNA-associated SM-like protein 4	NM_015816	1.62	1.62	1.62
Dr1 associated protein 1	BC002090	1.62	1.52	1.57
Sin3-associated polypeptide 18	AV023865	1.52	1.62	1.57
small nuclear ribonucleoprotein D1	NM_009226	1.52	1.52	1.52
splicing factor, arginine/serine rich 9 (25 kDa)	NM_025573	1.52	1.52	1.52
suppressor of Ty 4 homolog 2 (S. cerevisiae)	NM_011509	1.52	1.52	1.52
tripartite motif protein 33	BE915274	-1.74	-1.74	-1.74
zinc finger protein 397	BC021456	-1.62	-2.00	-1.81
interferon-related developmental regulator 1	NM_013562	-1.62	-2.00	-1.81
DEAD/H box polypeptide 20	NM_017397	-1.74	-2.00	-1.87
zinc finger protein 113	NM_019747	-1.74	-2.14	-1.94
deltex 2 homolog (Drosophila)	BB518874	-2.00	-2.14	-2.07
core promoter element binding protein	AV025472	-2.30	-2.00	-2.15
Notch gene homolog 1, (Drosophila)	BE952133	-1.74	-2.64	-2.19
inhibitor of DNA binding 3	NM_008321	-2.00	-2.46	-2.23
core promoter element binding protein	BG800611	-2.83	-1.87	-2.35
zinc finger protein 93	NM_009567	-2.46	-2.30	-2.38
zinc finger protein 54	NM_011760	-2.14	-2.83	-2.49

Gene description	Accession	Exp 1	Exp 2	Average
Transcription and splicing (continued)				
zinc finger protein BC027407	BC023090	-3.03	-2.14	-2.59
zinc finger protein 51	BC011183	-3.25	-2.14	-2.70
Jun oncogene	NM_010591	-2.64	-2.83	-2.73
activating transcription factor 4	M94087	-2.83	-3.03	-2.93
activating transcription factor 4	AV314773	-2.64	-3.73	-3.19
DNA-damage inducible transcript 3	NM_007837	-3.48	-4.00	-3.74
feminization 1 homolog b (C. elegans)	NM_010193	-2.30	-5.66	-3.98
Jun oncogene	BC002081	-3.73	-4.92	-4.33
Protein Degradation				
proteasome 26S subunit, non-ATPase, 13	NM_011875	1.52	2.30	1.91
ubiquitin-conjugating enzyme E2N	AY039837	1.87	1.87	1.87
ubiquitin-conjugating enzyme E2S	NM_133777	1.52	2.14	1.83
proteasome 26S subunit, non-ATPase, 8	AK003436	1.87	1.62	1.75
proteasome maturation factor domain	NM_025624	1.62	1.87	1.75
(ubiquitin thiolesterase)	AB033370	1.62	1.74	1.68
proteasome 28 subunit, beta	NM_011190	1.74	1.52	1.63
ubiquitin-conjugating enzyme E2D 2	NM_019912	1.62	1.52	1.57
ubiquitin-conjugating enzyme E2B, homology	AK010432	1.52	1.62	1.57
ubiquitin conjugating enzyme interacting protein 5	BM244352	-1.74	-1.87	-1.80
ubiquilin 2	NM_018798	-1.87	-2.14	-2.00

Figure 5.6: Functional classification of polysomal mRNAs whose levels changed by more than 2-fold or more than 1.5 fold in response to glucose stimulation for 1 hour

Polysomal mRNAs whose levels changed by more than 2 fold or more than 1.5 fold were functionally classified using NCBI databases (www.ncbi.nlm.nih.gov) according to known cellular functions or sequence similarity to genes of known functions. The proportional representation of each classification group was plotted on a pie chart. The numbers of genes that increased or decreased are displayed with the functional group labels.

a) 2-fold (39 genes)

Apoptosis, repair, DNA synthesis; 1 down

Cell signalling; 4 up, 3 down

Cytoskeletal; 1 up, 0 down

Translation; 1 up

Transcription and splicing; 4 up, 13 down

Metabolism and mitochondria; 6 up, 2 down

Unclassified; 2 up, 2 down

b) 1.5 fold (322 genes)

Protein degradation; 9 up, 2 down

Apoptosis, repair, DNA synthesis; 2 up, 9 down

Transcription and splicing; 31 up, 20 down

Cell signalling; 29 up, 8 down

Cytoskeletal; 10 up, 0 down

Secretion and protein folding; 15 up, 2 down

Translation; 44 up, 0 down

Unclassified; 53 up, 15 down

Metabolism and mitochondria; 70 up, 6 down

233

5.3.4: Analysis of Microarrays using dChip

Quality Control

The cell files were read into dChip and opened to show the image of the scanned probe array. Inspection of the images confirmed the absence of any marks that would have indicated hybridisation inefficiencies (figure 5.7).

After the cells files were read into dChip, the array summary file was generated to check the quality of the hybridisation and the comparability of the replicate experiments. The percentage of genes present was similar between all four arrays, confirming that the replicates were comparable (table 5.5).

To further check hybridisation efficiencies and control the quality of the data, dchip cross-referenced each array with the other arrays to identify any problematic array outliers (probe sets whose pattern is different to the consensus pattern of most other arrays). The % of array outliers in each array were provided in the array summary file. In these experiments all of the array outlier values were well below 5%, confirming that the quality of both the arrays in experiment 1 and 2 were good, and therefore the data was reliable (table 5.5).

Normalisation

The array summary file also contained the median probe intensity for each array, which determines the need for normalisation (table 5.5). Because, the median intensities were relatively different, especially between the two experiments, normalisation was necessary. Each array was normalised to the array with the median overall intensity (experiment 2, 20mM).

Normalisation plots of the normalisation array (experiment 2, 20mM glucose) against the other arrays were plotted before and after normalisation using R software. R software plotted the invariant probe sets in red and all other probe sets in black. The running median normalisation curves were calculated and plotted in green, while y=x was plotted in blue. Before normalisation of the arrays to the baseline array, (experiment 2, 20mM) the running median normalisation curve and y=x were far apart, showing that one array is

a) Experiment 1

0.5mM glucose 20mM glucose

b) Experiment 2

0.5mM glucose 20mM glucose

Figure 5.7: Image of scanned arrays in dChip
To check for any hybridisation problems, the scanned arrays were displayed
with dChip.

Array	Present call %	% Array outlier	Median Intensity (unnormalised)
Exp1 0.5	58.2	0.405	78
Exp1 20	60.1	0.524	75
Exp2 0.5	43.7	0.961	161
Exp2 20	62.3	0.185	85

Table 5.5: Quality control data generated by dChip

The array summary file was generated by dChip. Identity of columns from left to right: array (experiment 1 or 2, 0.5mM glucose or 20mM glucose), % of probe sets that were present, % of probe sets that were outliers (i.e. did not conform to the consensus probe set pattern across the other arrays), median intensity of the unnormalised arrays.

brighter than the other and therefore requires normalisation (figure 5.8). After normalisation, the running median normalisation curves and y=x largely overlap, showing that the overall brightness of the arrays are similar.

Identification of genes regulated by glucose using dChip data analysis

To identify glucose-regulated genes, comparison analysis was performed by the combined comparison method. In this way, dChip found the mean intensity for each probe set between the two experiments at low glucose and the mean intensity for each probe set between the two experiments at high glucose concentrations and then calculated the mean fold change between low and high glucose. Probe sets showing changes in levels of polysomal mRNAs were selected by the following criteria: 1) probe sets with a difference of less than 100 between the 0.5mM glucose and 20mM glucose arrays were excluded and 2) a threshold was set of more than a 1.5 fold or 2 fold change in levels of polysomal mRNAs. To increase the stringency of the analysis, a fold change of 1.5 fold or 2 fold was only included if the 90% confidence intervals were also within these boundaries.

Using the stringent criteria, dChip identified 76 and 16 glucose-responsive genes whose polysomal mRNA levels changed by more than 1.5 fold or 2 fold respectively. The list of polysomal mRNAs that are increased or decreased more than 2 fold or 1.5 fold by glucose stimulation are listed along with their Genbank accession numbers in table 5.6 and 5.7.

Glucose responsive genes whose polysomal mRNA levels increased 1.5 fold or more or 2 fold or more in dChip were functionally classified according to known cellular functions or sequence similarity to genes of known functions using NCBI databases (figure 5.9). Like the MAS5 analysis, more than 50% of probe sets that glucose stimulated a 2 fold or more change in polysomal mRNA were important in transcription or metabolism (figure 5.9). Transcription and metabolism were also the two largest functional groups that glucose stimulated more than a 1.5 fold change in levels of polysomal mRNA. As with MAS5 analysis, a large majority (78%) of polysomal mRNAs important in metabolism increased in response to an increase in high glucose concentration and only 22% of polysomal mRNAs important in metabolism decreased in response to an increase in high glucose concentration. However, a smaller proportion

Figure 5.8: Normalisation plots of polysomal mRNA levels
All arrays were normalised to the array with the overall median intensity, (experiment 2, 20mM) glucose. The intensity values of each probe set for experiment 2, 20mM (y-axis) were plotted against the intensity value for each normalised or unnormalised probe set for experiment 1, 0.5mM (a) or experiment 1, 20mM (b) or experiment 2, 0.5mM (c) (x-axis). Probes in the invariant set were plotted in red, the running median normalisation curve in green and y=x in blue.

a) Normalisation of experiment 1, 0.5mM glucose array
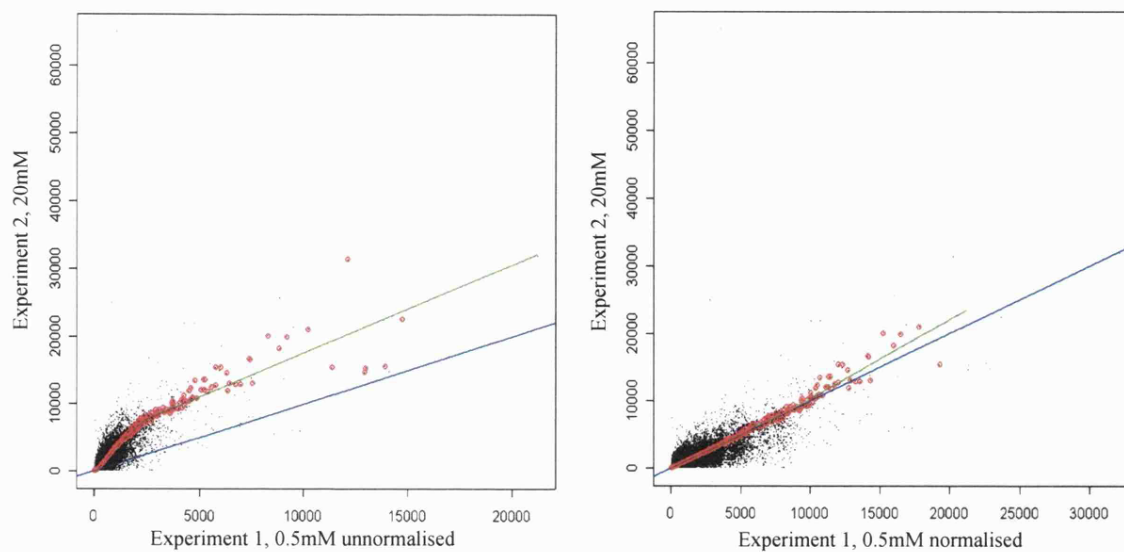
b) Normalisation of experiment 1, 20mM glucose array
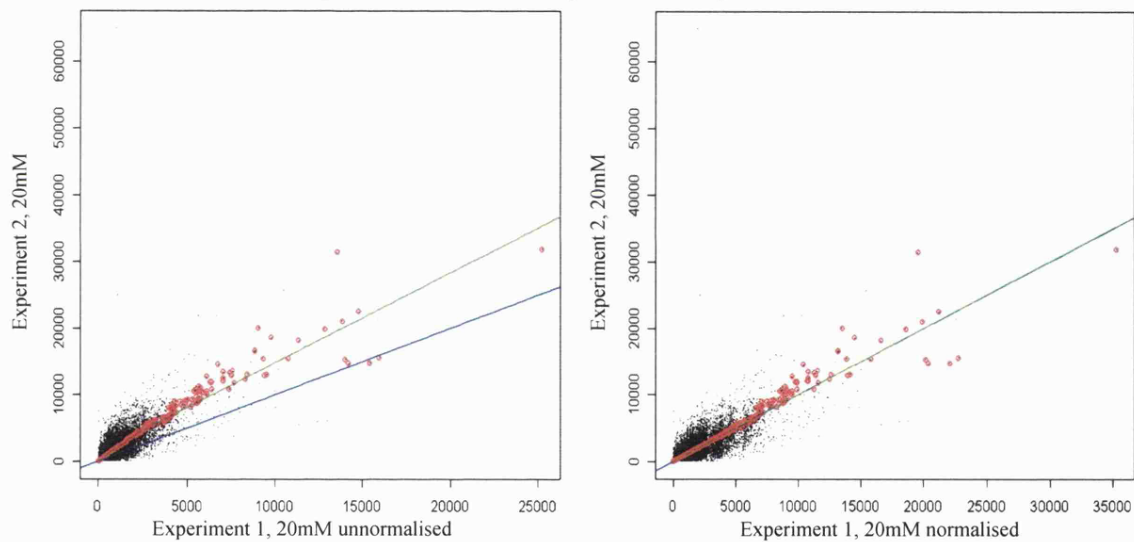
c) Normalisation of experiment 2, 0.5mM glucose array
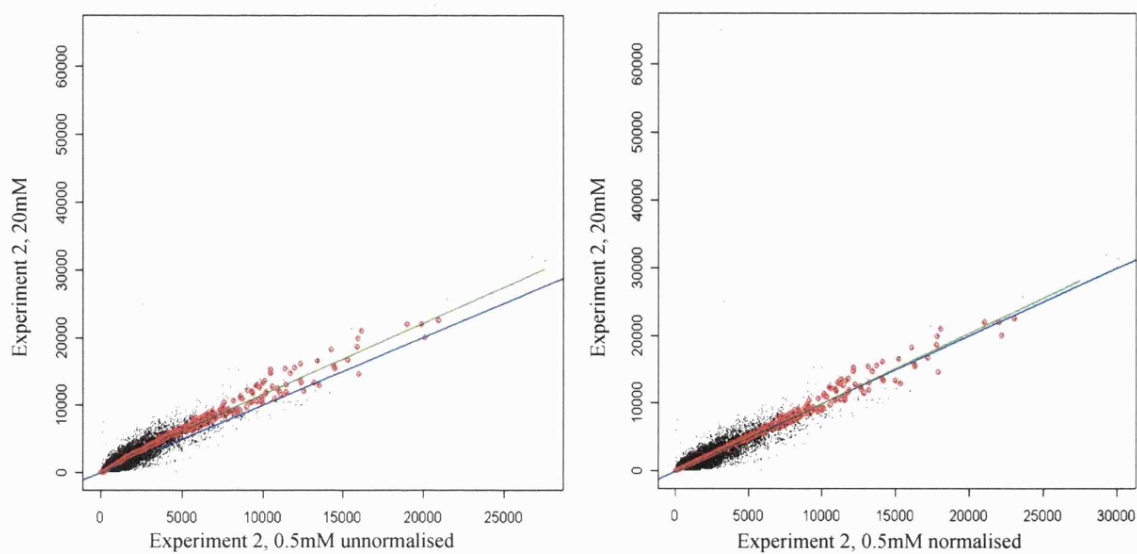
gene	Accession	0.5 mean	0.5 SE	20 mean	20 SE	fold
Cell signalling						
regulator of G-protein signaling 16	U94828	7.69	14.99	107.87	29.35	14.02
protein phosphatase 3, catalytic subunit	BE825122	56.88	10.16	169.14	18.19	2.97
Cd27 binding protein	AF033112	102.66	13.9	296.55	30.82	2.89
Cytoskeletal						
tubulin cofactor a	BB559082	124.08	21.17	331.38	26.03	2.67
Metabolism and mitochondria						
aquaporin 3	AF104416	-80.76	20.31	73.81	14.32	73.81
thioredoxin 2	NM_019913	16.7	20.07	128.84	26.78	7.71
cDNA sequence BC003494	BC018194	61.77	13.67	217.38	10.24	3.52
DNA segment	AK004219	71.91	13.11	200.5	9.8	2.79
sodium channel, nonvoltage-gated 1	NM_011326	153.33	44.6	19.81	18.25	-7.74
Unclassified						
testis specific X-linked gene	NM_009440	206.64	65.11	30.79	9.01	-6.71
Secretion/protein folding						
ubiquitously expressed transcript	NM_013840	90.21	10.87	252.22	31.14	2.8
surfeit gene 4	AV311750	61.61	12.5	168.86	4.95	2.74
Transcription and splicing						
FBJ osteosarcoma oncogene	AV026617	54.84	8.08	271.57	44.97	4.95
activating transcription factor 4	AV314773	1552.38	108.89	503.52	21.72	-3.08
Jun oncogene	NM_010591	775.76	57.06	222.15	18.04	-3.49
Jun oncogene	BC002081	972.77	106.72	211.26	22.73	-4.6

Table 5.6: List of polysomal mRNAs whose levels changed by more than 2-fold in response to glucose stimulation (dChip)

Polysomal mRNAs whose levels were shown to increase or decrease by more than 2 fold in response to 1 hour glucose stimulation are listed. Identity of columns from left to right: gene name, Genbank accession number; mean intensity of experiment 1 and experiment 2 at 0.5mM glucose as calculated by dChip, standard error of the mean intensity at 0.5mM glucose, mean intensity of experiment 1 and experiment 2 at 20mM glucose as calculated by dChip, standard error of the mean intensity at 20mM glucose, fold change between the mean intensity at high glucose vs low glucose.

gene	Accession	0.5 mean	0.5 SE	20 mean	20 SE	fold
Apoptosis, repair, DNA synthesis						
apoptosis-associated speck-like protein	NM_023258	81.38	7.76	191.4	14.01	2.35
origin recognition complex, subunit 6	NM_019716	134.07	15.5	253.09	17.49	1.89
Cell signalling						
regulator of G-protein signaling 16	U94828	7.69	14.99	107.87	29.35	14
Cd27 binding protein	NM_013929	21.18	25.64	131.33	26.13	6.2
calpactin	NM_009112	112.58	34.41	365.03	103.3	3.24
protein phosphatase 3	BE825122	56.88	10.16	169.14	18.19	2.97
Cd27 binding protein	AF033112	102.66	13.9	296.55	30.82	2.89
nephronophthisis 1 (juvenile) homolog	NM_016902	97.32	21.11	225.38	25.63	2.32
tumor necrosis factor receptor	BF580567	116.55	13.48	221.25	18.34	1.9
diazepam binding inhibitor	AV007315	221.06	16.75	399.18	32.23	1.81
interleukin 17	NM_010552	813.23	29.1	438.46	9.96	-1.9
CDC-like kinase	U21209	420.82	22.12	215.75	34.75	-2
insulin-like growth factor binding protein	NM_008340	257.64	30.68	126.51	15	-2
discs, large homolog 4 (Drosophila)	BC014807	198.51	21.37	81.1	14.02	-2.5
pleckstrin homology domainfamily A	BC021387	225.1	96.97	39.74	10.99	-5.7
Cytoskeletal						
tubulin cofactor a	BB559082	124.08	21.17	331.38	26.03	2.67
Translation						
ligatin	BC025036	104.27	13.76	235.49	38.01	2.26
EIF-5 homolog [Rattus norvegicus]	BQ176989	1537.42	205.7	774.29	54.1	-2
Metabolism and mitochondria						
aquaporin 3	AF104416	-80.76	20.31	73.81	14.32	73.8
thioredoxin 2	NM_019913	16.7	20.07	128.84	26.78	7.71
cDNA sequence BC003494	BC018194	61.77	13.67	217.38	10.24	3.52
S-adenosylmethionine decarboxylase 1	NM_009665	62.1	24.15	210.27	41.15	3.39
thioredoxin interacting protein	NM_023719	326.76	57.52	1087.67	270.1	3.33
thioredoxin-like 5	AK004219	71.91	13.11	200.5	9.8	2.79
mitochondrial ribosomal protein S18C	AK004139	137.45	29.27	329.09	55.28	2.39
peroxiredoxin 1	AI120393	137.48	22.16	323.89	11.26	2.36
translocator mitochondrial membrane	AF106620	128.07	18.33	287.52	33.24	2.25
protein O-fucosyltransferase 2	BB699319	141.82	17.88	305.89	18.16	2.16
RIKEN cDNA 5730591C18 gene	AK003189	123.45	22.13	259.61	21	2.1
mitochondrial carrier homolog 1	AF192558	373.41	42.14	768.39	74.69	2.06
mitochondrial ribosomal protein L51	BC021535	354.64	29.98	715.65	83.32	2.02
phosphomannomutase 1	BC006809	123.29	16.76	244.09	11.9	1.98
prostaglandin I2 (prostacyclin) synthase	NM_008968	810.84	118.2	383.52	37.31	-2.1
nicotinamide N-methyltransferase	AK006371	223.72	30.44	92.08	12.77	-2.4
solute carrier family 9	BF468098	186.22	26.68	66.03	24.73	-2.8
sodium channel, nonvoltage-gated	NM_011326	153.33	44.6	19.81	18.25	-7.7

Table 5.7: List of polysomal mRNAs whose levels changed by more than 1.5-fold in response to glucose stimulation (dChip)

Polysomal mRNAs whose levels were shown to increase or decrease by more than 1.5 fold in response to 1 hour glucose stimulation are listed. Identity of columns from left to right: gene name, Genbank accession number; mean intensity of experiment 1 and experiment 2 at 0.5mM glucose as calculated by dChip, standard error of the mean intensity at 0.5mM glucose, mean intensity of experiment 1 and experiment 2 at 20mM glucose as calculated by dChip, standard error of the mean intensity at 20mM glucose, fold change between the mean intensity at high glucose vs low glucose. (continued over page)

gene	Accession	0.5 mean	0.5 SE	20 mean	20 SE	fold
Unknown function or miscellaneous						
DNA segment, Chr 9	BI692686	76.38	27.27	237.66	35.84	3.11
RIKEN cDNA 5730536A07 gene	NM_026635	55.69	26.4	161.44	18.04	2.9
RIKEN cDNA 2810405K02 gene	AI836168	57.01	19.28	158.25	26.88	2.78
RIKEN cDNA 1700008C22 gene	BB650419	103.49	21.09	283.31	35.03	2.74
RIKEN cDNA 2010003O02 gene	C78790	160.7	40.41	367.63	29.03	2.29
RIKEN cDNA 1110019N10 gene	BF535957	105.49	12.62	233.1	23.02	2.21
RIKEN cDNA 2900010M23 gene	NM_026063	515.83	79.18	1130.16	92.01	2.19
RIKEN cDNA 2210016L21 gene	BG076998	165.94	17.17	344.3	29.6	2.07
RIKEN cDNA 9930116P15 gene	BG071611	119.95	7.06	243.52	30.9	2.03
LIM only 6	AV166926	332.29	14.6	665.23	18.43	2
hypothetical protein DKFZp434P0531	AV032559	165.15	19.38	316.53	17.6	1.92
RIKEN cDNA 1110025I09 gene	BC024620	148.94	11.7	263.17	16.41	1.77
Tal1 interrupting locus	BC004585	378.88	75.13	141.44	14.45	-2.7
testis specific X-linked gene	NM_009440	206.64	65.11	30.79	9.01	-6.7
Protein folding and secretion						
ubiquitously expressed transcript	NM_013840	90.21	10.87	252.22	31.14	2.8
RIKEN cDNA 2210409M21 gene	BF318739	93.58	18.93	207.36	24.33	2.22
vesicular membrain protein p24	NM_009513	75.23	9.16	180.08	29.36	2.39
clathrin, light polypeptide (Lcb)	BQ173953	61.7	25.81	179.74	6.88	2.91
surfeit gene 4	AV311750	61.61	12.5	168.86	4.95	2.74
prefoldin 2	NM_011070	302.57	24.29	647.74	80.3	2.14
endoplasmic reticulum protein 29	AK013303	144.18	25.31	306.14	28.84	2.12
sec11-like 3 (S. Cerevisea)	AK007641	106.78	17.89	219.28	18.68	2.05
Transcription and splicing						
FBJ osteosarcoma oncogene	AV026617	54.84	8.08	271.57	44.97	4.95
polymerase (RNA) II (DNA directed)	BC002306	71.48	10.99	216.4	53.93	3.03
Dr1 associated protein 1	BC002090	76.46	14.56	207.26	17.34	2.71
Sin3-associated polypeptide 18	BC006625	86.67	17.04	221.9	25.08	2.56
breakpoint cluster region protein 1	NM_011793	126.36	22.45	319.82	51.91	2.53
CREBBP/EP300 inhibitory protein 1	NM_025613	90.47	22.85	228.35	43.7	2.52
early growth response 1	NM_007913	434.98	62.66	1045.98	150.6	2.4
breakpoint cluster region protein 1	NM_011793	156.48	28.39	340.27	46.65	2.17
splicing factor, arginine/serine-rich 3	BB470806	111.78	6.38	219.32	6.2	1.96
RNA polymerase 1-3 (16 kDa subunit)	NM_009087	297.24	29.95	534.55	29.57	1.8
flap structure specific endonuclease 1	BB393998	1800.18	45.34	1050.03	38.33	-1.7
enhancer of polycomb homolog 1	NM_007935	721.26	54.47	381.41	26.1	-1.9
Treacher Collins Franceschetti syndrome	AW209012	187.19	5.99	85.56	9.46	-2.2
apolipoprotein B editing complex 1	BC003792	508.23	93.52	212.5	36.22	-2.4
activating transcription factor 4	AV314773	1552.38	108.9	503.52	21.72	-3.1
DNA-damage inducible transcript 3	NM_007837	1938.95	452.2	566.99	142.3	-3.4
Jun oncogene	NM_010591	775.76	57.06	222.15	18.04	-3.5
Jun oncogene	BC002081	972.77	106.7	211.26	22.73	-4.6

Table 5.7 (cont): List of polysomal mRNAs whose levels changed by more than 1.5-fold in response to glucose stimulation (dChip)

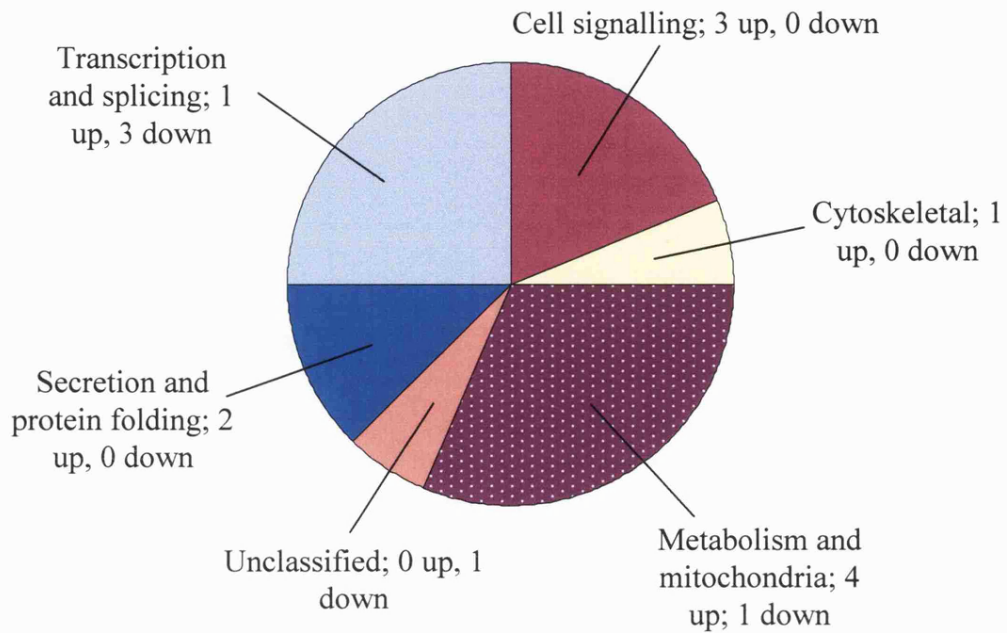**Figure 5.9: Functional classification of polysomal mRNAs whose levels changed by more than 2-fold or more than 1.5 fold in response to glucose stimulation (dChip)**
Polysomal mRNAs which dChip identified as changing by more than 2 fold or more than 1.5 fold were functionally classified using NCBI databases (www.ncbi.nlm.nih.gov) according to known cellular functions or sequence similarity to genes of known functions. The proportional representation of each classification group was plotted on a pie chart. The numbers of genes that increased or decreased are displayed with the functional group labels.

a) 2-fold (16 genes)

Cell signalling; 3 up, 0 down

Transcription and splicing; 1 up, 3 down

Cytoskeletal; 1 up, 0 down

Secretion and protein folding; 2 up, 0 down

Unclassified; 0 up, 1 down

Metabolism and mitochondria; 4 up; 1 down

b) 1.5 fold (76 genes)

Apoptosis, repair, DNA synthesis; 2 up. 0 down

Cell signalling; 8 up, 5 down

Transcription and splicing; 10 up, 8 down

Cytoskeletal; 1 up, 0 down

Translation; 1 up, 1 down

Secretion and protein folding; 8 up, 0 down

Metabolism and mitochondria; 14 up, 4 down

Unclassified; 12 up, 2 down

244

(56%) of polysomal mRNAs important in transcription increased in response to an increase in high glucose concentration.

5.3.5: Genes identified by both MAS5 and dChip

Polysomal mRNAs that were found to change between low and high glucose using both MAS5 and dChip analysis methods were selected using Excel. If both analysis programs identify a specific polysomal mRNA as glucose-regulated, the probability of it being a true positive is increased. 39 polysomal mRNAs changed more than 1.5 fold in both dChip and MAS5 (table 5.8); while only 6 polysomal mRNAs were found to change more than 2 fold in both MAS5 and dChip (table 5.9). The majority of polysomal mRNAs whose levels changed more than 1.5 fold in response to glucose were important in metabolism or transcription, while all polysomal mRNAs that were stimulated by glucose by more than 2 fold were involved in transcription or metabolism.

5.3.6: Confirmation of Microarray Results by Northern Blot Analysis

All of the polysomal mRNAs that changed by 2 fold or more in both MAS5 and dChip in response to increases in glucose concentration were important in metabolism or transcription, suggesting that the acute regulation of metabolism and transcription may be important for the β-cell to maintain the correct response to changes in glucose concentration. To confirm changes observed in the microarray analysis, changes in specific mRNAs were further investigated by Northern blot analysis of the polysomal and non-polysomal fractions. Furthermore, to determine if the change in amount of polysomal mRNA was due to an increase in total mRNA levels (most likely through an increase in transcription or mRNA stability), Northern blot analysis was performed on total RNA isolated from MIN6 cells incubated in low or high glucose.

Transcription Factors

Four out of the six probe sets that changed more than 2 fold in response to glucose in both dChip and MAS5 were important in transcription (table 5.7). Out of these, three were probe sets for the immediate early-response genes, c-jun and FBJ osteosarcoma oncogene (c-fos). Previous work has shown that glucose has no effect on the mRNA levels of c-jun or c-fos in INS-1 cells incubated in 3mM or 15mM glucose (Susini et al.,
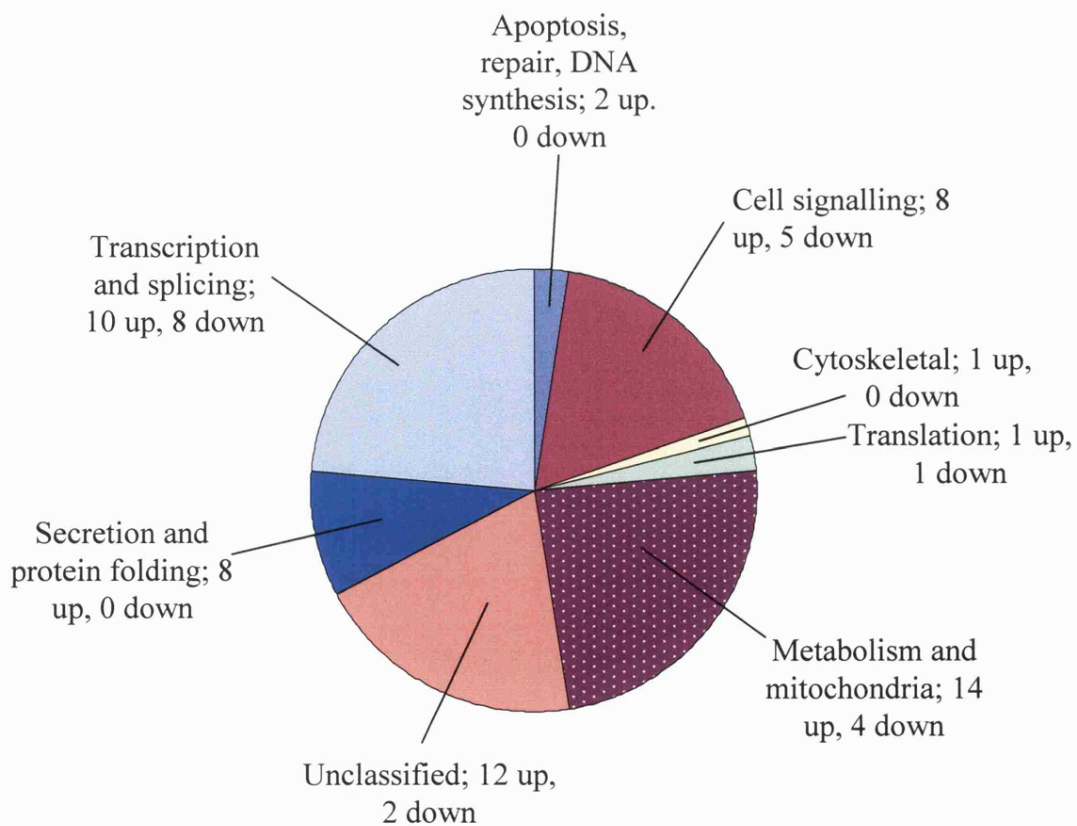
Table 5.8: List of polysomal mRNAs whose levels changed by more than 1.5-fold in response to glucose stimulation using dChip and MAS5

Polysomal mRNAs whose levels were shown to increase or decrease by more than 1.5 fold in response to 1 hour glucose stimulation in both dChip and MAS5 are listed. Identity of columns from left to right: gene name, Genbank accession number; mean fold change between experiment 1 and 2 as calculated by dChip, mean fold change between experiment 1 and 2 as calculated by MAS5.

gene	Accession	dchip	MAS5
Cell Signalling			
Cd27 binding protein (Hindu God of destruction)	NM_013929	6.2	7.78
S100 calcium binding protein A10 (calpactin)	NM_009112	3.24	2.07
Cd27 binding protein (Hindu God of destruction)	AF033112	2.89	1.76
nephronophthisis 1 (juvenile) homolog (human)	NM_016902	2.32	1.62
CDC-like kinase	U21209	-1.95	-2.02
Cytoskeletal			
tubulin cofactor a	BB559082	2.67	1.69
Translation			
ligatin	BC025036	2.26	1.51
Metabolism			
thioredoxin 2	NM_019913	7.71	8.31
cDNA sequence BC003494	BC018194	3.52	2.30
S-adenosylmethionine decarboxylase 1	NM_009665	3.39	2.15
thioredoxin interacting protein	NM_023719	3.33	3.78
mitochondrial ribosomal protein S18C	AK004139	2.39	2.07
translocator of inner mitochondrial membrane 17 kDa,	AF106620	2.25	1.80
protein O-fucosyltransferase 2	BB699319	2.16	1.74
mitochondrial carrier homolog 1	AF192558	2.06	2.00
mitochondrial ribosomal protein L51	BC021535	2.02	1.68
phosphomannomutase 1	BC006809	1.98	1.75
Miscellaneous			
DNA segment, Chr 9,	BI692686	3.11	2.10
RIKEN cDNA 1700008C22 gene	BB650419	2.74	2.16
RIKEN cDNA 2900010M23 gene	NM_026063	2.19	2.56
RIKEN cDNA 2210016L21 gene	BG076998	2.07	1.69
RIKEN cDNA 9930116P15 gene	BG071611	2.03	1.63
RIKEN cDNA 1110025I09 gene	BC024620	1.77	1.52
Secretion and protein folding			
ubiquitously expressed transcript	NM_013840	2.8	1.78
prefoldin 2	NM_011070	2.14	1.93
endoplasmic reticulum protein 29	AK013303	2.12	1.68
Transcription			
FBJ osteosarcoma oncogene	AV026617	4.95	2.75
polymerase (RNA) II (DNA directed) polypeptide H	BC002306	3.03	1.76
Dr1 associated protein 1 (negative cofactor 2 alpha)	BC002090	2.71	1.57
Sin3-associated polypeptide 18	BC006625	2.56	1.87
breakpoint cluster region protein 1	NM_011793	2.53	2.07
CREBBP/EP300 inhibitory protein 1	NM_025613	2.52	1.76
early growth response 1	NM_007913	2.4	2.23
breakpoint cluster region protein 1	NM_011793	2.17	2.00
RNA polymerase 1-3 (16 kDa subunit)	NM_009087	1.8	1.75
activating transcription factor 4	AV314773	-3.08	-3.19
DNA-damage inducible transcript 3	NM_007837	-3.42	-3.74
Jun oncogene	NM_010591	-3.49	-2.73
Jun oncogene	BC002081	-4.6	-4.33

Gene	Accession	dChip	MAS5
metabolism			
thioredoxin 2	NM_019913	7.71	8.31
cDNA sequence BC003494	BC018194	3.52	2.30
transcription			
FBJ osteosarcoma oncogene	AV026617	4.95	2.75
activating transcription factor 4	AV314773	-3.08	-3.19
Jun oncogene	NM_010591	-3.49	-2.73
Jun oncogene	BC002081	-4.6	-4.33

Table 5.9: List of polysomal mRNAs whose levels changed by more than 2-fold in response to glucose stimulation using dChip and MAS5

Polysomal mRNAs whose levels were shown to increase or decrease by more than 2 fold in response to 1 hour glucose stimulation in both dChip and MAS5 are listed. Identity of columns from left to right: gene name, Genbank accession number; mean fold change between experiment 1 and 2 as calculated by dChip, mean fold change between experiment 1 and 2 as calculated by MAS5.

1998). However, in the presence of a cAMP analog, glucose did stimulate the mRNA levels of c-jun and c-fos by 2 fold. (Susini et al., 1998). The microarray data here shows that while glucose stimulated an increase in the amount of polysomal c-fos mRNA, glucose inhibited the amount of polysomal c-jun mRNA by more than 3.5-fold (table 5.8). Microarray analysis also showed that the levels of polysomal mRNA encoding activating transcription factor 4 (ATF4) decreased more than 3-fold at high glucose concentrations. ATF4 has previously been shown to be regulated at the level of translation and transcription (Lu et al., 2004a; Scheuner et al., 2001; Vattem and Wek, 2004).

To confirm the microarray data that high glucose concentrations inhibited the amount of polysomal mRNAs encoding c-jun and ATF4, Northern blot analysis was carried out on polysomal and non-polysomal mRNA isolated from MIN6 cells that had been incubated in 0.5mM or 20mM glucose for one hour. In agreement with the microarray results, glucose stimulated a decrease in the amount of polysomal mRNAs encoding ATF4 and c-jun (figure 5.10a). These changes were not accompanied by glucose-stimulated increases in the non-polysomal fractions at high glucose, suggesting that these changes may be due to changes in the mRNA levels and not changes in the translation efficiency.

To confirm that the glucose-stimulated decrease in polysomal mRNA encoding c-jun and ATF4 were due to changes in total mRNA levels, Northern blot analysis for c-jun and ATF4 mRNA was carried out on total RNA isolated from MIN6 cells that were incubated for one hour in KRB supplemented with 0.5mM or 20mM glucose. Interestingly, Northern blot analysis confirmed the microarray data and showed that an increase in glucose concentration resulted in a 1.94-fold decrease in c-jun mRNA levels and a 1.32 fold decrease in ATF4 mRNA levels (figure 5.10b). This suggests that the synthesis of these proteins is most likely regulated at the level of transcription or mRNA stability.

It has been shown that ATF4 is translationally regulated under conditions of eIF2α phosphorylation and that low glucose concentrations induce eIF2α phosphorylation in MIN6 cells (Gomez et al., 2004; Lu et al., 2004a; Vattem and Wek, 2004). Therefore, to determine whether ATF4 was recruited into the polysome fractions at low glucose,

249

Figure 5.10: Analysis of mRNAs encoding proteins important in the regulation of transcription

a) MIN6 cells were incubated in KRB containing 0.5mM glucose for one hour and then incubated for a further hour in KRB containing 0.5mM glucose or 20mM glucose. RNA was purified by harvesting the cells in Tri-reagent. Purified R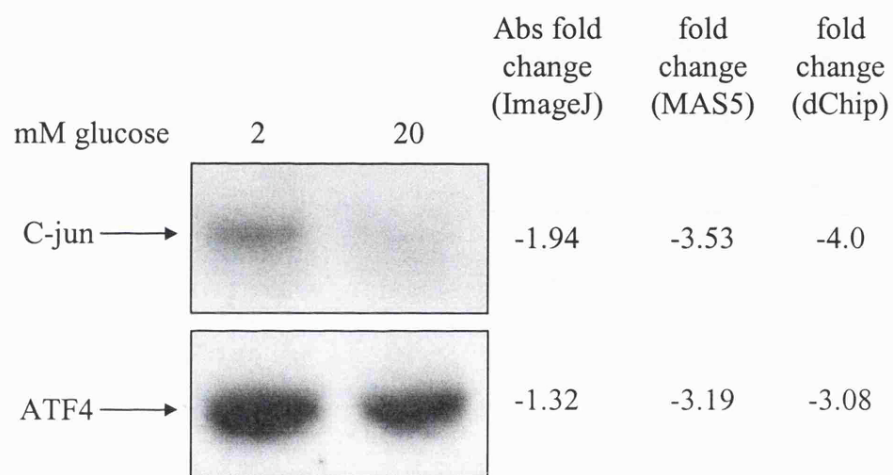NA was then run on a 1% agarose formaldehyde gel, transferred onto nylon membrane and probed for specific mRNAs as shown. The fold changes observed in the Northern blot between low and high glucose concentrations were quantified with ImageJ (fold change, ImageJ). The average fold change in MAS5 over the two experiments is also shown (fold change, MAS5). b) MIN6 cells were pre-incubated in KRB containing 0.5mM glucose for 1h followed by incubation in KRB containing 0.5mM or 20mM glucose for a further hour. 0.1mg/ml (final concentration) of cycloheximide was added to the cells 10 minutes prior to lysis to prevent ribosomal run-off. Cells were lysed and the lysates layered onto 7 - 47% sucrose gradients. The gradients were then centrifuged at 39000rpm at 4°C for 2h and fractionated from top to bottom using the ISCO gradient fractionator. The polysomal and non-polysomal fractions were pooled as shown in figure 3.2 and were run on a 1% agarose formaldehyde gel, transferred onto nylon membrane and probed for specific mRNAs as shown. The fold changes observed in the Northern blot between the amounts of polysomal mRNA at low and high glucose concentrations were quantified with ImageJ (fold change, ImageJ). The average fold change in MAS5 over the two experiments is also shown (fold change, MAS5). c) MIN6 cells were pre-incubated in KRB containing 0.5mM glucose for 1h followed by incubation in KRB containing 0.5mM or 20mM glucose for a further hour. 0.1mg/ml (final concentration) of cycloheximide was added to the cells 10 minutes prior to lysis to prevent ribosomal run-off. Cells were lysed and the lysates layered onto 7 - 47% sucrose gradients. The gradients were then centrifuged at 39000rpm at 4°C for 2h and fractionated from top (fraction 1) to bottom (fraction 20) using the ISCO gradient fractionator. Absorbance of the gradients was measured continually at 254nm to give polysome profiles. RNA was isolated from 20, 1ml fractions, run on a 1% agarose formaldehyde gel, transferred to nylon membrane and probed for specific mRNAs as shown. Abbreviations: ATF4: activating transcription factor 4. These results are representative of two separate experiments.

a)

		Non-polysomal		Polysomal		Abs fold change (ImageJ)	fold change (MAS5)	fold change (dChip)
mM glucose		2	20	2	20			
c-jun						-1.56	-3.53	-3.53
ATF4						-2.9	-3.19	-3.19

b)

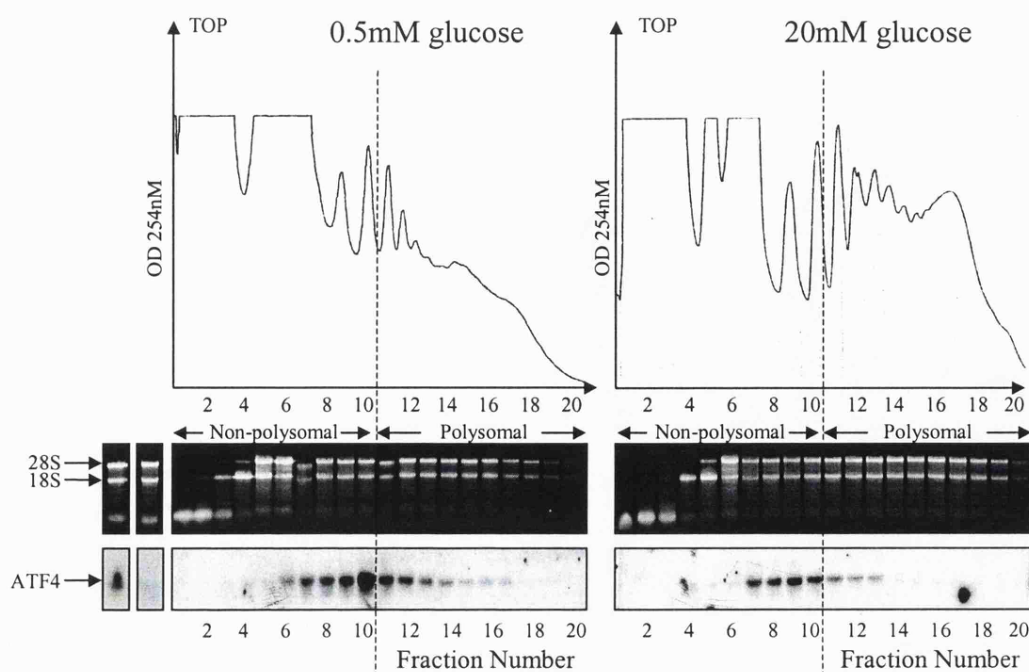|			Abs fold change (ImageJ)	fold change (MAS5)	fold change (dChip)
mM glucose	2	20			
C-jun			-1.94	-3.53	-4.0
ATF4			-1.32	-3.19	-3.08

c)

251
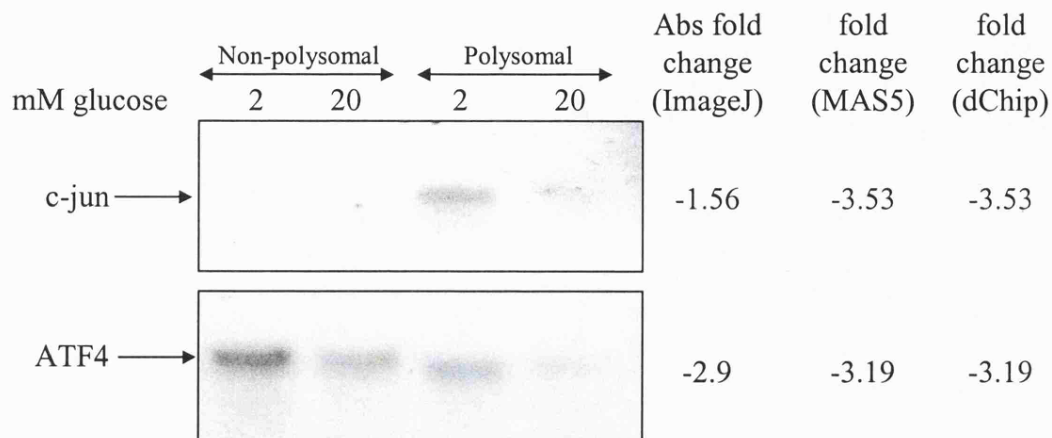
the recruitment of ribosomes onto ATF4 mRNA was examined more closely by Northern blot analysis of the sedimentation profiles of these mRNAs. MIN6 cells were incubated in KRB containing 0.5mM or 20mM glucose and lysed in high salt polysome buffer supplemented with 1% triton (figure 5.10). The cell lysates were layered on 7-47% sucrose gradients and polysome analysis was carried out as previously described (figure 5.2). Each gradient was fractionated into 20 fractions; RNA was isolated from each fraction, run on a formaldehyde gel and stained with ethidium bromide. The distribution of ATF4 was determined by Northern blot analysis and showed that low glucose concentrations stimulated the recruitment of ribosomes onto heavier polysomes (figure 5.10c).
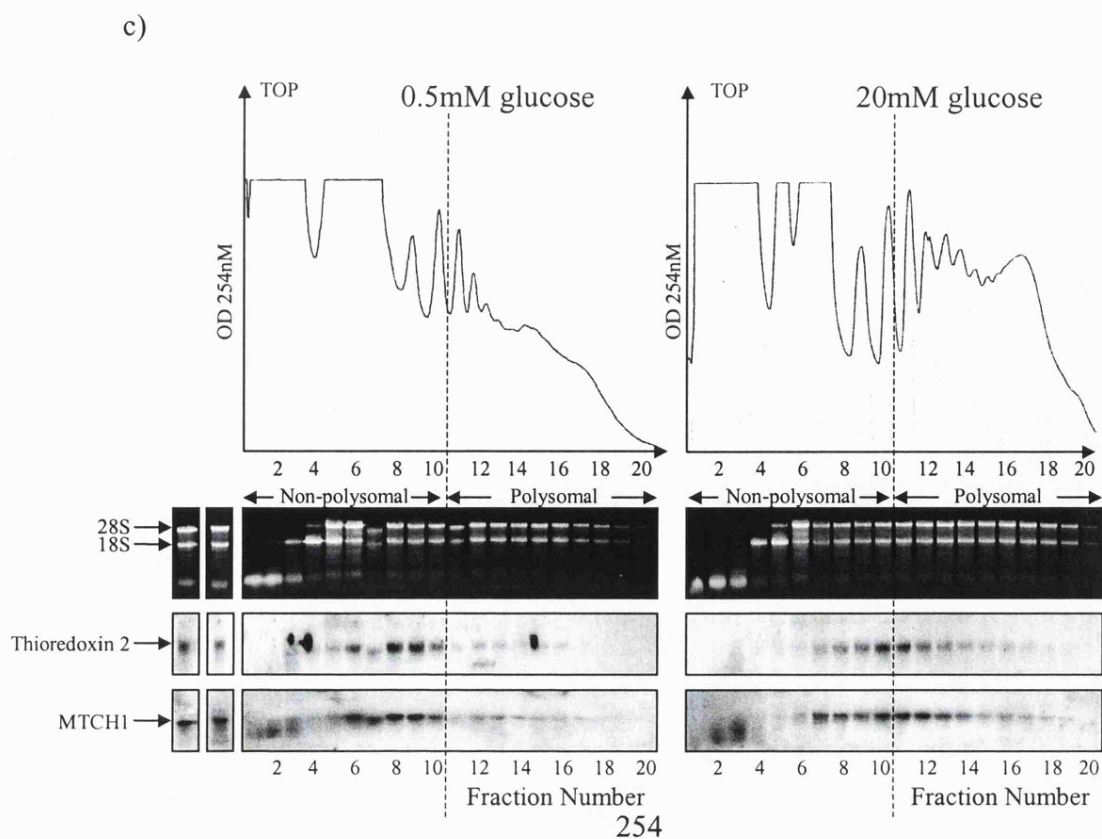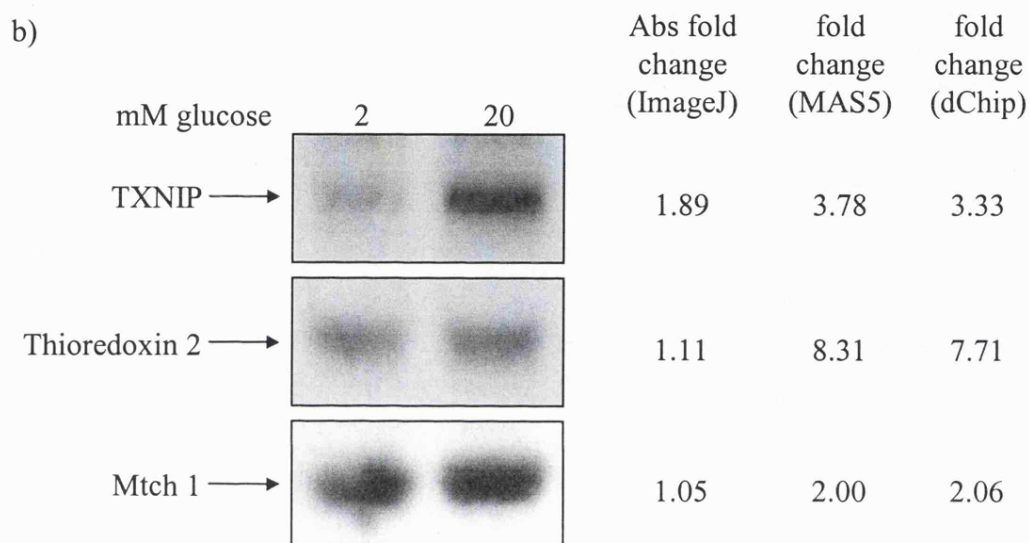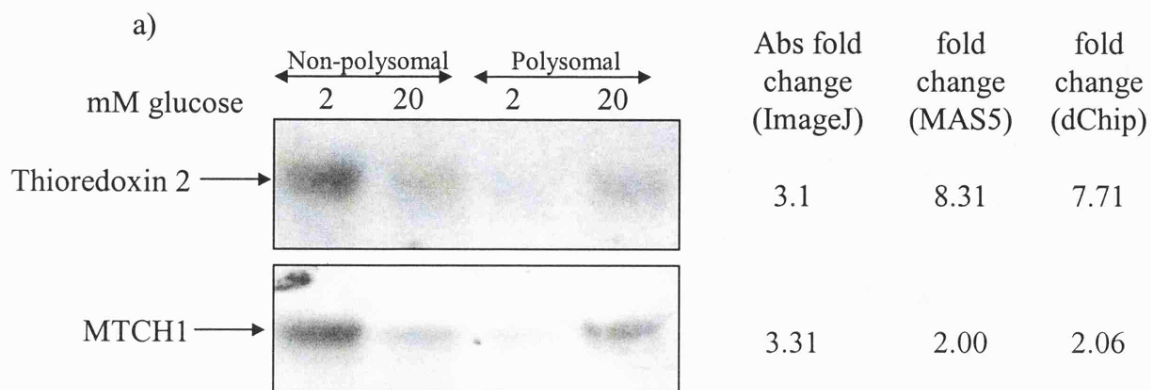
Anti-oxidative pathways

Microarray analysis showed that a large number of polysomal mRNAs important in metabolism were regulated by glucose and a large number of these metabolic genes were involved in the anti-oxidative pathway. Both dChip and MAS5 identified more than a 7.5-fold glucose-stimulated increase in the amount of polysomal thioredoxin 2 mRNA, a mitochondrial thioredoxin that plays an important role in the thiol antioxidative pathway. MAS5 also identified more than a 2-fold increase in polysomal mRNAs encoding thioredoxin interacting protein (TXNIP), and mitochondrial carrier homologue 1 (MTCH1). Using dChip, over a 2-fold increase in TXNIP and MTCH1 was observed, but these fold changes were not within the 90% confidence interval. Interestingly, recent work has shown that a kidney mitochondrial carrier protein is up-regulated in response to oxidative stress, suggesting that Mtch1 may be important in regulating the redox state of the cell (Haguenauer et al., 2005).

To confirm that glucose stimulated the amount of polysomal mRNAs encoding thioredoxin 2 and MTCH1, Northern blot analysis was carried out on polysomal and non-polysomal mRNA isolated from MIN6 cells that had been incubated in 0.5mM or 20mM glucose for one hour. Quantification of the Northern blots showed that glucose stimulated a 3.1 fold increase in the amount of polysomal mRNAs encoding thioredoxin 2 and a 3.31 fold increase in the amount of polysomal mRNA encoding MTCH1 (figure 5.11a). Moreover, these increases were accompanied by a glucose-stimulated decrease in the amount of non-polysomal mRNAs encoding MTCH1 and thioredoxin 2, suggesting that glucose stimulated the recruitment of non-polysomal MTCH1 and

Figure 5.11: Analysis of mRNAs encoding proteins important in the regulation of oxidative stress

mRNAs encoding specific proteins important in regulating oxidative stress were analysed as described in the figure legend to figure 5.10. These results are representative of two separate experiments

a)

	Non-polysomal		Polysomal		Abs fold change (ImageJ)	fold change (MAS5)	fold change (dChip)
mM glucose	2	20	2	20			
Thioredoxin 2					3.1	8.31	7.71
MTCH1					3.31	2.00	2.06

b)

			Abs fold change (ImageJ)	fold change (MAS5)	fold change (dChip)
mM glucose	2	20			
TXNIP			1.89	3.78	3.33
Thioredoxin 2			1.11	8.31	7.71
Mtch 1			1.05	2.00	2.06

c)

TOP   0.5mM glucose

OD 254nM

2 4 6 8 10 12 14 16 18 20

Non-polysomal   Polysomal

28S
18S

Thioredoxin 2

MTCH1

2 4 6 8 10 12 14 16 18 20

Fraction Number

TOP   20mM glucose

OD 254nM

2 4 6 8 10 12 14 16 18 20

Non-polysomal   Polysomal

2 4 6 8 10 12 14 16 18 20

Fraction Number

254

thioredoxin 2 into the polysomal fractions, indicative of an increase in the rate of initiation of translation.

To confirm that glucose did not change the levels of total thioredoxin 2 or MTCH1 mRNAs, Northern blot analysis was carried out on total RNA isolated from MIN6 cells that were incubated for one hour in KRB supplemented with 0.5mM or 20mM glucose. Quantification of the Northern blots showed that glucose did not stimulate a significant increase in the expression of mRNAs encoding thioredoxin 2 (1.11-fold) or MTCH1 mRNAs (1.05-fold, figure 5.11a).

Previous work has shown that TXNIP is transcriptionally up-regulated in human and mouse islets during a 24-hour incubation in high glucose (Minn et al., 2005a; Shalev et al., 2002b). Therefore, to identify whether the increases in polysomal mRNA encoding TXNIP was due to changes in levels of total mRNA, Northern blot analysis was carried out on total mRNA isolated from MIN6 cells that were incubated in 0.5mM glucose or 20mM glucose for one hour. Quantification of the Northern blots showed that glucose stimulated a 1.89-fold increase in TXNIP mRNA, suggesting that short term incubation in high glucose concentrations increased the stability of TXNIP mRNA or stimulated the transcription of mRNA encoding TXNIP (figure 5.11b).

Having established that mRNAs encoding MTCH1 and thioredoxin 2 were translationally regulated, the recruitment of ribosomes onto these mRNAs was examined more closely by Northern blot analysis of the sedimentation profiles of these mRNAs. At 0.5mM glucose concentration, the majority of mRNA encoding thioredoxin 2 and mitochondrial homologue 1 was associated with disomes or trisomes and almost no thioredoxin 2 or mitochondrial homologue 2 was associated with any larger polysomes (figure 5.11c). An increase in glucose from 0.5mM to 20mM resulted in the recruitment of a large amount of these mRNAs onto polysomes, indicative of an increase in the rate of initiation of translation.

Secretory proteins

Microarray analysis showed that neither PI nor carboxypeptidase H (CPH) was recruited onto polysomes in response to changes in glucose concentration. This contradicts our earlier data that showed glucose-stimulated recruitment of PPI mRNA

onto polysomes (figure 3.2). However, the microarray data does support reports that show that the synthesis of CPH is not regulated by glucose (Grimaldi et al., 1987; Guest et al., 1989; Martin et al., 1994; Skelly et al., 1996). Therefore, to further investigate the regulation of PI and carboxypeptidase H synthesis, Northern blot analysis was carried out on pooled polysomal and non-polysomal RNA that was isolated from MIN6 cells incubated in low or high glucose concentrations. Quantification of Northern blots of PPI and CPH mRNAs showed that glucose stimulated a 2.25-fold increase in PPI polysomal mRNA and a 1.3 fold increase in CPH polysomal mRNA (figure 5.12a). This contradicts microarray analysis, which showed that the levels of these polysomal mRNAs were not glucose-regulated.

To determine whether an increase in glucose resulted in an increase in PPI or CPH mRNA, Northern blot analysis was carried out on total mRNA isolated from MIN6 cells incubated in low or high glucose. Quantification of the Northern blots showed that glucose did not change the total levels of mRNAs encoding the secretory proteins, PPI or CPH (figure 5.12b), suggesting that neither PPI nor CPH mRNA transcription is acutely regulated by glucose.
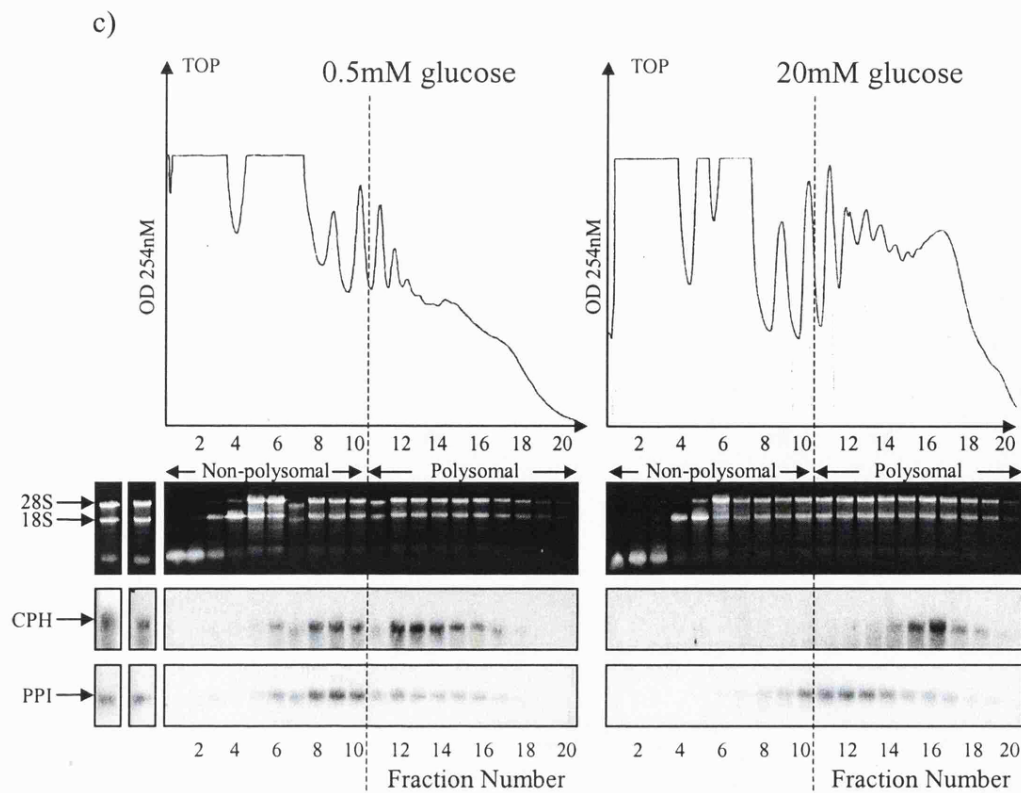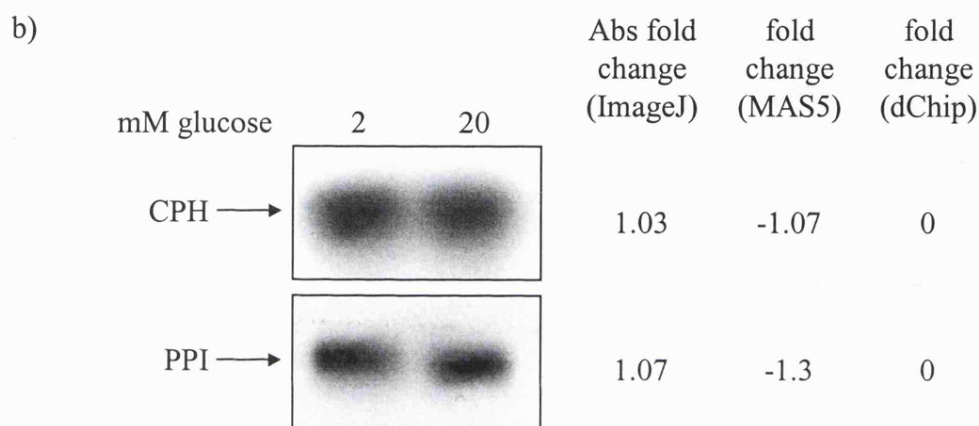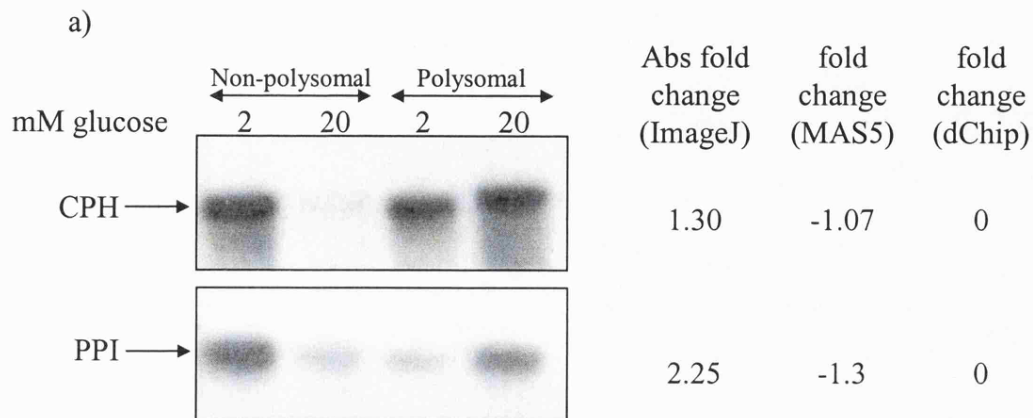
To investigate the recruitment of ribosomes onto PPI and CPH mRNAs more closely, the sedimentation profiles of these mRNAs were investigated by Northern blot analysis. There was no free PPI or CPH mRNA at low or high glucose. However, glucose clearly stimulated a significant recruitment of PPI and CPH mRNA that was associated with 1-3 ribosomes at low glucose onto heavier polysomes at high glucose concentrations, indicative of an increase in the rate of initiation (figure 5.12c).

Previous work has shown that glucose stimulates PI synthesis at the level of translation but does not stimulate the synthesis of carboxypeptidase H (Grimaldi et al., 1987; Guest et al., 1989; Martin et al., 1994; Skelly et al., 1996). However, although no increases in polysomal mRNAs encoding PPI and CPH were identified by Affymetrix microarray, Northern blot analysis did show a recruitment of PPI and CPH mRNAs onto heavier polysomes at high glucose (figure 5.12). This data therefore suggests that glucose stimulated the synthesis of carboxypeptidase H as well as PI. To determine whether the increase in the translation of carboxypeptidase H and PPI mRNAs were mirrored by an increase in PI and CPH proteins, MIN6 cells were incubated in KRB containing 0.5mM

glucose for 1 hour, followed by a one hour incubation in KRB containing 0.5mM or 20mM glucose and [^{35}S]-methionine. PI and CPH were then immunoprecipitated from the cell lysates with specific antibodies and then run on SDS-PAGE. Immunoprecipitations showed that glucose stimulated a large increase in both PI and CPH proteins (figure 5.13).

Figure 5.12: Analysis of mRNAs encoding specific secretory proteins
mRNAs encoding specific secretory proteins were analysed as described in the figure legend to figure 5.10. These results are representative of two separate experiments

a)

		Abs fold change (ImageJ)	fold change (MAS5)	fold change (dChip)
CPH		1.30	-1.07	0
PPI		2.25	-1.3	0

b)

		Abs fold change (ImageJ)	fold change (MAS5)	fold change (dChip)
CPH		1.03	-1.07	0
PPI		1.07	-1.3	0

c)

259
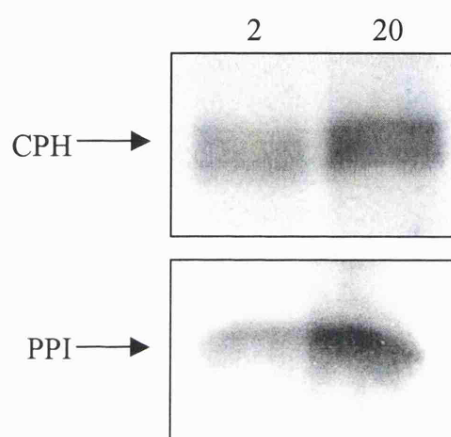
Figure 5.13: Glucose stimulates the synthesis of proinsulin and carboxypeptidase H

MIN6 cells were pre-incubated in KRB containing 0.5mM glucose for 1 hour followed by incubation in KRB containing 0.5mM or 20mM glucose for a further hour. The cells were lysed in MIN6 lysis buffer and proinsulin and CPH were immunoprecipitated from the lysates and resolved on 20% and 12.5% SDS-PAGE. These results are representative of three separate experiments.

5.4: Discussion

Previous work has investigated the effect of long-term and short-term incubations in glucose on β-cell expression profiles (Ohsugi et al., 2004; Shalev et al., 2002b; Webb et al., 2000; Webb et al., 2001). However, this is the first study that uses microarray analysis to identify changes in polysomal mRNA and therefore is the first study to identify mRNAs that may be regulated through changes in transcription or translation.

This study has identified 39 glucose-responsive polysomal mRNAs that change by 1.5 fold or more in both dChip and MAS5 and 6 glucose-responsive polysomal mRNAs that change 2 fold or more in both dChip and MAS5 (table 5.8 and 5.9). The 39 polysomal mRNAs that changed 1.5 fold or more encoded proteins with a wide range of functions that included cell signalling effectors, secretion and protein folding regulators, transcription factors, metabolic enzymes and components of the mitochondria (table 5.8). However, in both MAS5 and dChip, approximately 55% of polysomal mRNAs that changed more than 1.5 fold in response to glucose encoded transcription factors, proteins important in metabolism or components of the mitochondria (figures 5.6 and 5.9). Moreover, all of the polysomal mRNAs that changed by more than 2 fold in MAS5 and dChip were involved in metabolism or transcription.

5.4.1: Glucose increases the amount of polysomal mRNAs encoding regulators of oxidative stress

Functional analysis of glucose-regulated genes showed that 26% of polysomal mRNAs that changed 1.5 fold or more in both dChip and MAS5 were important in metabolism (table 5.9). Moreover, a large number of glucose-regulated metabolic or mitochondrial polysomal mRNAs that were identified by MAS5 or dChip, play important roles in the regulation of oxidative stress. Previous work has shown that the β-cell is particularly vulnerable to oxidative stress, probably due to its low anti-oxidative enzyme activity, which makes it difficult to inactivate reactive oxygen species (Grankvist et al., 1981; Lenzen et al., 1996; Tiedge et al., 1997). Moreover, this weakness of the β-cell to combat oxidative stress is thought to be important in the development of diabetes, as it

is believed to lead to β-cell dysfunction and apoptosis, a major form of β-cell loss in type I and type II diabetes (Kaneto et al., 1996).

The thiol anti-oxidative pathway uses thioredoxins to donate hydrogen ions and reduce reactive oxygenated species (eg O_2^-) via a reaction catalysed by peroxiredoxins ((Holmgren, 1985) figure 5.14). Meanwhile, thioredoxin binding proteins such as thioredoxin interacting protein (TXNIP) inhibit thioredoxins (Junn et al., 2000; Nishiyama et al., 2001). Previous work has shown that glucose regulates TXNIP, peroxiredoxin 2 and peroxiredoxin 6 (Ahmed and Bergsten, 2005) (Minn et al., 2005a) (Bast et al., 2002). Interestingly, over-expression of thioredoxin, protected mice from streptozotocin-induced diabetes (Hotta et al., 1998), while over-expression of TXNIP induced apoptosis in islets (Minn et al., 2005a). These studies have led to the suggestion that the thiol anti-oxidative pathway may be a key regulator of oxidative stress in pancreatic β-cells.

This work has shown that glucose stimulates a rapid increase in the levels of polysomal mRNAs encoding key members of the thiol anti-oxidative pathway including thioredoxin 2, TXNIP, peroxiredoxin 1 and 2 and thioredoxin-like 5 (table 5.4 and 4,7). Microarray and Northern blot analysis showed that glucose stimulated an increase in the levels of polysomal mRNAs encoding thioredoxin 2 through a recruitment of non-polysomal thioredoxin 2 mRNA at low glucose into the polysomal fractions at high glucose, indicative of an increase in the rate of initiation (figures 5.11a and 5.11c). Meanwhile glucose also increased the levels of polysomal mRNA encoding TXNIP by over 3.5-fold. However, this glucose-stimulated increase in TXNIP was also observed with total TXNIP mRNA (i.e. non-polysomal and polysomal), suggesting that the increase in TXNIP was due to an increase in TXNIP gene expression (transcription) or TXNIP mRNA stability (figure 5.11b). Previous work has shown that 24 hours incubation in high glucose stimulates transcription of TXNIP mRNA (Minn et al., 2005a); therefore it is likely that this rapid up-regulation of TXNIP is in fact due to the rapid up-regulation of TXNIP transcription. The simultaneous activation of thioredoxin 2, which reduces the number of reactive oxygen species and TXNIP, which inhibits thioredoxins, may be required to maintain the fine-tuning of the redox state of the β-cell and β-cell apoptosis. I suggest that by maintaining separate regulatory mechanisms of
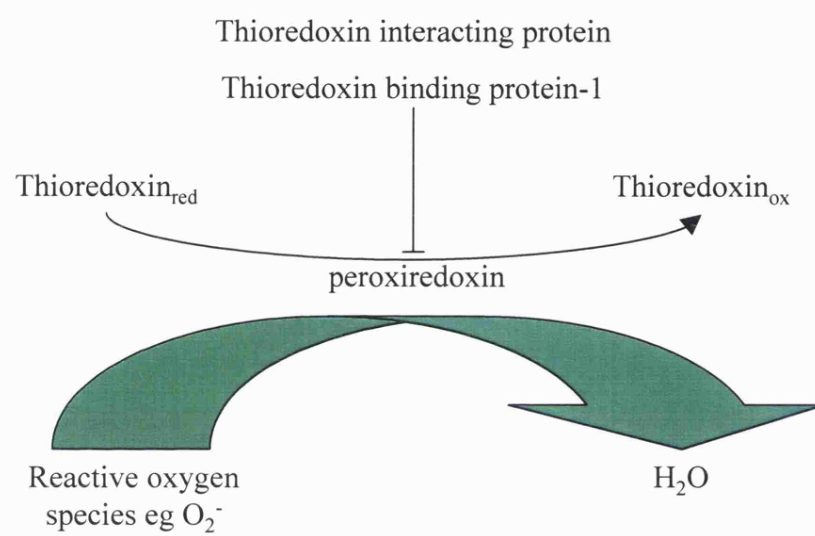
figure 5.14: Thiol anti-oxidative pathway

transcription of TXNIP and translation of thioredoxin 2, the β-cell can easily differentially regulate their expression when necessary.

Glucose also stimulated a 2-fold increase in levels of polysomal mRNA encoding MTCH1 through a recruitment of non-polysomal MTCH1 mRNA at low glucose into the polysomal fractions at high glucose, indicative of an increase in the rate of initiation (5.11a and 5.11c). The mitochondrial carrier proteins are a class of proteins that are responsible for the transport of small molecules across the mitochondrial membrane (Haguenauer et al., 2005; Palmieri, 2004). Recently, a new renal mitochondrial carrier protein was identified that is up regulated in response to oxidative stress (Haguenauer et al., 2005), therefore pancreatically-expressed MTCH1 may also be important in regulating the redox state of the β-cell.

5.4.2: Glucose regulates polysomal mRNAs encoding transcription factors

Microarray analysis of polysomal mRNA showed that incubation of β-cells in high glucose for one hour changed the amount of polysomal mRNA encoding a number of transcription factors, including immediate early genes and stress response transcription factors.

Immediate early genes

Increases in glucose concentration changed levels of polysomal mRNA encoding immediate early genes, including: c-jun, c-fos and early growth response 1 by 1.5 fold or more (table 5.9). Interestingly, previous microarray analysis has shown that a one hour incubation in 25mM glucose activated the expression of immediate early genes including c-fos and early growth response 1 (Susini et al., 1998) and in the presence of a cAMP analogue, glucose activated the expression of c-fos and c-jun (Ohsugi et al., 2004). However, while our microarray data showed that glucose increased the amount of polysomal mRNA encoding c-fos and early growth response 1, one of the largest decreases observed in response to an increase in glucose was the 3.5 fold decrease in the transcription factor, c-jun. c-jun is phosphorylated and activated by stress-activated c-jun NH_2-terminal kinase (JNK), and is required in certain apoptosis pathways (table 5.8, (Shaulian and Karin, 2002). Interestingly, in β-cells, the production of reactive oxygen

species, (which can also stimulate apoptosis) activates JNK, which in turn reduces insulin gene transcription and secretion (Kaneto et al., 2002; Matsuoka et al., 1997). Moreover, suppression of the JNK pathway can protect β-cells from reduced insulin gene transcription and secretion caused by oxidative stress (Kaneto et al., 2002). The glucose regulation of polysomal mRNA encoding c-jun (figure 5.10) suggests that the β-cell may protect against oxidative stress induced by high glucose through a decrease in the transcription of c-jun. In this way, insulin gene transcription and secretion may be maintained at high glucose in the presence of reactive oxygen species. Further insight into the glucose-regulation of c-jun and JNK signalling in pancreatic β-cells is clearly required and could be important in the understanding and prevention of diabetes.

The regulation of immediate early genes such as c-fos is most likely required to regulate the expression of many secondary genes. Previous work has shown that stimulation of MIN6 cells or rat FACS-sorted β-cells with glucose for 24 hours stimulated the expression of a large number of secretory and metabolic proteins (Flamez et al., 2002; Webb et al., 2000; Webb et al., 2001). The majority of these proteins that were glucose-regulated over 24 hours were not identified in this microarray analysis or in previous microarray analysis, where MIN6 cells were only stimulated with glucose for one hour (Ohsugi et al., 2004). Therefore, it is likely that the acute glucose-regulation of the immediate early genes is required for the long-term glucose-regulation of proteins important in secretion and metabolism.

Stress-induced transcription factors

An increase in glucose concentration resulted in a decrease in the amount of polysomal mRNA encoding the transcription factor ATF4 (table 5.9). This up-regulation of polysomal mRNA encoding ATF4 at low glucose is perhaps not surprising since translation of ATF4 is known to be up-regulated when eIF2α is phosphorylated (Harding et al., 2000a) and work has shown that eIF2α is phosphorylated in response to low glucose concentrations in MIN6 cells (Gomez et al., 2004). The data presented here suggests that total mRNA levels of ATF4 are increased at low glucose, suggesting that glucose deprivation also stimulates the transcription of ATF4 or increases the stability of ATF4 mRNA.

An increase in glucose concentration also resulted in a decrease in CHOP, which is a down stream target of ATF4 (table 5.9)(Harding et al., 2000a). This data confirms microarray analysis of MIN6 cells incubated in low or high glucose concentrations for 24 hours, which showed that CHOP expression was increased approximately 15 fold at low glucose concentrations (Webb et al., 2000; Webb et al., 2001). It is likely that the rapid up-regulation of ATF4 and CHOP is necessary for the β-cell to respond to stress induced by glucose deprivation.

5.4.3: Glucose increased the amount of polysomal mRNAs encoding secretory proteins

Previous work has shown that glucose stimulates the recruitment of ribosomes onto PPI mRNA [figure 3.2) (Itoh and Okamoto, 1980; Welsh et al., 1986; Welsh et al., 1991; Welsh et al., 1987). However, while Northern blot analysis showed that glucose did stimulate the recruitment of ribosomes onto PPI mRNA, microarray analysis showed that glucose did not regulate the levels of polysomal mRNAs encoding PI (figure 5.12). One possibility for the apparent contradiction between the microarray analysis and the Northern blot analysis is that the probes on the array for the highly expressed PPI mRNA may be saturated by the large quantity of PPI cRNA. Saturation of the probes would result in equal signal intensities and therefore no change between low and high glucose concentrations. Indeed, a comparison of the efficiencies of MAS5 and dChip showed that both programs failed to identify changes in transcripts that were high in concentration, most likely due to saturation of the signal (Rajagopalan, 2003).

Microarray analysis did not identify changes in the levels of polysomal mRNA encoding CPH, although Northern blot analysis did show a 1.3 fold increase in polysomal CPH mRNA at high glucose compared to low glucose concentrations (figure 5.12). Although CPH mRNA is far less abundant in β-cells than PPI mRNA, it was still approximately 10 times more abundant than TXNIP. Therefore, the high levels of polysomal CPH mRNA may have also saturated the array. Alternatively, because of the normalisation of the arrays, only mRNAs that are recruited into the polysome fractions above the recruitment of total RNA are identified by microarray analysis. Therefore, the 1.3 fold increase in polysomal CPH mRNA may not have been larger than the overall increase in the rate of initiation.

Previous work has shown that although glucose stimulates PI synthesis, glucose has no effect on the synthesis of CPH (Grimaldi et al., 1987; Guest et al., 1991; Guest et al., 1989; Martin et al., 1994; Skelly et al., 1996). However, the glucose-stimulated recruitment of CPH mRNA onto heavier polysomes suggests that glucose did stimulate an increase in the rate of initiation of translation for CPH (figure 5.12). Furthermore, the glucose stimulated increase in polysomal CPH mRNA was accompanied by an increase in CPH protein that paralleled the glucose stimulated increase in PI synthesis (figure 5.13). Therefore from this work, I have shown that CPH synthesis is regulated by glucose in MIN6 cells. Clearly further investigation is required to see if CPH synthesis is regulated in the same way as PI synthesis.

5.4.4: Restrictions of experimental procedures

The primary objective of this work was to identify proteins that are glucose-regulated at the level of translation. In addition to the identification of translationally regulated proteins such as thioredoxin 2, microarray analysis also identified transcriptionally regulated proteins such as TXNIP. To discriminate between transcriptionally and translationally regulated proteins microarray analysis has previously been performed on the non-polysomal and polysomal fractions of cells incubated in baseline or experimental conditions (Johannes et al., 1999). In this way, translationally activated proteins give fold change increases between the baseline and experimental polysomal arrays and the same fold change decreases between the non-polysomal arrays, indicative of a recruitment of the mRNA from the non-polysomal fractions at low glucose to the polysomal fractions at high glucose. Meanwhile, transcriptionally activated proteins may have increased amounts of polysomal mRNA, but there will not be a recruitment of non-polysomal mRNA at the baseline conditions into the polysomal fractions at the experimental conditions.

One limitation of this study is that a recruitment of mRNA into heavier polysomes might not actually reflect an increase in protein synthesis. Indeed, stalling of ribosomes or slowing of elongation (resulting in a decrease in protein synthesis) may actually cause the stacking of ribosomes and an increase in polysome size. To determine whether an increase in polysomal mRNA resulted in an increase in the synthesis of that specific protein, MIN6 cells were radiolabelled and CPH or PI were

immunoprecipitated (figure 5.13). However, this candidate protein approach is slow and requires a new antibody for each protein. 2-D gel electrophoresis and mass spectrometry has been used to identify large numbers of glucose-regulated proteins that are regulated by glucose over 24 hours (Ahmed and Bergsten, 2005). 2-D gel electrophoresis and mass spectrometry of β-cells incubated in low or high glucose concentrations for 1 hour would determine if the changes observed in the microarray analysis are correlated by changes in the proteins. However, there are also limitations with this technique. As this technique analyses changes in protein levels, it still does not distinguish between transcriptionally or translationally regulated proteins. Furthermore, many β-cell proteins are proteolytically processed (e.g. proinsulin is processed to insulin); therefore, there may be more than one spot for certain proteins.

5.4.5: Final Conclusions

Microarray analysis has shown that glucose regulates the levels of polysomal mRNAs involved in a variety of cellular functions. However, the majority of polysomal mRNAs that were regulated by glucose were important in transcription or metabolism. In particular, glucose regulated a number of polysomal mRNAs that encoded proteins responsible for regulating the redox state of the cell. Using the candidate gene approach I confirmed that glucose stimulated an increase in polysomal mRNAs encoding thioredoxin 2, TXNIP, and MTCH1 and a decrease in polysomal mRNA encoding c-jun and ATF4. This tight regulation of the redox state of the cell by glucose may be important in β-cell apoptosis and the development of diabetes. Therefore a better understanding of these processes may be important in the prevention of diabetes.

Chapter 6: Summary and General Discussion

6.1: Introduction

Within 60 minutes of stimulation of the pancreatic β-cell with glucose there is a 10 to 20 fold increase of proinsulin (PI) synthesis (Grimaldi et al., 1987; Guest et al., 1991; Itoh and Okamoto, 1980). However, there is no corresponding change in preproinsulin (PPI) mRNA abundance in the absence or presence of the transcription inhibitor, actinomycin D (Itoh and Okamoto, 1980) (Alarcon et al., 1993; Permutt and Kipnis, 1972a; Tillmar et al., 2002). Therefore, glucose stimulated PI synthesis is regulated at the post-transcriptional level, likely through an increase in the rate of protein synthesis. At present, however, the regulation of glucose-stimulated PI synthesis is poorly understood. Prior to this project, it has been reported that PI synthesis is post-transcriptionally regulated by glucose through changes in the rate of translational initiation and elongation, signal recognition particle arrest and mRNA stability (Tillmar et al., 2002; Watanabe, 1982; Welsh et al., 1986).

In addition to an increase in PI synthesis, glucose stimulates a 2 to 4 fold increase in the synthesis of more than 240 secretory granule proteins (Guest et al., 1991). A small number of these proteins have been identified and include PC2 and PC3, which are involved in the processing of PI to form insulin (Guest et al., 1989; Martin et al., 1994; Rhodes and Alarcon, 1994). However, the enzyme CPH, which is involved in the processing of PI to insulin, does not appear to be regulated by glucose (Grimaldi et al., 1987). It has been suggested that the glucose-regulated proteins are synthesised at a post-transcriptional level by the same mechanism as glucose-stimulated PI synthesis (Alarcon et al., 1993; Martin et al., 1994; Rhodes and Alarcon, 1994). Therefore, to improve the understanding of glucose stimulated protein synthesis in pancreatic β-cells; the objectives of this thesis were to further investigate the mechanism of glucose-regulated PI synthesis and to identify additional glucose-regulated proteins.

6.2: Summary

6.2.1: Glucose regulation of PI synthesis in pancreatic β-cells

Glucose stimulated the recruitment of ribosomes onto ribosome-associated PPI mRNA, indicative of an increase in the rate of initiation of translation (figure 3.2, 3.9, 3.13, 3.22). However, glucose did not stimulate an increase in de novo initiation, as all PPI mRNA was ribosome-bound at both low and high glucose concentrations (figure 3.2, 3.9, 3.13, 3.22).

Glucose also stimulated the recruitment of PPI, CPH and PC2 mRNAs to the ER (figure 3.9 and 3.13), therefore it is likely that glucose stimulates the recruitment of all secretory proteins to the ER. Furthermore, *in vitro* and *in situ* translations of PPI mRNA demonstrated that the recruitment of PPI mRNA is an important step in glucose-stimulation of PI synthesis (figure 3.21a and b). In addition to a general glucose-stimulated recruitment of secretory protein mRNAs to the ER, the association of PPI mRNA with the ER appears to be specifically regulated by glucose. At low glucose concentrations only 46% of PPI mRNA is associated with the ER while, 59% of CPH and 61% of PC2 mRNAs are associated with the ER at low glucose concentrations (figure 3.9). This data suggests that PPI mRNA is specifically inhibited from associating with the ER and two possible explanations for this exist: 1) mRNA binding proteins may prevent PPI mRNA from associating with the ER through a number of possible mechanisms; 2) PPI mRNA may be localised to specific sub-cellular compartment, thus preventing it from being targeted to the ER. To identify PPI mRNA binding proteins that may regulate PI synthesis, PPI-8MS2 mRNA was successfully pulled out of MIN6 cells. Unfortunately, the quantity of the mRNA and its binding proteins was too small to identify any proteins that were specifically bound to the PPI mRNA (figure 4.17). However, modifications to the technique, as discussed in chapter 4, should be able to overcome this problem.

6.2.2: Glucose regulation of total protein synthesis in pancreatic β-cells

Absorbance profiles of MIN6 cells show that an increase in the glucose concentration from 2mM to 20mM resulted in a large decrease in the 60S/80S peak and an increase in the polysome peaks (figure 3.2), indicative of an increase in the overall rate of initiation in MIN6 cells. Furthermore, polysome profiles of specific mRNAs showed that glucose stimulated the recruitment of ribosomes onto PC2, CPH, actin and S7 mRNAs as well as PPI mRNA (figure 3.2). This data therefore suggests that glucose stimulates an increase in the overall rate of initiation of translation for the majority of mRNAs.

To identify proteins that were differentially regulated by glucose through changes in the rate of initiation of translation, microarray analysis was carried out on polysomal mRNAs isolated from MIN6 cells incubated in low or high glucose concentrations. The microarrays at low and high glucose were normalised so that the analysis only identified mRNAs that were recruited onto polysomes above the average increase in the rate of initiation of translation. Furthermore, as changes in mRNA content also result in differential amounts of polysomal mRNAs, this method also identified changes in transcription or mRNA stability. Interestingly, glucose increased the amount of polysomal mRNA for a large number of mRNAs encoding metabolic enzymes, oxidative stress regulators and transcription factors. Moreover, Northern blot analysis confirmed that glucose stimulated a recruitment of ribosomes onto thioredoxin 2 and MTCH1 mRNA (figure 5.11). This recruitment was independent from any changes in total (polysomal and non-polysomal) mRNA encoding thioredoxin 2 or MTCH1 and therefore was indicative of an increase in the rate of initiation of translation. On the other hand, Northern blot analysis showed that glucose decreased the levels of total mRNA encoding c-jun and ATF4 mRNAs and increased the levels of total mRNA encoding TXNIP, suggesting that the synthesis of these proteins was regulated at the level of transcription or mRNA stability (figure 5.10 and 5.11). Interestingly, microarray analysis did not identify changes in levels of polysomal mRNAs encoding PI or the processing enzymes PC2, PC3 or CPH. However, Northern blot analysis did identify a glucose-stimulated recruitment of ribosomes onto both PPI (2.25 fold) and CPH (1.3 fold) mRNAs (figure 5.12). Moreover, immunoprecipitation of [^{35}S]-

methionine labelled MIN6 lysates showed that glucose also stimulated an increase in the amount of both PI and CPH proteins (figure 5.13).

6.3: General Discussion

Glucose stimulates a recruitment of ribosomes onto PPI mRNA (figure 3.2), indicative of an increase in the rate of initiation of translation. Moreover, glucose also stimulates a recruitment of ribosomes onto mRNAs encoding secretory proteins (e.g. CPH and PC2), cytosolic proteins (e.g. actin and S7) and mitochondrial proteins (e.g. thioredoxin 2 and MTCH1) (figure 3.2 and table 5.9). This suggests that glucose stimulates an increase in the rate of initiation of translation in the majority of mRNAs. It is likely that this glucose-stimulated increase in initiation is through an increase in ternary complex formation, as glucose stimulates the dephosphorylation of eIF2α and an increase in ternary complex formation (Gomez et al., 2004). However as the recruitment of ribosomes onto PPI, thioredoxin 2 and MTCH1 mRNAs was larger than the recruitment of ribosomes onto other mRNAs, such as CPH, it is likely that additional mechanisms are responsible for the larger glucose-stimulated increase in initiation for specific mRNAs. Interestingly, neither thioredoxin 2 nor MTCH1 are secretory or ER proteins, suggesting that the mechanism for their glucose-stimulated up-regulation may differ slightly from glucose stimulated PI synthesis.

Interestingly, previous work has demonstrated that the 5' and 3'UTRs of PPI mRNA regulate PI synthesis (Wicksteed et al., 2001). Therefore, it would be interesting to examine whether elements within the 5' and 3' UTRs of PPI mRNA are also present within the UTRs of thioredoxin 2 and MTCH1. The 5' and 3' UTRs of PPI mRNA have also been shown to act co-operatively to increase PI synthesis. One possible function for this co-operativity between the 5' and 3'UTRs of PPI mRNA may be to interact with each other and increase initiation through ribosome recycling. Evidence for ribosome recycling in vitro and in vivo has shown an interaction between PABP and eRF3, which interacts with the terminating ribosome though eRF1 (Cosson et al., 2002; Hoshino et al., 1999; Uchida et al., 2002). To characterise the effect of the interaction between PABP and eRF3 on translation, Uchida *et al* (2002) examined the effect of over-expression of the PABP binding domain of eRF3 (eRF3-N) on the synthesis of a bi-cistronic vector that expressed renilla luciferase (Rluc) in a cap-poly(A) dependent

manner and firefly luciferase (Fluc) in a cap-poly(A) independent manner. Overexpression of eRF3-N in HeLa cells increased the ratio of Fluc to Rluc, indicative of a decrease in cap-poly(A) dependent translation. To determine whether ribosome recycling is regulated by glucose, the effect of eRF3-N on PI synthesis at low and high glucose concentrations could be examined. To determine whether ribosome recycling is specific to a sub-set of proteins or a general effect on protein synthesis, the effect of eRF3-N on the synthesis of a large number of specific proteins could be examined by microarray analysis of polysomal mRNAs and/or 2-D gel electrophoresis and mass spectrometry.

In addition to an increase in initiation, glucose also stimulated an increase in the recruitment of PPI, CPH and PC2 mRNAs to the ER. Moreover, the glucose-stimulated increase in ER-associated PPI mRNA was larger than the increase in CPH or PC2 mRNAs. This presents the question: what triggers the increased recruitment of PPI mRNA over other secretory protein mRNAs? Interestingly, at low glucose, a higher proportion of PC2 (55%) and CPH (60%) mRNAs are associated with the membranes compared to PPI (46%) mRNA. This suggests that at low glucose, a specific mechanism is preventing PPI mRNA from being recruited to the ER. This selective recruitment of mRNAs encoding secretory proteins to the ER is a novel mechanism to regulate secretory protein expression and may prove a paradigm for the regulated expression of secretory membrane proteins in other secretory cells, for example neuro-endocrine cells.

How PPI mRNA is prevented from interacting with the ER is unclear. Previous work has shown that glucose increased the ratio of GTP to GDP from 2:1 to 4:1 (Hoenig and Matschinsky, 1987). It has been suggested that this increase will allow the SRP receptor to switch from its inactive GDP-bound state to its active GTP-bound state (Welsh et al., 1986). Furthermore, the non-hydrolysable analogue of GTP, GTP-γ-[S] stimulated recruitment of PPI mRNA to the ER in a similar manner to glucose (Welsh et al., 1991). Therefore, it was suggested that glucose might regulate the binding of SRP to the SRP receptor through the regulation of their GTP cycles. Flanagan *et al*, (2003) showed that SRP has a lower affinity for the PPI signal sequence than for the BiP signal sequence and suggest that this is to ensure that under cell stress conditions the efficient translation and translocation of BiP is a priority, since it is important for the unfolded protein

response. However, I propose that at low glucose concentrations, when GTP is limiting and a large proportion of SRP may be inactive, the weaker PPI signal sequence competes for SRP less efficiently than stronger signal sequences, such as BiP. In this way, secretory proteins with a stronger affinity for SRP e.g. BiP, will be preferentially recruited to the ER at low glucose concentrations. As a higher percentage of PC2 (59%) and CPH (61%) mRNAs are found associated with the ER at low glucose compared to PPI mRNA (46%), it would be interesting to determine whether SRP has a higher affinity for the signal sequences of PC2 and CPH than the PPI signal sequence.

A second reason why PPI mRNA may be prevented from interacting with the ER may be because of increased ribosome pausing at low glucose, which may prevent the synthesis of the signal peptide. Interestingly, rat PPI mRNA has numerous pause sites and translational pausing on PPI mRNA has been observed *in vitro* in the absence of SRP (Wolin and Walter, 1988). Therefore, at low glucose concentrations, PI synthesis may specifically pause at one of these sites, thereby specifically preventing the signal peptide from being synthesised and PPI mRNA from being recruited to the ER. One way to do identify the ribosome pause sites on PPI mRNA in β-cells incubated in low or high glucose could be using the method of heelprinting (Hollingsworth et al., 1998).

If the recruitment of PPI mRNA to the ER is regulated through ribosomal pausing, protein(s) would likely be required to bind PPI mRNA to control the specific pausing of PI synthesis at low glucose. Translational repression by protein binding to mRNA has been demonstrated in mammalian cells; for example, protein synthesis of ferritin is repressed when iron concentrations are low through the binding of IRP to its 5'UTR. However, the regulated inhibition of mRNA recruitment to the ER through protein binding to the mRNA has not been demonstrated. One example of inhibition of mRNA recruitment to the ER is the mechanism by which myristoylation of the emerging nascent polypeptide chain of NADH-cytochrome b(5) reductase (b5R) inhibits targeting of the b5R RNC to the ER by inhibiting the interaction of SRP with the signal peptide (Colombo et al., 2005). Myristoylated b5R that cannot be targeted to the ER is consequently targeted to the mitochondria. In this way, the extent of myristoylation determines the quantities of b5R that are targeted to the ER and the mitochondria.

The differential recruitment of PPI and CPH and PC2 mRNAs to the ER may simply reflect differences in the rates of initiation of these different mRNAs. Indeed, polysome analysis of PPI and PC2 mRNAs shows that PPI mRNA is associated with less ribosomes than PC2 mRNA at low glucose concentrations (figure 3.2). To determine whether the glucose-stimulated recruitment of PPI mRNA is linked to increases in the rate of initiation of translation of PI, the recruitment of PPI mRNA could be analysed in the presence of the translational inhibitor, cycloheximide. If the specific recruitment of PPI mRNA were not dependent on translation (for example if PPI mRNA recruitment was blocked at low glucose by inhibitory proteins binding the mRNA) glucose would still stimulate the recruitment of PPI mRNA to the ER. However, if the recruitment of PPI mRNA to the ER were dependent on the increased rate of initiation at high glucose, PPI mRNA would not be recruited to the ER at high glucose concentrations in the presence of cycloheximide.

While an increase in initiation may increase the recruitment of secretory protein mRNAs to the ER, the increased recruitment of mRNA to the ER at high glucose may enable an increased rate of initiation. This would still explain the larger glucose-stimulated increase in polysomal PPI mRNA compared to CPH mRNA, as the increased quantity of CPH at the ER at low glucose could result in more efficient initiation. Indeed, the lower fold change in levels of polysomal CPH mRNA compared to PPI mRNA appear to be due to a increased proportion of polysomal CPH mRNA at low glucose (figure 5.12). An increased rate of initiation at the ER could be attributed to the high concentration of available 60S ribosomal subunits that remain associated with the membranes after protein synthesis (Potter and Nicchitta, 2002; Seiser and Nicchitta, 2000). Additionally, the large amount of localised protein synthesis may ensure a high concentration of initiation factors, thereby contributing to high rates of initiation of translation at the ER.

Data presented in this thesis suggested that all ER-associated PPI mRNA is actively translating. However, further regulation at the ER may still occur. One possibility is that the rate of elongation could be faster at high glucose than at low glucose. Moreover, elongation of secretory proteins at the ER could be regulated through the regulated association of elongation factors with the ER. A second possibility is that translocation of the nascent chain into the ER lumen may be regulated. Indeed,

comparison of the early stages of translocation of different nascent chains suggests that the ribosome-translocon junction is regulated by the nature of the nascent chain (Rutkowski et al., 2001; Wolin and Walter, 1993). For example, some nascent chains such as the prion protein quickly formed tight ribosome-translocon junctions, while others such as pre β-lactamase remained exposed to the cytosol for longer. Interestingly, the β-subunit, which is believed to facilitate co-translational translocation of the nascent chain, is phosphorylated at high glucose concentrations in MIN6 cells (TP Herbert, unpublished observations). This preliminary data suggests that translocation of the nascent chain may be regulated in β-cells.

Final Summary

This thesis has shown that glucose stimulates proinsulin synthesis through an increase in the rate of initiation of translation and an increase in the recruitment of PPI mRNA to the ER. Furthermore, I show for the first time that PPI mRNA is preferentially recruited to the ER over other secretory protein mRNAs. This mechanism may prove a paradigm for the specific regulation of secretory protein synthesis in neuro-endocrine cells.

Additionally, microarray analysis was used to identify pancreatic β-cell polysomal mRNAs that are differentially distributed over one hour between low and high glucose concentrations. The majority of polysomal mRNAs whose levels changed between low and high glucose encoded proteins that play important roles in metabolism or transcription.

6.4: Relevance to Disease

The ability of the β-cell to release insulin in response to increases in blood glucose levels is essential for the maintenance of glucose homeostasis. However, in type II diabetes, increased insulin resistance leads to increased insulin demand and β-cell dysfunction, which is usually characterised by reduced insulin gene transcription and insulin secretion (Porte and Kahn, 2001). Interestingly, insulin secretion was impaired by the short-term (2 hours) inhibition of protein synthesis, suggesting that the rapid up-regulation of protein synthesis is also required for the β-cell to maintain the correct response to changes in plasma glucose concentrations (Garcia et al., 2001).

Importantly, we have shown that glucose stimulates the translational regulation of oxidative stress regulators, particularly in the thiol anti oxidative pathway. Previous work has shown that reactive oxygen species are produced during hyperglycaemia and that oxidative stress is likely to be involved in the progression of β-cell dysfunction during type II diabetes (Kajimoto and Kaneto, 2004). Therefore, it is likely that this rapid up-regulation of oxidative stress regulators is important in protecting the cell from oxidative stress caused by hyperglycaemia that may otherwise lead to β-cell dysfunction. Clearly, further understanding in the translational control of both PI and total protein synthesis in pancreatic β-cells will increase the understanding in the pathogenesis of β-cell dysfunction.

Appendix 1: Cloning Strategies

A1.1: PPI and Fluc containing eight MS2 binding sites

A1.1.1: pShuttle CMV PPI-8MS2 SDM2

To insert 8 MS2 binding sites into the coding sequence of PPI mRNA (figure A1.1), the 3' end of PPI (bases 270-443) was amplified from pGEM-PPI (pGEM-3Zf containing the PPI mRNA sequence cloned into the EcoRI and HindIII sites), with the 5' primer, PPI-2xMS2-F, containing a 5' tail of 2 MS2 binding sites with a XmaI site at the 5' end of the primer and a BspEI site directly 3' of the MS2 binding sites, followed by the 17 bases complementary to the PPI sequencee that is downstream of base pair 270, and a 3' primer complementary to bases 426-451 of pGEM3Zf (pGEM-R-451). The resulting PCR product was digested with XmaI and HindIII to leave a 268 bp fragment, containing the 2 MS2 binding sites followed by the 3' end of PPI. This 268 bp fragment was then ligated into pGEM-PPI that had been digested with XmaI and HindIII to result in a plasmid containing 2 MS2 binding sites in the centre of the coding sequence for proinsulin (pGEM-PPI-2MS2). To increase the number of binding sites to 4, pGEM-PPI-2MS2 was digested with XmaI and HindIII to give a 268 bp fragment containing the MS2 binding sites and the 3' end of PPI. pGEM-PPI-2MS2 was then digested with BspEI and HindIII to result in a 3605 bp fragment containing pGEM-3Zf, the 5' end of PPI and 2 MS2 binding sites. The 268 bp and 3605 bp fragments were then ligated, with the ligation of XmaI and BspEI resulting in the deletion of these sites. The resulting plasmid (pGEM-PPI-4MS2) therefore contained 4 MS2 binding sites and this process was repeated to result in pGEM-PPI-8MS2. The presence of 8MS2 binding sites was confirmed by digestion with EcoRI and HindIII to release the insert (figure A1.2) and then confirmed by sequencing.

To clone PPI-8MS2 into pShuttle CMV (figure A1.3), PPI-8MS2 was amplified by PCR with the 5' primer, PPI-8MS2F that was complementary to the 5' end of PPI and contained a BglII site at the 5' end and the 3' primer, PPI-8MS2R that was complementary to the 3' end of PPI and contained an HpaI restriction site at the 3' end. The amplified product was then digested with BglII and HpaI and ligated into
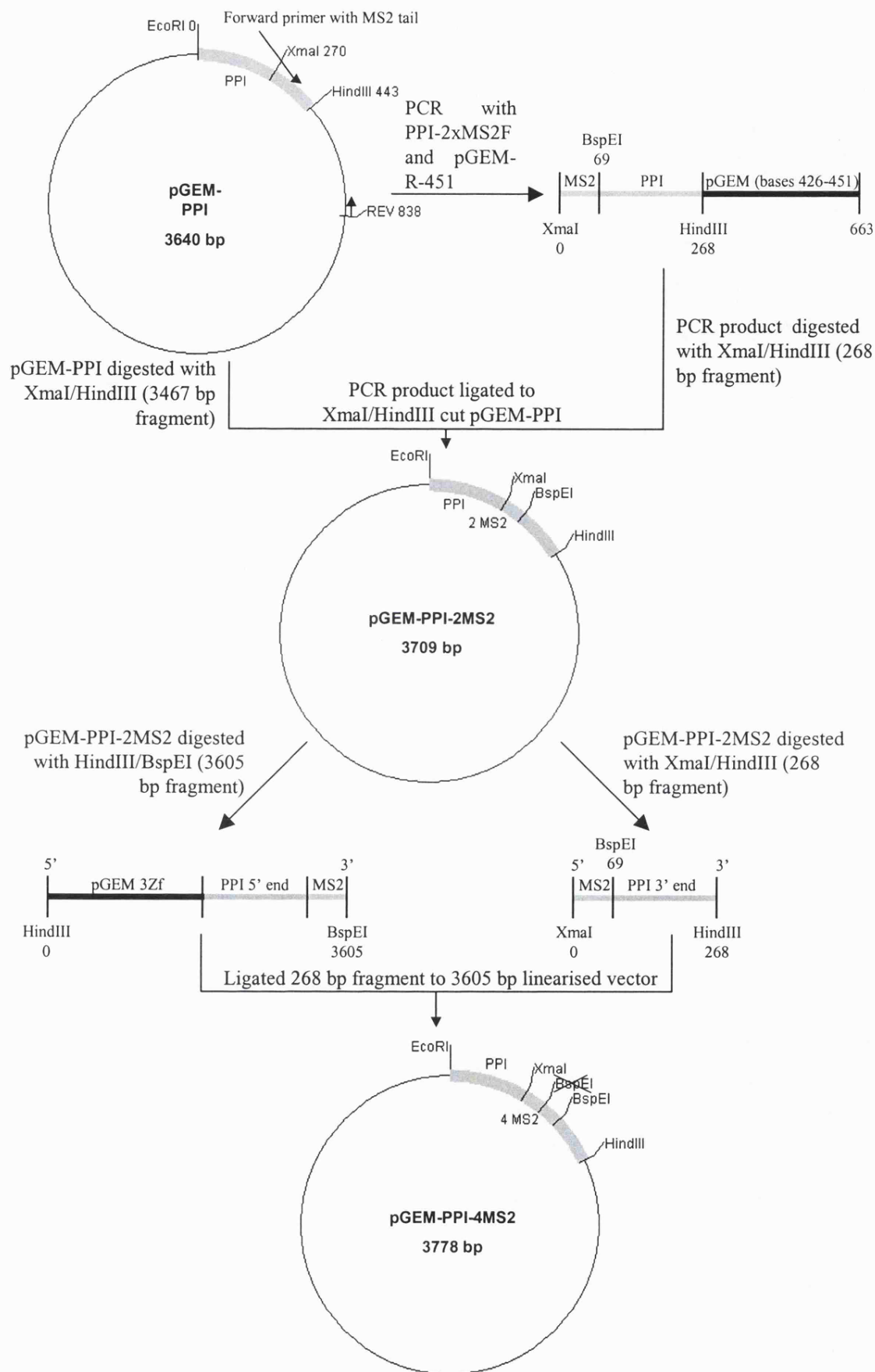
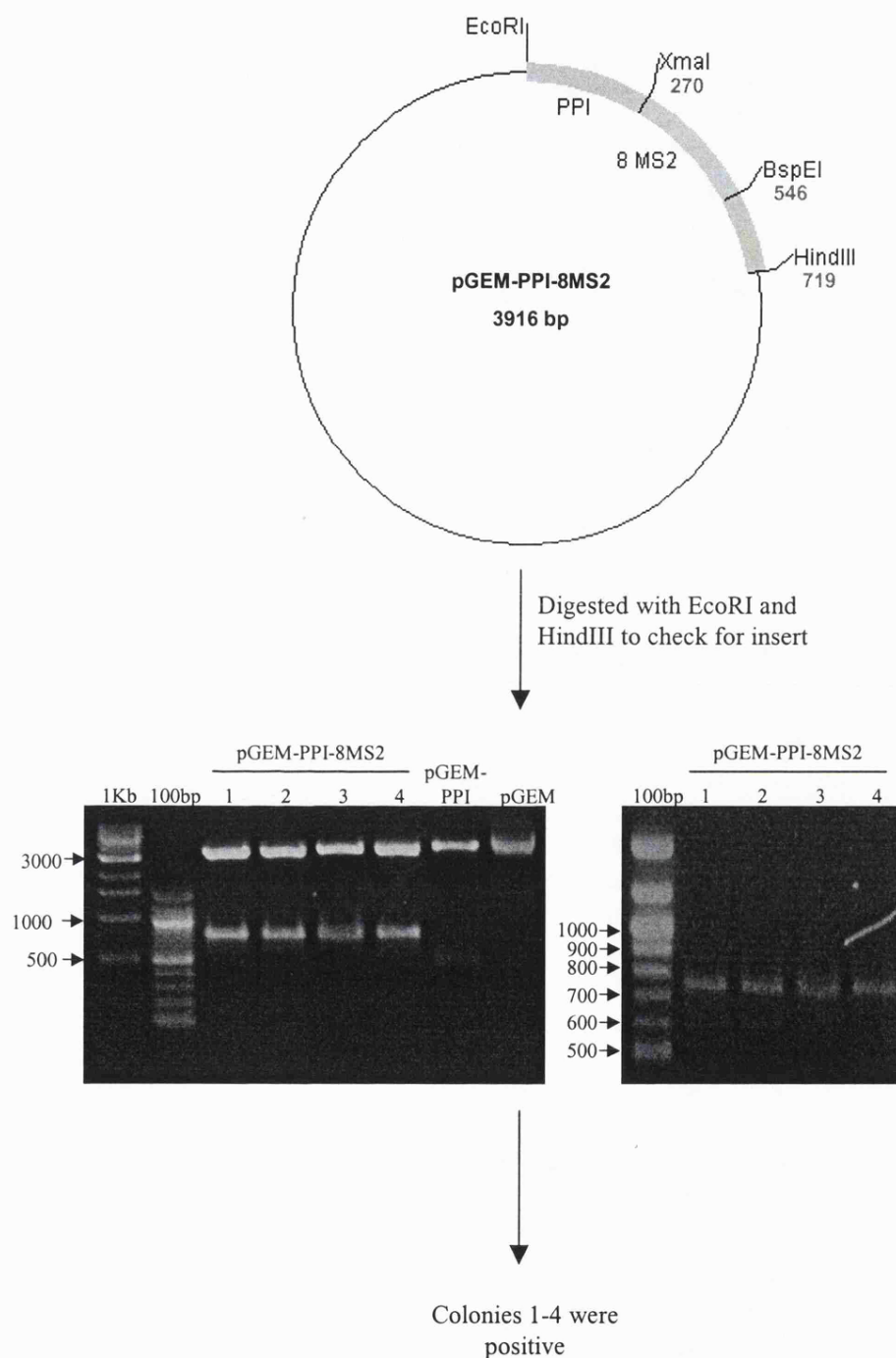**Figure A1.1: Construction of pGEM-PPI-4MS2**
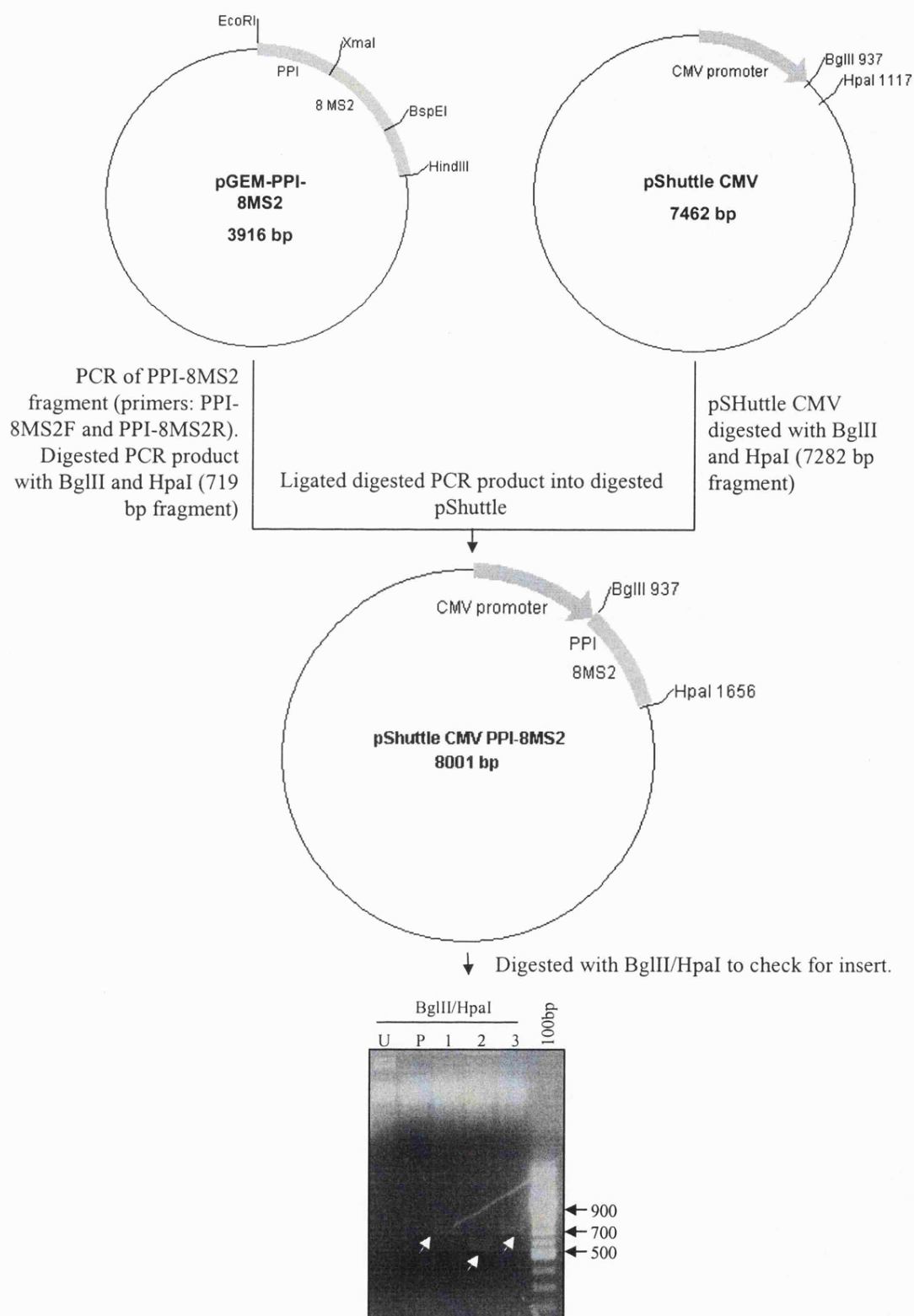
279

Figure A1.2: Construction of pGEM-PPI-8MS2 and confirmation of insert
Plasmid DNA was isolated from four colonies and digested with EcoRI and BamHI
to check for positive pGEM-PPI-8MS2 colonies. pGEM-PPI and pGEM-3Z(f) were
also digested with EcoRI and BamHI as controls. The digested plasmid DNA was
then run on 1.5% agarose gel and stained with ethidium bromide.

280

Figure A1.3: Construction of pShuttle-PPI-8MS2 and confirmation of insert
Plasmid DNA was isolated from three colonies and digested with BglII and HpaI to check for positive pShuttle-PPI-8MS2 colonies. Uncut pShuttle-CMV (U) and pShuttle CMV that had been cut with BglII and HpaI (P) were run on a 1% agarose gel containing ethidium bromide, alongside the digested plasmid DNA (1-3) to check for the correct insert size. Inserts are shown with white arrows.

PCR of PPI-8MS2 fragment (primers: PPI-8MS2F and PPI-8MS2R). Digested PCR product with BglII and HpaI (719 bp fragment)

pSHuttle CMV digested with BglII and HpaI (7282 bp fragment)

Ligated digested PCR product into digested pShuttle

Digested with BglII/HpaI to check for insert.

Site-directed mutagenesis using colony 1 removed the 18 bases between the transcription start site and the 5' end of PPI (primers: PPI-SDM1-903F and PPI-SDM1-903R for 1st round and PPI-SDM2-903F and PPI-SDM2-903R for 2nd round). Sequencing confirmed the positive clones.

282

pShuttle CMV that had been digested with BglII and HpaI. Restriction digestion with BglII and HpaI confirmed the presence of the insert (figure A1.3). PPI-8MS2 was ligated into BglII and HpaI because these sites were the closest to the transcription start site and the poly(A) tail respectively. However, after ligation , there were still 18 base pairs between the transcription start site and the first base of PPI, which may interfere with the influence that the 5'-UTR has on glucose-regulated proinsulin synthesis. Therefore, site-directed mutagenesis was carried out in two stages to remove these 18 bases and result in the plasmid: pShuttle PPI-8MS2 SDM2. Sequencing with the 5' primer, pShut-seq874F that was complementary to the 18 bases downstream of base pair 874 of pShuttle CMV and the 3' primer PShut-seq1168R that was complementary to the 18 bases upstream of base pair 1168 of pShuttle CMV, confirmed the positive clones.

A1.1.2: pShuttle CMV 3'8MS2 SDM

To clone the 8MS2 binding sites at the 3' end of PPI, the 8MS2 binding sites were amplified by PCR with a 5' primer, 8MS2HindIIIF that was complementary to the 5' end of the first MS2 binding site and the adjacent 6 bases of PPI, and a 3' primer, 8MS2HindIIIR that was complementary to the 3' end of the last MS2 binding site and the adjacent 6 bases of PPI (figure A1.4). Both primers contained 5' HindIII restriction sites. The PCR product was digested with HindIII and ligated into pGEM-PPI that had been cut with HindIII and dephosphorylated with CIAP.

PPI-3'8MS2 was then amplified by PCR with the 5' primer, PPI-8MS2 and the 3' primer, 8MS2HpaIF, which was complementary to the 3' end of the final MS2 binding site and contained an HpaI restriction site at the 5' end (figure A1.4). The 719 bp fragment was then digested with BglII and HpaI and ligated into pShuttle CMV that had also been digested with BglII and HpaI. The presence of insert was confirmed in positive clones 3 and 5 by digestion with BglII and HpaI (figure A1.5).

To remove the 18 bases between the transcription start site and the first base of PPI 5'-UTR, pShuttle-PPI-3'8MS2 was digested with SexA1 and the 3000 base pair fragment that contained the 3' end of PPI and the 8MS2 binding sites was ligated to
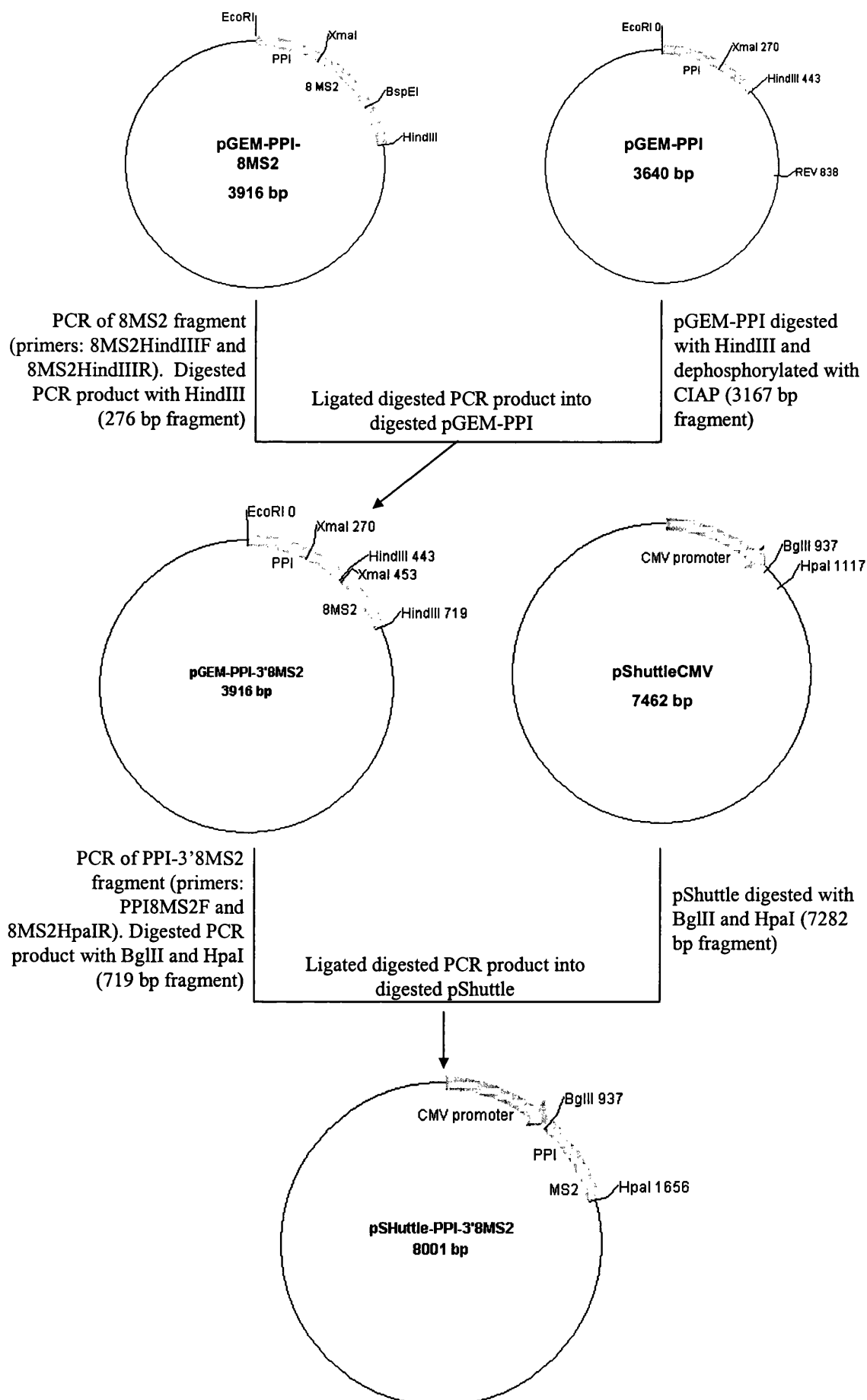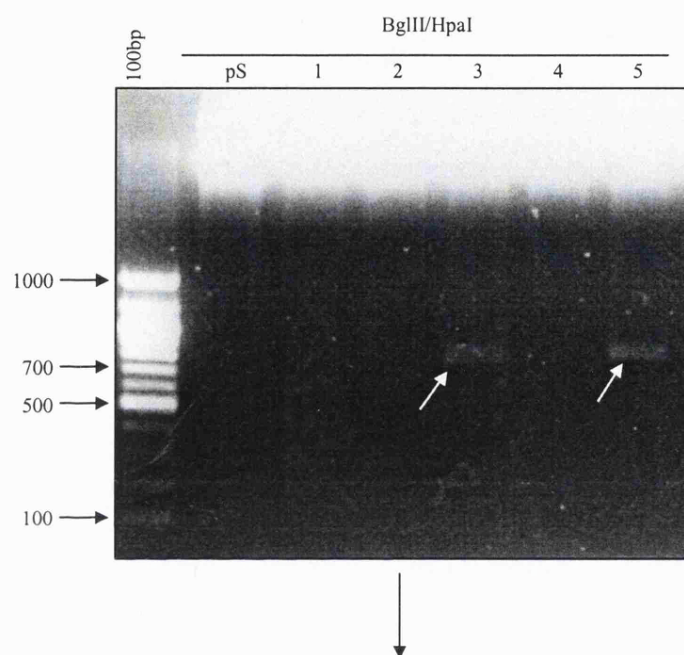
Figure A1.4: Construction of pShuttle-PPI-3'8MS2

Colonies 3 and 5 were positive.

Figure A1.5: Confirmation of pShuttle-PPI-3'8MS2

Plasmid DNA was isolated from five colonies (from fig 5.6) and digested with BglII and HpaI to check for positive pShuttle-PPI-3'8MS2 colonies. pShuttle CMV that had been cut with BglII and HpaI (pS) were run on a 1% agarose gel containing ethidium bromide, alongside the digested plasmid DNA (1-5) to check for the correct insert size. Inserts are shown with white arrows.

the 4983 base pair fragment resulting from the digestion of pShuttle PPI-8MS2 SDM2 with SexA1 that contained the 5' end of PPI and the CMV promoter (figure A1.6). The positive colony was confirmed by digestion with BamHI and HpaI (figure A1.7).

A1.1.3: pShuttle Fluc-8MS2

To insert eight MS2 binding sites into the centre of the coding region of Fluc, 8MS2 binding sites were amplified from pShuttle CMV PPI-8MS2 using the 5' primer, 8MS2F, which was complementary to the 5' end of the first MS2 binding site and 6 bases of PPI adjacent to the first MS2 binding site and the 3' primer, 8MS2R, which was complementary to the 3' end of the last MS2 binding site and the 6 bases of PPI adjacent to this (figure A1.8). Both 8MS2F and 8MS2R contained BsrGI restriction sites at their 5' ends. The resulting PCR product was cut with BsrGI and ligated into pGl3-Fluc, which had been digested with BsrGI and dephosphorylated with CIAP. Digestion with BsrGI confirmed the insert size and digestion with XmaI confirmed the orientation of the insert.

For insertion into pShuttle CMV, Fluc-8MS2 was amplified from pGL3-Fluc-8MS2 using the 5' primer, Fluc-8MS2F, which was complementary to the 5' end of Fluc and contained a BglII restriction site at its 5' end, and the 3' primer, Fluc-8MS2R, which was complementary to the 3' end of Fluc and contained an HpaI site at its 5' end (figure A1.9). The resultant PCR product was then ligated into pShuttle CMV that had been digested with BglII and HpaI, to make the resultant plasmid, pShuttle-Fluc-8MS2. Positive colonies were confirmed by restriction digest with BglII and HpaI and then by sequencing.

A1.1.4: pShuttle Fluc 3'8MS2

To clone pShuttle Fluc 3'8MS2, Fluc was amplified by PCR from pGL3-Fluc, using the 5' primer Fluc8MS2F, which was complementary to the 5' end of Fluc and contained a BglII restriction site at its 5' end, and the 3' primer, FlucHindIIIR, which was complementary to the 3' end of Fluc and contained a HindIII site at its 5' end
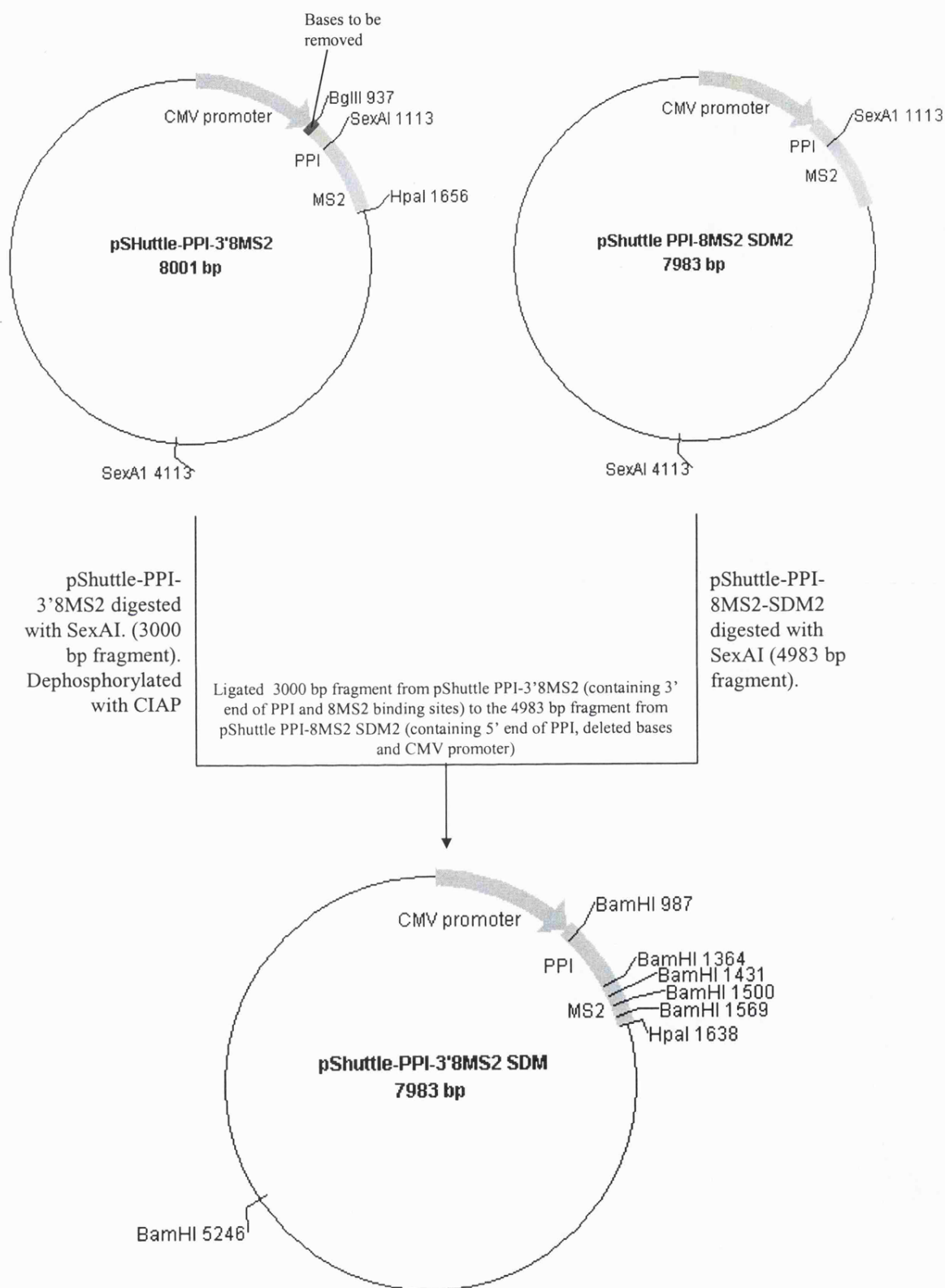
Figure A1.6: Construction of pShuttle-PPI-3'8MS2 SDM
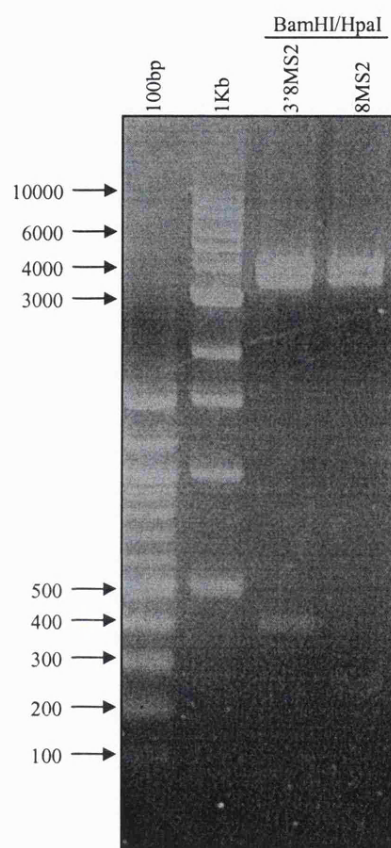
Figure A1.7: Confirmation of pShuttle-PPI-3'8MS2 SDM Plasmid DNA was isolated from one colony and digested with BamHI and HpaI to check for positive pShuttle-PPI-3'8MS2 SDM colonies. pShuttle-PPI-8MS2 SDM that had been cut with BamHI and HpaI (pS) was run on a 1% agarose gel containing ethidium bromide, alongside the digested plasmid DNA to check for the correct fragment sizes.

Figure A1.8: Construction of pGL3-Fluc-8MS2 and confirmation of insert
Plasmid DNA was isolated from 4 colonies and digested with BsrGI to check for insert and with XmaI to check the insert orientation. pShuttle-CMV that had been cut with BsrGI or XmaI (P) were run on a 1% agarose gel containing ethidium bromide, alongside the digested plasmid DNA to check for the correct fragment sizes.
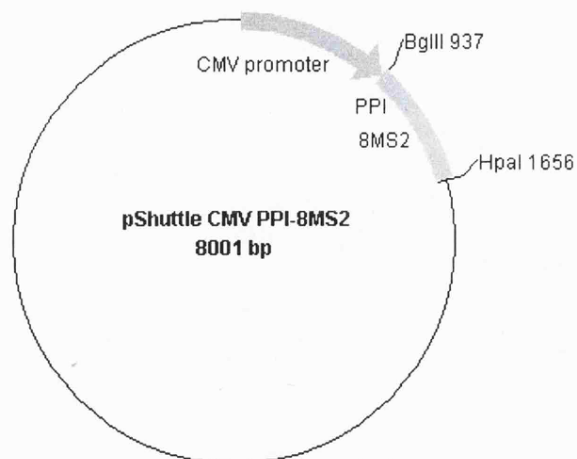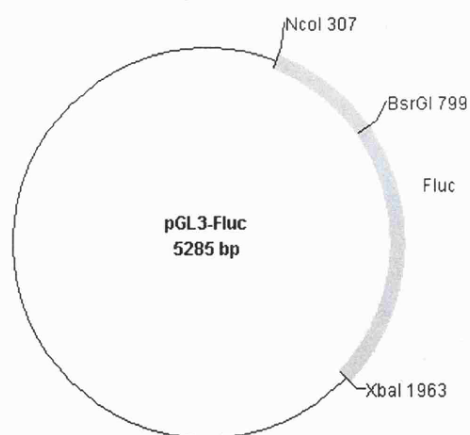
Digested with BsrGI and dephosphorylated with CIAP (5285 bp fragment)
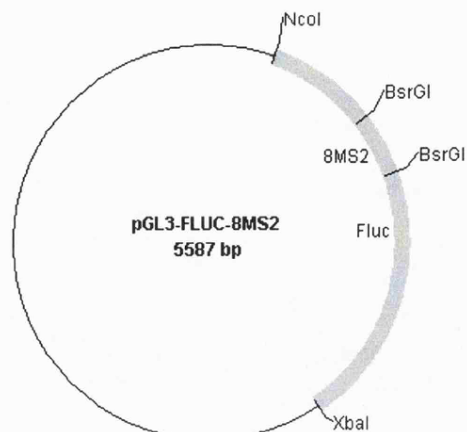
PCR of 8MS2 fragment, introducing BsrGI sites (primers: 8MS2F and 8MS2R). (276 bp fragment)

Ligated 8MS2 fragment to linearised pGL3-Fluc

Digested with BsrGI to check for insert and XmaI to check orientation

High exposure

Low exposure

Colony 1 was positive and used for further cloning

290

Figure A1.9: Construction of pShuttle-Fluc-8MS2 and confirmation of insert
Plasmid DNA was isolated from four colonies (1-4) and digested with BglII and HpaI to check for positive pShuttle-Fluc-3'8MS2 colonies. Uncut pShuttle CMV (U) was run on a 1% agarose gel containing ethidium bromide, alongside the digested plasmid DNA to check for the correct fragment sizes.

Sequencing confirmed that colony 1 was
positive 292

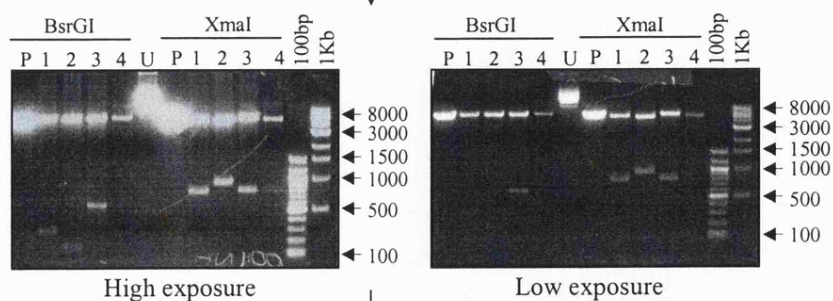(figure A1.10). The resultant PCR product was digested with BglII and HindIII and cloned into the 7558 bp fragment that resulted from the digestion of pShuttle CMV PPI-3'8MS2 with BglII and HindIII. Digestion with BglII and HpaI confirmed the presence of Fluc-8MS2 and digestion with BglII and HindIII confirmed the presence of Fluc.

A1.2: Expression of Adenoviruses

Due to the poor transfection efficiency of MIN6 cells, the cDNA for all mRNAs and proteins to be expressed in MIN6 cells were cloned into pShuttle CMV, for making adenoviruses: AdPPI-8MS2, AdPPI-3'8MS2, AdFluc-8MS2, AdFluc-3'8MS2. To confirm the presence of the sequences for PPI-3'8MS2 or Fluc-3'8MS2 in AdPPI-3'8MS2 and AdFluc-3'8MS2, the sequences were amplified by PCR from the virus and from the recombinant and pShuttle vectors. PPI-3'8MS2 was amplified using the primers PPI8MS2F and 8MS2HpaIR and Fluc-3'8MS2 was amplified using the primers, Fluc-8MS2F and 8MS2HpaIR. PCR of PPI-3'8MS2 confirmed the presence of a fragment of just over 700 base pairs in the virus, recombinant and shuttle vector that is the correct size for PPI-3'8MS2 (figure A1.11). There was also a small amount of shorter fragments that most likely corresponded to amplifications where the 3' primer has annealed to the end of the second, fourth or sixth MS2 binding site, instead of the final eighth binding site. PCR of Fluc-3'8MS2 confirmed the presence of an approximately 2000 base pair fragment in both the shuttle vector and virus, which presumably corresponds to Fluc-3'8MS2. As the PCR of the same amount of PPI-3'8MS2 or Fluc-3'8MS2 shuttle vector resulted in far less amplified Fluc-3'8MS2 than amplified PPI-3'8MS2, it is likely that the PCR of Fluc-3'8MS2 is less efficient than that of PPI-3'8MS2. Poor PCR efficiency is probably why Fluc-3'8MS2 did not amplify from the recombinant vector, even when Fluc-3'8MS2 was present in the virus.
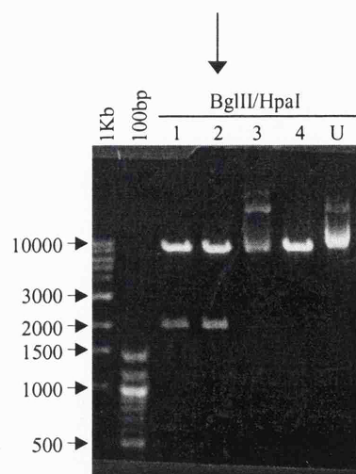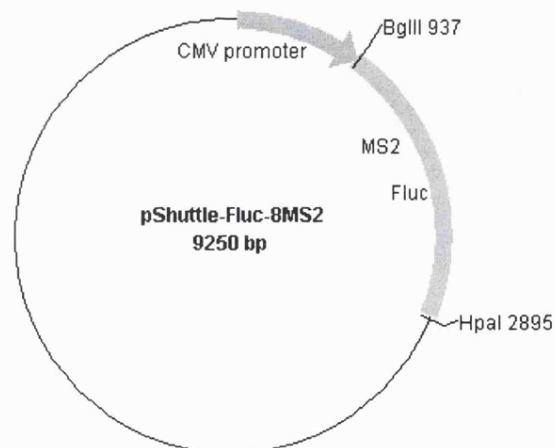
Figure A1.10: Construction of pShuttle-Fluc-3'8MS2 and confirmation of insert
Plasmid DNA was isolated from four colonies (1-4) and digested with BglII and HpaI or BglII and HindIII to check for positive pShuttle-Fluc-3'8MS2 colonies. pShuttle-Fluc-8MS2 was also cut with BglII and HpaI as a control (P). The digested plasmid DNA was run on a 1% agarose gel and DNA was stained with ethidium bromide.
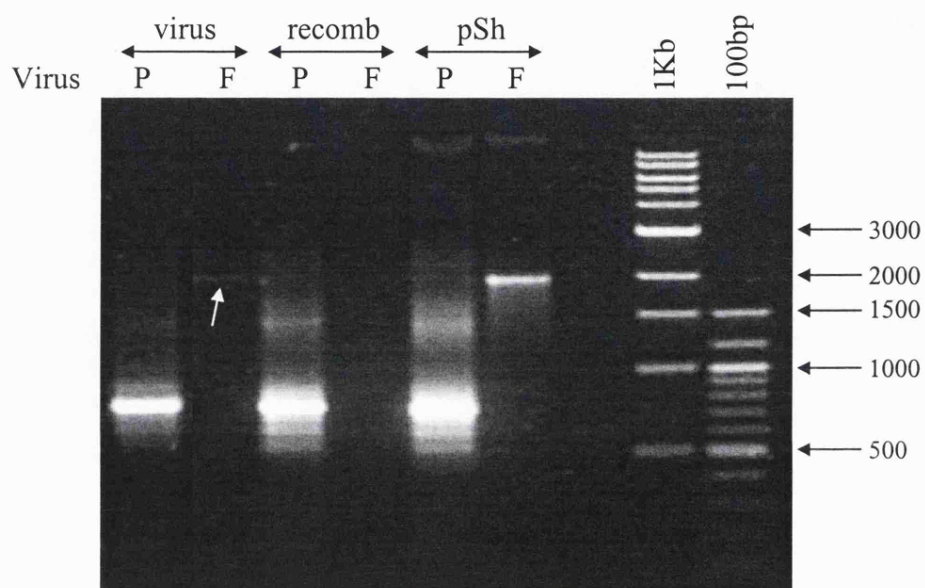
figure A1.11: PCR confirmed the presence of PPI-3'8MS2 and Fluc-3'8MS2 in the adenoviral genome

PPI-3'8MS2 (P) or Fluc-3'8MS2 (F) was amplified by PCR from 0.1μl of high titre virus, 100ng of recombinant plasmid DNA or 100ng of pShuttle plasmid DNA using the forward primers PPI-8MS2F or Fluc-8MS2F and the reverse primer, 8MS2R. 1/5 of each PCR reaction was run on a 1% agarose gel containing ethidium bromide.

A1.3: MS2 protein plasmids

A1.3.1: pShuttle-MS2

The cDNA sequence for MS2 protein was provided as pEGFP C1-MS2-NLS. A 1262 bp fragment containing EGFP-MS2-NLS was released by digestion of pEGFP C1-MS2-NLS with NheI and XbaI and ligated into pShuttle CMV that had been cut with XbaI and dephosphorylated with CIAP (figure A1.12). Positive colonies were confirmed by digestion with EcoRV and NotI to remove the insert and digestion with KpnI to check the orientation.

A1.3.2: pGEX4T3 MS2

To make a bacterial expression vector that would express MS2 fused to GST, MS2 was amplified from pEGFP C1-MS2-NLS with the 5' primer MS2-EXF that was complementary to the 5' end of MS2 and contained a BamHI restriction site at the 5' end and the 3' primer, MS2-EXR, that was complementary to the 3' end of MS2 and contained a XhoI restriction site at the 5' end (figure A1.13). The resultant PCR product was digested with BamHI and XhoI and ligated into pGEX4T3 that had also been digested with BamHI and XhoI. Positive colonies were confirmed by digestion with BamHI and XhoI or EcoRI and SalI.

Figure A1.12: Construction of pShuttle-GFP-MS2-NLS and confirmation of insert
Plasmid DNA was isolated from four colonies (1-4) and digested with NotI and EcoRV
to check for positive pShuttle-GFP-MS2-NLS colonies and with KpnI to check insert
orientation. pShuttle-CMV was also cut with NotI and EcoRV or KpnI as a control
(pS). The digested plasmid DNA was run on a 1-% agarose gel and DNA was stained
with ethidium bromide.

pShuttle CMV
7462 bp

KpnI 961
NotI 974
XbaI 996
EcoRV 1002

CMV promoter

pEGFP C1-MS2-NLS
5200 bp

NheI

EGFP

MS2 binding protein

Nuclear localisation signal
XbaI

Digested pShuttle CMV with XbaI, dephosphorylated with CIAP (7462 bp fragment)

Digested with NheI and XbaI to release EGFP-MS2-NLS (1262 bp fragment)

Ligated EGFP-MS2-NLS into digested pShuttle CMV

CMV promoter
KpnI 961
NotI 974
NheI ligated to XbaI 996

EGFP

pShuttle CMV-MS2
8724 bp

MS2

NLS

KpnI 2231
XbaI 2258
EcoRV 2264

Digested with NotI/EcoRV to remove insert and KpnI to check orientation

KpnI   NotI/EcoRV
1 2 3 4 pS 1Kb 100bp pS 1 2 3 4

← 10000
← 3000
← 1500
← 1000
← 500
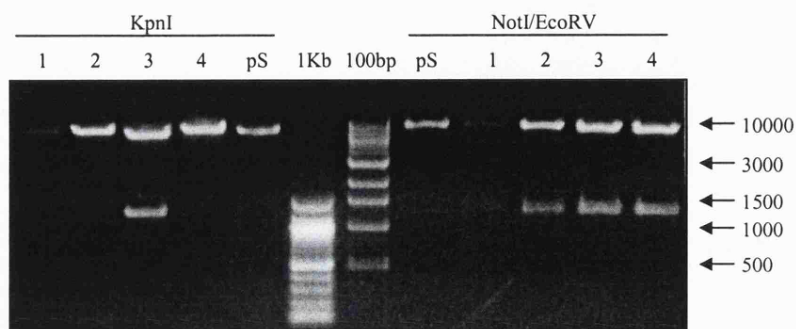
Colony 3 was positive

299

Figure A1.13: Construction of pGEX4T3 MS2 and confirmation of insert
Plasmid DNA was isolated from four colonies (1-3) and digested with BamHI and XhoI or SalI and EcoRI to check for positive pGGEX4T3 MS2 colonies. The digested plasmid DNA was run alongside the uncut plasmid on a 1-% agarose gel and DNA was stained with ethidium bromide.

pEGFP C1-MS2-NLS
5200 bp

NheI
EGFP
MS2 binding protein
Nuclear localisation signal
XbaI

pGEX4T3
4900 bp

tac promoter
GST
BamHI 930
XhoI 955
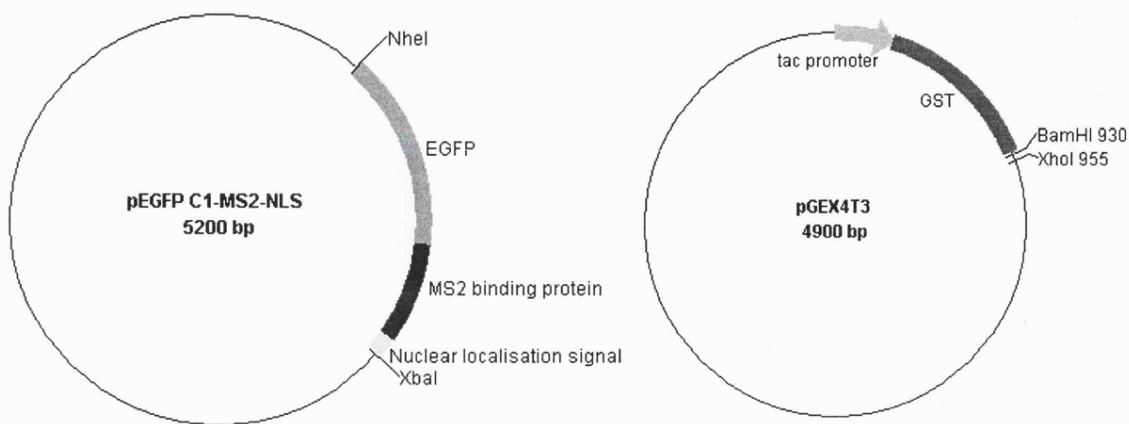
PCR of MS2 (primers: MS2-EXF and MS2-EXR). Digested PCR product with BamHI and XhoI (403 bp fragment)

pGEX4T3 digested with BamHI and XhoI (4875 bp fragment)

Ligated digested PCR product into digested pGEX4T3

pGEX4T3 MS2
5293 bp

tac promoter
GST
MS2
BamHI 930
SalI 961
EcoRI 1224
XhoI 1323
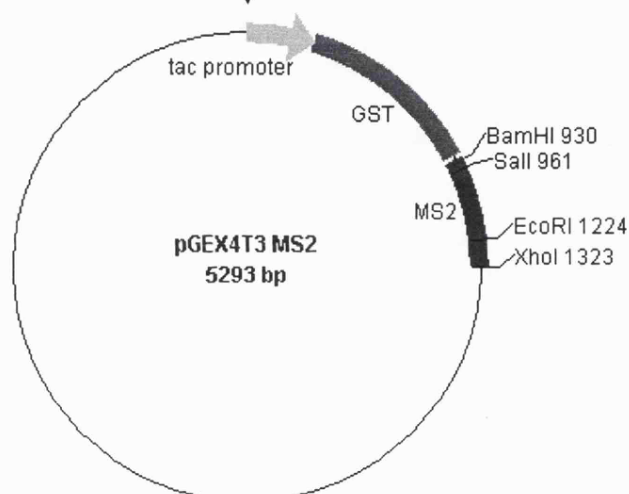
Digested with BamHI/XhoI and SalI/EcoRI to check insert

uncut   100bp 1Kb   BamHI/XhoI   SalI/EcoRI
1   2   3   1   2   3   1   2   3

← 10000
← 3000
← 2000
← 1500
← 1000
← 500
← 300
← 100
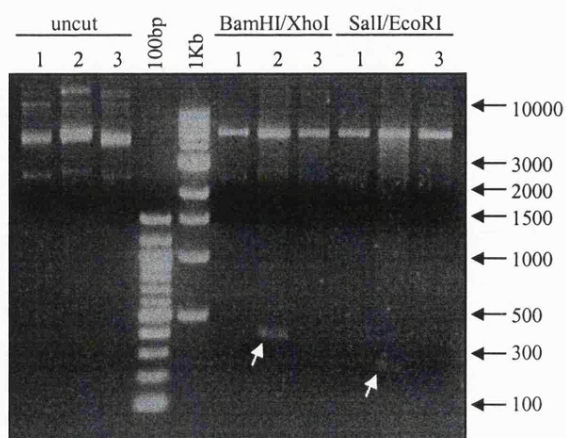
Colony 2 was positive

301

References

Abramson, R. D., Browning, K. S., Dever, T. E., Lawson, T. G., Thach, R. E., Ravel, J. M., and Merrick, W. C. (1988). Initiation factors that bind mRNA. A comparison of mammalian factors with wheat germ factors. J Biol Chem *263*, 5462-5467.

Abramson, R. D., Dever, T. E., Lawson, T. G., Ray, B. K., Thach, R. E., and Merrick, W. C. (1987). The ATP-dependent interaction of eukaryotic initiation factors with mRNA. J Biol Chem *262*, 3826-3832.

Adelman, M. R., Sabatini, D. D., and Blobel, G. (1973). Ribosome-membrane interaction. Nondestructive disassembly of rat liver rough microsomes into ribosomal and membranous components. J Cell Biol *56*, 206-229.

Ahmed, M., and Bergsten, P. (2005). Glucose-induced changes of multiple mouse islet proteins analysed by two-dimensional gel electrophoresis and mass spectrometry. Diabetologia *48*, 477-485.

Ainger, K., Avossa, D., Diana, A. S., Barry, C., Barbarese, E., and Carson, J. H. (1997). Transport and localization elements in myelin basic protein mRNA. J Cell Biol *138*, 1077-1087.

Alarcon, C., Lincoln, B., and Rhodes, C. (1993). The biosynthesis of the subtilisin-related proprotein convertase PC3, but not that of PC2 convertase, is regulated by glucose in parallel to proinsulin biosynthesis in rat pancreatic islets. The Journal of Biological Chemistry *268*, 4276-4280.

Alarcon, C., Wicksteed, B., Prentki, M., Corkey, B. E., and Rhodes, C. J. (2002). Succinate is a preferential metabolic stimulus-coupling signal for glucose-induced proinsulin biosynthesis translation. Diabetes *51*, 2496-2504.

Asano, K., Shalev, A., Phan, L., Nielsen, K., Clayton, J., Valasek, L., Donahue, T. F., and Hinnebusch, A. G. (2001). Multiple roles for the C-terminal domain of eIF5 in translation initiation complex assembly and GTPase activation. Embo J *20*, 2326-2337.

Ashcroft, S. J. (1980). Glucoreceptor mechanisms and the control of insulin release and biosynthesis. Diabetologia *18*, 5-15.

Ashcroft, S. J., Bunce, J., Lowry, M., Hansen, S. E., and Hedeskov, C. J. (1978). The effect of sugars on (pro)insulin biosynthesis. Biochem J *174*, 517-526.

Astrom, S. U., von Pawel-Rammingen, U., and Bystrom, A. S. (1993). The yeast initiator tRNAMet can act as an elongator tRNA(Met) in vivo. J Mol Biol *233*, 43-58.

Bacher, G., Pool, M., and Dobberstein, B. (1999). The ribosome regulates the GTPase of the beta-subunit of the signal recognition particle receptor. J Cell Biol *146*, 723-730.

Banerjee, A. K. (1980). 5'-terminal cap structure in eucaryotic messenger ribonucleic acids. Microbiol Rev *44*, 175-205.

Banerjee, D., and Slack, F. (2002). Control of developmental timing by small temporal RNAs: a paradigm for RNA-mediated regulation of gene expression. Bioessays *24*, 119-129.

Bardwell, V. J., and Wickens, M. (1990). Purification of RNA and RNA-protein complexes by an R17 coat protein affinity method. Nucleic Acids Res *18*, 6587-6594.

Bast, A., Wolf, G., Oberbaumer, I., and Walther, R. (2002). Oxidative and nitrosative stress induces peroxiredoxins in pancreatic beta cells. Diabetologia *45*, 867-876.

Batey, R. T., Rambo, R. P., Lucast, L., Rha, B., and Doudna, J. A. (2000). Crystal structure of the ribonucleoprotein core of the signal recognition particle. Science *287*, 1232-1239.

Beckmann, R., Bubeck, D., Grassucci, R., Penczek, P., Verschoor, A., Blobel, G., and Frank, J. (1997). Alignment of conduits for the nascent polypeptide chain in the ribosome-Sec61 complex. Science *278*, 2123-2126.

Beretta, L., Gingras, A. C., Svitkin, Y. V., Hall, M. N., and Sonenberg, N. (1996). Rapamycin blocks the phosphorylation of 4E-BP1 and inhibits cap-dependent initiation of translation. Embo J *15*, 658-664.

Bernstein, H. D., Poritz, M. A., Strub, K., Hoben, P. J., Brenner, S., and Walter, P. (1989). Model for signal sequence recognition from amino-acid sequence of 54K subunit of signal recognition particle. Nature *340*, 482-486.

Bertolotti, A., Zhang, Y., Hendershot, L. M., Harding, H. P., and Ron, D. (2000). Dynamic interaction of BiP and ER stress transducers in the unfolded-protein response. Nat Cell Biol *2*, 326-332.

Bi, X., and Goss, D. J. (2000). Wheat germ poly(A)-binding protein increases the ATPase and the RNA helicase activity of translation initiation factors eIF4A, eIF4B, and eIF-iso4F. J Biol Chem *275*, 17740-17746.

Biegel, D., and Pachter, J. S. (1992). mRNA association with the cytoskeletal framework likely represents a physiological binding event. J Cell Biochem *48*, 98-106.

Birse, D. E., Kapp, U., Strub, K., Cusack, S., and Aberg, A. (1997). The crystal structure of the signal recognition particle Alu RNA binding heterodimer, SRP9/14. Embo J *16*, 3757-3766.

Bollheimer, L. C., Skelly, R. H., Chester, M. W., McGarry, J. D., and Rhodes, C. J. (1998). Chronic exposure to free fatty acid reduces pancreatic beta cell insulin content by increasing basal insulin secretion that is not compensated for by a corresponding increase in proinsulin biosynthesis translation. J Clin Invest *101*, 1094-1101.

Bonneau, A. M., and Sonenberg, N. (1987). Involvement of the 24-kDa cap-binding protein in regulation of protein synthesis in mitosis. J Biol Chem *262*, 11134-11139.

Borman, A. M., Michel, Y. M., and Kean, K. M. (2000). Biochemical characterisation of cap-poly(A) synergy in rabbit reticulocyte lysates: the eIF4G-PABP interaction increases the functional affinity of eIF4E for the capped mRNA 5'-end. Nucleic Acids Res *28*, 4068-4075.

Brawerman, G. (1981). The Role of the poly(A) sequence in mammalian messenger RNA. CRC Crit Rev Biochem *10*, 1-38.

Breyton, C., Haase, W., Rapoport, T. A., Kuhlbrandt, W., and Collinson, I. (2002). Three-dimensional structure of the bacterial protein-translocation complex SecYEG. Nature *418*, 662-665.

Brunel, C., and Ehresmann, C. (2004). Secondary structure of the 3' UTR of bicoid mRNA. Biochimie *86*, 91-104.

Brunn, G. J., Hudson, C. C., Sekulic, A., Williams, J. M., Hosoi, H., Houghton, P. J., Lawrence, J. C., Jr., and Abraham, R. T. (1997). Phosphorylation of the translational repressor PHAS-I by the mammalian target of rapamycin. Science *277*, 99-101.

Brunstedt, J., and Chan, S. J. (1982). Direct effect of glucose on the preproinsulin mRNA level in isolated pancreatic islets. Biochem Biophys Res Commun *106*, 1383-1389.

Bu, X., Haas, D. W., and Hagedorn, C. H. (1993). Novel phosphorylation sites of eukaryotic initiation factor-4F and evidence that phosphorylation stabilizes interactions of the p25 and p220 subunits. J Biol Chem *268*, 4975-4978.

Calzone, F. J., Angerer, R. C., and Gorovsky, M. A. (1982). Regulation of protein synthesis in Tetrahymena: isolation and characterization of polysomes by gel filtration and precipitation at pH 5.3. Nucleic Acids Res *10*, 2145-2161.

Campbell, I. L., Hellquist, L. N. B., and Taylor, K. W. (1982). Insulin biosynthesis and its regulation. Clinical Science *62*, 449-455.

Campbell, L. E., Wang, X., and Proud, C. G. (1999). Nutrients differentially regulate multiple translation factors and their control by insulin. Biochem J *344 Pt 2*, 433-441.

Carrera, P., Johnstone, O., Nakamura, A., Casanova, J., Jackle, H., and Lasko, P. (2000). VASA mediates translation through interaction with a Drosophila yIF2 homolog. Mol Cell *5*, 181-187.

Ceci, M., Gaviraghi, C., Gorrini, C., Sala, L. A., Offenhauser, N., Marchisio, P. C., and Biffo, S. (2003). Release of eIF6 (p27BBP) from the 60S subunit allows 80S ribosome assembly. Nature *426*, 579-584.

Chakrabarti, A., and Maitra, U. (1991). Function of eukaryotic initiation factor 5 in the formation of an 80 S ribosomal polypeptide chain initiation complex. J Biol Chem *266*, 14039-14045.

Chaudhuri, J., Chowdhury, D., and Maitra, U. (1999). Distinct functions of eukaryotic translation initiation factors eIF1A and eIF3 in the formation of the 40 S ribosomal preinitiation complex. J Biol Chem *274*, 17975-17980.

Chaudhuri, J., Si, K., and Maitra, U. (1997). Function of eukaryotic translation initiation factor 1A (eIF1A) (formerly called eIF-4C) in initiation of protein synthesis. J Biol Chem *272*, 7883-7891.

Chen, J. J., Crosby, J. S., and London, I. M. (1994). Regulation of heme-regulated eIF-2 alpha kinase and its expression in erythroid cells. Biochimie *76*, 761-769.

Choi, S. K., Lee, J. H., Zoll, W. L., Merrick, W. C., and Dever, T. E. (1998). Promotion of met-tRNAiMet binding to ribosomes by yIF2, a bacterial IF2 homolog in yeast. Science *280*, 1757-1760.

Choi, S. K., Olsen, D. S., Roll-Mecak, A., Martung, A., Remo, K. L., Burley, S. K., Hinnebusch, A. G., and Dever, T. E. (2000). Physical and functional interaction between the eukaryotic orthologs of prokaryotic translation initiation factors IF1 and IF2. Mol Cell Biol *20*, 7183-7191.

Chou, T. (2003). Ribosome recycling, diffusion, and mRNA loop formation in translational regulation. Biophys J *85*, 755-773.

Clemens, M. J. (1997). PKR--a protein kinase regulated by double-stranded RNA. Int J Biochem Cell Biol *29*, 945-949.

Clemens, M. J., Pain, V. M., Wong, S. T., and Henshaw, E. C. (1982). Phosphorylation inhibits guanine nucleotide exchange on eukaryotic initiation factor 2. Nature *296*, 93-95.

Cohen, N., Sharma, M., Kentsis, A., Perez, J. M., Strudwick, S., and Borden, K. L. (2001). PML RING suppresses oncogenic transformation by reducing the affinity of eIF4E for mRNA. Embo J *20*, 4547-4559.

Colombo, S., Longhi, R., Alcaro, S., Ortuso, F., Sprocati, T., Flora, A., and Borgese, N. (2005). N-myristoylation determines dual targeting of mammalian NADH-cytochrome b5 reductase to ER and mitochondrial outer membranes by a mechanism of kinetic partitioning. J Cell Biol *168*, 735-745.

Colthurst, D. R., Campbell, D. G., and Proud, C. G. (1987). Structure and regulation of eukaryotic initiation factor eIF-2. Sequence of the site in the alpha subunit phosphorylated by the haem-controlled repressor and by the double-stranded RNA-activated inhibitor. Eur J Biochem *166*, 357-363.

Connolly, T., and Gilmore, R. (1989). The signal recognition particle receptor mediates the GTP-dependent displacement of SRP from the signal sequence of the nascent polypeptide. Cell *57*, 599-610.

Connolly, T., and Gilmore, R. (1993). GTP hydrolysis by complexes of the signal recognition particle and the signal recognition particle receptor. J Cell Biol *123*, 799-807.

Connolly, T., Rapiejko, P. J., and Gilmore, R. (1991). Requirement of GTP hydrolysis for dissociation of the signal recognition particle from its receptor. Science *252*, 1171-1173.

Cosson, B., Couturier, A., Chabelskaya, S., Kiktev, D., Inge-Vechtomov, S., Philippe, M., and Zhouravleva, G. (2002). Poly(A)-binding protein acts in translation termination via eukaryotic release factor 3 interaction and does not influence [PSI(+)] propagation. Mol Cell Biol *22*, 3301-3315.

Crowley, K. S., Liao, S., Worrell, V. E., Reinhart, G. D., and Johnson, A. E. (1994). Secretory proteins move through the endoplasmic reticulum membrane via an aqueous, gated pore. Cell *78*, 461-471.

Crowley, K. S., Reinhart, G. D., and Johnson, A. E. (1993). The signal sequence moves through a ribosomal tunnel into a noncytoplasmic aqueous environment at the ER membrane early in translocation. Cell *73*, 1101-1115.

da Silva Xavier, G., Varadi, A., Ainscow, E. K., and Rutter, G. A. (2000). Regulation of gene expression by glucose in pancreatic beta -cells (MIN6) via insulin secretion and activation of phosphatidylinositol 3'-kinase. J Biol Chem *275*, 36269-36277.

Das, S., Ghosh, R., and Maitra, U. (2001). Eukaryotic translation initiation factor 5 functions as a GTPase-activating protein. J Biol Chem *276*, 6720-6726.

Das, S., and Maitra, U. (2001). Functional significance and mechanism of eIF5-promoted GTP hydrolysis in eukaryotic translation initiation. Prog Nucleic Acid Res Mol Biol 70, 207-231.

Delepine, M., Nicolino, M., Barrett, T., Golamaully, M., Lathrop, G. M., and Julier, C. (2000). EIF2AK3, encoding translation initiation factor 2-alpha kinase 3, is mutated in patients with Wolcott-Rallison syndrome. Nat Genet 25, 406-409.

Deshaies, R. J., and Schekman, R. (1987). A yeast mutant defective at an early stage in import of secretory protein precursors into the endoplasmic reticulum. J Cell Biol 105, 633-645.

Dever, T. E., Chen, J. J., Barber, G. N., Cigan, A. M., Feng, L., Donahue, T. F., London, I. M., Katze, M. G., and Hinnebusch, A. G. (1993). Mammalian eukaryotic initiation factor 2 alpha kinases functionally substitute for GCN2 protein kinase in the GCN4 translational control mechanism of yeast. Proc Natl Acad Sci U S A 90, 4616-4620.

Donaldson, R. W., Hagedorn, C. H., and Cohen, S. (1991). Epidermal growth factor or okadaic acid stimulates phosphorylation of eukaryotic initiation factor 4F. J Biol Chem 266, 3162-3166.

Duggan, D. J., Bittner, M., Chen, Y., Meltzer, P., and Trent, J. M. (1999). Expression profiling using cDNA microarrays. Nature Genetics 21, 10-14.

Duncan, R., Milburn, S. C., and Hershey, J. W. (1987). Regulated phosphorylation and low abundance of HeLa cell initiation factor eIF-4F suggest a role in translational control. Heat shock effects on eIF-4F. J Biol Chem 262, 380-388.

Duncan, R. F., and Hershey, J. W. (1989). Protein synthesis and protein phosphorylation during heat stress, recovery, and adaptation. J Cell Biol 109, 1467-1481.

Ephrussi, A., Dickinson, L. K., and Lehmann, R. (1991). Oskar organizes the germ plasm and directs localization of the posterior determinant nanos. Cell 66, 37-50.

Esnault, Y., Blondel, M. O., Deshaies, R. J., Scheckman, R., and Kepes, F. (1993). The yeast SSS1 gene is essential for secretory protein translocation and encodes a conserved protein of the endoplasmic reticulum. Embo J 12, 4083-4093.

Esnault, Y., Feldheim, D., Blondel, M. O., Schekman, R., and Kepes, F. (1994). SSS1 encodes a stabilizing component of the Sec61 subcomplex of the yeast protein translocation apparatus. J Biol Chem 269, 27478-27485.

Farruggio, D., Chaudhuri, J., Maitra, U., and RajBhandary, U. L. (1996). The A1 x U72 base pair conserved in eukaryotic initiator tRNAs is important specifically for binding to the eukaryotic translation initiation factor eIF2. Mol Cell Biol *16*, 4248-4256.

Finke, K., Plath, K., Panzner, S., Prehn, S., Rapoport, T. A., Hartmann, E., and Sommer, T. (1996). A second trimeric complex containing homologs of the Sec61p complex functions in protein transport across the ER membrane of S. cerevisiae. Embo J *15*, 1482-1494.

Flamez, D., Berger, V., Kruhoffer, M., Orntoft, T., Pipeleers, D., and Schuit, F. C. (2002). Critical role for cataplerosis via citrate in glucose-regulated insulin release. Diabetes *51*, 2018-2024.

Flanagan, J. J., Chen, J. C., Miao, Y., Shao, Y., Lin, J., Bock, P. E., and Johnson, A. E. (2003). Signal recognition particle binds to ribosome-bound signal sequences with fluorescence-detected subnanomolar affinity that does not diminish as the nascent chain lengthens. J Biol Chem *278*, 18628-18637.

Flynn, A., and Proud, G. (1996). Insulin-stimulated phosphorylation of initiation factor 4E is mediated by the MAP kinase pathway. FEBS Lett *389*, 162-166.

Fons, R. D., Bogert, B. A., and Hegde, R. S. (2003). Substrate-specific function of the translocon-associated protein complex during translocation across the ER membrane. J Cell Biol *160*, 529-539.

Frederickson, R. M., Mushynski, W. E., and Sonenberg, N. (1992). Phosphorylation of translation initiation factor eIF-4E is induced in a ras-dependent manner during nerve growth factor-mediated PC12 cell differentiation. Mol Cell Biol *12*, 1239-1247.

Frey, S., Pool, M., and Seedorf, M. (2001). Scp160p, an RNA-binding protein, polysome-associated protein, localizes to the endoplasmic reticulum of *Saccharomyces cerevisea* in a microtubule-dependent manner. The Journal of Biological Chemistry *276*, 15905-15912.

Freymann, D. M., Keenan, R. J., Stroud, R. M., and Walter, P. (1997). Structure of the conserved GTPase domain of the signal recognition particle. Nature *385*, 361-364.

Freymann, D. M., Keenan, R. J., Stroud, R. M., and Walter, P. (1999). Functional changes in the structure of the SRP GTPase on binding GDP and Mg2+GDP. Nat Struct Biol *6*, 793-801.

Fukunaga, R., and Hunter, T. (1997). MNK1, a new MAP kinase-activated protein kinase, isolated by a novel expression screening method for identifying protein kinase substrates. Embo J *16*, 1921-1933.

Fulga, T. A., Sinning, I., Dobberstein, B., and Pool, M. R. (2001). SRβ coordinates signal sequence release from SRP with ribosome binding to the translocon. EMBO Journal *20*, 2338-2347.

Gallie, D. R. (1991). The cap and poly(A) tail function synergistically to regulate mRNA translational efficiency. Genes Dev *5*, 2108-2116.

Garcia, M. J., Ravier, M. A., Rolland, J. F., Gilon, P., Nenquin, M., and Henquin, J. C. (2001). Inhibition of protein synthesis sequentially impairs distinct steps of stimulus-secretion coupling in pancreatic beta cells. Endocrinology *142*, 299-307.

Garcia, P. D., and Walter, P. (1988). Full-length prepro-alpha-factor can be translocated across the mammalian microsomal membrane only if translation has not terminated. J Cell Biol *106*, 1043-1048.

Gavis, E. R., and Lehmann, R. (1992). Localization of nanos RNA controls embryonic polarity. Cell *71*, 301-313.

Giddings, S. J., Chirgwin, J., and Permutt, M. A. (1982). Effects of glucose on proinsulin messenger RNA in rats in vivo. Diabetes *31*, 624-629.

Gilligan, M., Welsh, G. I., Flynn, A., Bujalska, I., Diggle, T. A., Denton, R. M., Proud, C. G., and Docherty, K. (1996). Glucose stimulates the activity of the guanine nucleotide-exchange factor eIF2B in isolated rat islets of Langerhans. The Journal of Biological Chemistry *271*, 2121-2125.

Gingras, A. C., Kennedy, S. G., O'Leary, M. A., Sonenberg, N., and Hay, N. (1998). 4E-BP1, a repressor of mRNA translation, is phosphorylated and inactivated by the Akt(PKB) signaling pathway. Genes Dev *12*, 502-513.

Gingras, A. C., Raught, B., and Sonenberg, N. (1999). eIF4 initiation factors: effectors of mRNA recruiment to ribosomes and regulators of translation. Annual Review Biochemistry *68*, 913-963.

Gomez, E., Powell, M. L., Greenman, I. C., and Herbert, T. P. (2004). Glucose-stimulated protein synthesis in pancreatic beta-cells parallels an increase in the availability of the translational ternary complex (eIF2-GTP.Met-tRNAi) and the dephosphorylation of eIF2 alpha. J Biol Chem *279*, 53937-53946.

Gorlich, D., Hartmann, E., Prehn, S., and Rapoport, T. A. (1992). A protein of the endoplasmic reticulum involved early in polypeptide translocation. Nature *357*, 47-52.

Gorlich, D., and Rapoport, T. A. (1993). Protein translocation into proteoliposomes reconstituted from purified components of the endoplasmic reticulum membrane. Cell *75*, 615-630.

Goss, D. J., Rounds, D., Harrigan, T., Woodley, C. L., and Wahba, A. J. (1988). Effects of eucaryotic initiation factor 3 on eucaryotic ribosomal subunit equilibrium and kinetics. Biochemistry *27*, 1489-1494.

Goyer, C., Altmann, M., Lee, H. S., Blanc, A., Deshmukh, M., Woolford, J. L., Jr., Trachsel, H., and Sonenberg, N. (1993). TIF4631 and TIF4632: two yeast genes encoding the high-molecular-weight subunits of the cap-binding protein complex (eukaryotic initiation factor 4F) contain an RNA recognition motif-like sequence and carry out an essential function. Mol Cell Biol *13*, 4860-4874.

Grankvist, K., Marklund, S. L., and Taljedal, I. B. (1981). CuZn-superoxide dismutase, Mn-superoxide dismutase, catalase and glutathione peroxidase in pancreatic islets and other tissues in the mouse. Biochem J *199*, 393-398.

Grifo, J. A., Tahara, S. M., Leis, J. P., Morgan, M. A., Shatkin, A. J., and Merrick, W. C. (1982). Characterization of eukaryotic initiation factor 4A, a protein involved in ATP-dependent binding of globin mRNA. J Biol Chem *257*, 5246-5252.

Grimaldi, K. A., Siddle, K., and Hutton, J. C. (1987). Biosynthesis of insulin secretory granule membrane proteins. Control by glucose. Biochemical Journal.

Grund, E. M., Spyropoulos, D. D., Watson, D. K., and Muise-Helmericks, R. C. (2005). Interleukins 2 and 15 regulate Ets1 expression via ERK1/2 and MNK1 in human natural killer cells. J Biol Chem *280*, 4772-4778.

Guest, C., Bailyes, E. M., Rutherford, N. G., and Hutton, J. C. (1991). Insulin secretory granule biogenesis. Co-ordinateregulation of the biosynthesis of the majority of constituent proteins. Biochemical Journal *274*, 73-78.

Guest, P. C., Rhodes, C., and Hutton, J. C. (1989). Regulation of the biosynthesis of insulin secretory granule proteins. Co-ordinate translational control is exerted on some, but not all, granule matrix constituents. Biochemical Journal *257*, 411-437.

Gundelfinger, E. D., Krause, E., Melli, M., and Dobberstein, B. (1983). The organization of the 7SL RNA in the signal recognition particle. Nucleic Acids Res *11*, 7363-7374.

Haghighat, A., Mader, S., Pause, A., and Sonenberg, N. (1995). Repression of cap-dependent translation by 4E-binding protein 1: competition with p220 for binding to eukaryotic initiation factor-4E. Embo J *14*, 5701-5709.

Haguenauer, A., Raimbault, S., Masscheleyn, S., Gonzalez-Barroso, M. D., Criscuolo, F., Plamondon, J., Miroux, B., Ricquier, D., Richard, D., Bouillaud, F., and Pecqueur,

C. (2005). A new renal mitochondrial carrier, KMCP1, is upregulated during tubular cell regeneration and induction of antioxidant enzymes. J Biol Chem.

Hainzl, T., Huang, S., and Sauer-Eriksson, A. E. (2002). Structure of the SRP19 RNA complex and implications for signal recognition particle assembly. Nature *417*, 767-771.

Halic, M., Becker, T., Pool, M. R., Spahn, C. M., Grassucci, R. A., Frank, J., and Beckmann, R. (2004). Structure of the signal recognition particle interacting with the elongation-arrested ribosome. Nature *427*, 808-814.

Hamman, B. D., Chen, J. C., Johnson, E. E., and Johnson, A. E. (1997). The aqueous pore through the translocon has a diameter of 40-60 A during cotranslational protein translocation at the ER membrane. Cell *89*, 535-544.

Hamman, B. D., Hendershot, L. M., and Johnson, A. E. (1998). BiP maintains the permeability barrier of the ER membrane by sealing the lumenal end of the translocon pore before and early in translocation. Cell *92*, 747-758.

Hanein, D., Matlack, K. E., Jungnickel, B., Plath, K., Kalies, K. U., Miller, K. R., Rapoport, T. A., and Akey, C. W. (1996). Oligomeric rings of the Sec61p complex induced by ligands required for protein translocation. Cell *87*, 721-732.

Harding, H. P., Novoa, I., Zhang, Y., Zeng, H., Wek, R., Schapira, M., and Ron, D. (2000a). Regulated translation initiation controls stress-induced gene expression in mammalian cells. Molecular cell *6*, 1099-1108.

Harding, H. P., Novoa, I., Zhang, Y., Zeng, H., Wek, R., Schapira, M., and Ron, D. (2000b). Regulated translation initiation controls stress-induced gene expression in mammalian cells. Mol Cell *6*, 1099-1108.

Harding, H. P., Zeng, H., Zhang, Y., Jungries, R., Chung, P., Plesken, H., Sabatini, D. D., and Ron, D. (2001). Diabetes mellitus and exocrine pancreatic dysfunction in perk-/- mice reveals a role for translational control in secretory cell survival. Mol Cell *7*, 1153-1163.

Harding, H. P., Zhang, Y., Bertolotti, A., Zeng, H., and Ron, D. (2000c). Perk is essential for translational regulation and cell survival during the unfolded protein response. Mol Cell *5*, 897-904.

Harding, H. P., Zhang, Y., and Ron, D. (1999). Protein translation and folding are coupled by an endoplasmic-reticulum-resident kinase. Nature *397*, 271-274.

Hattori, S., Ulsh, L. S., Halliday, K., and Shih, T. Y. (1985). Biochemical properties of a highly purified v-rasH p21 protein overproduced in Escherichia coli and inhibition of its activities by a monoclonal antibody. Mol Cell Biol *5*, 1449-1455.

Hauser, S., Bacher, G., Dobberstein, B., and Lutcke, H. (1995). A complex of the signal sequence binding protein and the SRP RNA promotes translocation of nascent proteins. Embo J *14*, 5485-5493.

He, H., von der Haar, T., Singh, C. R., Ii, M., Li, B., Hinnebusch, A. G., McCarthy, J. E., and Asano, K. (2003). The yeast eukaryotic initiation factor 4G (eIF4G) HEAT domain interacts with eIF1 and eIF5 and is involved in stringent AUG selection. Mol Cell Biol *23*, 5431-5445.

He, T., Zhou, S., Da Costa, L. T., Yu, J., Kinzler, K. W., and Vogelstein, B. (1998). A simplified system for generating recombinant adenoviruses. PNAS *95*, 2509-2514.

Hegde, R. S., Voigt, S., Rapoport, T. A., and Lingappa, V. R. (1998). TRAM regulates the exposure of nascent secretory proteins to the cytosol during translocation into the endoplasmic reticulum. Cell *92*, 621-631.

Helmers, J., Schmidt, D., Glavy, J. S., Blobel, G., and Schwartz, T. (2003). The beta-subunit of the protein-conducting channel of the endoplasmic reticulum functions as the guanine nucleotide exchange factor for the beta-subunit of the signal recognition particle receptor. J Biol Chem *278*, 23686-23690.

Hentze, M. W. (1997). eIF4G: a multipurpose ribosome adaptor. Science *275*, 500-501.

Herbert, T. P., Kilhams, G. R., Batty, I., and Proud, C. (2000). Distinct signalling pathways mediate insulin and phorbal ester-stimulated Eukaryotic Initiation Factor 4F assembly and protein synthesis in HEK 293 cells. The Journal of Biological Chemistry *275*, 11249-11256.

Hershey, J., and Merrick, W. C. (2000). Pathway and mechanism of initiation and protein synthesis. In Translational Control of Gene Expression, N. Sonenberg, J. Hershey, and M. Matthews, eds. (New York, Cold Spring Harbor Laboratory Press), pp. 33-89.

Hesketh, J. E., and Pryme, I. F. (1991). Interaction between mRNA, ribosomes and the cytoskeleton. Biochem J *277 (Pt 1)*, 1-10.

Hinnebusch, A. G. (2000). Mechanism and regulation of intiator methionyl tRNA binding to ribosomes. In Translational Control of Gene Expression, N. Sonenberg, J. Hershey, and M. Matthews, eds. (New York, Cold Spring Harbor Laboratory Press), pp. 185-243.

Hiremath, L. S., Webb, N. R., and Rhoads, R. E. (1985). Immunological detection of the messenger RNA cap-binding protein. J Biol Chem *260*, 7843-7849.

Hoek, K. S., Kidd, G. J., Carson, J. H., and Smith, R. (1998). hnRNP A2 selectively binds the cytoplasmic transport sequence of myelin basic protein mRNA. Biochemistry *37*, 7021-7029.

Hoenig, M., and Matschinsky, F. M. (1987). HPLC analysis of nucleotide profiles in glucose-stimulated perifused rat islets. Metabolism *36*, 295-301.

Hollingsworth, M. J., Kim, J. K., and Stollar, N. E. (1998). Heelprinting analysis of in vivo ribosome pause sites. Methods Mol Biol *77*, 153-165.

Holmgren, A. (1985). Thioredoxin. Annu Rev Biochem *54*, 237-271.

Hoshino, S., Imai, M., Kobayashi, T., Uchida, N., and Katada, T. (1999). The eukaryotic polypeptide chain releasing factor (eRF3/GSPT) carrying the translation termination signal to the 3'-Poly(A) tail of mRNA. Direct association of erf3/GSPT with polyadenylate-binding protein. J Biol Chem *274*, 16677-16680.

Hotta, M., Tashiro, F., Ikegami, H., Niwa, H., Ogihara, T., Yodoi, J., and Miyazaki, J. (1998). Pancreatic beta cell-specific expression of thioredoxin, an antioxidative and antiapoptotic protein, prevents autoimmune and streptozotocin-induced diabetes. J Exp Med *188*, 1445-1451.

Huang, H. K., Yoon, H., Hannig, E. M., and Donahue, T. F. (1997). GTP hydrolysis controls stringent selection of the AUG start codon during translation initiation in Saccharomyces cerevisiae. Genes Dev *11*, 2396-2413.

Hunt, S. L., Hsuan, J. J., Totty, N., and Jackson, R. J. (1999). unr, a cellular cytoplasmic RNA-binding protein with five cold-shock domains, is required for internal initiation of translation of human rhinovirus RNA. Genes Dev *13*, 437-448.

Iizuka, N., Najita, L., Franzusoff, A., and Sarnow, P. (1994). Cap-dependent and cap-independent translation by internal initiation of mRNAs in cell extracts prepared from Saccharomyces cerevisiae. Mol Cell Biol *14*, 7322-7330.

Imataka, H., Gradi, A., and Sonenberg, N. (1998). A newly identified N-terminal amino acid sequence of human eIF4G binds poly(A)-binding protein and functions in poly(A)-dependent translation. Embo J *17*, 7480-7489.

Itoh, N., and Okamoto, H. (1980). Translational control of proinsulin synthesis by glucose. Nature *283*, 100-102.

Itoh, N., Sei, T., Nose, K., and Okamoto, H. (1978). Glucose stimulation of the proinsulin synthesis in isolated pancreatic islets without increasing amount of proinsulin mRNA. FEBS Lett *93*, 343-347.

Jagath, J. R., Rodnina, M. V., and Wintermeyer, W. (2000). Conformational changes in the bacterial SRP receptor FtsY upon binding of guanine nucleotides and SRP. J Mol Biol *295*, 745-753.

Jagus, R., Joshi, B., and Barber, G. N. (1999). PKR, apoptosis and cancer. Int J Biochem Cell Biol *31*, 123-138.

Jahr, H., Schroder, D., Ziegler, B., Ziegler, M., and Zuhlke, H. (1980a). Transcriptional and translational control of glucose-stimulated (pro)insulin biosynthesis. European Journal Biochemistry *110*, 499-505.

Jahr, H., Schroder, D., Ziegler, B., Ziegler, M., and Zuhlke, H. (1980b). Transcriptional and translational control of glucose-stimulated (pro)insulin biosynthesis. Eur J Biochem *110*, 499-505.

Johannes, G., Carter, M. S., Eisen, M. B., Brown, P. O., and Sarnow, P. (1999). Identification of eukaryotic mRNAs that are translated at reduced cap binding complex eIF4F concentrations using a cDNA microarray. Proc Natl Acad Sci U S A *96*, 13118-13123.

Johannes, G., and Sarnow, P. (1998). Cap-independent polysomal association of natural mRNAs encoding c-myc, BiP, and eIF4G conferred by internal ribosome entry sites. Rna *4*, 1500-1513.

Joshi, B., Cai, A. L., Keiper, B. D., Minich, W. B., Mendez, R., Beach, C. M., Stepinski, J., Stolarski, R., Darzynkiewicz, E., and Rhoads, R. E. (1995). Phosphorylation of eukaryotic protein synthesis initiation factor 4E at Ser-209. J Biol Chem *270*, 14597-14603.

Jousse, C., Oyadomari, S., Novoa, I., Lu, P., Zhang, Y., Harding, H. P., and Ron, D. (2003). Inhibition of a constitutive translation initiation factor 2alpha phosphatase, CReP, promotes survival of stressed cells. J Cell Biol *163*, 767-775.

Jungnickel, B., and Rapoport, T. A. (1995). A posttargeting signal sequence recognition event in the endoplasmic reticulum membrane. Cell *82*, 261-270.

Junn, E., Han, S. H., Im, J. Y., Yang, Y., Cho, E. W., Um, H. D., Kim, D. K., Lee, K. W., Han, P. L., Rhee, S. G., and Choi, I. (2000). Vitamin D3 up-regulated protein 1 mediates oxidative stress via suppressing the thioredoxin function. J Immunol *164*, 6287-6295.

Kahvejian, A., Svitkin, Y. V., Sukarieh, R., M'Boutchou, M. N., and Sonenberg, N. (2005). Mammalian poly(A)-binding protein is a eukaryotic translation initiation factor, which acts via multiple mechanisms. Genes Dev *19*, 104-113.

Kajimoto, Y., and Kaneto, H. (2004). Role of oxidative stress in pancreatic beta-cell dysfunction. Ann N Y Acad Sci *1011*, 168-176.

Kalies, K. U., Gorlich, D., and Rapoport, T. A. (1994). Binding of ribosomes to the rough endoplasmic reticulum mediated by the Sec61p-complex. J Cell Biol *126*, 925-934.

Kalies, K. U., Rapoport, T. A., and Hartmann, E. (1998). The beta subunit of the Sec61 complex facilitates cotranslational protein transport and interacts with the signal peptidase during translocation. J Cell Biol *141*, 887-894.

Kaminski, A., and Jackson, R. J. (1998). The polypyrimidine tract binding protein (PTB) requirement for internal initiation of translation of cardiovirus RNAs is conditional rather than absolute. Rna *4*, 626-638.

Kaneto, H., Fujii, J., Myint, T., Miyazawa, N., Islam, K. N., Kawasaki, Y., Suzuki, K., Nakamura, M., Tatsumi, H., Yamasaki, Y., and Taniguchi, N. (1996). Reducing sugars trigger oxidative modification and apoptosis in pancreatic beta-cells by provoking oxidative stress through the glycation reaction. Biochem J *320 (Pt 3)*, 855-863.

Kaneto, H., Xu, G., Fujii, N., Kim, S., Bonner-Weir, S., and Weir, G. C. (2002). Involvement of c-Jun N-terminal kinase in oxidative stress-mediated suppression of insulin gene expression. J Biol Chem *277*, 30010-30018.

Kapp, L. D., and Lorsch, J. R. (2004). The molecular mechanics of eukaryotic translation. Annu Rev Biochem *73*, 657-704.

Katahira, H., Nagamatsu, S., Ozawa, S., Nakamichi, Y., Yamaguchi, S., Furukawa, H., Takizawa, M., Yoshimoto, K., Itagaki, E., and Ishida, H. (2001). Acute inhibition of proinsulin biosynthesis at the translational level by palmitic acid. Biochem Biophys Res Commun *282*, 507-510.

Keenan, R. J., Freymann, D. M., Stroud, R. M., and Walter, P. (2001). The signal recognition particle. Annual Review of Biochemistry *70*, 755-775.

Knight, S. W., and Docherty, K. (1992). RNA-protein interactions in the 5' untranslated region of preproinsulin mRNA. Journal of Molecular Endocrinology *8*, 1-10.

Knoch, K. P., Bergert, H., Borgonovo, B., Saeger, H. D., Altkruger, A., Verkade, P., and Solimena, M. (2004). Polypyrimidine tract-binding protein promotes insulin secretory granule biogenesis. Nat Cell Biol *6*, 207-214.

Kojima, E., Takeuchi, A., Haneda, M., Yagi, A., Hasegawa, T., Yamaki, K., Takeda, K., Akira, S., Shimokata, K., and Isobe, K. (2003). The function of GADD34 is a recovery from a shutoff of protein synthesis induced by ER stress: elucidation by GADD34-deficient mice. Faseb J *17*, 1573-1575.

Korneeva, N. L., First, E. A., Benoit, C. A., and Rhoads, R. E. (2004). Interaction between the NH2-terminal domain of eIF4A and the central domain of eIF4G modulates RNA-stimulated ATPase activity. J Biol Chem.

Koromilas, A. E., Lazaris-Karatzas, A., and Sonenberg, N. (1992). mRNAs containing extensive secondary structure in their 5' non-coding region translate efficiently in cells overexpressing initiation factor eIF-4E. Embo J *11*, 4153-4158.

Kozak, M. (1980a). Evaluation of the "scanning model" for initiation of protein synthesis in eucaryotes. Cell *22*, 7-8.

Kozak, M. (1980b). Role of ATP in binding and migration of 40S ribosomal subunits. Cell *22*, 459-467.

Kozak, M. (1986a). Influences of mRNA secondary structure on initiation by eukaryotic ribosomes. Proc Natl Acad Sci U S A *83*, 2850-2854.

Kozak, M. (1986b). Point mutations define a sequence flanking the AUG initiator codon that modulates translation by eukaryotic ribosomes. Cell *44*, 283-292.

Kozak, M. (1987a). An analysis of 5'-noncoding sequences from 699 vertebrate messenger RNAs. Nucleic Acids Res *15*, 8125-8148.

Kozak, M. (1987b). At least six nucleotides preceding the AUG initiator codon enhance translation in mammalian cells. J Mol Biol *196*, 947-950.

Kozak, M. (1989a). Circumstances and mechanisms of inhibition of translation by secondary structure in eucaryotic mRNAs. Mol Cell Biol *9*, 5134-5142.

Kozak, M. (1989b). The scanning model for translation: an update. J Cell Biol *108*, 229-241.

Kozak, M. (1992). Regulation of translation in eukaryotic systems. Anuual Review of Cell Biology *8*, 197-225.

Kozak, M. (2004). How strong is the case for regulation of the initiation step of translation by elements at the 3' end of eukaryotic mRNAs? Gene *343*, 41-54.

Krieg, U. C., Walter, P., and Johnson, A. E. (1986). Photocrosslinking of the signal sequence of nascent preprolactin to the 54-kilodalton polypeptide of the signal recognition particle. Proc Natl Acad Sci U S A *83*, 8604-8608.

Kurzchalia, T. V., Wiedmann, M., Girshovich, A. S., Bochkareva, E. S., Bielka, H., and Rapoport, T. A. (1986). The signal sequence of nascent preprolactin interacts with the 54K polypeptide of the signal recognition particle. Nature *320*, 634-636.

Lachance, P. E., Miron, M., Raught, B., Sonenberg, N., and Lasko, P. (2002). Phosphorylation of eukaryotic translation initiation factor 4E is critical for growth. Mol Cell Biol *22*, 1656-1663.

Lago, H., Parrott, A. M., Moss, T., Stonehouse, N. J., and Stockley, P. G. (2001). Probing the kinetics of formation of the bacteriophage MS2 translational operator complex: identification of a protein conformer unable to bind RNA. J Mol Biol *305*, 1131-1144.

Lamphear, B. J., Kirchweger, R., Skern, T., and Rhoads, R. E. (1995). Mapping of functional domains in eukaryotic protein synthesis initiation factor 4G (eIF4G) with picornaviral proteases. Implications for cap-dependent and cap-independent translational initiation. J Biol Chem *270*, 21975-21983.

Lamphear, B. J., and Panniers, R. (1990). Cap binding protein complex that restores protein synthesis in heat- shocked Ehrlich cell lysates contains highly phosphorylated eIF-4E. The Journal of Biological Chemistry *265*, 5333-5336.

Lang, B. D., and Fridovich-Keil, J. L. (2000). Scp160p, a multiple KH-domain protein, is a component of mRNP complexes in yeast. Nucleic Acids Res *28*, 1576-1584.

Lawson, T. G., Ray, B. K., Dodds, J. T., Grifo, J. A., Abramson, R. D., Merrick, W. C., Betsch, D. F., Weith, H. L., and Thach, R. E. (1986). Influence of 5' proximal secondary structure on the translational efficiency of eukaryotic mRNAs and on their interaction with initiation factors. J Biol Chem *261*, 13979-13989.

Le, H., Tanguay, R. L., Balasta, M. L., Wei, C. C., Browning, K. S., Metz, A. M., Goss, D. J., and Gallie, D. R. (1997). Translation initiation factors eIF-iso4G and eIF-4B interact with the poly(A)-binding protein and increase its RNA binding activity. J Biol Chem *272*, 16247-16255.

Lee, H. C., and Bernstein, H. D. (2001). The targeting pathway of Escherichia coli presecretory and integral membrane proteins is specified by the hydrophobicity of the targeting signal. Proc Natl Acad Sci U S A *98*, 3471-3476.

Lee, J. H., Pestova, T. V., Shin, B. S., Cao, C., Choi, S. K., and Dever, T. E. (2002). Initiation factor eIF5B catalyzes second GTP-dependent step in eukaryotic translation initiation. Proc Natl Acad Sci U S A *99*, 16689-16694.

Lee, K. A., Guertin, D., and Sonenberg, N. (1983). mRNA secondary structure as a determinant in cap recognition and initiation complex formation. ATP-Mg2+ independent cross-linking of cap binding proteins to m7I-capped inosine-substituted reovirus mRNA. J Biol Chem *258*, 707-710.

Legate, K. R., and Andrews, D. W. (2003). The beta-subunit of the signal recognition particle receptor is a novel GTP-binding protein without intrinsic GTPase activity. J Biol Chem *278*, 27712-27720.

Leibiger, B., Leibiger, I. B., Moede, T., Kemper, S., Kulkarni, R. N., Kahn, C. R., de Vargas, L. M., and Berggren, P. O. (2001). Selective insulin signaling through A and B insulin receptors regulates transcription of insulin and glucokinase genes in pancreatic beta cells. Mol Cell *7*, 559-570.

Leibiger, B., Moede, T., Schwarz, T., Brown, G. R., Kohler, M., Leibiger, I. B., and Berggren, P. (1998). Short-term regulation of insulin gene transcription by glucose. PNAS *95*, 9307-9312.

Leibiger, B., Moede, T., Uhles, S., Berggren, P. O., and Leibiger, I. B. (2002). Short-term regulation of insulin gene transcription. Biochem Soc Trans *30*, 312-317.

Leibiger, B., Wahlander, K., Berggren, P., and Leibiger, I. B. (2000). Glucose-stimulated insulin biosynthesis depends on insulin-stimulated insulin gene transcription. The Journal of Biological Chemistry *275*, 30153-30156.

Leibowitz, G., Uckaya, G., Oprescu, A. I., Cerasi, E., Gross, D. J., and Kaiser, N. (2002). Glucose-regulated proinsulin gene expression is required for adequate insulin production during chronic glucose exposure. Endocrinology *143*, 3214-3220.

Lenzen, S., Drinkgern, J., and Tiedge, M. (1996). Low antioxidant enzyme gene expression in pancreatic islets compared with various other mouse tissues. Free Radic Biol Med *20*, 463-466.

Lerner, R. S., Seiser, R. M., Zheng, T., Lager, P. J., Reedy, M. C., Keene, J. D., and Nicchitta, C. V. (2003). Partitioning and translation of mRNAs encoding soluble proteins on membrane-bound ribosomes. Rna *9*, 1123-1137.

Levy, R., Wiedmann, M., and Kreibich, G. (2001). In vitro binding of ribosomes to the beta subunit of the Sec61p protein translocation complex. J Biol Chem *276*, 2340-2346.

Liang, Y., and Matschinsky, F. M. (1991). Content of CoA-esters in perifused rat islets stimulated by glucose and other fuels. Diabetes *40*, 327-333.

Liao, S., Lin, J., Do, H., and Johnson, A. E. (1997). Both lumenal and cytosolic gating of the aqueous ER translocon pore are regulated from inside the ribosome during membrane protein integration. Cell *90*, 31-41.

Lin, B. J., and Haist, R. E. (1973). Effects of some modifiers of insulin secretion on insulin biosynthesis. Endocrinology *92*, 735-742.

Lin, T. A., Kong, X., Haystead, T. A., Pause, A., Belsham, G., Sonenberg, N., and Lawrence, J. C., Jr. (1994). PHAS-I as a link between mitogen-activated protein kinase and translation initiation. Science *266*, 653-656.

Ling, Z., Kiekens, R., Mahler, T., Schuit, F. C., Pipeleers-Marichal, M., Sener, A., Kloppel, G., Malaisse, W. J., and Pipeleers, D. G. (1996). Effects of chronically elevated glucose levels on the functional properties of rat pancreatic beta-cells. Diabetes *45*, 1774-1782.

Lipp, J., Dobberstein, B., and Haeuptle, M. T. (1987). Signal recognition particle arrests elongation of nascent secretory and membrane proteins at multiple sites in a transient manner. J Biol Chem *262*, 1680-1684.

Lipshitz, H. D., and Smibert, C. A. (2000). Mechanisms of RNA localization and translational regulation. Curr Opin Genet Dev *10*, 476-488.

Lipshutz, R. J., Fodor, S. P. A., Gingeras, T. R., and Lockhart, D. J. (1999). High density synthetic oligonucleotide arrays. Nature Genetics *21*, 20-24.

Lodish, H. (1976). Translational control of protein synthesis. Annual Review Biochemistry *45*, 39-72.

Lodish, H. F. (1974). Model for the regulation of mRNA translation applied to haemoglobin synthesis. Nature *251*, 385-388.

Lodish, H. F., Alton, T., Dottin, R. P., Weiner, A. M., and Margolskee, J. P. (1976). Synthesis and translation of messenger RNA during differentiation of the cellular slime mold Dictyostelium discoideum. Symp Soc Dev Biol, 75-103.

Lodish, H. F., and Small, B. (1976). Different lifetimes of reticulocyte messenger RNA. Cell *7*, 59-65.

Lomedico, P. T., and Saunders, G. F. (1977). Cell-free modulation of proinsulin synthesis. Science *198*, 620-622.

Lu, P. D., Harding, H. P., and Ron, D. (2004a). Translation reinitiation at alternative open reading frames regulates gene expression in an integrated stress response. J Cell Biol *167*, 27-33.

Lu, P. D., Jousse, C., Marciniak, S. J., Zhang, Y., Novoa, I., Scheuner, D., Kaufman, R. J., Ron, D., and Harding, H. P. (2004b). Cytoprotection by pre-emptive conditional phosphorylation of translation initiation factor 2. Embo J *23*, 169-179.

Lu, Y., Qi, H. Y., Hyndman, J. B., Ulbrandt, N. D., Teplyakov, A., Tomasevic, N., and Bernstein, H. D. (2001). Evidence for a novel GTPase priming step in the SRP protein targeting pathway. Embo J *20*, 6724-6734.

Lutcke, H., High, S., Romisch, K., Ashford, A. J., and Dobberstein, B. (1992). The methionine-rich domain of the 54 kDa subunit of signal recognition particle is sufficient for the interaction with signal sequences. Embo J *11*, 1543-1551.

Lutcke, H., Prehn, S., Ashford, A. J., Remus, M., Frank, R., and Dobberstein, B. (1993). Assembly of the 68- and 72-kD proteins of signal recognition particle with 7S RNA. J Cell Biol *121*, 977-985.

MacDonald, P. M. (1990). bicoid mRNA localization signal: phylogenetic conservation of function and RNA secondary structure. Development *110*, 161-171.

Macdonald, P. M., and Struhl, G. (1988). cis-acting sequences responsible for anterior localization of bicoid mRNA in Drosophila embryos. Nature *336*, 595-598.

Mader, S., Lee, H., Pause, A., and Sonenberg, N. (1995). The translation initiation factor eIF-4E binds to a common motif shared by the translation factor eIF-4 gamma and the translational repressors 4E-binding proteins. Mol Cell Biol *15*, 4990-4997.

Majumdar, R., Bandyopadhyay, A., and Maitra, U. (2003). Mammalian translation initiation factor eIF1 functions with eIF1A and eIF3 in the formation of a stable 40 S preinitiation complex. J Biol Chem *278*, 6580-6587.

Mandon, E. C., Jiang, Y., and Gilmore, R. (2003). Dual recognition of the ribosome and the signal recognition particle by the SRP receptor during protein targeting to the endoplasmic reticulum. J Cell Biol *162*, 575-585.

Manzella, J. M., Rychlik, W., Rhoads, R. E., Hershey, J. W., and Blackshear, P. J. (1991). Insulin induction of ornithine decarboxylase. Importance of mRNA secondary structure and phosphorylation of eucaryotic initiation factors eIF-4B and eIF-4E. J Biol Chem *266*, 2383-2389.

Marcotrigiano, J., Gingras, A. C., Sonenberg, N., and Burley, S. K. (1997). Cocrystal structure of the messenger RNA 5' cap-binding protein (eIF4E) bound to 7-methyl-GDP. Cell *89*, 951-961.

Martin, S. K., Carroll, R., Benig, M., and Steiner, D. (1994). Regulation by glucose of the biosynthesis of PC2, PC3 and proinsulin in (ob/ob) mouse Islets of Langerhans. FEBS Letters *356*, 279-282.

Mason, N., Ciufo, L. F., and Brown, J. D. (2000). Elongation arrest is a physiologically important function of signal recognition particle. Embo J *19*, 4164-4174.

Matsuo, H., Li, H., McGuire, A. M., Fletcher, C. M., Gingras, A. C., Sonenberg, N., and Wagner, G. (1997). Structure of translation factor eIF4E bound to m7GDP and interaction with 4E-binding protein. Nat Struct Biol *4*, 717-724.

Matsuoka, T., Kajimoto, Y., Watada, H., Kaneto, H., Kishimoto, M., Umayahara, Y., Fujitani, Y., Kamada, T., Kawamori, R., and Yamasaki, Y. (1997). Glycation-dependent, reactive oxygen species-mediated suppression of the insulin gene promoter activity in HIT cells. J Clin Invest *99*, 144-150.

Mauro, V. P., and Edelman, G. M. (1997). rRNA-like sequences occur in diverse primary transcripts: implications for the control of gene expression. Proc Natl Acad Sci U S A *94*, 422-427.

McKendrick, L., Morley, S. J., Pain, V. M., Jagus, R., and Joshi, B. (2001). Phosphorylation of eukaryotic initiation factor 4E (eIF4E) at Ser209 is not required for protein synthesis in vitro and in vivo. Eur J Biochem *268*, 5375-5385.

Menetret, J. F., Neuhof, A., Morgan, D. G., Plath, K., Radermacher, M., Rapoport, T. A., and Akey, C. W. (2000). The structure of ribosome-channel complexes engaged in protein translocation. Mol Cell *6*, 1219-1232.

Meyer, D. I., Louvard, D., and Dobberstein, B. (1982). Characterization of molecules involved in protein translocation using a specific antibody. J Cell Biol *92*, 579-583.

Meyer, T. H., Menetret, J. F., Breitling, R., Miller, K. R., Akey, C. W., and Rapoport, T. A. (1999). The bacterial SecY/E translocation complex forms channel-like structures similar to those of the eukaryotic Sec61p complex. J Mol Biol *285*, 1789-1800.

Michel, Y. M., Poncet, D., Piron, M., Kean, K. M., and Borman, A. M. (2000). Cap-Poly(A) synergy in mammalian cell-free extracts. Investigation of the requirements for poly(A)-mediated stimulation of translation initiation. J Biol Chem *275*, 32268-32276.

Mikulits, W., Pradet-Balade, B., Habermann, B., Beug, H., Garcia-Sanz, J. A., and Mullner, E. W. (2000). Isolation of translationally controlled mRNAs by differential screening. Faseb J *14*, 1641-1652.

Miller, J. D., Tajima, S., Lauffer, L., and Walter, P. (1995). The beta subunit of the signal recognition particle receptor is a transmembrane GTPase that anchors the alpha

subunit, a peripheral membrane GTPase, to the endoplasmic reticulum membrane. J Cell Biol *128*, 273-282.

Miller, J. D., Wilhelm, H., Gierasch, L., Gilmore, R., and Walter, P. (1993). GTP binding and hydrolysis by the signal recognition particle during initiation of protein translocation. Nature *366*, 351-354.

Minich, W. B., Balasta, M. L., Goss, D. J., and Rhoads, R. E. (1994). Chromatographic resolution of in vivo phosphorylated and nonphosphorylated eukaryotic translation initiation factor eIF-4E: increased cap affinity of the phosphorylated form. Proc Natl Acad Sci U S A *91*, 7668-7672.

Minn, A. H., Hafele, C., and Shalev, A. (2005a). Thioredoxin-Interacting Protein Is Stimulated by Glucose through a Carbohydrate Response Element and Induces {beta}-Cell Apoptosis. Endocrinology *146*, 2397-2405.

Minn, A. H., Kayton, M., Lorang, D., Hoffmann, S. C., Harlan, D. M., Libutti, S. K., and Shalev, A. (2004). Insulinomas and expression of an insulin splice variant. Lancet *363*, 363-367.

Minn, A. H., Lan, H., Rabaglia, M. E., Harlan, D. M., Peculis, B. A., Attie, A. D., and Shalev, A. (2005b). Increased insulin translation from an insulin splice-variant overexpressed in diabetes, obesity, and insulin resistance. Mol Endocrinol *19*, 794-803.

Montoya, G., Kaat, K., Moll, R., Schafer, G., and Sinning, I. (2000). The crystal structure of the conserved GTPase of SRP54 from the archaeon Acidianus ambivalens and its comparison with related structures suggests a model for the SRP-SRP receptor complex. Structure Fold Des *8*, 515-525.

Montoya, G., Svensson, C., Luirink, J., and Sinning, I. (1997). Crystal structure of the NG domain from the signal-recognition particle receptor FtsY. Nature *385*, 365-368.

Morgan, D. G., Menetret, J. F., Neuhof, A., Rapoport, T. A., and Akey, C. W. (2002). Structure of the mammalian ribosome-channel complex at 17A resolution. J Mol Biol *324*, 871-886.

Morley, S. J., and Pain, V. M. (1995). Translational regulation during activation of porcine peripheral blood lymphocytes: association and phosphorylation of the alpha and gamma subunits of the initiation factor complex eIF-4F. Biochem J *312 (Pt 2)*, 627-635.

Moser, C., Mol, O., Goody, R. S., and Sinning, I. (1997). The signal recognition particle receptor of Escherichia coli (FtsY) has a nucleotide exchange factor built into the GTPase domain. Proc Natl Acad Sci U S A *94*, 11339-11344.

Mothes, W., Prehn, S., and Rapoport, T. A. (1994). Systematic probing of the environment of a translocating secretory protein during translocation through the ER membrane. Embo J *13*, 3973-3982.

Muckenthaler, M., Gray, N. K., and Hentze, M. W. (1998). IRP-1 binding to ferritin mRNA prevents the recruitment of the small ribosomal subunit by the cap-binding complex eIF4F. Mol Cell *2*, 383-388.

Munro, T. P., Magee, R. J., Kidd, G. J., Carson, J. H., Barbarese, E., Smith, L. M., and Smith, R. (1999). Mutational analysis of a heterogeneous nuclear ribonucleoprotein A2 response element for RNA trafficking. J Biol Chem *274*, 34389-34395.

Munroe, D., and Jacobson, A. (1990). mRNA poly(A) tail, a 3' enhancer of translational initiation. Mol Cell Biol *10*, 3441-3455.

Murphy, E. C., 3rd, Zheng, T., and Nicchitta, C. V. (1997). Identification of a novel stage of ribosome/nascent chain association with the endoplasmic reticulum membrane. J Cell Biol *136*, 1213-1226.

Nagai, K., Oubridge, C., Kuglstatter, A., Menichelli, E., Isel, C., and Jovine, L. (2003). Structure, function and evolution of the signal recognition particle. The EMBO Journal (2003) **22**, 3479–3485.

Nagamatsu, S., Nakamichi, Y., and Katahira, H. (1997). Syntaxin, but not soluble NSF attachment protein (SNAP), biosynthesis by rat pancreatic islets is regulated by glucose in parallel with proinsulin biosynthesis. Diabetologia *40*, 1396-1402.

Nakamura, A., Sato, K., and Hanyu-Nakamura, K. (2004). Drosophila cup is an eIF4E binding protein that associates with Bruno and regulates oskar mRNA translation in oogenesis. Dev Cell *6*, 69-78.

Nakaya, K., Ranu, R. S., and Wool, I. G. (1973). Dissociation of eukaryotic ribosomes by purified initiation factor EIF-3. Biochem Biophys Res Commun *54*, 246-255.

Naranda, T., MacMillan, S. E., Donahue, T. F., and Hershey, J. W. (1996). SUI1/p16 is required for the activity of eukaryotic translation initiation factor 3 in Saccharomyces cerevisiae. Mol Cell Biol *16*, 2307-2313.

Neuhof, A., Rolls, M. M., Jungnickel, B., Kalies, K. U., and Rapoport, T. A. (1998). Binding of signal recognition particle gives ribosome/nascent chain complexes a competitive advantage in endoplasmic reticulum membrane interaction. Mol Biol Cell *9*, 103-115.

Newitt, J. A., and Bernstein, H. D. (1997). The N-domain of the signal recognition particle 54-kDa subunit promotes efficient signal sequence binding. Eur J Biochem *245*, 720-729.

Nicchitta, C. V., Migliaccio, G., and Blobel, G. (1991). Biochemical fractionation and assembly of the membrane components that mediate nascent chain targeting and translocation. Cell *65*, 587-598.

Niedzwiecka, A., Marcotrigiano, J., Stepinski, J., Jankowska-Anyszka, M., Wyslouch-Cieszynska, A., Dadlez, M., Gingras, A. C., Mak, P., Darzynkiewicz, E., Sonenberg, N., *et al.* (2002). Biophysical studies of eIF4E cap-binding protein: recognition of mRNA 5' cap structure and synthetic fragments of eIF4G and 4E-BP1 proteins. J Mol Biol *319*, 615-635.

Nielsen, D. A., Welsh, M., Casadaban, M. J., and Steiner, D. F. (1985). Control of insulin gene expression in pancreatic beta-cells and in an insulin-producing cell line, RIN-5F cells. I. Effects of glucose and cyclic AMP on the transcription of insulin mRNA. J Biol Chem *260*, 13585-13589.

Nishiyama, A., Masutani, H., Nakamura, H., Nishinaka, Y., and Yodoi, J. (2001). Redox regulation by thioredoxin and thioredoxin-binding proteins. IUBMB Life *52*, 29-33.

Novoa, I., and Carrasco, L. (1999). Cleavage of eukaryotic translation initiation factor 4G by exogenously added hybrid proteins containing poliovirus 2Apro in HeLa cells: effects on gene expression. Mol Cell Biol *19*, 2445-2454.

Ogg, S. C., Barz, W. P., and Walter, P. (1998). A functional GTPase domain, but not its transmembrane domain, is required for function of the SRP receptor beta-subunit. J Cell Biol *142*, 341-354.

Ogg, S. C., and Walter, P. (1995). SRP samples nascent chains for the presence of signal sequences by interacting with ribosomes at a discrete step during translation elongation. Cell *81*, 1075-1084.

Ohsugi, M., Cras-Meneur, C., Zhou, Y., Warren, W., Bernal-Mizrachi, E., and Permutt, M. A. (2004). Glucose and insulin treatment of insulinoma cells results in transcriptional regulation of a common set of genes. Diabetes *53*, 1496-1508.

Oldfield, S., Jones, B. L., Tanton, D., and Proud, C. G. (1994). Use of monoclonal antibodies to study the structure and function of eukaryotic protein synthesis initiation factor eIF-2B. Eur J Biochem *221*, 399-410.

Olsen, D. S., Savner, E. M., Mathew, A., Zhang, F., Krishnamoorthy, T., Phan, L., and Hinnebusch, A. G. (2003). Domains of eIF1A that mediate binding to eIF2, eIF3 and eIF5B and promote ternary complex recruitment in vivo. Embo J *22*, 193-204.

Ostareck, D. H., Ostareck-Lederer, A., Shatsky, I. N., and Hentze, M. W. (2001). Lipoxygenase mRNA silencing in erythroid differentiation: The 3'UTR regulatory complex controls 60S ribosomal subunit joining. Cell *104*, 281-290.

Ostareck, D. H., Ostareck-Lederer, A., Wilm, M., Thiele, B. J., Mann, M., and Hentze, M. W. (1997). mRNA silencing in erythroid differentiation: hnRNP K and hnRNP E1 regulate 15-lipoxygenase translation from the 3' end. Cell *89*, 597-606.

Oubridge, C., Kuglstatter, A., Jovine, L., and Nagai, K. (2002). Crystal structure of SRP19 in complex with the S domain of SRP RNA and its implication for the assembly of the signal recognition particle. Mol Cell *9*, 1251-1261.

Palade, G. (1975). Intracellular aspects of the process of protein synthesis. Science *189*, 347-358.

Palmieri, F. (2004). The mitochondrial transporter family (SLC25): physiological and pathological implications. Pflugers Arch *447*, 689-709.

Parry, D. G., and Taylor, K. W. (1966). The effects of sugars on incorporation of [3H)leucine into insulins. Biochem J *100*, 2C-4C.

Pause, A., Belsham, G. J., Gingras, A. C., Donze, O., Lin, T. A., Lawrence, J. C., Jr., and Sonenberg, N. (1994). Insulin-dependent stimulation of protein synthesis by phosphorylation of a regulator of 5'-cap function. Nature *371*, 762-767.

Peabody, D. S. (1993). The RNA binding site of bacteriophage MS2 coat protein. EMBO *12*, 595-600.

Peluso, P., Shan, S. O., Nock, S., Herschlag, D., and Walter, P. (2001). Role of SRP RNA in the GTPase cycles of Ffh and FtsY. Biochemistry *40*, 15224-15233.

Permutt, M. A. (1974). Effect of glucose on intitation and elongation rates in isolated rat pancreatic islets. The Journal of Biological Chemistry *245*, 2738-2742.

Permutt, M. A., and Kipnis, D. M. (1972a). Insulin biosynthesis I. On the mechanism of glucose stimulation. The Journal of Biological Chemistry *247*, 1194-1199.

Permutt, M. A., and Kipnis, D. M. (1972b). Insulin biosynthesis. II. Effect of glucose on ribonucleic acid synthesis in isolated rat islets. J Biol Chem *247*, 1200-1207.

Permutt, M. A., and Kipnis, D. M. (1973). Glucose regulation of insulin biosynthesis in isolated rat islets. Mt Sinai J Med *40*, 323-333.

Pestka, S. (1974). The use of inhibitors in studies on protein synthesis. Methods Enzymol *30*, 261-282.

Pestova, T. V., Borukhov, S. I., and Hellen, C. U. (1998). Eukaryotic ribosomes require initiation factors 1 and 1A to locate initiation codons. Nature *394*, 854-859.

Pestova, T. V., and Kolupaeva, V. G. (2002). The roles of individual eukaryotic translation initiation factors in ribosomal scanning and initiation codon selection. Genes Dev *16*, 2906-2922.

Pestova, T. V., Kolupaeva, V. G., Lomakin, I. B., Pilipenko, E. V., Shatsky, I. N., Agol, V. I., and Hellen, C. U. (2001). Molecular mechanisms of translation initiation in eukaryotes. Proc Natl Acad Sci U S A *98*, 7029-7036.

Pestova, T. V., Lomakin, I. B., Lee, J. H., Choi, S. K., Dever, T. E., and Hellen, C. U. (2000). The joining of ribosomal subunits in eukaryotes requires eIF5B. Nature *403*, 332-335.

Phan, L., Zhang, X., Asano, K., Anderson, J., Vornlocher, H. P., Greenberg, J. R., Qin, J., and Hinnebusch, A. G. (1998). Identification of a translation initiation factor 3 (eIF3) core complex, conserved in yeast and mammals, that interacts with eIF5. Mol Cell Biol *18*, 4935-4946.

Pipeleers, D. G., Marichal, M., and Malaisse, W. J. (1973a). The stimulus-secretion coupling of glucose-induced insulin release. XIV. Glucose regulation of insular biosynthetic activity. Endocrinology *93*, 1001-1011.

Pipeleers, D. G., Marichal, M., and Malaisse, W. J. (1973b). The stimulus-secretion coupling of glucose-induced insulin release. XV. Participation of cations in the recognition of glucose by the beta-cell. Endocrinology *93*, 1012-1018.

Piron, M., Vende, P., Cohen, J., and Poncet, D. (1998). Rotavirus RNA-binding protein NSP3 interacts with eIF4GI and evicts the poly(A) binding protein from eIF4F. Embo J *17*, 5811-5821.

Pisarev, A. V., Skabkin, M. A., Thomas, A. A., Merrick, W. C., Ovchinnikov, L. P., and Shatsky, I. N. (2002). Positive and negative effects of the major mammalian messenger ribonucleoprotein p50 on binding of 40 S ribosomal subunits to the initiation codon of beta-globin mRNA. J Biol Chem *277*, 15445-15451.

Plath, K., Mothes, W., Wilkinson, B. M., Stirling, C. J., and Rapoport, T. A. (1998). Signal sequence recognition in posttranslational protein transport across the yeast ER membrane. Cell *94*, 795-807.

Ponka, P., Beaumont, C., and Richardson, D. R. (1998). Function and regulation of transferrin and ferritin. Seminars in Hematology *35*, 35-54.

Pool, M. R., Stumm, J., Fulga, T. A., Sinning, I., and Dobberstein, B. (2002). Distinct modes of signal recognition particle interaction with the ribosome. Science *297*, 1345-1348.

Poritz, M. A., Bernstein, H. D., Strub, K., Zopf, D., Wilhelm, H., and Walter, P. (1990). An E. coli ribonucleoprotein containing 4.5S RNA resembles mammalian signal recognition particle. Science *250*, 1111-1117.

Poritz, M. A., Strub, K., and Walter, P. (1988). Human SRP RNA and E. coli 4.5S RNA contain a highly homologous structural domain. Cell *55*, 4-6.

Porksen, N. (2002). The in vivo regulation of pulsatile insulin secretion. Diabetologia *45*, 3-20.

Porte, D., Jr., and Kahn, S. E. (2001). beta-cell dysfunction and failure in type 2 diabetes: potential mechanisms. Diabetes *50*, S160-163.

Potter, M. D., and Nicchitta, C. V. (2002). Endoplasmic reticulum-bound ribosomes reside in stable association with the translocon following termination of protein synthesis. J Biol Chem *277*, 23314-23320.

Potter, M. D., Seiser, R. M., and Nicchitta, C. V. (2001). Ribosome exchange revisited: a mechanism for translation-coupled ribosome detachment from the ER membrane. Trends Cell Biol *11*, 112-115.

Powers, T., and Walter, P. (1995). Reciprocal stimulation of GTP hydrolysis by two directly interacting GTPases. Science *269*, 1422-1424.

Powers, T., and Walter, P. (1996). The nascent polypeptide-associated complex modulates interactions between the signal recognition particle and the ribosome. Curr Biol *6*, 331-338.

Preiss, T., and Hentze, M. W. (1998). Dual function of the messenger RNA cap structure in poly(A)-tail-promoted translation in yeast. Nature *392*, 516-520.

Prentki, M. (1996). New insights into pancreatic beta-cell metabolic signaling in insulin secretion. Eur J Endocrinol *134*, 272-286.

Prentki, M., Tornheim, K., and Corkey, B. E. (1997). Signal transduction mechanisms in nutrient-induced insulin secretion. Diabetologia *40 Suppl 2*, S32-41.

Price, N., and Proud, C. (1994). The guanine nucleotide-exchange factor, eIF-2B. Biochimie *76*, 748-760.

Prinz, A., Behrens, C., Rapoport, T. A., Hartmann, E., and Kalies, K. U. (2000). Evolutionarily conserved binding of ribosomes to the translocation channel via the large ribosomal RNA. Embo J *19*, 1900-1906.

Proud, C., Wang, W., Patel, J. V., Campbell, L. E., Kleijn, M., Li, W., and Browne, G. J. (2001). Interplay between insulin and nutrients in the regulation of translation factors. Biochemical Society Transactions *29*, 541-547.

Proud, C. G. (2002). Regulation of mammalian translation factors by nutrients. Eur J Biochem *269*, 5338-5349.

Pyronnet, S., Imataka, H., Gingras, A. C., Fukunaga, R., Hunter, T., and Sonenberg, N. (1999). Human eukaryotic translation initiation factor 4G (eIF4G) recruits mnk1 to phosphorylate eIF4E. Embo J *18*, 270-279.

Raden, D., Song, W., and Gilmore, R. (2000). Role of the cytoplasmic segments of Sec61α in the ribosome-binding and translocation-promoting activities of the Sec61 somplex. The Journal of Cell Biology *150,* 53-64.

Rajagopalan, D. (2003). A comparison of statistical methods for analysis of high density oligonucleotide array data. Bioinformatics *19*, 1469-1476.

Rajkowitsch, L., Vilela, C., Berthelot, K., Ramirez, C. V., and McCarthy, J. E. (2004). Reinitiation and recycling are distinct processes occurring downstream of translation termination in yeast. J Mol Biol *335*, 71-85.

Ramaiah, K. V., Davies, M. V., Chen, J. J., and Kaufman, R. J. (1994). Expression of mutant eukaryotic initiation factor 2 alpha subunit (eIF-2 alpha) reduces inhibition of guanine nucleotide exchange activity of eIF-2B mediated by eIF-2 alpha phosphorylation. Mol Cell Biol *14*, 4546-4553.

Rapiejko, P. J., and Gilmore, R. (1992). Protein translocation across the ER requires a functional GTP binding site in the alpha subunit of the signal recognition particle receptor. J Cell Biol *117*, 493-503.

Rapiejko, P. J., and Gilmore, R. (1994). Signal sequence recognition and targeting of ribosomes to the endoplasmic reticulum by the signal recognition particle do not require GTP. Mol Biol Cell *5*, 887-897.

Rapiejko, P. J., and Gilmore, R. (1997). Empty site forms of the SRP54 and SRα GTPases mediate targeting of ribosome-nascent chain complexes to the endoplasmic reticulum. Cell *89*, 703-713.

Rau, M., Ohlman, T., Monley, S. J., and Pain, V. M. (1996). A Reevaluation of the Cap-binding Protein, eIF4E, as a Rate-limiting Factor for Initiation of Translation in Reticulocyte Lysate. The Journal of Biological Chemistry *271*, 8983-8990.

Raught, B., Gingras, A. C., Gygi, S. P., Imataka, H., Morino, S., Gradi, A., Aebersold, R., and Sonenberg, N. (2000). Serum-stimulated, rapamycin-sensitive phosphorylation sites in the eukaryotic translation initiation factor 4GI. Embo J *19*, 434-444.

Rhodes, C., and Alarcon, C. (1994). Diabetes *43*, 511-517.

Richter, N. J., Rogers, G. W., Jr., Hensold, J. O., and Merrick, W. C. (1999). Further biochemical and kinetic characterization of human eukaryotic initiation factor 4H. J Biol Chem *274*, 35415-35424.

Richter-Cook, N. J., Dever, T. E., Hensold, J. O., and Merrick, W. C. (1998). Purification and characterization of a new eukaryotic protein translation factor. Eukaryotic initiation factor 4H. J Biol Chem *273*, 7579-7587.

Rogers, G. W., Jr., Richter, N. J., and Merrick, W. C. (1999). Biochemical and kinetic characterization of the RNA helicase activity of eukaryotic initiation factor 4A. J Biol Chem *274*, 12236-12244.

Romisch, K., Webb, J., Lingelbach, K., Gausepohl, H., and Dobberstein, B. (1990). The 54-kD protein of signal recognition particle contains a methionine-rich RNA binding domain. J Cell Biol *111*, 1793-1802.

Rook, M. S., Lu, M., and Kosik, K. S. (2000). CaMKIIalpha 3'-untranslated region-directed mRNA translocation in living neurons: visualisation by GFP linkage. Journal of Neuroscience *207*, 6385-6393.

Rosenwald, I. B., Rhoads, D. B., Callanan, L. D., Isselbacher, K. J., and Schmidt, E. V. (1993). Increased expression of eukaryotic translation initiation factors eIF-4E and eIF-2 alpha in response to growth induction by c-myc. Proc Natl Acad Sci U S A *90*, 6175-6178.

Rousseau, D., Kaspar, R., Rosenwald, I., Gehrke, L., and Sonenberg, N. (1996). Translation initiation of ornithine decarboxylase and nucleocytoplasmic transport of cyclin D1 mRNA are increased in cells overexpressing eukaryotic initiation factor 4E. Proc Natl Acad Sci U S A *93*, 1065-1070.

Rowlands, A. G., Panniers, R., and Henshaw, E. C. (1988). The catalytic mechanism of guanine nucleotide exchange factor action and competitive inhibition by phosphorylated eukaryotic initiation factor 2. J Biol Chem *263*, 5526-5533.

Roy, A., and Wonderlin, W. F. (2003). The permeability of the endoplasmic reticulum is dynamically coupled to protein synthesis. J Biol Chem *278*, 4397-4403.

Rutkowski, D. T., Lingappa, V. R., and Hegde, R. S. (2001). Substrate-specific regulation of the ribosome- translocon junction by N-terminal signal sequences. Proc Natl Acad Sci U S A *98*, 7823-7828.

Rutter, G. A. (2001). Nutrient-secretion coupling in the pancreatic islet beta-cell: recent advances. Mol Aspects Med *22*, 247-284.

Sachs, A. B., and Davis, R. W. (1989). The poly(A) binding protein is required for poly(A) shortening and 60S ribosomal subunit-dependent translation initiation. Cell *58*, 857-867.

Schadt, E. E., Li, C., Ellis, B., and Wong, W. H. (2001). Feature extraction and normalization algorithms for high-density oligonucleotide gene expression array data. J Cell Biochem Suppl *Suppl 37*, 120-125.

Scheper, G. C., Morrice, N. A., Kleijn, M., and Proud, C. G. (2001). The mitogen-activated protein kinase signal-integrating kinase Mnk2 is a eukaryotic initiation factor 4E kinase with high levels of basal activity in mammalian cells. Mol Cell Biol *21*, 743-754.

Scheper, G. C., van Kollenburg, B., Hu, J., Luo, Y., Goss, D. J., and Proud, C. G. (2002). Phosphorylation of eukaryotic initiation factor 4E markedly reduces its affinity for capped mRNA. J Biol Chem *277*, 3303-3309.

Scheuner, D., Song, B., McEwen, E., Liu, C., Laybutt, R., Gillespie, P., Saunders, T., Bonner-Weir, S., and Kaufman, R. J. (2001). Translational control is required for the unfolded protein response and in vivo glucose homeostasis. Mol Cell *7*, 1165-1176.

Schmitt, E., Blanquet, S., and Mechulam, Y. (2002). The large subunit of initiation factor aIF2 is a close structural homologue of elongation factors. Embo J *21*, 1821-1832.

Schratt, G. M., Nigh, E. A., Chen, W. G., Hu, L., and Greenberg, M. E. (2004). BDNF regulates the translation of a select group of mRNAs by a mammalian target of rapamycin-phosphatidylinositol 3-kinase-dependent pathway during neuronal development. J Neurosci *24*, 7366-7377.

Schwartz, T., and Blobel, G. (2003). Structural basis for the function of the beta subunit of the eukaryotic signal recognition particle receptor. Cell *112*, 793-803.

Searfoss, A., Dever, T. E., and Wickner, R. (2001). Linking the 3' poly(A) tail to the subunit joining step of translation initiation: relations of Pab1p, eukaryotic translation initiation factor 5b (Fun12p), and Ski2p-Slh1p. Mol Cell Biol *21*, 4900-4908.

Seiser, R. M., and Nicchitta, C. V. (2000). The fate of membrane-bound ribosomes following the termination of protein synthesis. J Biol Chem *275*, 33820-33827.

Shalev, A., Blair, P. J., Hoffmann, S. C., Hirshberg, B., Peculis, B. A., and Harlan, D. M. (2002a). A proinsulin gene splice variant with increased translation efficiency is expressed in human pancreatic islets. Endocrinology *143*, 2541-2547.

Shalev, A., Pise-Masison, C. A., Radonovich, M., Hoffmann, S. C., Hirshberg, B., Brady, J. N., and Harlan, D. M. (2002b). Oligonucleotide microarray analysis of intact human pancreatic islets: identification of glucose-responsive genes and a highly regulated TGFbeta signaling pathway. Endocrinology *143*, 3695-3698.

Shan, S. O., and Walter, P. (2003). Induced nucleotide specificity in a GTPase. Proc Natl Acad Sci U S A *100*, 4480-4485.

Shaulian, E., and Karin, M. (2002). AP-1 as a regulator of cell life and death. Nat Cell Biol *4*, E131-136.

Shi, Y., Vattem, K. M., Sood, R., An, J., Liang, J., Stramm, L., and Wek, R. C. (1998). Identification and characterization of pancreatic eukaryotic initiation factor 2 alpha-subunit kinase, PEK, involved in translational control. Mol Cell Biol *18*, 7499-7509.

Shin, B. S., Maag, D., Roll-Mecak, A., Arefin, M. S., Burley, S. K., Lorsch, J. R., and Dever, T. E. (2002). Uncoupling of initiation factor eIF5B/IF2 GTPase and translational activities by mutations that lower ribosome affinity. Cell *111*, 1015-1025.

Siegel, V., and Walter, P. (1985). Elongation arrest is not a prerequisite for secretory protein translocation across the microsomal membrane. J Cell Biol *100*, 1913-1921.

Siegel, V., and Walter, P. (1986). Removal of the Alu structural domain from signal recognition particle leaves its protein translocation activity intact. Nature *320*, 81-84.

Siegel, V., and Walter, P. (1988). Each of the activities of signal recognition particle (SRP) is contained within a distinct domain: analysis of biochemical mutants of SRP. Cell *52*, 39-49.

Simon, S. M., and Blobel, G. (1991). A protein-conducting channel in the endoplasmic reticulum. Cell *65*, 371-380.

Skelly, R. H., Bollheimer, L. C., Wicksteed, B. L., Corkey, B. E., and Rhodes, C. J. (1998). A distinct difference in the metabolic stimulus-response coupling pathways for

regulating proinsulin biosynthesis and insulin secretion that lies at the level of a requirement for fatty acyl moieties. Biochem J *331 (Pt 2)*, 553-561.

Skelly, R. H., Schuppin, G. T., Ishihara, H., Oka, Y., and Rhodes, C. J. (1996). Glucose-regulated translational control of proinsulin biosynthesis with that of the proinsulin endopeptidases PC2 and PC3 in the insulin-producing MIN6 cell line. Diabetes *45*, 37-43.

Skogerson, L., and Moldave, K. (1968). Evidence for aminoacyl-tRNA binding, peptide bond synthesis, and translocase activities in the aminoacyl transfer reaction. Arch Biochem Biophys *125*, 497-505.

Smith, K. E., and Henshaw, E. C. (1975). Binding of Met-tRNAf to native 40 S ribosomal subunits in Ehrlich ascites tumor cells. J Biol Chem *250*, 6880-6884.

Song, W., Raden, D., Mandon, E. C., and Gilmore, R. (2000). Role of Sec61α in the regulated transfer of the ribosome-nascent chain complex from the signal recognition particle to the translocation channel. Cell *100*, 333-343.

Sood, R., Porter, A. C., Olsen, D. A., Cavener, D. R., and Wek, R. C. (2000). A mammalian homologue of GCN2 protein kinase important for translational control by phosphorylation of eukaryotic initiation factor-2alpha. Genetics *154*, 787-801.

Sprinzl, M., Hartmann, T., Meissner, F., Moll, J., and Vorderwulbecke, T. (1987). Compilation of tRNA sequences and sequences of tRNA genes. Nucleic Acids Res *15 Suppl*, r53-188.

St Johnston, D. (2005). Moving messages: the intracellular localization of mRNAs. Nat Rev Mol Cell Biol.

Susini, S., Roche, E., Prentki, M., and Schlegel, W. (1998). Glucose and glucoincretin peptides synergize to induce c-fos, c-jun, junB, zif-268, and nur-77 gene expression in pancreatic beta(INS-1) cells. Faseb J *12*, 1173-1182.

Svitkin, Y. V., Ovchinnikov, L. P., Dreyfuss, G., and Sonenberg, N. (1996). General RNA binding proteins render translation cap dependent. Embo J *15*, 7147-7155.

Tajima, S., Lauffer, L., Rath, V. L., and Walter, P. (1986). The signal recognition particle receptor is a complex that contains two distinct polypeptide chains. J Cell Biol *103*, 1167-1178.

Tarun, S. Z., Jr., and Sachs, A. B. (1996). Association of the yeast poly(A) tail binding protein with translation initiation factor eIF-4G. Embo J *15*, 7168-7177.

Terzi, L., Pool, M. R., Dobberstein, B., and Strub, K. (2004). Signal recognition particle Alu domain occupies a defined site at the ribosomal subunit interface upon signal sequence recognition. Biochemistry *43*, 107-117.

Thomas, T., Kulkarni, G. D., Gallo, M. A., Greenfield, N., Lewis, J. S., Shirahata, A., and Thomas, T. J. (1997). Effects of natural and synthetic polyamines on the conformation of an oligodeoxyribonucleotide with the estrogen response element. Nucleic Acids Res *25*, 2396-2402.

Tiedge, M., Lortz, S., Drinkgern, J., and Lenzen, S. (1997). Relation between antioxidant enzyme gene expression and antioxidative defense status of insulin-producing cells. Diabetes *46*, 1733-1742.

Tillmar, L., Carlsson, C., and Welsh, N. (2002). Control of insulin mRNA stability in rat pancreatic islets. Regulatory role of a 3' - untranslated region pyrimidine-rich sequence. The Journal of Biological Chemistry *277*, 1099-1106.

Topisirovic, I., Culjkovic, B., Cohen, N., Perez, J. M., Skrabanek, L., and Borden, K. L. (2003). The proline-rich homeodomain protein, PRH, is a tissue-specific inhibitor of eIF4E-dependent cyclin D1 mRNA transport and growth. Embo J *22*, 689-703.

Topisirovic, I., Ruiz-Gutierrez, M., and Borden, K. L. (2004). Phosphorylation of the eukaryotic translation initiation factor eIF4E contributes to its transformation and mRNA transport activities. Cancer Res *64*, 8639-8642.

Tuazon, P. T., Merrick, W. C., and Traugh, J. A. (1989). Comparative analysis of phosphorylation of translational initiation and elongation factors by seven protein kinases. J Biol Chem *264*, 2773-2777.

Tuazon, P. T., Morley, S. J., Dever, T. E., Merrick, W. C., Rhoads, R. E., and Traugh, J. A. (1990). Association of initiation factor eIF-4E in a cap binding protein complex (eIF-4F) is critical for and enhances phosphorylation by protein kinase C. J Biol Chem *265*, 10617-10621.

Tuxworth, W. J., Jr., Saghir, A. N., Spruill, L. S., Menick, D. R., and McDermott, P. J. (2004). Regulation of protein synthesis by eIF4E phosphorylation in adult cardiocytes: the consequence of secondary structure in the 5'-untranslated region of mRNA. Biochem J *378*, 73-82.

Uchida, N., Hoshino, S., Imataka, H., Sonenberg, N., and Katada, T. (2002). A novel role of the mammalian GSPT/eRF3 associating with poly(A)-binding protein in Cap/Poly(A)-dependent translation. J Biol Chem *277*, 50286-50292.

Ueda, T., Watanabe-Fukunaga, R., Fukuyama, H., Nagata, S., and Fukunaga, R. (2004). Mnk2 and Mnk1 are essential for constitutive and inducible phosphorylation of eukaryotic initiation factor 4E but not for cell growth or development. Mol Cell Biol *24*, 6539-6549.

Valent, Q. A., Kendall, D. A., High, S., Kusters, R., Oudega, B., and Luirink, J. (1995). Early events in preprotein recognition in E. coli: interaction of SRP and trigger factor with nascent polypeptides. Embo J *14*, 5494-5505.

Van den Berg, B., Clemons, W. M., Jr., Collinson, I., Modis, Y., Hartmann, E., Harrison, S. C., and Rapoport, T. A. (2004). X-ray structure of a protein-conducting channel. Nature *427*, 36-44.

Vattem, K. M., and Wek, R. C. (2004). Reinitiation involving upstream ORFs regulates ATF4 mRNA translation in mammalian cells. Proc Natl Acad Sci U S A *101*, 11269-11274.

Vega Laso, M. R., Zhu, D., Sagliocco, F., Brown, A. J., Tuite, M. F., and McCarthy, J. E. (1993). Inhibition of translational initiation in the yeast Saccharomyces cerevisiae as a function of the stability and position of hairpin structures in the mRNA leader. J Biol Chem *268*, 6453-6462.

Voigt, S., Jungnickel, B., Hartmann, E., and Rapoport, T. A. (1996). Signal sequence-dependent function of the TRAM protein during early phases of protein transport across the endoplasmic reticulum membrane. J Cell Biol *134*, 25-35.

von Pawel-Rammingen, U., Astrom, S., and Bystrom, A. S. (1992). Mutational analysis of conserved positions potentially important for initiator tRNA function in Saccharomyces cerevisiae. Mol Cell Biol *12*, 1432-1442.

Walsh, D., and Mohr, I. (2004). Phosphorylation of eIF4E by Mnk-1 enhances HSV-1 translation and replication in quiescent cells. Genes Dev *18*, 660-672.

Walter, P., and Blobel, G. (1980). Purification of a membrane-associated protein complex required for protein translocation across the endoplasmic reticulum. Proc Natl Acad Sci U S A *77*, 7112-7116.

Walter, P., and Blobel, G. (1981). Translocation of proteins across the endoplasmic reticulum III. Signal recognition protein (SRP) causes signal sequence-dependent and site-specific arrest of chain elongation that is released by microsomal membranes. J Cell Biol *91*, 557-561.

Walter, P., and Blobel, G. (1982). Signal recognition particle contains a 7S RNA essential for protein translocation across the endoplasmic reticulum. Nature *299*, 691-698.

Walter, P., and Johnson, A. E. (1994). Signal sequence recognition and protein targeting to the endoplasmic reticulum. Annual Review Cell Biology *10*, 87-119.

Wang, X., Campbell, L. E., Miller, C. M., and Proud, C. G. (1998a). Amino acid availability regulates p70 S6 kinase and multiple translation factors. Biochem J *334 (Pt 1)*, 261-267.

Wang, X., Flynn, A., Waskiewicz, A. J., Webb, B. L., Vries, R. G., Baines, I. A., Cooper, J. A., and Proud, C. G. (1998b). The phosphorylation of eukaryotic initiation factor eIF4E in response to phorbol esters, cell stresses, and cytokines is mediated by distinct MAP kinase pathways. J Biol Chem *273*, 9373-9377.

Wang, X., Janmaat, M., Beugnet, A., Paulin, F. E., and Proud, C. G. (2002). Evidence that the dephosphorylation of Ser(535) in the epsilon-subunit of eukaryotic initiation factor (eIF) 2B is insufficient for the activation of eIF2B by insulin. Biochem J *367*, 475-481.

Wang, X., Paulin, F. E., Campbell, L. E., Gomez, E., O'Brien, K., Morrice, N., and Proud, C. G. (2001). Eukaryotic initiation factor 2B: identification of multiple phosphorylation sites in the epsilon-subunit and their functions in vivo. Embo J *20*, 4349-4359.

Waskiewicz, A. J., Flynn, A., Proud, C. G., and Cooper, J. A. (1997). Mitogen-activated protein kinases activate the serine/threonine kinases Mnk1 and Mnk2. Embo J *16*, 1909-1920.

Waskiewicz, A. J., Johnson, J. C., Penn, B., Mahalingam, M., Kimball, S. R., and Cooper, J. A. (1999). Phosphorylation of the cap-binding protein eukaryotic translation initiation factor 4E by protein kinase Mnk1 in vivo. Mol Cell Biol *19*, 1871-1880.

Watanabe, Y. (1982). Translational control of proinsulin synthesis by glucose. In Endocrinology, International Congress Series no 598, K. Shizume, H. Imura, and N. Shimizu, eds. (Amsterdam, Elsevier), pp. 266-270.

Webb, B. L. J., and Proud, C. G. (1997). eIF2B. The International Journal of Biochemistry and Cell Biology *29*, 1127-1131.

Webb, G. C., Akbar, M. S., Zhao, C., and Steiner, D. (2000). Expression profiling of pancreatic beta cells: glucose regulation of secretory and metabolic pathway genes. PNAS *97*, 5773-5778.

Webb, G. C., Akbar, M. S., Zhao, C., and Steiner, D. (2001). Expression profiling of pancreatic beta cells: Glucose regulation of secretory and metabolic pathway genes. Diabetes *50*, S135-S136.

Weichenrieder, O., Wild, K., Strub, K., and Cusack, S. (2000). Structure and assembly of the Alu domain of the mammalian signal recognition particle. Nature *408*, 167-173.

Wells, S. E., Hillner, P. E., Vale, R. D., and Sachs, A. B. (1998). Circularization of mRNA by eukaryotic translation initiation factors. Mol Cell *2*, 135-140.

Welsh, G. I., Miller, C. M., Loughlin, A. J., Price, N. T., and Proud, C. G. (1998). Regulation of eukaryotic initiation factor eIF2B: glycogen synthase kinase-3 phosphorylates a conserved serine which undergoes dephosphorylation in response to insulin. FEBS Lett *421*, 125-130.

Welsh, M., Nielsen, D. A., MacKrell, A. J., and Steiner, D. F. (1985). Control of insulin gene expression in pancreatic beta-cells and in an insulin-producing cell line, RIN-5F cells. II. Regulation of insulin mRNA stability. J Biol Chem *260*, 13590-13594.

Welsh, M., Scherberg, N., Gilmore, R., and Steiner, D. (1986). Translational control of insulin biosynthesis. Evidence for regulation of elongation, initiation and signal-recognition-particle-mediated translational control. Biochemical Journal *235*, 459-467.

Welsh, N., Oberg, C., and Welsh, M. (1991). P-binding proteins may stimulate insulin biosynthesis in rat pancreatic islets by enhancing the signal-recogntion-particle-dependent-translaocation of the insulin mRNA poly-/mono-some complex to the endoplasmic reticulum. Biochemical Journal *275*, 23-28.

Welsh, N., Welsh, M., Steiner, D. F., and Hellerstrom, C. (1987). Mechanisms of leucine- and theophylline-stimulated insulin biosynthesis in isolated rat pancreatic islets. Biochemical Journal *246*, 245-248.

Whalen, S. G., Gingras, A. C., Amankwa, L., Mader, S., Branton, P. E., Aebersold, R., and Sonenberg, N. (1996). Phosphorylation of eIF-4E on serine 209 by protein kinase C is inhibited by the translational repressors, 4E-binding proteins. J Biol Chem *271*, 11831-11837.

Wicksteed, B., Herbert, T. P., Alarcon, C., Lingohr, M., Moss, L. G., and Rhodes, C. (2001). Cooperativity between the preproinsulin mRNA untranslated regions is necessary for glucose-stimulated translation. The Journal of Biological Chemistry *276*, 22553-22558.

Wiedmann, M., Kurzchalia, T. V., Bielka, H., and Rapoport, T. A. (1987). Direct probing of the interaction between the signal sequence of nascent preprolactin and the signal recognition particle by specific cross-linking. J Cell Biol *104*, 201-208.

Wilhelm, J. E., Hilton, M., Amos, Q., and Henzel, W. J. (2003). Cup is an eIF4E binding protein required for both the translational repression of oskar and the recruitment of Barentsz. J Cell Biol *163*, 1197-1204.

Wilkinson, B. M., Critchley, A. J., and Stirling, C. J. (1996). Determination of the transmembrane topology of yeast Sec61p, an essential component of the endoplasmic reticulum translocation complex. J Biol Chem *271*, 25590-25597.

Wolin, S. L., and Walter, P. (1988). Ribosome pausing and stacking during translation of a eukaryotic mRNA. Embo J *7*, 3559-3569.

Wolin, S. L., and Walter, P. (1989). Signal recognition particle mediates a transient elongation arrest of preprolactin in reticulocyte lysate. J Cell Biol *109*, 2617-2622.

Wolin, S. L., and Walter, P. (1993). Discrete nascent chain lengths are required for the insertion of presecretory proteins into microsomal membranes. J Cell Biol *121*, 1211-1219.

Woolhead, C. A., McCormick, P. J., and Johnson, A. E. (2004). Nascent membrane and secretory proteins differ in FRET-detected folding far inside the ribosome and in their exposure to ribosomal proteins. Cell *116*, 725-736.

Wu, H., MacFarlane, W. M., Tadayyon, M., Arch, J. R., James, R. F., and Docherty, K. (1999). Insulin stimulates pancreatic-duodenal homoeobox factor-1 (PDX1) DNA-binding activity and insulin promoter activity in pancreatic beta cells. Biochem J *344 Pt 3*, 813-818.

Xu, G., Marshall, C. A., Lin, T., Kwon, G., Munivenkatappa, R. B., Hill, J. R., Lawrence, J. C., and McDaniel, M. L. (1998). Insulin mediates glucose-stimulated phosphorylation of PHAS-1 by pancreatic beta cells. The Journal of Biological Chemistry *273*, 4485-4491.

Xu, G. G., and Rothenberg, P. L. (1998). Insulin receptor signaling in the beta-cell influences insulin gene expression and insulin content: evidence for autocrine beta-cell regulation. Diabetes *47*, 1243-1252.

Yahr, T. L., and Wickner, W. T. (2000). Evaluating the oligomeric state of SecYEG in preprotein translocase. Embo J *19*, 4393-4401.

Yan, L., Nairn, A. C., Palfrey, H. C., and Brady, M. J. (2003). Glucose regulates EF-2 phosphorylation and protein translation by a protein phosphatase-2A-dependent mechanism in INS-1-derived 832/13 cells. J Biol Chem *278*, 18177-18183.

Yang, R., Wek, S. A., and Wek, R. C. (2000). Glucose limitation induces GCN4 translation by activation of Gcn2 protein kinase. Mol Cell Biol *20*, 2706-2717.

Yoon, H. J., and Donahue, T. F. (1992). The sui1 suppressor locus in Saccharomyces cerevisiae encodes a translation factor that functions during tRNA(iMet) recognition of the start codon. Mol Cell Biol *12*, 248-260.

Young, J. C., and Andrews, D. W. (1996). The signal recognition particle receptor alpha subunit assembles co-translationally on the endoplasmic reticulum membrane during an mRNA-encoded translation pause in vitro. Embo J *15*, 172-181.

Young, J. C., Ursini, J., Legate, K. R., Miller, J. D., Walter, P., and Andrews, D. W. (1995). An amino-terminal domain containing hydrophobic and hydrophilic sequences binds the signal recognition particle receptor alpha subunit to the beta subunit on the endoplasmic reticulum membrane. J Biol Chem *270*, 15650-15657.

Zheng, N., and Gierasch, L. M. (1997). Domain interactions in E. coli SRP: stabilization of M domain by RNA is required for effective signal sequence modulation of NG domain. Mol Cell *1*, 79-87.

Zopf, D., Bernstein, H. D., Johnson, A. E., and Walter, P. (1990). The methionine-rich domain of the 54 kd protein subunit of the signal recognition particle contains an RNA binding site and can be crosslinked to a signal sequence. Embo J *9*, 4511-4517.

Zopf, D., Bernstein, H. D., and Walter, P. (1993). GTPase domain of the 54-kD subunit of the mammalian signal recognition particle is required for protein translocation but not for signal sequence binding. J Cell Biol *120*, 1113-1121.

Zwieb, C. (1985). The secondary structure of the 7SL RNA in the signal recognition particle: functional implications. Nucleic Acids Res *13*, 6105-6124.